CHARACTERIZATION AND ELUCIDATION OF LYSOGENY ON HOST PHYSIOLOGY AND METABOLISM IN A ONE-HOST-TWO-PHAGE ROSEOBACTER MODEL SYSTEM

A Dissertation Presented for the
Doctor of Philosophy
Degree
The University of Tennessee, Knoxville

Jonelle Tamara Rose Basso
December 2019

DEDICATION

I dedicate this dissertation to my family. I wish to dedicate this dissertation to my parents, Roger Basso and Cheryl Basso, and my brother Gregory. I also dedicate this to my grandmother, Bernice Basso, who continues to be a force to be reckoned with and a true inspiration, as well as my uncles, aunts and cousins.

ACKNOWLEDGEMENTS

Words cannot truly express my gratitude in having Dr. Alison Buchan as my PI and mentor. I would first like to offer appreciation for the opportunity to be a part of the lab. I have grown as a phage microbial ecologist and scientist through her guidance, support and encouragement. I also wish to acknowledge my committee members, Dr. Steven Wilhelm, Dr. Sarah Lebeis, and Dr. Gladys Alexandre, who have provided invaluable expertise, support and direction throughout my academic journey.

I am also grateful for the current and past Buchan lab members, for all their help from the very beginning. Special thanks go to Dr. Nana Ankrah, who without his encouragement, I quite possibly would not have considered attending the University of Tennessee for this program. He was my official mentor, and still continues in this role today. I am also truly grateful for Matthew Tuttle, for his expertise and support in a way that propels me to a better scientist and person every day. I am grateful for the rest of my lab family, Ashley Frank, Michelle Chua, Lauren Quigley, April Armes, and Mary Hadden, who have been great people to work with. I am humbled by the wonderful undergraduates I have mentored and who have contributed to the research reported herein: Alex Grossman, Avery Bullock, Kaylee Jacobs and Julie Xu. I have had the pleasure of collaborating with some amazing people from the Chemistry department, Geography department and College of Engineering, and I am indebted to every one of them: Katarina Jones, Haley Fielland, Courtney Christopher, Michael Campanovo and Michael Allen. I am also indebted to Dr. Dunlap for his expertise on Transmission Electron and Confocal Microscopy.

A special thank you also goes out my incredible support system which comprises the East Tennessee Caribbean Community, the UT Nepali students' association, the Knoxville Gambian community, the PEER program and AVW friends. Particular thanks are extended to Bikash Bogati, Dr. Sanjeev Dahal and Pragya Poudel, Dembo Jammeh, Leondra Lawson, Mivy Drexler, the Jacobs family and the Aidoo family, who have all significantly contributed to my well-being in many ways throughout my PhD process.

Lastly, but certainly not least, I am so grateful for my family's support from across the miles.

ABSTRACT

Marine bacteria are key components of the marine food web and are influenced by the viruses that infect them. Viruses are the most abundant biological entities on the planet. Bacteriophages (phages) can cause lytic infections or form long-term relationships with their bacterial hosts, though aspects of the lysogenic to lytic switch remain poorly understood. Phages can manipulate host genetic diversity, metabolism, evolution and fitness, as well as offer host competitive advantage through conferring immunity to superinfecting phages. Phages can influence nutrient availability in ecosystems through cell lysis of their hosts. Lysogeny is prevalent in marine systems due to high incidence of temperate phage signatures from well-characterized bacteria. Exposure to stressors can effect prophage induction, though minute quantities of induction can occur in the absence of an obvious stressor. This phenomenon, described as spontaneous prophage induction (SPI), is now proposed to benefit lysogenized populations as a form of "biological weaponry". SPI has historically been studied in *E. coli*, which is not ecologically relevant. Furthermore, many systems currently use lytic phages to study facets of phage-host interactions. Therefore, how temperate phages affect host physiology, modulate SPI, and manipulate metabolism is considerably less understood and investigated especially in non-model systems. Here, I used an environmentally relevant one-host-two-phage *Roseobacter* model system to characterize and elucidate the influence of lysogeny on host physiology and metabolism. I observed that temperate prophages influence physiology. Competition experiments reveal that our strains have increased fitness when grown together in biofilm but reduced fitness in liquid culture. Host range studies determine very high host specificity of our phages, and highlight modulation of growth dynamic, cell size, biomass and SPI according to vessel type, culture volume and substrate. We show that discrete metabolites are responsible for observed differences in the metabolome and lipidome between our strains when grown on standard marine media, glutamate or acetate. In summary, these findings offer insight into key genetic and metabolic mechanisms of host-phage dynamics as they relate to host fitness, evolution, and regulation of nutrients into the marine environment. This work helps elucidate the biological and ecological factors affecting such phage-host systems in nature.

TABLE OF CONTENTS

LIST OF TABLES

LIST OF FIGURES

CHAPTER 1

INTRODUCTION

Ocean systems comprise the majority of the total surface of the Earth, of which microbial exploration has been conducted anywhere from coastal seawaters to deep-sea (Kobayashi et al 2008, Moran et al 2004). Microorganisms are ubiquitous and ecologically relevant groups form driving forces of global biogeochemical cycles (reviewed in Buchan et al 2014). Representative groups are integral players in the production of global oxygen, for example, which is crucial for the survival and success of all aerobic terrestrial and marine organisms. Marine bacteria are important components of the marine food web and form intimate relationships with phytoplankton and viruses (reviewed in Buchan et al 2014, Sule and Belas 2013, Zhan and Chen 2019). Viruses are also ubiquitous, with global estimates residing upwards of the 10^{30} range (Bergh et al 1989, Fuhrman 1999, Hambly and Suttle 2005, Hendrix 2002, Suttle 2007). Viruses significantly contribute to shuttling of carbon and nutrients in marine systems and is described as the viral shunt (Wilhelm and Suttle 1999). Viruses infecting bacteria, bacteriophages, carry out a variety of cycles, of which lytic and lysogenic ones describe either end of the spectrum (reviewed in Sturino and Klaenhammer 2006). Phages can carry out active lysogeny or pseudolysogeny, and virus-virus communication may help control the decision for the lysogenic to lytic switch (Erez et al 2017, reviewed in Feiner et al 2015, reviewed in Los and Wegrzyn 2012). Phages significantly affect bacterial mortality, facilitate horizontal gene transfer (HGT), manipulate gene regulation, and modify host metabolism (Ankrah et al 2014d, reviewed in Breitbart 2012, reviewed in Breitbart et al 2018, Canchaya et al 2003, Chen et al 2005, Dodd et al 2005, Hurwitz et al 2013, Thomas et al 2011, reviewed in Warwick-Dugdale et al 2019). Phages influence host fitness and evolution and have also been described as "biological weapons", providing competitive advantage over non-lysogenized bacteria (Chen et al 2005, Davies et al 2016a, Davies et al 2016b, reviewed in Harrison and Brockhurst 2017, Lai et al 2018, Li et al 2017, Yu et al 2015).

Factors such as temperature, UV radiation, pH and nutrient availability can affect phage infectivity and induction (Eichenbaum and Livneh 1998, Mojica and Brussaard 2014). Seasonal changes are linked to fluctuations in phage abundance (Jiang and Paul 1994, Sahlsten 1998). Spontaneous prophage induction (SPI), describing the phenomenon of phages undergoing a lysogenic to lytic switch due to an unknown factor, may be

promoted by intrinsic factors (reviewed in Nanda et al 2015). SPI occurs at low frequencies and may influence biofilm formation ((Helfrich et al 2015, reviewed in Nanda et al 2015, Pennington and Rosenberg 2007, Simmons et al 2009). Previous research pertaining to SPI has been solely conducted on *E. coli* and thus identifies a paucity of data that describes this phenomenon in other systems (Czyz et al 2001). Phages exhibit host-range variability (Boyd et al 2000, Hambly and Suttle 2005, Ross et al 2016, Tzipilevich et al 2017, Wang and Chen 2008). Infection may be limited to one virus per host, as observed in *Salmonella* phages and *Lactobacillus casei* Shirota phage PL-1 (Joerger 2003, Stetter 1977). Alternatively, phage infection of more than one host has been illustrated where CTX ϕ infects both *Vibrio cholerae* and *Vibrio minicus* (Boyd et al 2000) and ϕ-OTB infects Serratia strain ATCC:39006 and Pantoea *agglomerans*, 9Rz4 (Evans et al 2010). Host-range dynamics have implications concerning HGT and proliferation of virulence genes (Casas et al 2006).

The prevalence of lysogeny is described in a variety of host-phage systems, where more than half of well characterized bacteria are lysogens (Paul 2008, Touchon et al 2016). Mesocosm experiments help in the discovery of new lysogens and temperate phages (Ankrah et al 2014a, Ankrah et al 2014c). Some systems even show incidence of polylysogeny where the symbiosis is beneficial to the host (Espeland et al 2004, Wang et al 2010). Here we define polylysogeny as the instance whereby a singular host is lysogenized by more than one phage. A delicate balance is acknowledged however, between lysogeny and lytic infection and how this influences microbial ecology (Obeng et al 2016, Payet and Suttle 2013). Ecological factors such as seasonal changes can in turn have influence on incidence of lysogeny (Jiang and Paul 1994). The triggers of lysogenic to lytic conversion of is current debate and ecological models have been proposed to help demystify these mechanisms.

Considerations are given for the 'Piggyback the Winner' (PtW) strategy, whereby the ratio of virus/bacteria is dictated by lysogeny with preference for rapid host growth rates and high host density (Knowles et al 2016). Others suggest alternative strategies such as 'Kill the Winner' (KtW) (Thingstad and Lignell 1997) or 'King of the Mountain' (KoM) (Breitbart et al 2018), which hypothesize increased rates of viral immunity but operate

through different mechanisms. KtW suggests an expense for competitiveness for obtaining resources, in contrast to KoM which suggests the presence of a positive feedback loop that drives better competition for resources, thus increasing geochemical cycling contributions (Giovannoni et al 2013, Thingstad and Lignell 1997). Most of these are focused on host productivity and other external factors, such as resource and nutrient availability (Giovannoni et al 2013, Jiang and Paul 1998, Knowles et al 2016, Thingstad and Lignell 1997, Weinbauer and Suttle 1999), spatial and temporal variability (Luo et al 2017), and the subsequent stress triggers resulting in relief of phage gene repression (reviewed in Howard-Varona et al 2017, Jiang and Paul 1996, Mojica and Brussaard 2014).

Temperate phages were previously described as "time bombs" (Paul 2008). Lysogeny represents one end of the sprectrum of host-virus interactions. The proposed "virocell" terminology can be described as an infected cell anywhere on the continuum of lysogeny to lysis (Forterre 2013). This new vocabulary aims to better conceptualize this much more complex phage-host relationship where, for example, metabolism of the virocell entity is distinctly unique from uninfected counterparts (Rosenwasser et al 2016).

Despite the complexity, prevalence and interesting nature of lysogeny, much more research continues to be conducted on their lytic counterparts instead. Much knowledge of phage-host interactions stems from studies historically conducted with *E. coli* and other medically relevant systems, such as *Salmonella* species and *Clostridium difficile* (Bossi et al 2003, Butala et al 2008, Lai et al 2018, Randall-Hazelbauer and Schwartz 1973, Susskind et al 1974a., Thanki et al 2018). There is a paucity of studies conducted using ecologically relevant marine phage-host model systems. The depth and characterization of temperate phage influence in terms of host range, physiology, biofilm formation, carbon and lipid metabolism, superinfection exclusion and the phenomenon of SPI in the marine environment is yet to be revealed.

Members of the ecologically relevant Roseobacter clade are ubiquitous, with isolations conducted from a myriad of locations around the world (Brinkhoff et al 2008, Buchan et al 2003, Fuhrman et al 1994, Gonzalez et al 2003, Mas-Lladó et al 2014, Moran et al 2007). They contribute to global biogeochemical cycles (Billerbeck et al 2016, Buchan et al 2014) and can form biofilms (Cude et al 2015, Slightom and Buchan 2009).

Roseobacters form close association with lytic and temperate phages, where more than thirty roseophages have been isolated and described (Ankrah et al 2014a, Ankrah et al 2014b, Ankrah et al 2014c, Zhan and Chen 2019), and have been shown to have metabolic activity modulated by lytic phage (Ankrah et al 2014d). The ease of isolation and culturing of several roseobacters strains adds to the attractive nature of their use for laboratory experiments. Roseobacters thus provide a collection of hosts and phages to adequately perform host-phage investigation of marine systems.

For the research contained within this dissertation, we used and developed an ecologically relevant roseobacter-roseophage system that is comprised on *Sulfitobacter* sp. strain CB-D, which is lysogenized by prophage ϕ-D, and *Sulfitobacter* sp. strain CB-A, which is lysogenized by prophage ϕ-A. Hosts and phages were obtained from mesocosm studies conducted in Raunefjorden, Norway (Ankrah et al 2014a, Ankrah et al 2014b). While *Sulfitobacter* sp. strain CB-D (lysogenized by ϕ-D) was directly derived from the mesocosm experiment, CB-A was generated through superinfection experiments conducted with ϕ-A and CB-D in the laboratory. We used this two-phage-one-host model system to address the overarching research objectives, which were to 1) elucidate host-phage interactions of a model using ecologically important micro-components 2) investigate and characterize the system 3) determine phage-host specificity and 4) characterize lysogenic-lytic switching in these strains.

The scientific investigations of this dissertation are discussed within research chapters 2-5. Chapter 2 describes the characterization of temperate roseophages, ϕ-A and ϕ-D, influence on physiology in our model roseobacter-roseophage system. Chapter 3 discusses the determination of host specificity of roseophages ϕ-A and ϕ-D on a suite of roseobacter sp. strains. Chapter 4 seeks to determine the influence of lysogeny, and modification host-phage interactions in a complex medium, on the lysogenic-lytic switch. Chapter 5 determines the influence of lysogeny, and modification of host-phage interactions in defined media, on the lysogenic-lytic switch.

My work builds on the need for documentation of the effect of lysogeny on roseobacter virocells, in order to better characterize the roseobacter-roseophage model system. It also provides insight into the biological factors affecting prophage conversion

and transfer of genetic material in the marine environment. Assays have been included that characterize potential growth costs associated with an established virocells on a variety of minimal and rich media and addresses how lysogeny affects host cell metabolism. Altogether, these studies provide insight into the genetic and metabolic mechanisms underlying host-phage dynamics in various niches and help in the understanding of environmental and biological factors that affect virocells in the natural environment.

REFERENCES

Ankrah NYD, Budinoff CR, Wilson WH, Wilhelm SW, Buchan A (2014a). Genome Sequences of Two Temperate Phages, ΦCB2047-A and ΦCB2047-C, Infecting Sulfitobacter sp. Strain 2047. *Genome Announcements* **2**.

Ankrah NYD, Budinoff CR, Wilson WH, Wilhelm SW, Buchan A (2014b). Genome Sequence of the Sulfitobacter sp. Strain 2047-Infecting Lytic Phage ΦCB2047-B. *Genome Announcements* **2**.

Ankrah NYD, Lane T, Budinoff CR, Hadden MK, Buchan A (2014c). Draft Genome Sequence of Sulfitobacter sp. CB2047, a Member of the Roseobacter Clade of Marine Bacteria, Isolated from an Emiliania huxleyi Bloom. *Genome Announcements* **2**.

Ankrah NYD, May AL, Middleton JL, Jones DR, Hadden MK, Gooding JR *et al* (2014d). Phage infection of an environmentally relevant marine bacterium alters host metabolism and lysate composition. *Isme Journal* **8:** 1089-1100.

Bergh O, Borsheim KY, Bratbak G, Heldal M (1989). High Abundance of Viruses Found in Aquatic Environments. *Nature* **340:** 467-468.

Billerbeck S, Wemheuer B, Voget S, Poehlein A, Giebel HA, Brinkhoff T *et al* (2016). Biogeography and environmental genomics of the Roseobacter-affiliated pelagic CHAB-I-5 lineage. *Nature Microbiology* **1**.

Bossi L, Fuentes JA, Mora G, Figueroa-Bossi N (2003). Prophage contribution to bacterial population dynamics. *Journal of Bacteriology* **185:** 6467-6471.

Boyd EF, Moyer KE, Shi L, Waldor MK (2000). Infectious CTXPhi and the vibrio pathogenicity island prophage in Vibrio mimicus: evidence for recent horizontal transfer between V. mimicus and V. cholerae. *Infection and immunity* **68:** 1507-1513.

Breitbart M (2012). Marine Viruses: Truth or Dare. In: Carlson CA, Giovannoni SJ (eds). *Annual Review of Marine Science, Vol 4*. pp 425-448.

Breitbart M, Bonnain C, Malki K, Sawaya NA (2018). Phage puppet masters of the marine microbial realm. *Nature Microbiology* **3:** 754-766.

Brinkhoff T, Giebel HA, Simon M (2008). Diversity, ecology, and genomics of the Roseobacter clade: a short overview. *Archives of Microbiology* **189:** 531-539.

Buchan A, Newell SY, Butler M, Biers EJ, Hollibaugh JT, Moran MA (2003). Dynamics of bacterial and fungal communities on decaying salt marsh grass. *Applied and Environmental Microbiology* **69:** 6676-6687.

Buchan A, LeCleir GR, Gulvik CA, Gonzalez JM (2014). Master recyclers: features and functions of bacteria associated with phytoplankton blooms. *Nature Reviews Microbiology* **12:** 686-698.

Butala M, Žgur-Bertok D, Busby SJW (2008). The bacterial LexA transcriptional repressor. *Cellular and Molecular Life Sciences* **66:** 82.

Canchaya C, Fournous G, Chibani-Chennoufi S, Dillmann ML, Brussow H (2003). Phage as agents of lateral gene transfer. *Current Opinion in Microbiology* **6:** 417-424.

Casas V, Miyake J, Balsley H, Roark J, Telles S, Leeds S *et al* (2006). Widespread occurrence of phage-encoded exotoxin genes in terrestrial and aquatic environments in Southern California. *Fems Microbiology Letters* **261:** 141-149.

Chen Y, Golding I, Sawai S, Guo L, Cox EC (2005). Population fitness and the regulation of Escherichia coli genes by bacterial viruses. *Plos Biology* **3:** 1276-1282.

Cude WN, Prevatte CW, Hadden MK, May AL, Smith RT, Swain CL *et al* (2015). Phaeobacter sp Strain Y4I Utilizes Two Separate Cell-to-Cell Communication Systems To Regulate Production of the Antimicrobial Indigoidine. *Applied and Environmental Microbiology* **81:** 1417-1425.

Czyz A, Los M, Wrobel B, Wegrzyn G (2001). Inhibition of spontaneous induction of lambdoid prophages in Escherichia coli cultures: simple procedures with possible biotechnological applications. *BMC Biotechnology* **1:** 1-1.

Davies EV, James CE, Kukavica-Ibrulj I, Levesque RC, Brockhurst MA, Winstanley C (2016a). Temperate phages enhance pathogen fitness in chronic lung infection. *Isme Journal* **10:** 2553-2555.

Davies EV, James CE, Williams D, O'Brien S, Fothergill JL, Haldenby S *et al* (2016b). Temperate phages both mediate and drive adaptive evolution in pathogen biofilms. *Proceedings of the National Academy of Sciences* **113:** 8266-8271.

Dodd IB, Shearwin KE, Egan JB (2005). Revisited gene regulation in bacteriophage lambda. *Current Opinion in Genetics & Development* **15:** 145-152.

Eichenbaum Z, Livneh Z (1998). UV light induces IS10 transposition in Escherichia coli. *Genetics* **149:** 1173-1181.

Erez Z, Steinberger-Levy I, Shamir M, Doron S, Stokar-Avihail A, Peleg Y *et al* (2017). Communication between viruses guides lysis-lysogeny decisions. *Nature* **541:** 488-493.

Espeland EM, Lipp EK, Huq A, Colwell RR (2004). Polylysogeny and prophage induction by secondary infection in Vibrio cholerae. *Environmental Microbiology* **6:** 760-763.

Evans TJ, Crow MA, Williamson NR, Orme W, Thomson NR, Komitopoulou E *et al* (2010). Characterization of a broad-host-range flagellum-dependent phage that mediates high-efficiency generalized transiduction in, and between, Serratia and Pantoea. *Microbiology-Sgm* **156:** 240-247.

Feiner R, Argov T, Rabinovich L, Sigal N, Borovok I, Herskovits AA (2015). A new perspective on lysogeny: prophages as active regulatory switches of bacteria. *Nature Reviews Microbiology* **13:** 641-650.

Forterre P (2013). The virocell concept and environmental microbiology. *Isme Journal* **7:** 233-236.

Fuhrman JA, Lee SH, Masuchi Y, Davis AA, Wilcox RM (1994). Characterization of Marine Prokaryotic Communities via DNA and RNA. *Microbial Ecology* **28:** 133-145.

Fuhrman JA (1999). Marine viruses and their biogeochemical and ecological effects. *Nature* **399:** 541-548.

Giovannoni S, Temperton B, Zhao YL (2013). SAR11 viruses and defensive host strains reply. *Nature* **499:** E4-E5.

Gonzalez JM, Covert JS, Whitman WB, Henriksen JR, Mayer F, Scharf B *et al* (2003). Silicibacter pomeroyi sp nov and Roseovarius nubinhibens sp nov.,

dimethylsulfoniopropionate-demethylating bacteria from marine environments. *International Journal of Systematic and Evolutionary Microbiology* **53:** 1261-1269.

Hambly E, Suttle CA (2005). The viriosphere, diversity, and genetic exchange within phage communities. *Current Opinion in Microbiology* **8:** 444-450.

Harrison E, Brockhurst MA (2017). Ecological and Evolutionary Benefits of Temperate Phage: What Does or Doesn't Kill You Makes You Stronger. *BioEssays* **39:** 1700112.

Helfrich S, Pfeifer E, Kramer C, Sachs CC, Wiechert W, Kohlheyer D *et al* (2015). Live cell imaging of SOS and prophage dynamics in isogenic bacterial populations. *Molecular Microbiology* **98:** 636-650.

Hendrix RW (2002). Bacteriophages: Evolution of the majority. *Theoretical Population Biology* **61:** 471-480.

Howard-Varona C, Hargreaves KR, Abedon ST, Sullivan MB (2017). Lysogeny in nature: mechanisms, impact and ecology of temperate phages. *Isme Journal* **11:** 1511-1520.

Hurwitz BL, Hallam SJ, Sullivan MB (2013). Metabolic reprogramming by viruses in the sunlit and dark ocean. *Genome biology* **14:** R123-R123.

Jiang SC, Paul JH (1994). Seasonal and Diel Abundance of Viruses and Occurrence of Lysogeny/Bacteriocinogeny in the Marine Environment. *Marine Ecology Progress Series* **104:** 163-172.

Jiang SC, Paul JH (1996). Occurrence of lysogenic bacteria in marine microbial communities as determined by prophage induction. *Marine Ecology Progress Series* **142:** 27-38.

Jiang SC, Paul JH (1998). Significance of lysogeny in the marine environment: Studies with isolates and a model of lysogenic phage production. *Microbial Ecology* **35:** 235-243.

Joerger RD (2003). Alternatives to antibiotics: Bacteriocins, antimicrobial peptides and bacteriophages. *Poultry Science* **82:** 640-647.

Knowles B, Silveira CB, Bailey BA, Barott K, Cantu VA, Cobian-Guemes AG *et al* (2016). Lytic to temperate switching of viral communities. *Nature* **531:** 466-+.

Kobayashi T, Koide O, Mori K, Shimamura S, Matsuura T, Miura T *et al* (2008). Phylogenetic and enzymatic diversity of deep subseafloor aerobic microorganisms in organics- and methane-rich sediments off Shimokita Peninsula. *Extremophiles* **12:** 519-527.

Lai JYH, Zhang H, Chiang MHY, Lun CHI, Zhang R, Lau SCK (2018). The putative functions of lysogeny in mediating the survivorship of Escherichia coli in seawater and marine sediment. *Fems Microbiology Ecology* **94**.

Li XY, Lachnit T, Fraune S, Bosch TCG, Traulsen A, Sieber M (2017). Temperate phages as self-replicating weapons in bacterial competition. *Journal of the Royal Society Interface* **14**.

Los M, Wegrzyn G (2012). Pseudolysogeny. In: Lobocka M, Szybalski WT (eds). *Advances in Virus Research, Vol 82: Bacteriophages, Pt A*. pp 339-349.

Luo E, Aylward FO, Mende DR, DeLong EF (2017). Bacteriophage Distributions and Temporal Variability in the Ocean's Interior. *Mbio* **8**.

Mas-Lladó M, Piña-Villalonga JM, Brunet-Galmés I, Nogales B, Bosch R (2014). Draft Genome Sequences of Two Isolates of the Roseobacter Group, Sulfitobacter sp. Strains 3SOLIMAR09 and 1FIGIMAR09, from Harbors of Mallorca Island (Mediterranean Sea). *Genome Announcements* **2:** e00350-00314.

Mojica KDA, Brussaard CPD (2014). Factors affecting virus dynamics and microbial host-virus interactions in marine environments. *Fems Microbiology Ecology* **89:** 495-515.

Moran MA, Buchan A, Gonzalez JM, Heidelberg JF, Whitman WB, Kiene RP *et al* (2004). Genome sequence of Silicibacter pomeroyi reveals adaptations to the marine environment. *Nature* **432:** 910-913.

Moran MA, Belas R, Schell MA, Gonzalez JM, Sun F, Sun S *et al* (2007). Ecological genomics of marine roseobacters. *Applied and Environmental Microbiology* **73:** 4559-4569.

Nanda AM, Thormann K, Frunzke J (2015). Impact of Spontaneous Prophage Induction on the Fitness of Bacterial Populations and Host-Microbe Interactions. *Journal of Bacteriology* **197:** 410-419.

Obeng N, Pratama AA, van Elsas JD (2016). The Significance of Mutualistic Phages for bacterial Ecology and Evolution. *Trends in Microbiology* **24:** 440-449.

Paul JH (2008). Prophages in marine bacteria: dangerous molecular time bombs or the key to survival in the seas? *Isme Journal* **2:** 579-589.

Payet JP, Suttle CA (2013). To kill or not to kill: The balance between lytic and lysogenic viral infection is driven by trophic status. *Limnology and Oceanography* **58:** 465-474.

Pennington JM, Rosenberg SM (2007). Spontaneous DNA breakage in single living Escherichia coli cells. *Nat Genet* **39:** 797-802.

Randall-Hazelbauer L, Schwartz M (1973). Isolation of the bacteriophage lambda receptor from Escherichia coli. *Journal of bacteriology* **116:** 1436-1446.

Rosenwasser S, Ziv C, Van Creveld SG, Vardi A (2016). Virocell Metabolism: Metabolic Innovations During Host-Virus Interactions in the Ocean. *Trends in Microbiology* **24:** 821-832.

Ross A, Ward S, Hyman P (2016). More Is Better: Selecting for Broad Host Range Bacteriophages. *Frontiers in Microbiology* **7**.

Sahlsten E (1998). Seasonal abundance in Skagerrak-Kattegat coastal waters and host specificity of viruses infecting the marine photosynthetic flagellate Micromonas pusilla. *Aquatic Microbial Ecology* **16:** 103-108.

Simmons LA, Goranov AI, Kobayashi H, Davies BW, Yuan DS, Grossman AD *et al* (2009). Comparison of Responses to Double-Strand Breaks Double-Strand Breaks between Escherichia coli and Bacillus subtilis Reveals Different Requirements for SOS Inductions. *Journal of Bacteriology* **191:** 1152.

Slightom RN, Buchan A (2009). Surface Colonization by Marine Roseobacters: Integrating Genotype and Phenotype. *Applied and Environmental Microbiology* **75:** 6027-6037.

Stetter KO (1977). Evidence for frequent lysogeny in lactobacilli: temperate bacteriophages within the subgenus Streptobacterium. *Journal of virology* **24:** 685-689.

Sturino JM, Klaenhammer TR (2006). Engineered bacteriophage-defence systems in bioprocessing. *Nature Reviews Microbiology* **4:** 395-404.

Sule P, Belas R (2013). A Novel Inducer of Roseobacter Motility Is Also a Disruptor of Algal Symbiosis. *Journal of Bacteriology* **195:** 637-646.

Susskind MM, Botstein D, Wright A (1974a.). Superinfection exclusion by P22 prophage in lysogens of Salmonella typhimurium III. Failure of superinfecting phage DNA to enter sieA+ lysogens. *Virology* **62:** 350-366.

Suttle CA (2007). Marine viruses - major players in the global ecosystem. *Nature Reviews Microbiology* **5:** 801-812.

Thanki AM, Taylor-Joyce G, Dowah A, Nale JY, Malik D, Clokie MRJ (2018). Unravelling the Links between Phage Adsorption and Successful Infection in Clostridium difficile. *Viruses-Basel* **10**.

Thingstad TF, Lignell R (1997). Theoretical models for the control of bacterial growth rate, abundance, diversity and carbon demand. *Aquatic Microbial Ecology* **13:** 19-27.

Thomas R, Berdjeb L, Sime-Ngando T, Jacquet S (2011). Viral abundance, production, decay rates and life strategies (lysogeny versus lysis) in Lake Bourget (France). *Environmental Microbiology* **13:** 616-630.

Touchon M, Bernheim A, Rocha EPC (2016). Genetic and life-history traits associated with the distribution of prophages in bacteria. *Isme Journal* **10:** 2744-2754.

Tzipilevich E, Habusha M, Ben-Yehuda S (2017). Acquisition of Phage Sensitivity by Bacteria through Exchange of Phage Receptors. *Cell* **168:** 186-+.

Wang K, Chen F (2008). Prevalence of highly host-specific cyanophages in the estuarine environment. *Environmental Microbiology* **10:** 300-312.

Wang X, Kim Y, Ma Q, Hong SH, Pokusaeva K, Sturino JM *et al* (2010). Cryptic prophages help bacteria cope with adverse environments. *Nature Communications* **1:** 147.

Warwick-Dugdale J, Buchholz HH, Allen MJ, Temperton B (2019). Host-hijacking and planktonic piracy: how phages command the microbial high seas. *Virology Journal* **16:** 15.

Weinbauer MG, Suttle CA (1999). Lysogeny and prophage induction in coastal and offshore bacterial communities. *Aquatic Microbial Ecology* **18:** 217-225.

Wilhelm SW, Suttle CA (1999). Viruses and Nutrient Cycles in the Sea - Viruses play critical roles in the structure and function of aquatic food webs. *Bioscience* **49:** 781-788.

Yu Z-C, Chen X-L, Shen Q-T, Zhao D-L, Tang B-L, Su H-N *et al* (2015). Filamentous phages prevalent in Pseudoalteromonas spp. confer properties advantageous to host survival in Arctic sea ice. *The ISME journal* **9:** 871-881.

Zhan YC, Chen F (2019). Bacteriophages that infect marine roseobacters: genomics and ecology. *Environmental Microbiology* **21:** 1885-1895.

CHAPTER 2

GENETICALLY SIMILAR TEMPERATE PHAGES FORM COALITIONS WITH THEIR SHARED HOST THAT LEAD TO NICHE-SPECIFIC FITNESS EFFECTS

A version of this chapter has been submitted for publication in the International Society for Microbial Ecology Journal, ISME J by Jonelle T.R. Basso, Nana Y.D. Ankrah, Matthew J. Tuttle, Alex S. Grossman and Alison Buchan.

NYDA conducted qPCR analyses, including phage enumeration, and original sequencing of strains. DNA extractions for resequencing of strains was conducted by JRTB. Co-culture experiments were conducted by AB, MJT, and AGM. Biofilm assays were conducted by MJT, JTRB and ASG. SPI experiments were conducted by MJT. Statistical analyzes were conducted by NYDA, JTRB and AB. JTRB drafted the manuscript. AB aided with crafting the manuscript. AB also aided with the design and data interpretation of the study. All authors reviewed and approved the final manuscript.

ABSTRACT

Temperate phages engage in long-term associations with their hosts that may lead to mutually beneficial interactions, the full extent of which is presently unknown. Here we describe an environmentally relevant model system with a single host, a species of the Roseobacter clade of marine bacteria, and two genetically similar phages (ϕ-A and ϕ-D). Superinfection of a ϕ-D lysogenized strain (CB-D) with ϕ-A particles resulted in a lytic infection, prophage induction, and lysogenic conversion of a subset of the host population, leading to isolation of a newly ϕ-A lysogenized strain (CB-A). Phenotypic differences, predicted to result from divergent lysogenic-lytic switch mechanisms, are evident between these lysogens. As strains are susceptible to infection by the opposing phage type, co-culture competitions were performed to test fitness effects. When grown planktonically, CB-A outcompeted CB-D three to one. During biofilm growth, CB-D outcompeted CB-A three to one. These results contribute to growing evidence that lysogenized bacteria can use prophages as weapons in competition against susceptible hosts and, given the reciprocal nature of the attack, reveals a new layer of complexity in this interaction. These findings have implications for enhanced understanding of the eco-evolutionary dynamics of host-phage interactions that are pervasive in all ecosystems.

INTRODUCTION

Temperate phages may engage in long-term association with their bacterial hosts that can lead to mutually beneficial interactions. It is well established that prophages can offer their hosts benefits, including immunity to superinfection by homologous phages (Bondy-Denomy and Davidson 2014, Brussow et al 2004, Canchaya et al 2003, Paul 2008) and enhanced virulence through prophage encoded toxins (e.g., Brussow et al. 2004; Feiner et al. 2015; Nanda et al. 2015). However, the roles of prophages in enhancing both host and phage fitness is broadening in scope and complexity (Feiner et al 2015, Touchon et al 2016).

Prophages have frequently been referred to as "time bombs" (*e.g.*, Paul 2008), in which the nature of the host-phage relationship hinges upon the physiological status of the host. The most commonly cited trigger of prophage induction is damage of the host's DNA, typically the result of extrinsic factors such as UV radiation or chemical toxins, which induces a molecular cascade of events culminating in expression of prophage-encoded lytic genes (Feiner et al 2015, Fortier and Sekulovic 2013). However, intrinsic factors may also promote activation of the lytic life cycle, a process termed spontaneous prophage induction (SPI) (Nanda et al 2015). Even under seemingly optimal cultivation conditions, SPI occurs with low frequency in populations (range 0.09-3.1%; Helfrich et al 2015, Kamenšek et al 2010, Nanda et al 2014, Pennington and Rosenberg 2007, Simmons et al 2009). SPI is often considered a detrimental process for the host as a fraction of cells is continuously lost by phage-mediated cell lysis. Yet, benefits of SPI on bacterial fitness have recently been recognized, including the release of extracellular DNA, which can be important for biofilm formation (Nanda et al 2015) and production of phages as weapons in competition with susceptible hosts (Harrison and Brockhurst 2017).

Lysogeny is hypothesized to be prevalent in marine environments (Leitet et al 2006, Stopar et al 2004). Approximately half of sequenced bacterial genomes contain prophage signatures, suggesting a high proportion of marine bacteria are lysogenized (Paul 2008, Touchon et al 2016). The abundance of marine temperate viruses is further supported by culture-independent approaches (Duhaime et al 2012, Hurwitz et al 2014). Quantitative

estimates of the prevalence of lysogeny in the ocean are principally derived from field-based mitomycin C induction experiments and vary widely, ranging from 0-71% (Brum et al 2016, Payet and Suttle 2013, Williamson et al 2002). This observed variation is predicted to reflect environmental conditions (e.g., host productivity and abundance) that drive temperate phages into either a lysogenic or lytic state (Brum et al 2016, Giovannoni et al 2013, Jiang and Paul 1998, Luo et al 2017, Thingstad and Lignell 1997, Weinbauer and Suttle 1999) and has been the focus of considerable debate (e.g., Knowles et al 2016, Weitz et al 2017). In contrast, a role for spontaneous induction has not been broadly considered in a marine context.

Roseobacters are abundant members of microbial assemblages in both planktonic and surface-associated marine niches (Billerbeck et al 2016, Buchan et al 2005, Slightom and Buchan 2009) and prophages are common in genomes of cultured representatives (Chen et al 2006, Zhao et al 2010). Thus, this environmentally relevant group of heterotrophic marine bacteria presents an opportunity to study host-phage interactions in the context of lysogeny. *Sulfitobacter* sp. strain CB2047 and its infecting temperate phage ϕ-A were originally isolated from a phytoplankton bloom (Ankrah et al 2014a, Ankrah et al 2014b). Genome sequence analyses of the host revealed it was lysogenized with a prophage, denoted ϕ-D, that shares a high degree (79%) of nucleotide identity with ϕ-A (Ankrah et al 2014b). Here we report the complex interactions of this two-phage shared-host system.

MATERIALS AND METHODS

Bacterial growth, prophage induction, and infection.

Sulfitobacter sp. strain CB2047 (henceforth CB-D) was originally isolated from an *Emiliania huxleyi* phytoplankton bloom in Raunefjorden, Norway, (Ankrah et al 2014b). CB-D, and its derivative CB-A, were routinely grown at 25ºC in the dark at 200 rpm on Standard Marine Media (SMM), an artificial sea water medium supplemented with 0.11% yeast extract and 0.2% tryptone (Budinoff and Hollibaugh 2007). Phages were propagated by induction of exponentially growing lysogenic cultures with mitomycin C (0.5 µg/ml) following standard approaches (Ankrah 2015). Superinfections were performed by phage addition to early exponential phase cultures of permissive hosts (OD_{540nm} = 0.17) at a multiplicity of infection (MOI) of 0.06. These infections yield mixed phage populations due to concurrent induction of the resident prophage.

Phage enumeration.

Phage abundance was monitored using plaque assay and quantitative PCR (qPCR). Plaque assays were performed on SMM using standard approaches (Kropinski et al 2009). qPCR assays used unique phage-specific primers (Table S2.1) and were performed with a DNA Engine Opticon 2 system with the Opticon Monitor 3.1.32 software package (Bio-Rad Laboratories, Inc., Hercules, CA). qPCRs were in 25 µl reactions with 12.5 µl SYBR Premix Ex Taq cocktail RR041 (Perfect Real Time; Takara Bio, Inc., Shiga, Japan), 500 nM primers, and 10 µl of phage DNA. Thermocycling conditions were as follows: 95ºC for 2 min, 40 cycles of 95ºC for 20 s, 57ºC for 20 s, 72ºC for 20 s, followed by 72ºC for 5 min. Melt curves consistently showed single peaks per primer set, indicating high specificity. Standards were developed from plasmids containing cloned sequences and standard curves (correlation between log of gene copy numbers and Ct) devised. Correlation coefficients for all standard curves were ≥ 0.99.

Gene expression assays.

Gene expression was quantified using quantitative reverse transcription-PCR (RT-qPCR) assays. Nucleic acids were extracted using AllPrep DNA/RNA Mini Kits (Qiagen, Valencia, CA) following manufacturer's instructions. After extraction of RNA, DNA was removed using the TURBO DNA-free Kit (Ambion, Austin, TX). The resulting RNA samples were converted to cDNA using M-MLV Reverse Transcriptase and random hexamers (Invitrogen, Carlsbad, CA) following manufacturer's instructions. M-MLV RT was heat inactivated by 15 min at 70°C. qPCR was performed as described above.

Transcripts diagnostics of the host SOS response, phage DNA replication/repair, phage excision/cell lysis and prophage integration were quantified and normalized to the expression of three host reference genes (*alaS*, *map*, and *rpoC*) selected using previously described criteria (Nieto et al 2009). Primers are shown in Table S2.1. (All tables and figures are located in the appendix).

Genome analysis.

Genomic DNA was isolated for both CB-A and CB-D using standard phenol/chloroform extraction procedures (Green 2012) and sequenced with the Illumina HiSeq platform at the Genomic Services Lab (HudsonAlpha Institute for Biotechnology, Huntsville, AL). *Sulfitobacter* sp. strain CB-D was re-sequenced to confirm the original sequence (Ankrah et al 2014b). Genome reads were assembled using CLC Genomics Workbench version 7.5.1 (QIAGEN). Reads were independently mapped to the original CB-D genome sequence (JPOY00000000) using Map Reads to Reference, followed by Local Sequence Realignment. Average read coverage was 278 for CB-D and 292 for CB-A. The Fixed Ploidy Variant Detection tool was used to identify nucleotide differences between assembled genome contigs.

Biofilm assays.

Clear flat-bottomed 96-well polypropylene plates (co-culture experiments) or 5 ml polypropylene tubes (monoculture experiments) were inoculated with 100 µl and 1 ml of

overnight cultures, respectively, grown in SMM (diluted in fresh medium to an OD_{540nm} of 0.15-0.18; ~10^7 CFU/ml) and incubated at 25°C. Relative biofilm formation of strains was quantified using a crystal violet assay and measured at OD_{600nm} using either a DU800 spectrophotometer (Beckman Coulter, Inc., CA) or a fluorescent plate reader (BioTek Instruments Inc, Vermont), as previously described (Cude et al 2015).

Co-culture competition assays.

Overnight monocultures of both lysogens were sub-cultured into fresh medium and grown to mid-log phase (ca. 1.0 x 10^8 CFU/ml). Cells were harvested by gentle centrifugation (5000 x *g* for 10 min), rinsed with fresh media to remove unbound phages and resuspended in fresh media. Lysogens were mixed at a ratio of 1:1 at an OD_{540} of 0.17 (~10^7 CFU/ml) and incubated at 25°C, with shaking, for broth culture competition experiments. After 24 hours, samples were collected for: (i) genomic DNA extraction from bacteria and viruses; (ii) viable counts; and (iii) plaque assays. The relative abundance of each strain was determined using qPCR of genomic DNA isolated from mixed cellular biomass collected by centrifugation, following procedures outlined above. Virus particles were enumerated from cell-free filtrate (0.2 µm) as described above. Samples were first treated with Fermentas DNAse at 5 U/ml for 30 min at 37°C to destroy any free genomic DNA from lysed host cells. DNAase was heat inactivated by incubation of samples at 65°C for 10 min. For qPCR of phages, samples were heated for 10 min at 95°C and 2.5 µl was used as template in 25 µl reactions. Co-culture biofilm experiments were performed in a similar fashion with the following exceptions: 100 µl of 1:1 lysogen mixtures were added to individual wells of a 96-well microtiter dish and incubated at 25°C for 48 hours. qPCR was performed using extracted DNA from microbial biomass. Due to the adherent nature of the biofilm matrix, it was not possible to separate cells from the matrix which contains free phage particles.

Statistical analysis

RT-qPCR data analysis and the normalized relative transcript quantity was calculated using the qBASE method (Hellemans et al 2007). Student's t-tests were used to determine significant difference using GraphPad Prism (GraphPad Software, Inc.).

Nucleotide sequence accession numbers.

The genome sequence for *Sulfitobacter* sp. strain CB-A was deposited in GenBank under the accession number PYUG00000000. Genome sequences for ϕ-A and CB-D (with ϕ-D within) were previously reported as HQ332142 and NC_027299, respectively (Ankrah et al 2014a, Ankrah et al 2014b).

RESULTS

Genome comparisons of temperate ϕ-A and prophage ϕ-D reveal high sequence similarity

Within the genome of *Sulfitobacter* sp. CB-D lies the prophage ϕ-D, which is distinct from, yet highly similar to, ϕ-A, a temperate virus isolated from the same waters as CB-D (Fig 1). Genome-wide nucleotide similarity alignment of ϕ-A and ϕ-D show that they share 79% identity. A CoreGenesUniqueGenes (CGUG) (Mahadevan et al 2009) analysis identified 58 highly homologous genes (BLASTp threshold score, 75) between ϕ-A and ϕ-D. Both phages carry a suite of genes for phage structure, replication/host regulations, host integration/excision, lysis/structure, and share the same DNA Bre-C-like integrase anticipated to facilitate integration into the host genome (Ankrah et al 2014a, Ankrah et al 2014b).

The sequence variation between ϕ-A and ϕ-D is localized to two 4-6 kb regions, which primarily encode genes of unknown function, but also includes putative tail fibers protein genes, expected to be important for binding to host cell surface receptors, and transcriptional regulators that may repress lytic genes during lysogeny. The putative

transcriptional regulators encoded within each phage have low sequence identity to one another: <30% identity at amino acid level for all pairwise alignments. ϕ-D harbors two ORFs (SUFP_003; SUFP_050) that fall within the XRE transcriptional regulator superfamily. Both contain an XRE-family HTH domain but lack the *lexA*/signal peptidase superfamily domain common to characterized phage repressors within this family (Sauer et al. 1982). ϕ-D also harbors an ORF (SUFP_063) with homology to the single stranded DNA binding protein family, with members involved in DNA replication via binding of ssDNA at the primosome assembly site (Hellweger et al. 2016). ϕ-A possesses two ORFs that belong to the XRE-superfamily and lack specific catalytic domains (SUFA_030 and SUFA_031).

A temperate virus causes lytic infection and prophage induction.

Infection of *Sulfitobacter* sp. CB-D with the temperate phage ϕ-A results in prophage induction, production of both phage types and cell lysis. The growth dynamics of *Sulfitobacter* sp. CB-D cultures infected with ϕ-A are indistinguishable from uninfected controls until the onset of cell lysis at ~5 hours post infection (h.p.i.), when significant differences in cultures are observed (Fig 2A). By 10 h.p.i., optical densities in the infected cultures are approximately 40% of the uninfected controls and both phages are produced at unequal abundances (Fig 2). Infection of *Sulfitobacter* sp. CB-A with temperate phage ϕ-D also results in prophage induction, production of both phage types and cell lysis, with an apparent decrease in the latent period (3 hr h.p.i.) relative to CB-D ϕ-A superinfections (Fig 2B). Using qPCR as a proxy for phage abundance, each of the superinfecting phage are present in at least 10-fold higher abundance than the resident prophage 24 h.p.i. (Fig S2.1).

Quantitative RT-PCR of genes diagnostic for the host *Sulfitobacter* sp. strain CB-D, ϕ-D, and ϕ-A provide further evidence that a mixed lytic-lysogenic infection occurs. Expression of host genes indicative of the SOS response, *recA* and *lexA,* as well as select phage genes involved in the presumptive lysogenic-lytic switch (XRE-type repressor [*rep/XRE*]), ϕ-D phage DNA replication and repair (single stranded DNA binding protein

gene [*ssb*]), ϕ-D double stranded DNA break repair gene [*rad52*]) and cell lysis (endolysin [*pepG*]) were monitored at two discrete time points preceding and following measurable culture lysis (3 and 6 h.p.i., respectively) (Fig 3). Consistent with the differences in phage production, the relative increase of ϕ-A gene expression is greater than that observed for prophage (ϕ-D) genes (Fig 3B and 3C). The ϕ-A XRE-type gene (SUAG_00031) is upregulated 66-fold 6 h.p.i. compared to an 8-fold expression increase of the ϕ-D *ssb* gene (SUFP050) at the same time point (Fig 3B and 3C). Similarly, endolysin gene expression (SUAG_00073) of the superinfecting phage ϕ-A is upregulated 2700-fold 6 h.p.i, while ϕ-D endolysin gene expression (SUFP_019) is upregulated 44-fold at the same time point, relative to initial expression levels (Fig 3B and 3C). Collectively, these data suggest both phages are actively employing lysogenic and lytic lifestyles that are likely influenced by the activities of the other.

Lysogenic conversion and generation of Sulfitobacter sp. strain CB-A.

Within the genome of CB-D, the ϕ-D prophage is flanked by a 15 bp GC-rich direct terminal repeat (designated *attB*), within the 3' end of a host tRNA-leu gene (Fig 1A), consistent with the observation that many phages and other genetic elements have high affinity for integration into tRNA genes (Fouts 2006). ϕ-A harbors a single copy of this sequence, designated *attP*. Thus, we hypothesized that this putative attachment site could direct ϕ-A viral DNA to the appropriate integration site in its host, generating a new lysogen. To test this hypothesis, a superinfection experiment was conducted using ϕ-A and *Sulfitobacter* sp. strain CB-D. Four and 8 hours post infection, aliquots of ϕ-A-infected *Sulfitobacter* sp. CB-D cultures were spread onto agar dishes. Fifty randomly selected colonies from each timepoint were then screened by PCR assay using phage-specific primers. Lysogens that were PCR positive for ϕ-A are recovered with relatively high frequency (~10% and ~20% of colonies at 4 and 8 h.p.i., respectively) (Table S2.2). Additionally, this screening method provided evidence of transient polylysogens (PCR positive for both ϕ-A and ϕ-D). These putative polylysogens were not stably maintained, reverting to single-lysogens following 3 or fewer passages on fresh medium.

A representative ϕ-A positive strain, denoted CB-A, was selected for further study. Genome sequence analysis of CB-A revealed the integration of ϕ-A at the *attB* site. The ϕ-D prophage was not present, indicative of a heteroimmune substitution (Fig 1B). Genome comparisons of CB-A and CB-D show that for all contigs to which CB-A Illumina reads mapped to the original CB-D genome, there are no nucleotide differences between these two strains outside of the regions of variation found in the prophages. The genome of CB-D was re-sequenced and shows no difference from the original sequence described in 2014 (Ankrah et al 2014b).

Immunity and differing physiologies of lysogens.

Each of the two lysogens demonstrates homoimmunity: CB-D is immune to infection with ϕ-D and CB-A is immune to infection with ϕ-A. Yet each strain is susceptible to lytic infection by the other phage genotype which is accompanied by induction of the resident prophage (Fig S2.1). In addition, under routine laboratory cultivation conditions the growth phenotypes of each lysogen were noticeably different. This qualitative assessment prompted quantitative phenotypic characterizations of these strains in liquid and surface associated growth modes. In liquid culture, CB-D has a shorter generation time and greater maximum cell density than CB-A (Fig 4A). Doubling times of the CB-D and CB-A lysogens were 75 and 100 min, respectively. In stationary phase, CB-A viable counts are half of CB-D (2.51×10^9 [$\pm 7.00 \times 10^8$] CFU/ml compared to 4.86×10^9 [$\pm 1.48 \times 10^8$] CFU/ml). In contrast, CB-A formed more robust biofilms relative to CB-D (Fig 4B). This bulk measurement is supported by confocal microscopy images of CB-A and CB-D biofilms that show substantial differences in biofilm structure (Fig S2.2). *Sulfitobacter* sp. strain CB-A has an average thickness (biomass) of 5.13um, compared to 3.48um for CB-D. The maximum biomass thickness was also larger for CB-A than CB-D and had a larger range (5.49-13.24um compared to 3.57-5.65um, respectively) (Fig S2.3, Table S2.3).

Titers of free-phage suggest lysogens have different rates of spontaneous prophage induction

Given the discrepancy in growth dynamics of the two strains, we next determined whether there were quantifiable differences in free-phage titers in CB-A and CB-D cultures. CB-A stationary and mid-log phase cultures yielded 1.63 x 10^6 (±2.08x10^6) PFU/ml and 5.2 x 10^5 (±8.5x10^4) PFU/ml respectively. CB-D cultures of the same growth states do not yield quantifiable phage using plaque assays, indicating values below the 45 PFU/ml limit of detection for our assay.

Prophage type determines outcome in head-to-head competition assays

The differences in spontaneous induction coupled with the susceptibility of each lysogen to infection by the opposing viral type, which in turn is accompanied by induction of the resident prophage, prompted us to perform competition experiments with these strains. In head-to-head competition (1:1 initial ratio) in broth culture, the ratio of CB-A to CB-D gene copies were 3.26 (range 2.00-4.73) after 24 hours of co-culture. The co-cultures were ~90% and ~65% lower than typical densities for monocultures of CB-A and CB-D, respectively (Fig 5A). The number of phage particles present in cell free filtrates of these mixed cultures were six to one (ϕ-A:ϕ-D); ϕ-A and ϕ-D gene copies were 6.84 x 10^9 (± 2.18 x 10^9) copies/ml and 1.18 x 10^9 (±0.27 x 10^8) copies/ml, respectively. Head-to-head competition assays on during growth on a surface showed an opposite response: co-culture biofilms had 29% and 55% greater biomass than CB-A and CB-D monoculture biofilms, respectively (Fig 5B). In addition, total ϕ-D gene copies were 3.4 times as high as phage A (range 2.7-3.8; Fig 5B); the biofilm matrix prevented physical separation of cells and unattached viruses, so summed values are presented.

DISCUSSION

Virus-mediated lysis of microbial cells in marine systems leads to quantitatively important impacts on food webs and biogeochemical cycles (Fuhrman 1999). Yet, our understanding of marine host-virus interactions that give rise to host death, or otherwise influence host fitness, are limited. This is particularly true for temperate viruses of heterotrophic marine bacteria. Here, we describe a new marine host-phage system that advances our understanding of the complex interactions found amongst temperate phages and susceptible hosts.

Lysogenized bacteria can exhibit resistance to superinfection (secondary infection) by homologous phages through immunity strategies (reviewed in Weinbauer 2004). ϕ-A and ϕ-D are certainly homologous from a genomic perspective, showing a reasonably high degree of nucleotide identity across the full length of their ~40kb genomes (79%) (Ankrah et al 2014b). Yet, we demonstrate here these lysogens are susceptible to infection by a genetically similar phage. Consistent with the mosaicism commonly observed amongst related phage (Dorscht et al 2009), the genomic differences between ϕ-A and ϕ-D are principally restricted to two 4-6 kb regions that appear to encode transcriptional regulators and tail fibers. Tail fiber adsorption to specific bacterial cell surface receptors forms part of the initial steps of successful phage infection (Randall-Hazelbauer and Schwartz 1973, Wang et al 2000). Thus, differences in the primary sequence of the ϕ-A and ϕ-D tail fiber proteins may indicate distinct cell-surface targets for each of these phages, which have yet to be elucidated. Furthermore, the putative transcriptional regulatory proteins encoded on ϕ-A and ϕ-D map to broad, but distinct, protein families indicating a likelihood for genotypic-phenotypic mismatching leading to the observed symmetrical infection profiles (Mavrich and Hatfull 2019).

Infection of CB-D with ϕ-A leads to the simultaneous production of ϕ-A and ϕ-D, indicative of both a lytic infection and prophage induction. While we do not yet know the proteins that mediate the lysogenic-lytic switch in this system, gene expression assays from infected cell populations support quantitative measurements of phage abundance (i.e. plaque assays). A putative peptidase (*pepG*) encoded by ϕ-A is upregulated during

superinfection. Similarly, upregulation of the CB-D host genes *recA* and *lexA* indicates activation of the global SOS response, which has been shown to mediate the lysogenic to lytic switch in various bacteria (e.g., *Salmonella enterica*, *Escherichia coli* and *Pseudomonas aeruginosa*; reviewed in Butala et al 2008, Campoy et al 2006, Cirz et al 2006). Indeed, superinfection by other phages has been shown to be a biotic factor influencing prophage induction, presumably through induction of the SOS response (Campos et al. 2003; Espeland et al. 2004). In contrast, a ϕ-A putative transcriptional regulator (*xre*-like), is below the limit of detection, perhaps suggesting a role for this gene's product in suppression of phage lytic genes during the lysogenic state. As the ϕ-A and ϕ-D encoded transcriptional regulators lack conserved catalytic domains common to well characterized phage repressors, these proteins may be valuable targets for future studies aimed at deciphering the lysogenic-lytic switch in our *Sulfitobacter*-phage pairs. An aspect of lytic activation of prophages in response to superinfection that has not been explored in our, or other systems, is whether lytic infection and prophage induction occur simultaneously in an individual cell or within distinct subpopulations of cells, one undergoing lytic infection by an exogenous phage and the other undergoing lytic activation of a previously quiescent prophage. It is possible that a subpopulation superinfected with one phage could communicate with non-superinfected counterparts, thus initiating a lytic induction, a phenomenon that has only recently been reported for a *Bacillus* phage (Erez et al 2017).

In addition to a mixed infection resulting in the production of both ϕ-A and ϕ-D viral particles, infection of CB-D with ϕ-A also yields new lysogens in which the prophage appears to have been replaced by the superinfecting phage. The mechanism whereby this presumptive substitution occurs is not yet clear, but several possibilities exist. It could have been achieved through homologous recombination between the phage genomes, an oft-cited mechanism of viral evolution (Bouchard and Moineau 2000, Clark et al 2001, De Paepe et al 2014). Alternatively, eviction of the prophage followed by integration of the ϕ-A genome could have led to the production of CB-A variants. While an intriguing possibility, there is presently little evidence in the literature to suggest such interactions occur amongst phages. A third possibility is that a subpopulation of host cells in our

cultures lack a prophage, freeing the attachment site for integration. Using quantitative PCR across the integration site, we estimate that a small subpopulation (ranging from 0.02-0.08% of *Sulfitobacter* sp. CB-D cultures) lack a prophage at the *attB* site (data not shown). Such individual cells would have increased susceptibility to lysogeny by ϕ-A invasion. Finally, integration of both prophages in tandem could result in the establishment of transient polylysogens. Due to an intrinsic instability arising from the high degree of nucleotide identity between the two phages, such presumed polylysogenic events might be expected to readily revert to a single phage type. Regardless of the apparent replacement mechanism, the relatively high frequency with which new lysogens are recovered from superinfections suggests either genotypic switching is prevalent with this two-phage-one-host system and/or that one host-phage pair (CB-A) displays higher fitness than the other (CB-D) in a given environmental context.

Our data indicate a competitive interaction between the two host-phage pairs that is based on a fundamental difference in the lysogenic-lytic switch between the pairs. One manifestation of these differences is altered frequencies of spontaneous prophage induction (SPI) that influence growth dynamics when the strains are cultivated planktonically and as biofilms. Rates of SPI are anticipated to be the combined result of stochasticity in gene expression (genetic noise) and induction of the SOS response. It has been observed that either a drop in phage repressor protein levels below a given threshold concentration or sporadic expression of integrase genes may initiate the lytic cycle (Broussard et al 2013). Noise is pervasive in gene regulatory networks and can provide selective advantage to populations by increasing phenotypic heterogeneity within individual species and complex microbial communities (reviewed in Nanda et al 2015). Thus, prophages may exploit genetic noise to modulate the frequency of spontaneous activation. In contrast, the apparent instability of the lysogenic state in CB-A may indicate a non-optimal pairing between host and phage. A recent example with nearly genetically identical marine *Bacteriodetes* strains reveals variation in infection efficiency across strains challenged with the same phage (Howard-Varona et al 2017). Regardless of the underlying mechanism(s) that give rise to the observed variation SPI in these two lysogens, this variation directly influences interactions amongst them.

Until recently, SPI was considered detrimental as some fraction of the cells is continuously lost by phage-induced cell lysis. However, benefits of SPI on bacterial fitness are now recognized, and include the release of extracellular DNA, which facilitates and enhances biofilm formation (Carrolo et al 2010, Nanda et al 2015), consistent with our findings. It has also been suggested that SPI dictates the maintenance and propagation of lysogeny in *Salmonella enterica*, which is important for the evolution and diversity of host populations (Bossi et al 2003). Relevant to this study, is the notion that lysogens may use SPI as a form of weaponry against susceptible cell types. *Salmonella enterica* studies demonstrate selective eradication of non-immune hosts in mixed populations as a means of a competing strategy by Gifsy 2 lysogenized strains (Bossi et al 2003). Rat model competition studies show that *Pseudomonas aeruginosa* strains lysogenized by Liverpool Epidemic Strain (LES) prophages use the phages as anti-competitor weapons against phage-susceptible bacterial populations in chronic lung infection murine model (Davies et al 2016). Studies using *E. coli* MG1655 lysogenized with λ reveal the competitive nature of this type of inaction is anticipated to be time-limited, as lysogenization of susceptible hosts ultimately diminishes non-lysogenized "competitors" (Gama et al 2013). Finally, in a more complicated scenario involving members of the microbiome of the fresh water metazoan, *Hydra vulgaris*, one microbiome member, a *Curvibacter* species, possesses an inducible prophage that lytically infects another microbome member, a *Duganella* strain. Mathematical modeling predicts this interaction may modulate competition amongst microbiome members (Li et al 2017).

Our system provides a new element to this type of interaction: the reciprocal attack by genetically similar, but hetero-susceptible phages that share an integration site in their shared host. Head-to-head competition experiments between CB-A and CB-D indicate different fates depending upon mode of bacterial growth: planktonic or biofilm, two modes in which Roseobacters, in general, and *Sulfitobacters*, in particular, thrive in nature (Buchan et al 2014). The maintenance of both phage types within the population may be advantageous to the bacterium over multiple generations and across marine landscapes. In this way, we might consider these discrete populations as analogous to populations that undergo phase variation. Phase variation has been described as an interchange between

"states", and is exemplified by the antigenic components, H1 and H2, in motile and non-motile strains of *Salmonella enterica* (formerly known as *Salmonella cholerae-suis*) (Lederberg and Iino 1956). We can consider the generation of *Sulfitobacter* sp. strain CB-A a modulated form of *Sulfitobacter* sp. strain CB-D, which exhibits different physiology in their shared host.

To better reflect the consequence of physiological differences in a natural marine environment, we conducted direct competition assays to probe fitness consequences of lysogenization of the same host by one of two genetically similar phage. We demonstrate that in liquid culture, co-cultures exhibit significantly lower cell densities than monocultures and that the CB-A host-phage pair dominates over the CB-D pair. The opposite outcome is seen in co-culture biofilms. Thus, in instances where the 'swim' phenotype may be more prevalent, ϕ-A may offer a greater competitive advantage to its host. Alternatively, in cases of cell surface adhesion ('stick' phenotype), the resident prophage (ϕ-D) may offer competitive advantage. These data support the hypothesis that the phage-influenced physiological state of the cell can dictate competitive advantage in a shared host. Some studies have indicated that cryptic prophages offer their hosts advantages for coping with adverse conditions (Wang et al 2010). In hosts with established Shiga toxin-producing *E. coli* (STEC) populations, SPI increases bacterial population fitness through priming effects, thus influencing biofilm formation and pathogen virulence (reviewed in Nanda et al 2015). We propose that SPI of CB-A acts as a highly specialized weapon against susceptible CB-D, which in turn causes new prophage induction and the production of ϕ-D. Newly generated ϕ-D can in turn counter attack CB-A, causing a chain reaction of inductions which may ultimately result in some community level equilibrium, that could vary based on environmental conditions and selective pressures experienced by the community.

Lysogeny is widespread in nature and has recently received considerable attention in the context of marine systems where focus has been on elucidation of the environmental factors that drive temperate phage into either a lytic or lysogenic state (e.g., Knowles et al 2016, Weitz et al 2017). Our work reveals the importance of intrinsic factors in influencing host-phage interactions and highlights the value of considering states that lie between the

bilateral viewpoint of wholesale lysogeny or rampant lysis within a population. Characterization of a two-phage-one-host model system reveals new mechanisms of microbial competition and cooperation in which host-phage pairs form coalitions to challenge one another. The outcomes of these "challenges" are context dependent leading to niche specific quasi-state equilibria. The extent to which these cooperative behaviors are influenced by other environmental factors (e.g., nutrients, temperature) and modulate community composition remains to be determined. Another open question is the prevalence of these types of host-phage interactions in marine systems. Given the extent of genetic microheterogenity present in both marine microbial and viral communities, we might predict these types of coalitions represent an important, but previously overlooked component of host-phage interactions in the seas.

ACKNOWLEDGEMENTS

The authors wish to thank Mary Hadden and Yi Ting Jiang for the generation of *Sulfitobacter* sp. strain CB-A. We also thank Mary Hadden for qPCR expertise. We are indebted to Dr. John Dunlap for confocal microscopy expertise. This research was supported by the NSF Biological Oceanography program (OCE OCE#1737237) to AB.

REFERENCES

Ankrah NYD, Budinoff CR, Wilson WH, Wilhelm SW, Buchan A (2014a). Genome Sequences of Two Temperate Phages, ΦCB2047-A and ΦCB2047-C, Infecting Sulfitobacter sp. Strain 2047. *Genome Announcements* **2**.

Ankrah NYD, Lane T, Budinoff CR, Hadden MK, Buchan A (2014b). Draft Genome Sequence of Sulfitobacter sp. CB2047, a Member of the Roseobacter Clade of Marine Bacteria, Isolated from an Emiliania huxleyi Bloom. *Genome Announcements* **2**.

Ankrah NYD (2015). Elucidating the Impact of Roseophage on Roseobacter Metabolism and Marine Nutrient Cycles.

Billerbeck S, Wemheuer B, Voget S, Poehlein A, Giebel HA, Brinkhoff T *et al* (2016). Biogeography and environmental genomics of the Roseobacter-affiliated pelagic CHAB-I-5 lineage. *Nature Microbiology* **1**.

Bondy-Denomy J, Davidson AR (2014). When a Virus is not a Parasite: The Beneficial Effects of Prophages on Bacterial Fitness. *Journal of Microbiology* **52:** 235-242.

Bossi L, Fuentes JA, Mora G, Figueroa-Bossi N (2003). Prophage contribution to bacterial population dynamics. *Journal of Bacteriology* **185:** 6467-6471.

Bouchard JD, Moineau S (2000). Homologous recombination between a lactococcal bacteriophage and the chromosome of its host strain. *Virology* **270:** 65-75.

Broussard GW, Oldfield LM, Villanueva VM, Lunt BL, Shine EE, Hatfull GF (2013). Integration-Dependent Bacteriophage Immunity Provides Insights into the Evolution of Genetic Switches. *Molecular Cell* **49:** 237-248.

Brum JR, Hurwitz BL, Schofield O, Ducklow HW, Sullivan MB (2016). Seasonal time bombs: dominant temperate viruses affect Southern Ocean microbial dynamics. *Isme Journal* **10:** 437-449.

Brussow H, Canchaya C, Hardt WD (2004). Phages and the evolution of bacterial pathogens: From genomic rearrangements to lysogenic conversion. *Microbiology and Molecular Biology Reviews* **68:** 560-+.

Buchan A, Gonzalez JM, Moran MA (2005). Overview of the marine Roseobacter lineage. *Applied and Environmental Microbiology* **71:** 5665-5677.

Buchan A, LeCleir GR, Gulvik CA, Gonzalez JM (2014). Master recyclers: features and functions of bacteria associated with phytoplankton blooms. *Nature Reviews Microbiology* **12:** 686-698.

Budinoff CR, Hollibaugh JT (2007). Ecophysiology of a mono lake picocyanobacterium. *Limnology and Oceanography* **52:** 2484-2495.

Butala M, Žgur-Bertok D, Busby SJW (2008). The bacterial LexA transcriptional repressor. *Cellular and Molecular Life Sciences* **66:** 82.

Campoy S, Hervàs A, Busquets N, Erill I, Teixidó L, Barbé J (2006). Induction of the SOS response by bacteriophage lytic development in Salmonella enterica. *Virology* **351:** 360-367.

Canchaya C, Fournous G, Chibani-Chennoufi S, Dillmann ML, Brussow H (2003). Phage as agents of lateral gene transfer. *Current Opinion in Microbiology* **6:** 417-424.

Carrolo M, Frias MJ, Pinto FR, Melo-Cristino J, Ramirez M (2010). Prophage Spontaneous Activation Promotes DNA Release Enhancing Biofilm Formation in Streptococcus pneumoniae. *Plos One* **5**.

Chen F, Wang K, Stewart J, Belas R (2006). Induction of multiple prophages from a marine bacterium: a genomic approach. *Applied and Environmental Microbiology* **72:** 4995-5001.

Cirz RT, O'Neill BM, Hammond JA, Head SR, Romesberg FE (2006). Defining the Pseudomonas aeruginosa SOS Response and Its Role in the Global Response to the Antibiotic Ciprofloxacin. *Journal of Bacteriology* **188:** 7101-7110.

Clark AJ, Inwood W, Cloutier T, Dhillon TS (2001). Nucleotide sequence of coliphage HK620 and the evolution of lambdoid phages1 1Edited by M. Gottesman. *Journal of Molecular Biology* **311:** 657-679.

Cude WN, Prevatte CW, Hadden MK, May AL, Smith RT, Swain CL *et al* (2015). Phaeobacter sp Strain Y4I Utilizes Two Separate Cell-to-Cell Communication Systems To Regulate Production of the Antimicrobial Indigoidine. *Applied and Environmental Microbiology* **81:** 1417-1425.

Davies EV, James CE, Kukavica-Ibrulj I, Levesque RC, Brockhurst MA, Winstanley C (2016). Temperate phages enhance pathogen fitness in chronic lung infection. *Isme Journal* **10:** 2553-2555.

De Paepe M, Hutinet G, Son O, Amarir-Bouhram J, Schbath S, Petit M-A (2014). Temperate phages acquire DNA from defective prophages by relaxed homologous recombination: the role of Rad52-like recombinases. *PLoS Genet* **10:** e1004181-e1004181.

Dorscht J, Klumpp J, Bielmann R, Schmelcher M, Born Y, Zimmer M *et al* (2009). Comparative Genome Analysis of Listeria Bacteriophages Reveals Extensive Mosaicism, Programmed Translational Frameshifting, and a Novel Prophage Insertion Site. *Journal of Bacteriology* **191:** 7206.

Duhaime MB, Deng L, Poulos BT, Sullivan MB (2012). Towards quantitative metagenomics of wild viruses and other ultra-low concentration DNA samples: a rigorous assessment and optimization of the linker amplification method. *Environmental Microbiology* **14:** 2526-2537.

Erez Z, Steinberger-Levy I, Shamir M, Doron S, Stokar-Avihail A, Peleg Y *et al* (2017). Communication between viruses guides lysis-lysogeny decisions. *Nature* **541:** 488-493.

Feiner R, Argov T, Rabinovich L, Sigal N, Borovok I, Herskovits AA (2015). A new perspective on lysogeny: prophages as active regulatory switches of bacteria. *Nature Reviews Microbiology* **13:** 641-650.

Fortier LC, Sekulovic O (2013). Importance of prophages to evolution and virulence of bacterial pathogens. *Virulence* **4:** 354-365.

Fouts DE (2006). Phage_Finder: Automated identification and classification of prophage regions in complete bacterial genome sequences. *Nucleic Acids Research* **34:** 5839-5851.

Fuhrman JA (1999). Marine viruses and their biogeochemical and ecological effects. *Nature* **399:** 541-548.

Gama JA, Reis AM, Domingues I, Mendes-Soares H, Matos AM, Dionisio F (2013). Temperate Bacterial Viruses as Double-Edged Swords in Bacterial Warfare. *Plos One* **8**.

Giovannoni S, Temperton B, Zhao YL (2013). SAR11 viruses and defensive host strains reply. *Nature* **499:** E4-E5.

Green MR (2012). Molecular cloning : a laboratory manual. In: Sambrook J (ed), 4th ed.. edn. Cold Spring Harbor, N.Y. : Cold Spring Harbor Laboratory Press: Cold Spring Harbor, N.Y.

Harrison E, Brockhurst MA (2017). Ecological and Evolutionary Benefits of Temperate Phage: What Does or Doesn't Kill You Makes You Stronger. *BioEssays* **39:** 1700112.

Helfrich S, Pfeifer E, Kramer C, Sachs CC, Wiechert W, Kohlheyer D *et al* (2015). Live cell imaging of SOS and prophage dynamics in isogenic bacterial populations. *Molecular Microbiology* **98:** 636-650.

Hellemans J, Mortier G, De Paepe A, Speleman F, Vandesompele J (2007). qBase relative quantification framework and software for management and automated analysis of real-time quantitative PCR data. *Genome Biology* **8:** R19.

Howard-Varona C, Roux S, Dore H, Solonenko NE, Holmfeldt K, Markillie LM *et al* (2017). Regulation of infection efficiency in a globally abundant marine Bacteriodetes virus. *The ISME Journal* **11:** 284-295.

Hurwitz BL, Westveld AH, Brum JR, Sullivan MB (2014). Modeling ecological drivers in marine viral communities using comparative metagenomics and network analyses. *Proceedings of the National Academy of Sciences of the United States of America* **111:** 10714-10719.

Jiang SC, Paul JH (1998). Significance of lysogeny in the marine environment: Studies with isolates and a model of lysogenic phage production. *Microbial Ecology* **35:** 235-243.

Kamenšek S, Podlesek Z, Gillor O, Zgur-Bertok D (2010). Genes regulated by the Escherichia coli SOS repressor LexA exhibit heterogeneous expression. *BMC Microbiol* **10:** 283-283.

Knowles B, Silveira CB, Bailey BA, Barott K, Cantu VA, Cobian-Guemes AG *et al* (2016). Lytic to temperate switching of viral communities. *Nature* **531:** 466-+.

Kropinski AM, Mazzocco A, Waddell TE, Lingohr E, Johnson RP (2009). Enumeration of Bacteriophages by Double Agar Overlay Plaque Assay. In: Clokie MRJ, Kropinski AM (eds). *Bacteriophages: Methods and Protocols, Volume 1: Isolation, Characterization, and Interactions*. Humana Press: Totowa, NJ. pp 69-76.

Lederberg J, Iino T (1956). Phase Variation in Salmonella. *Genetics* **41:** 743-757.

Leitet C, Riemann L, Hagstrom A (2006). Plasmids and prophages in Baltic Sea bacterioplankton isolates. *Journal of the Marine Biological Association of the United Kingdom* **86:** 567-575.

Li XY, Lachnit T, Fraune S, Bosch TCG, Traulsen A, Sieber M (2017). Temperate phages as self-replicating weapons in bacterial competition. *Journal of the Royal Society Interface* **14**.

Luo E, Aylward FO, Mende DR, DeLong EF (2017). Bacteriophage Distributions and Temporal Variability in the Ocean's Interior. *Mbio* **8**.

Mahadevan P, King JF, Seto D (2009). CGUG: in silico proteome and genome parsing tool for the determination of "core" and unique genes in the analysis of genomes up to ca. 1.9 Mb. *BMC Research Notes* **2:** 168-168.

Mavrich TN, Hatfull GF (2019). Evolution of Superinfection Immunity in Cluster A Mycobacteriophages. *mBio* **10:** e00971-00919.

Nanda AM, Heyer A, Krämer C, Grünberger A, Kohlheyer D, Frunzke J (2014). Analysis of SOS-Induced Spontaneous Prophage Induction in Corynebacterium glutamicum at the Single-Cell Level. *Journal of Bacteriology* **196:** 180.

Nanda AM, Thormann K, Frunzke J (2015). Impact of Spontaneous Prophage Induction on the Fitness of Bacterial Populations and Host-Microbe Interactions. *Journal of Bacteriology* **197:** 410-419.

Nieto PA, Covarrubias PC, Jedlicki E, Holmes DS, Quatrini R (2009). Selection and evaluation of reference genes for improved interrogation of microbial transcriptomes: case study with the extremophile Acidithiobacillus ferrooxidans. *BMC Molecular Biology* **10:** 63-63.

Paul JH (2008). Prophages in marine bacteria: dangerous molecular time bombs or the key to survival in the seas? *Isme Journal* **2:** 579-589.

Payet JP, Suttle CA (2013). To kill or not to kill: The balance between lytic and lysogenic viral infection is driven by trophic status. *Limnology and Oceanography* **58:** 465-474.

Pennington JM, Rosenberg SM (2007). Spontaneous DNA breakage in single living Escherichia coli cells. *Nat Genet* **39:** 797-802.

Randall-Hazelbauer L, Schwartz M (1973). Isolation of the bacteriophage lambda receptor from Escherichia coli. *Journal of bacteriology* **116:** 1436-1446.

Simmons LA, Goranov AI, Kobayashi H, Davies BW, Yuan DS, Grossman AD *et al* (2009). Comparison of Responses to Double-Strand Breaks Double-Strand Breaks between Escherichia coli and Bacillus subtilis Reveals Different Requirements for SOS Inductions. *Journal of Bacteriology* **191:** 1152.

Slightom RN, Buchan A (2009). Surface Colonization by Marine Roseobacters: Integrating Genotype and Phenotype. *Applied and Environmental Microbiology* **75:** 6027-6037.

Stopar D, Cerne A, Zigman M, Poljsak-Prijatelj M, Turk V (2004). Viral abundance and a high proportion of lysogens suggest that viruses are important members of the microbial community in the Gulf of Trieste. *Microbial Ecology* **47:** 1-8.

Thingstad TF, Lignell R (1997). Theoretical models for the control of bacterial growth rate, abundance, diversity and carbon demand. *Aquatic Microbial Ecology* **13:** 19-27.

Touchon M, Bernheim A, Rocha EPC (2016). Genetic and life-history traits associated with the distribution of prophages in bacteria. *Isme Journal* **10:** 2744-2754.

Wang J, Hofnung M, Charbit A (2000). The C-Terminal Portion of the Tail Fiber Protein of Bacteriophage Lambda Is Responsible for Binding to LamB, Its Receptor at the Surface of Escherichia coli K-12. *Journal of Bacteriology* **182:** 508.

Wang XX, Kim Y, Ma Q, Hong SH, Pokusaeva K, Sturino JM *et al* (2010). Cryptic prophages help bacteria cope with adverse environments. *Nature Communications* **1**.

Weinbauer MG, Suttle CA (1999). Lysogeny and prophage induction in coastal and offshore bacterial communities. *Aquatic Microbial Ecology* **18:** 217-225.

Weinbauer MG (2004). Ecology of prokaryotic viruses. *Fems Microbiology Reviews* **28:** 127-181.

Weitz JS, Beckett SJ, Brum JR, Cael BB, Dushoff J (2017). Lysis, lysogeny and virus-microbe ratios. *Nature* **549:** E1-E3.

Williamson SJ, Houchin LA, McDaniel L, Paul JH (2002). Seasonal variation in lysogeny as depicted by prophage induction in Tampa Bay, Florida. *Applied and Environmental Microbiology* **68:** 4307-4314.

Zhao YL, Wang K, Ackermann HW, Halden RU, Jiao NZ, Chen F (2010). Searching for a "Hidden" Prophage in a Marine Bacterium. *Applied and Environmental Microbiology* **76:** 589-595.

APPENDIX

Table legend.

Table S2.1. Oligonucleotides used in this study.

Table S2.2. Frequency (percentage) of ϕ-A PCR positive colonies from superinfection studies (MOI 0.06).

Table S2.3. Comstat2 analysis shown by Z stack data for *Sulfitobacter* sp. strains CB-D and CB-A. Analysis was conducted for biomass ($\mu m^3/\mu m^2$), maximum thickness (μm), roughness Coefficient (Ra*), average thickness (Entire area) (μm), and Average thickness (Biomass) (μm).

Table S2.1. Oligonucleotides used in this study.

Primer name	Primer sequence (5'-3')	Gene target	Purpose/experiment
alaS_577for	GGAGAGAGTGACGCATGGAT	alanine tRNA hydrolase	Host reference gene
alaS_719rev	CAGCTGTCGAGATGGACGTA	alanine tRNA hydrolase	Host reference gene
map_164for	TCACGCAGATGATCGAAGAC	methionine aminopeptidase	Host reference gene
map_334rev	CATCGACAATTACGGTGACG	methionine aminopeptidase	Host reference gene
rpoC_3196for	AAAAAGTCCGTCGTGGTGAC	RNA polymerase	Host reference gene
rpoC_3356rev	AACGGCATGTCTTCCATAGG	RNA polymerase	Host reference gene
2047LexA_for	ACTCGATCTGCTGGCCTTTA	*lexA* transcriptional regulator	Host SOS response
2047LexA_rev	TCGGGCAGTTTCACTACCTC	*lexA* transcriptional regulator	Host SOS response
2047RecA_for	CTGATTTCCCAGCCTGACAC	recombinase *recA*	Host SOS response
2047RecA_rev	AGCCTGTCAGCTTACGCATT	recombinase *recA*	Host SOS response
Pro PEPG_for	CTATGAAGGCATGGGCGATA	endolysin	ϕ-NYA Induction
Pro PEPG_rev	GGCGATCGATCCAACACT	endolysin	ϕ-NYA Induction
Pro Rad_for	TGGCCCTCTACGACAAAGAC	Rad52/22 dsDNA break repair	ϕ-NYA Induction
Pro Rad_rev	TCGTTTAGTTCGTGCTGCAT	Rad52/22 dsDNA break repair	ϕ-NYA Induction
Pro SSB_for	GCCTTGGAACGTCAATTCAT	ssDNA binding protein (*ssb*)	ϕ-NYA Induction
Pro SSB_rev	ACAACGGCAAGGACAAGAAC	ssDNA binding protein (*ssb*)	ϕ-NYA Induction
Pro rep_rev	CCGTGCCATTATTTGGCTAT	phage repressor	ϕ-NYA Induction
Pro rep_rev	GCTAATGTGCTGGGCCTTAG	phage repressor	ϕ-NYA Induction
int772_for	TGGGTCATTCTAACGCTGGT	integrase	Phage lysogeny establishment
int937_rev	ATTCCACAATCTCAAGCGCC	integrase	Phage lysogeny establishment
47AHTH_XRE_for	CAAAAGCTGACGCAGACTCA	phage repressor	ϕ-47A lysogeny establishment
47AHTH_XRE_rev	ATATCCCGCATCAGCTCAAC	phage repressor	ϕ-47A lysogeny establishment
47A PEPG_for	GTGTTTGCATAATCGGCAAG	endolysin	ϕ-47A replication
47A PEPG_rev	CGGATCTGGAAAACCAGCTT	endolysin	ϕ-47A replication
2047PP1_for	TATTCATAGCGAGGCGCAGT	endolysin	ϕ-NYA enumeration
2047PP1_rev	ATACCTGCCCAACGTCACAG	endolysin	ϕ-NYA enumeration

Table # S2.1 continued

Primer name	Primer sequence (5'-3')	Gene target	Purpose/experiment
2047A-C_for	CCCATGTGTATGTCGCCTCT	endolysin	ϕ-47A enumeration
2047A-C_rev	CAGCGTTGAAAAAGGCTCTG	endolysin	ϕ-47A enumeration
jxn761U_for	GGCCAGCATAACCGTTTCC	histidine kinase	Phage Integration site identification
int937_rev	ATTCCACAATCTCAAGCGCC	integrase	Phage Integration site identification
jxn1105D_rev	TGTCGCCAACACCTCTACC	HTH transcriptional regulator	Phage Integration site identification
jxn1105D_for	GGGAGGCATGAGCGTAGAA	hypothetical protein	Phage Integration site identification

Table S2.2. Frequency (percentage) of ϕ-A PCR positive colonies from superinfection studies (MOI 0.06).

Time (h.p.i.)	Replicate 1	Replicate 2	Replicate 3	Average
4	0	5	20	8
8	15	10	30	18

Table S2.3. Comstat2 analysis shown by Z stack data for *Sulfitobacter* sp. strains CB-D and CB-A. Analysis was conducted for biomass ($\mu m^3/\mu m^2$), maximum thickness (µm), roughness Coefficient (Ra*), average thickness (Entire area) (µm), and Average thickness (Biomass) (µm).

	Biomass	**Maximum thickness**	**Roughness coefficient**	**Thickness distribution**	
Organism name and Z stack field of view number	**Biomass ($\mu m^3/\mu m^2$):**	**Maximum thickness (µm):**	**Roughness Coefficient (Ra*):**	**Average thickness (Entire area) (µm):**	**Average thickness (Biomass) (µm):**
Sulfitobacter sp. strain CB-A. Z stack field of view: 1	1.18876	5.4879	1.00278	2.46208	4.91842
Sulfitobacter sp. strain CB-A. Z stack field of view: 2	1.46763	6.1336	1.00804	2.03385	3.78813
Sulfitobacter sp. strain CB-A. Z stack field of view: 3	1.71986	5.4879	0.7344	3.01986	4.72083
Sulfitobacter sp. strain CB-A. Z stack field of view: 4	0.11164	13.2356	1.90794	0.32584	7.07645
Sulfitobacter sp. strain CB-D. Z stack field of view: 1	0.53438	3.5706	1.28152	0.63001	1.73872
Sulfitobacter sp. strain CB-D. Z stack field of view: 2	0.32996	5.6534	1.73059	0.60152	4.44958
Sulfitobacter sp. strain CB-D. Z stack field of view: 3	0.53916	5.6534	1.36748	0.74707	2.34794
Sulfitobacter sp. strain CB-D. Z stack field of view: 4	0.22374	5.6534	1.73358	0.66207	4.95401
Sulfitobacter sp. strain CB-D. Z stack field of view: 5	2.31132	5.6534	0.22504	4.5969	4.82112
Sulfitobacter sp. strain CB-D. Z stack field of view: 6	0.34321	5.6534	1.56043	0.39356	1.78002
Sulfitobacter sp. strain CB-D. Z stack field of view: 7	0.14941	5.6534	1.85548	0.29573	4.09248
Sulfitobacter sp. strain CB-D. Z stack field of view: 8	0.32476	5.6534	1.68187	0.73548	4.58514
Sulfitobacter sp. strain CB-D. Z stack field of view: 9	0.31593	5.6534	1.62062	0.47826	2.51737

Figure legend.

Fig 2.1. Overview of roseophage-host system. (A) Potential outcomes of superinfection of *Sulfitobacter* sp. strain CB-D with ϕ-A viral particles. (B) Alignment of ϕ-A genome and ϕ-D prophage within CB-D genome. Plots shown in purple indicate regions of identity between phages at the nucleotide level. ϕ-D is flanked by a 15bp GC-rich direct terminal repeat (*attB*), within the 3' end of a host tRNA-Leu gene. ϕ-A harbors a single copy of this sequence (termed *attP*). (C) Growth dynamics of CB-D superinfected with ϕ-A (open squares), compared to uninfected controls (closed squares). Averages of biological triplicates are reported. Error bars denote standard deviations and are obscured by the data markers in some instances.

Fig 2.2. CB-D and CB-A susceptibility tests ϕ-D and ϕ-A. (A) CB-D growth dynamics of cultures superinfected with ϕ-A (open circles), ϕ-D (open triangles), and uninfected controls (closed squares). (B) CB-A growth dynamics of cultures superinfected with ϕ-D (open triangles), ϕ-A (open circles), and uninfected controls (closed squares). (C) Phage abundance (as estimated by gene copies/ml culture) during superinfection of CB-D with ϕ-A shown in (A), of ϕ-A gene copies (closed diamonds) and ϕ-D gene copies (closed inverted triangles). Averages of biological triplicates are reported for all treatments. Error bars denote standard deviations and are obscured by the data markers in some instances.

Fig 2.3. Relative gene expression of host and phage gene transcripts 3- and 6-hours post-infection, relative to uninfected controls. (A) Fold change of host SOS response genes (*recA* and *lexA*). (B) Fold change of ϕ-A genes, peptidase (*pepG*) and XRE-like transcriptional regulator (*xre*). (C) Fold change of prophage (ϕ-D) genes, peptidase (*pepG*), ssDNA break repair protein (*rad52*), and DNA replication and repair protein (*ssb*). Significant differences (Student's T-tests) are denoted by asterisks (* = $p<0.05$; ** = $p<0.01$; *** = $p<0.001$; n.s. = not significant). Averages of biological triplicates are reported for all treatments and error bars denote standard deviations.

Fig 2.4. Physiological characteristics of CB-D and CB-A during different modes of growth. (A) Growth dynamics of CB-D (light grey) and CB-A (dark grey) liquid cultures grown in standard marine medium. (B) 24-hour biofilm formation as determined by crystal violet assay. Asterisks denote significant differences as determined by Student's T-tests (* = p <0.05). Averages of biological and technical triplicates are reported for all treatments. Error bars denote standard deviation and are obscured by the data markers in some instances.

Fig 2.5. Head-to-head competition in liquid cultures and biofilms. (A) Final (24-hour) culture densities of liquid CB-A monocultures (dark grey), CB-D monocultures (light grey), and co-cultures (black) grown in standard marine medium. Horizontal bar graphs depict ratios of CB-D:CB-A and ϕ-A:ϕ-D in liquid culture as determined by qPCR. (B) Final 24-hour crystal violet biofilm assays for CB-A monocultures (light grey), CB-D monocultures (dark grey), and co-cultures (black) grown as biofilms. qPCR was used to quantify total number of gene copies of CB-D (+ϕ-D):CB-A (ϕ-A), as represented in horizontal bar graph. Significant differences (Student's T-tests) are denoted by asterisks (* = p<0.05; ** = p<0.01; *** = p<0.001; **** = p<0.0001; n.s. = not significant). Averages of biological triplicates are reported for all treatments and error bars denote standard deviations.

Fig S2.1. Quantification of each phage during homo- and heteroimmunity tests. (A) ϕ-A and (B) ϕ-D gene copies during infection of *Sulfitobacter* sp. strain CB-D. (C) ϕ-A and (D) ϕ-D gene copies during infection of *Sulfitobacter* sp. strain CB-A. Averages of biological triplicates are reported for all treatments. Error bars represent the standard deviation of the mean. Different letters denote columns with significantly different (p<0.05) phage gene copy numbers within a given plot.

Fig S2.2. 3D analysis of (A) CB-D and (B) CB-A biofilms. Overnight cultures of each strain were sub-cultured, diluted, and grown to early exponential phase (OD_{540nm} = 0.17). 3 ml of each strain was added to FlouroDish glass dishes (World Precision

Instruments, Inc.) and incubated without agitation overnight at room temperature. Planktonic bacteria were removed by gentle inversion of the glass dishes and washed twice with standard marine media (SMM). Dishes were left to dry for 15 min, then stained with 3 ml 25X SYBR Gold (ThermoFisher Scientific SYBR™ Gold Nucleic Acid Gel Stain) for 30 min. Images were generated using confocal laser microscopy and visualized using a Leica SP8 white light Laser Confocal System. Biofilm reconstruction was performed with the Leica Application Suite X (Las X) software. Confocal microscopy methods were greatly adapted from previously described literature (Townsley and Yildiz 2015) and data were analyzed using Comstat2 (Heydorn et al 2000, Vorregaard 2008). *Sulfitobacter* sp. strains were grown in triplicates and at least three images were generated per sample.

Fig S2.3. Comstat2 analysis of CB-D and CB-A biofilm confocal microscopy data. Biofilm (A) biomass, (B) average thickness, (C) Comstat max thickness, (D) roughness coefficient, and (E) average thickness. Each data point represents a separate Z stack field of view of the FlouroDish. All parameters showed no significant difference (Student's t-tests; $p<0.05$).

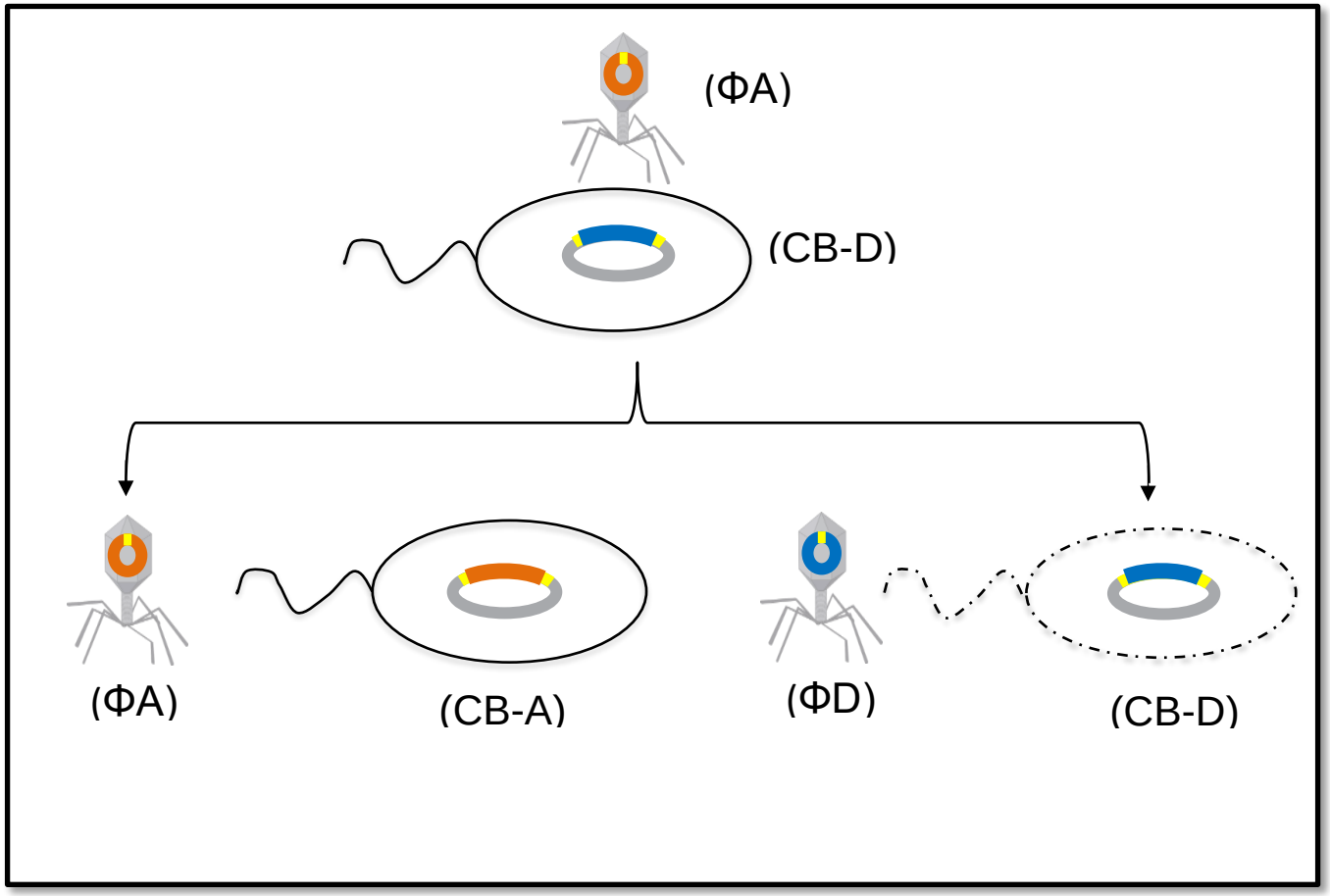

Fig 2.1A. Overview of roseophage-host system. Potential outcomes of superinfection of *Sulfitobacter* sp. strain CB-D with ϕ-A viral particles

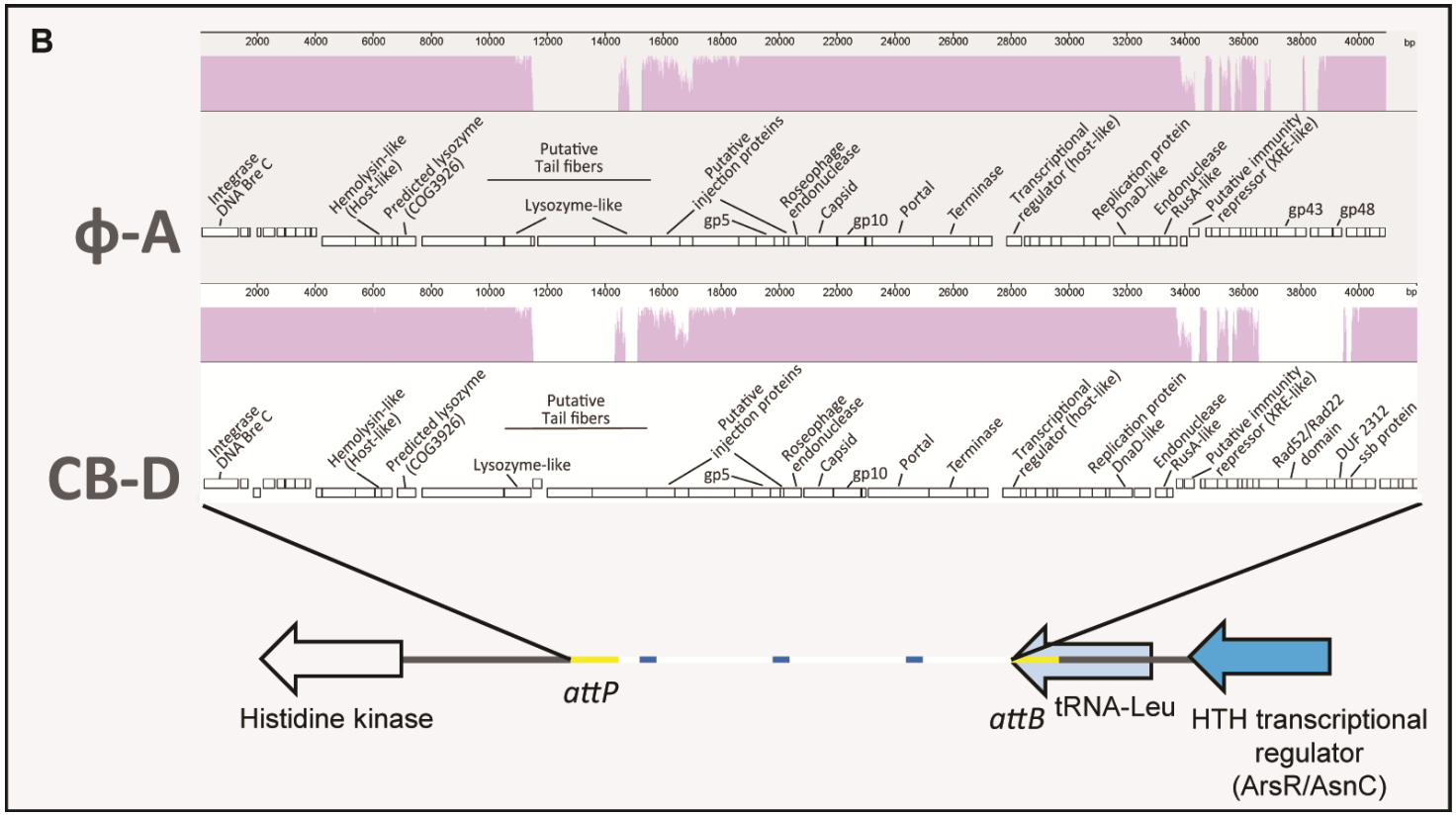

Fig 2.1B. Overview of roseophage-host system. Alignment of ϕ-A genome and ϕ-D prophage within CB-D genome. Plots shown in purple indicate regions of identity between phages at the nucleotide level. ϕ-D is flanked by a 15bp GC-rich direct terminal repeat (*attB*), within the 3' end of a host tRNA-Leu gene. ϕ-A harbors a single copy of this sequence (termed *attP*).

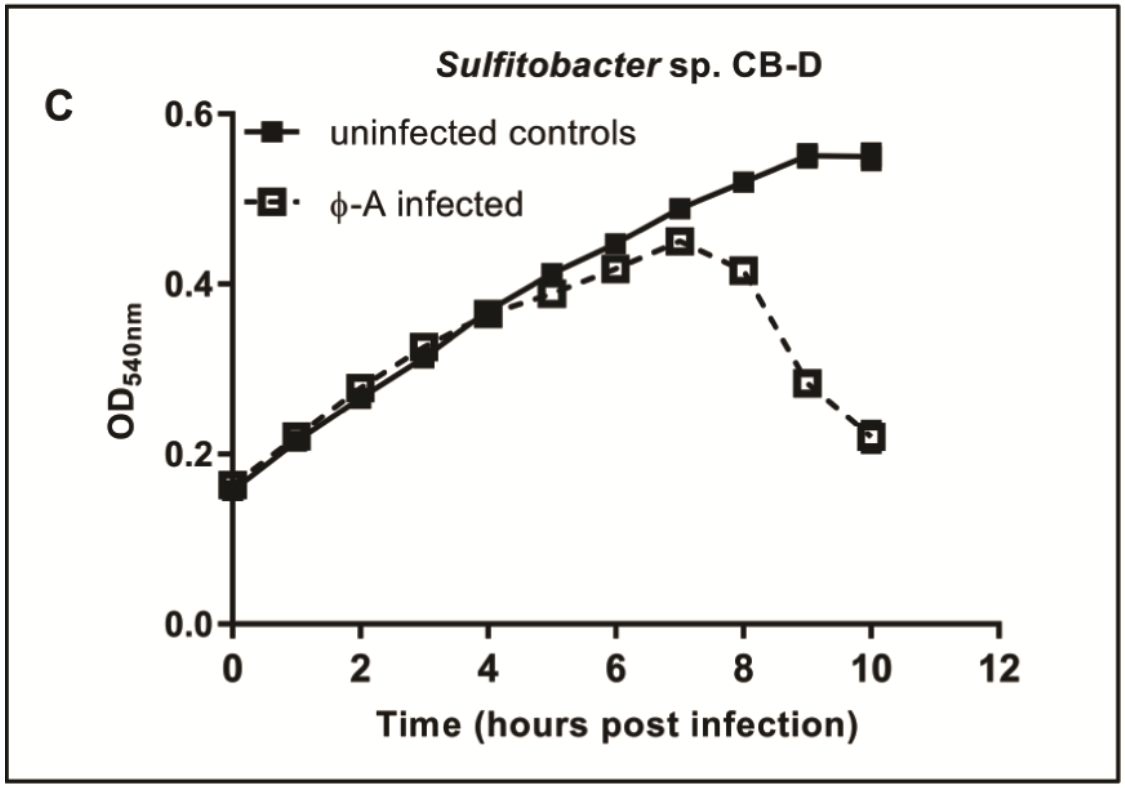

Fig 2.1C. Overview of roseophage-host system. Growth dynamics of CB-D superinfected with ϕ-A (open squares), compared to uninfected controls (closed squares). Averages of biological triplicates are reported. Error bars denote standard deviations and are obscured by the data markers in some instances.

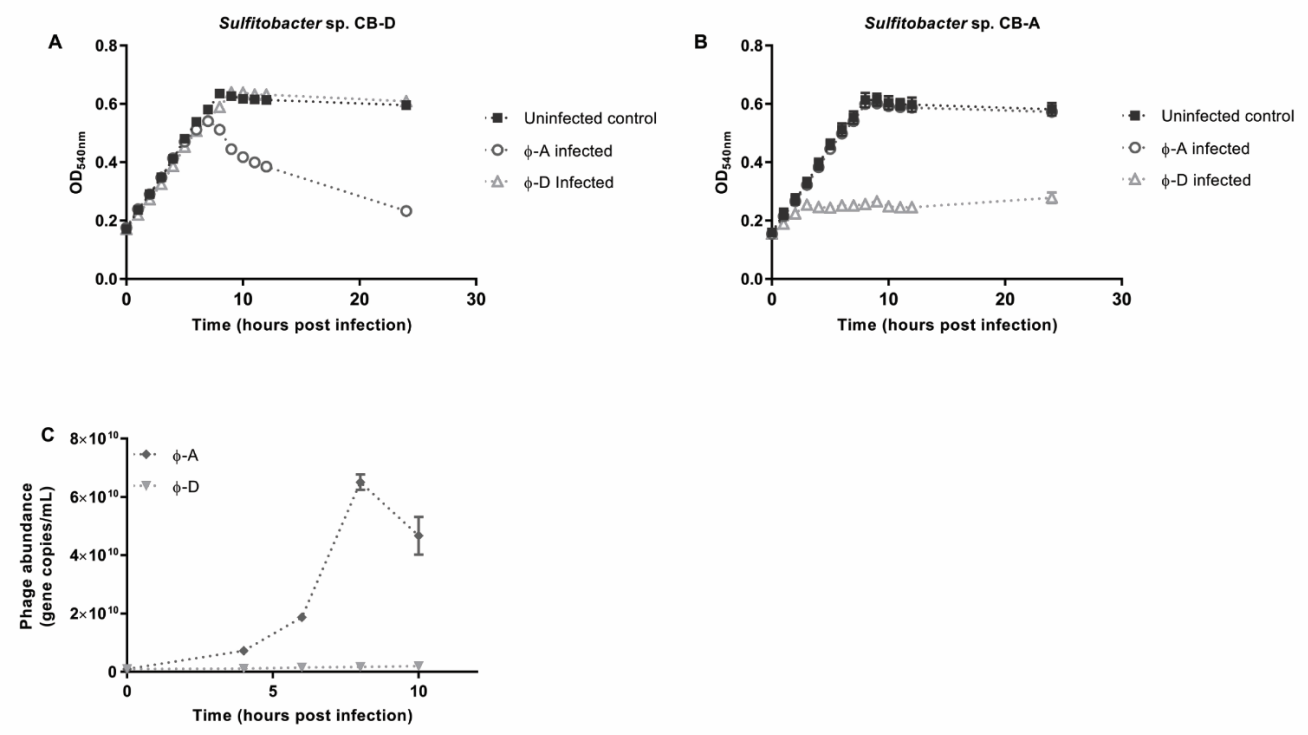

Fig 2.2. CB-D and CB-A susceptibility tests ϕ-D and ϕ-A. **(A)** CB-D growth dynamics of cultures superinfected with ϕ-A (open circles), ϕ-D (open triangles), and uninfected controls (closed squares). **(B)** CB-A growth dynamics of cultures superinfected with ϕ-D (open triangles), ϕ-A (open circles), and uninfected controls (closed squares). **(C)** Phage abundance (as estimated by gene copies/ml culture) during superinfection of CB-D with ϕ-A shown in (A), of ϕ-A gene copies (closed diamonds) and ϕ-D gene copies (closed inverted triangles). Averages of biological triplicates are reported for all treatments. Error bars denote standard deviations and are obscured by the data markers in some instances.

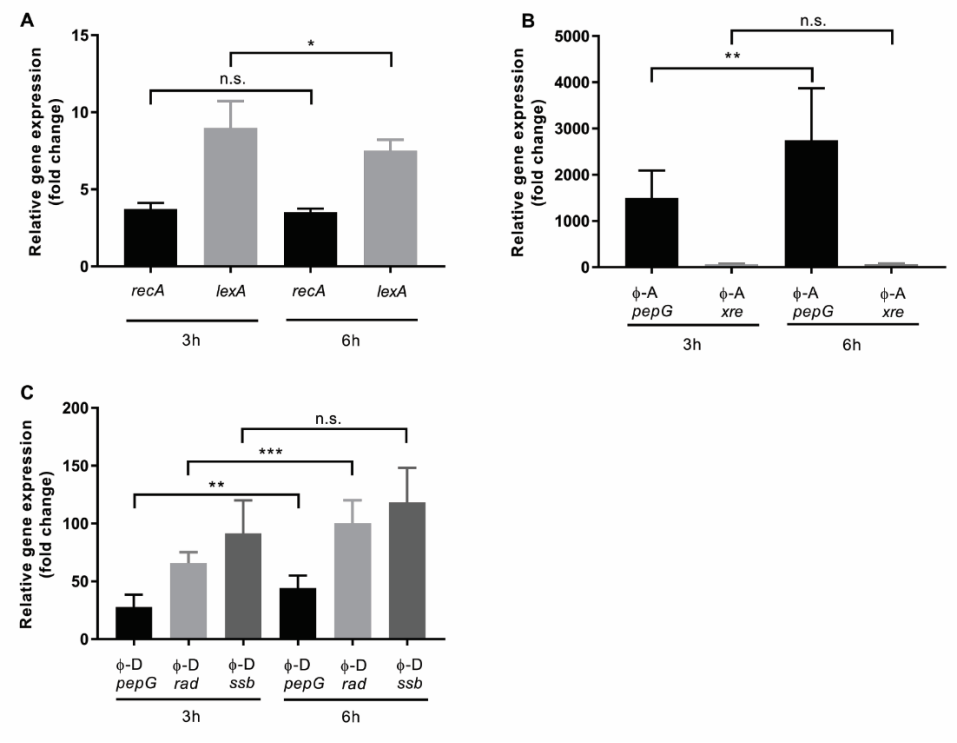

Fig 2.3. Relative gene expression of host and phage gene transcripts 3- and 6-hours post-infection, relative to uninfected controls. **(A)** Fold change of host SOS response genes (*recA* and *lexA*). **(B)** Fold change of ϕ-A genes, peptidase (*pepG*) and XRE-like transcriptional regulator (*xre*). **(C)** Fold change of prophage (ϕ-D) genes, peptidase (*pepG*), ssDNA break repair protein (*rad52*), and DNA replication and repair protein (*ssb*). Significant differences (Student's T-tests) are denoted by asterisks (* = $p<0.05$; ** = $p<0.01$; *** = $p<0.001$; n.s. = not significant). Averages of biological triplicates are reported for all treatments and error bars denote standard deviations.

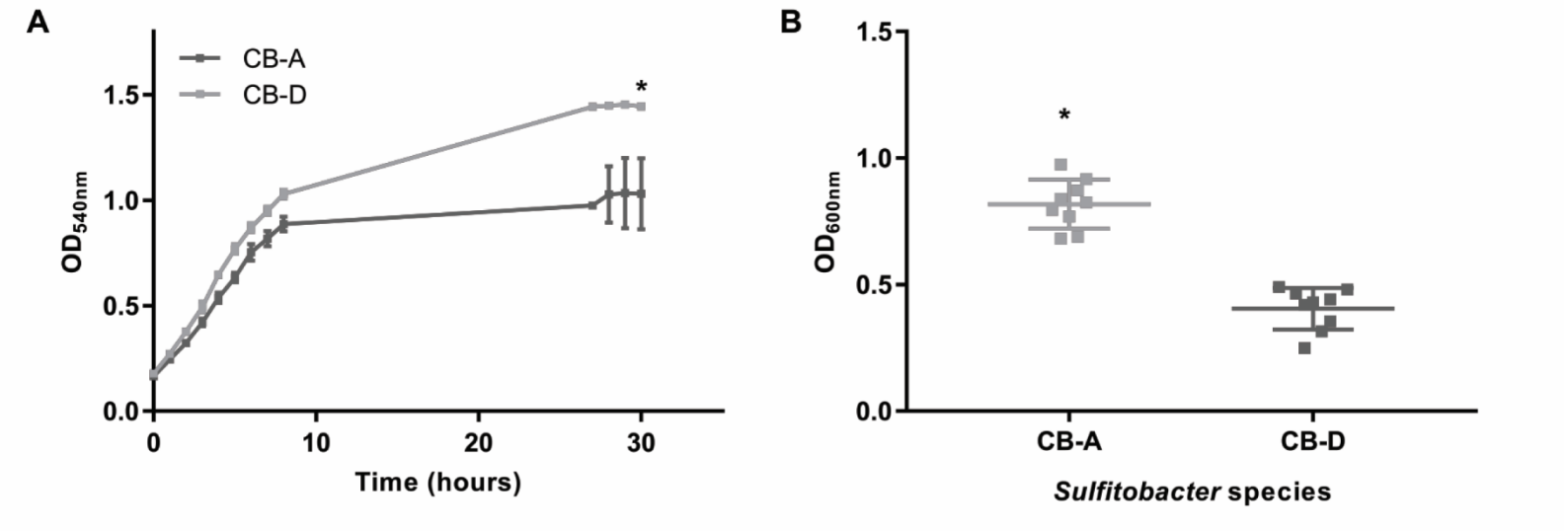

Fig 2.4. Physiological characteristics of CB-D and CB-A during different modes of growth. **(A)** Growth dynamics of CB-D (light grey) and CB-A (dark grey) liquid cultures grown in standard marine medium. **(B)** 24-hour biofilm formation as determined by crystal violet assay. Asterisks denote significant differences as determined by Student's T-tests (* = $p < 0.05$). Averages of biological and technical triplicates are reported for all treatments. Error bars denote standard deviation and are obscured by the data markers in some instances.

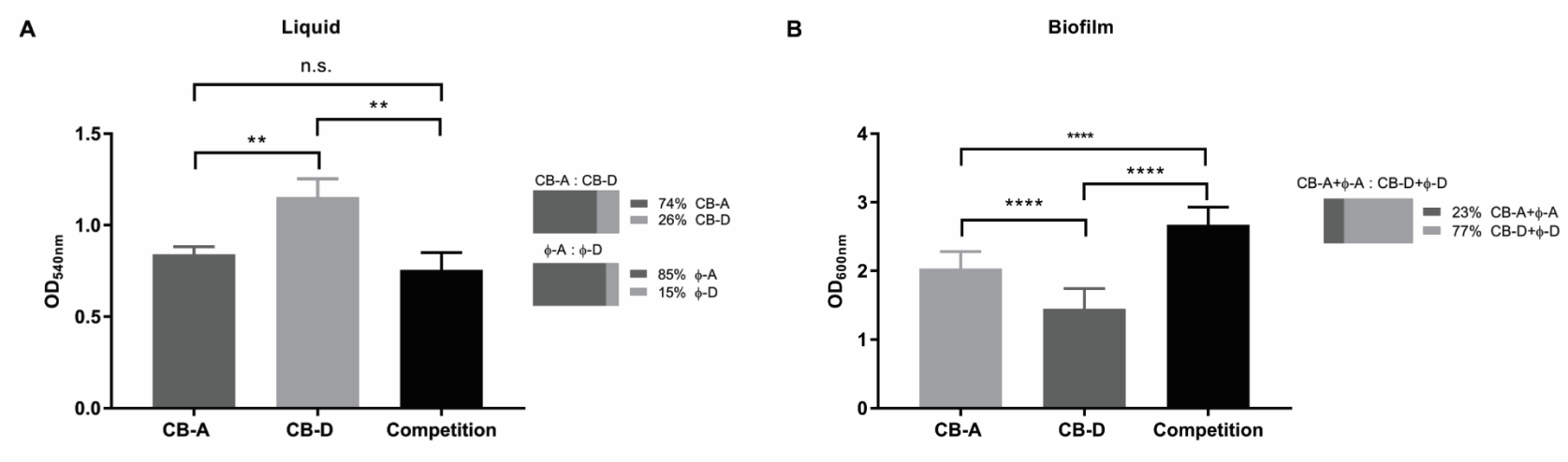

Fig 2.5. Head-to-head competition in liquid cultures and biofilms. **(A)** Final (24-hour) culture densities of liquid CB-A monocultures (dark grey), CB-D monocultures (light grey), and co-cultures (black) grown in standard marine medium. Horizontal bar graphs depict ratios of CB-D:CB-A and ϕ-A:ϕ-D in liquid culture as determined by qPCR. **(B)** Final 24-hour crystal violet biofilm assays for CB-A monocultures (light grey), CB-D monocultures (dark grey), and co-cultures (black) grown as biofilms. qPCR was used to quantify total number of gene copies of CB-D (+ϕ-D):CB-A (ϕ-A), as represented in horizontal bar graph. Significant differences (Student's T-tests) are denoted by asterisks (* = $p<0.05$; ** = $p<0.01$; *** = $p<0.001$; **** = $p<0.0001$; n.s. = not significant). Averages of biological triplicates are reported for all treatments and error bars denote standard deviations.

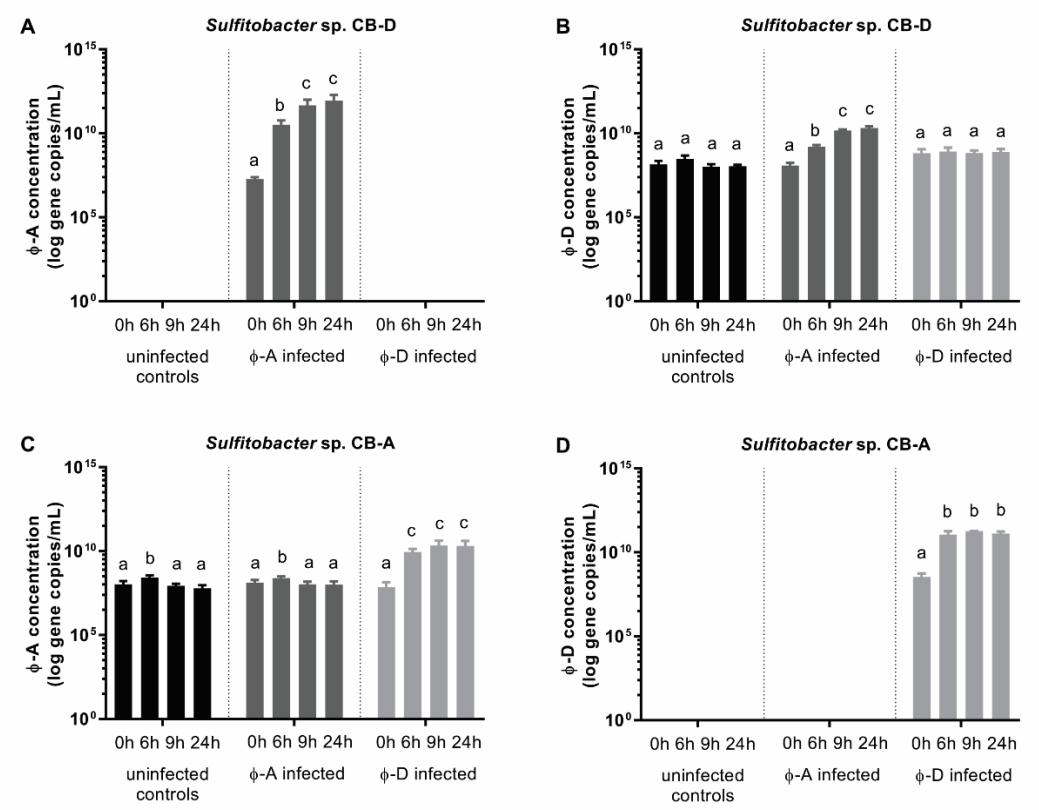

Fig S2.1. Quantification of each phage during homo- and heteroimmunity tests. **(A)** ϕ-A and **(B)** ϕ-D gene copies during infection of *Sulfitobacter* sp. strain CB-D. **(C)** ϕ-A and **(D)** ϕ-D gene copies during infection of *Sulfitobacter* sp. strain CB-A. Averages of biological triplicates are reported for all treatments. Error bars represent the standard deviation of the mean. Different letters denote columns with significantly different ($p<0.05$) phage gene copy numbers within a given plot.

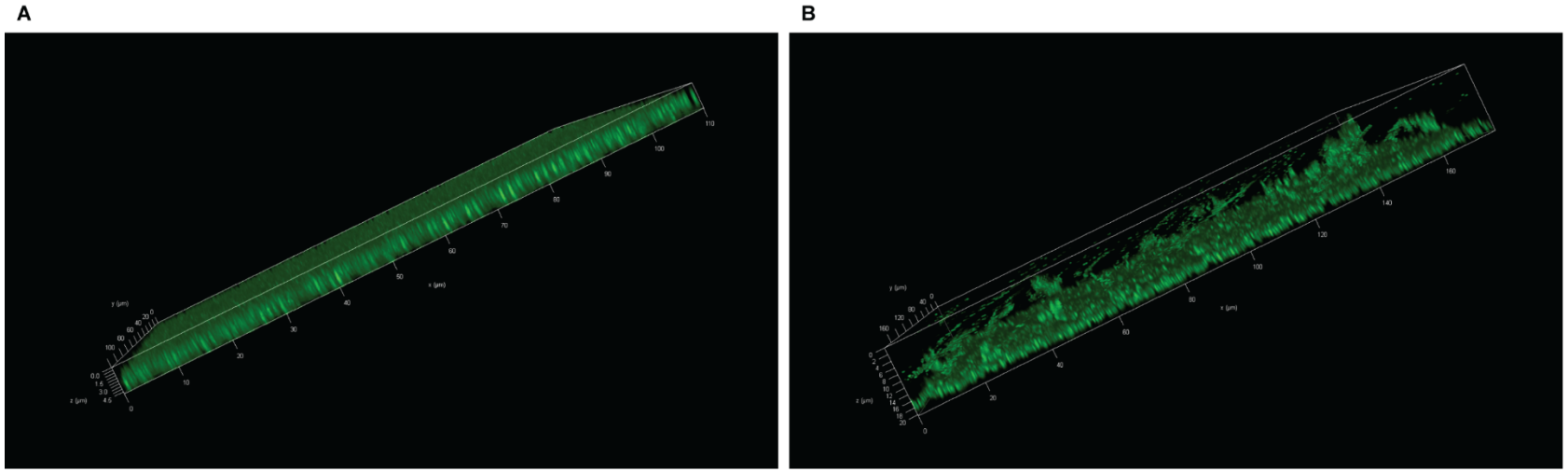

Fig S2.2. 3D analysis of **(A)** CB-D and **(B)** CB-A biofilms. Overnight cultures of each strain were sub-cultured, diluted, and grown to early exponential phase (OD_{540nm} = 0.17). 3 ml of each strain was added to FlouroDish glass dishes (World Precision Instruments, Inc.) and incubated without agitation overnight at room temperature. Planktonic bacteria were removed by gentle inversion of the glass dishes and washed twice with standard marine media (SMM). Dishes were left to dry for 15 min, then stained with 3 ml 25X SYBR Gold (ThermoFisher Scientific SYBR™ Gold Nucleic Acid Gel Stain) for 30 min. Images were generated using confocal laser microscopy and visualized using a Leica SP8 white light Laser Confocal System. Biofilm reconstruction was performed with the Leica Application Suite X (Las X) software. Confocal microscopy methods were greatly adapted from previously described literature (Townsley and Yildiz 2015) and data were analyzed using Comstat2 (Heydorn et al 2000, Vorregaard 2008). *Sulfitobacter* sp. strains were grown in triplicates and at least three images were generated per sample.

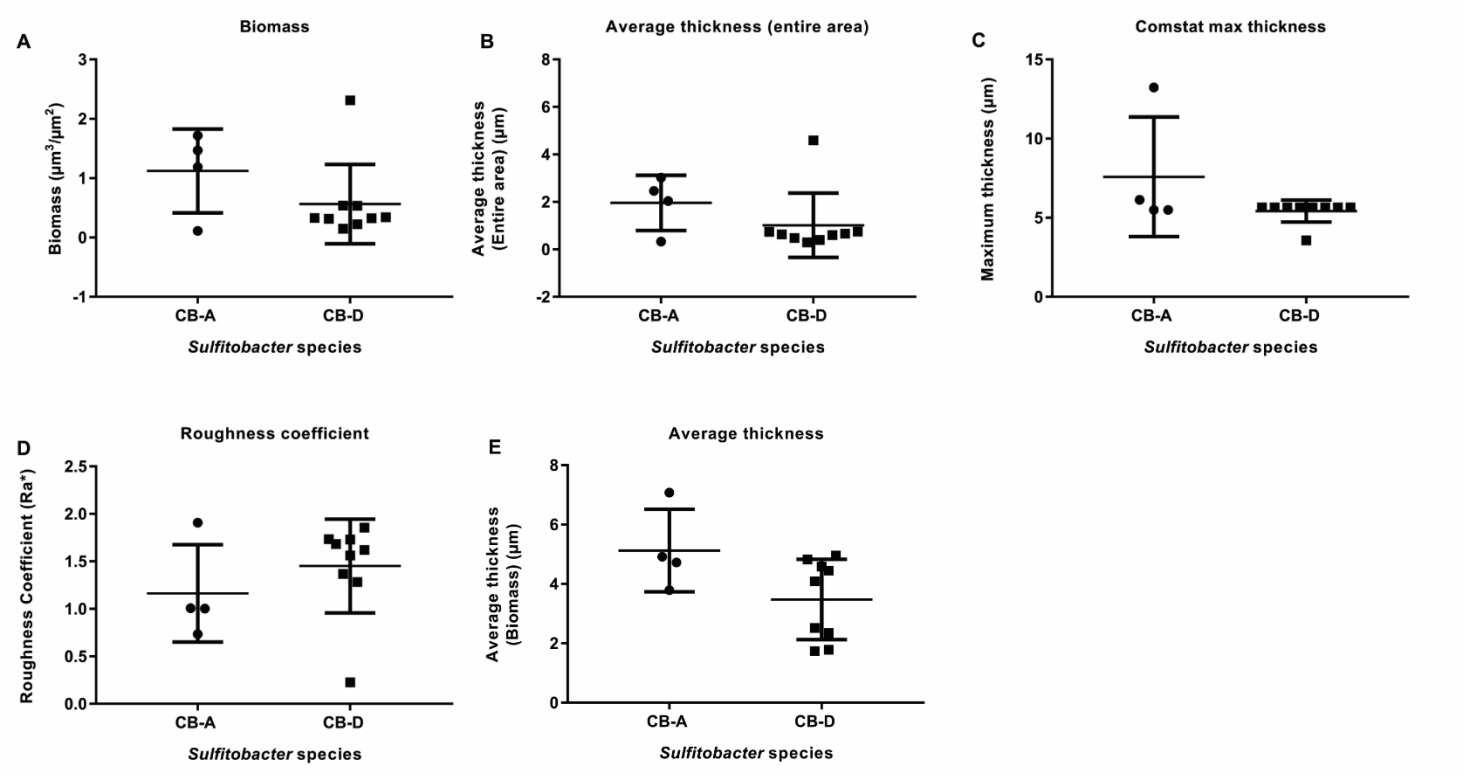

Fig S2.3. Comstat2 analysis of CB-D and CB-A biofilm confocal microscopy data. Biofilm **(A)** biomass, **(B)** average thickness, **(C) C**omstat max thickness, **(D)** roughness coefficient, and **(E)** average thickness. Each data point represents a separate Z stack field of view of the FlouroDish. All parameters showed no significant difference (Student's t-tests; $p<0.05$).

CHAPTER 3

THERE CAN BE ONLY ONE: TEMPERATE PHAGES EXHIBIT HIGH INCIDENCE OF HOST SPECIFICITY AS SEEN IN A SUITE OF ROSEOBACTER SP. STRAINS

A version of this chapter will be submitted for publication by Jonelle T.R. Basso, Nana Y.D. Ankrah, Matthew J. Tuttle and Alison Buchan.

NYDA conducted sequence alignment of *Sulfitobacter* strains. JTRB conducting culturing, spot plating, and screening of the bacterial strains used for the study, as well as generation of the phylogenetic tree, data interpretation, and drafting of the manuscript. AB helped in the design and data interpretation of the study. Alex Grossman conducted presence/absence screening of ϕ-A in 01FIGIMAR (JEMU00000000). Avery Bullock contributed to the development of proposed selection methods of *Sulfitobacter* sp. strains. Michael Camponovo generated ArcGIS maps (UTK Geography department). MJT and Helena Pound provided expertise for phylogenic tree building. Spiro Papoulis identified restriction modification systems. MJT and AB reviewed this manuscript.

ABSTRACT

Phage-host interactions demonstrate a level of complexity which still requires considerable exploration. Bacterial host lysis is described through methods of lysis induction, namely lysis from within or from without. Though previous systems have illustrated both broad and narrow host range, there is continued debate as to how host range is tested and defined. Furthermore, the extent of temperate phage host range is poorly understood among the roseobacter lineage. Here, we assessed the host range of temperate roseophages ϕ-D and ϕ-A, which share 79% sequence identity, and form part of a two-phage-one-host model system. We conducted a series of integration and infection experiments on eighteen roseobacter strains isolated from various locations and with varying degrees of relatedness to the primary hosts, two *Sulfitobacter* species. Five additional *Sulfitobacter* strains encoded a previously identified 15bp putative phage integration site that both ϕ-D and ϕ-A contain, denoted *attB,* within their genomes. Apart from *Sulfitobacter* sp. strains CB-D and CB-A, none of these roseobacters contained prophages. We hypothesized that integration or infection is likely in hosts that encode an *attB* site. However, we observe phage plaques only where *Sulfitobacter* sp. strain CB-D and CB-A are infected by ϕ-A and ϕ-D respectively. We also highlight that partial plaque formation is evident where *Sagittula stellata* E-37, *Rhodobacteraceae* strain pspc.2, *Rhodobacteraceae* strain SE62, *Phaeobacter* sp. strain Y3F, or *Silicibacter lacuscaerulensis* ITI-1157 are infected by ϕ-D and ϕ-A, and likely the result of lysis from without. These findings give evidence for high host specificity among two very similar roseophages and their hosts, with true indication of infectivity of a singular host. These data help in the elucidation of intracellular factors that influence host-phage interactions in a myriad of environments.

INTRODUCTION

Microorganisms belonging to the Roseobacter clade are ubiquitously distributed and abundant in various marine environments (Billerbeck et al 2016, Buchan et al 2005). Strains have been isolated from diverse locations, including Islandic geothermal lakes, Mallorca island, Spain, the Caribbean Sea, and off the coastal Eastern United States (Brinkhoff et al 2008, Fuhrman et al 1994, Gonzalez et al 2003, Mas-Lladó et al 2014, Slightom and Buchan 2009). Roseobacters are known to be infected by temperate phages (Zhan and Chen 2019), thus forming intimate relationships which may influence key components of biogeochemical cycling (Zhan and Chen 2019). Marine viruses exhibit great abundance (Hambly and Suttle 2005), with global viral population estimates upwards of 10^{30} viral particles (Hendrix 2002), and quantification of 10 million phages/ml of water collected from oceans and lakes (Bergh et al 1989). Phages affect bacterial mortality (Thomas et al 2011), facilitate increased host genomic diversity through horizontal gene transfer (HGT) (Canchaya et al 2003), influence host metabolism (Ankrah et al 2014c) and regulate host gene expression (reviewed in Breitbart 2012, reviewed in Hargreaves et al 2014).

Successful phage adsorption is the result of host receptor recognition to phage anti-receptors. There are several adsorption inhibition mechanisms by which phage infection can be halted, including cell surface alterations, mutations of single receptors, use of restriction mechanisms and abortive approaches (reviewed in Hyman and Abedon 2010). Successful phage adsorption can, broadly speaking, result in lytic or lysogenic modes of infection. Following injection of viral genetic information, subversion and synthesis, assembly and release of new phages tends to be quite rapid in lytic cycles (reviewed in Sturino and Klaenhammer 2006). In contrast, temperate phages may integrate with the host genome (reviewed in Sturino and Klaenhammer 2006) while exerting active lysogeny or remain in a plasmid-type form (Feiner et al 2015). Lysogeny is typically described as a dormant state that is maintained until a stressor (though spontaneous prophage induction [SPI] is possible) causes induction, and there is resumption of a lytic cycle (Sturino and Klaenhammer 2006). Lysogeny is prevalent in marine bacteria, with upwards of 50% of well-characterized marine bacterial genomes containing signature prophage genomes (Paul

2008, Touchon et al 2016). Of the thirty-two bacteriophages that infect marine roseobacters, twelve encode an integrase/repressor gene (Zhan and Chen 2019). Even though lysogeny is widespread, to our knowledge, few model systems are characterized for temperate phages.

As previously described, our system is comprised of *Sulfitobacter* sp. strain CB-D (accession no. JPOY00000000); its resident prophage, ϕ-D; and temperate phage, ϕ-A; all isolated from Raunefjorden, Norway (Ankrah et al 2014a, Ankrah et al 2014b). During laboratory superinfection experiments with addition of ϕ-A to CB-D, *Sulfitobacter* sp. strain CB-A was generated through lysogenic conversion (PYUG00000000). ϕ-A and ϕ-D exhibit 79% sequence identity and differ in regions coding for putative tail fiber and transcriptional regulator genes. A putative host integration site (*attB*) is located within a tRNA-Leu gene and a homologous site on the phage genome (*attP*), was predicted to facilitate phage integration (Chapter 2 of this dissertation).

The current paradigm suggests that immunity is conferred to lysogenized bacterial host in instances of superinfection from like phages (Susskind et al 1974a.). In our one-host-two-phage system, we observe homoimmunity and hetero-susceptibility. ϕ-A and ϕ-D are both capable of successful infection of a single host but exhibit variation in the stability of a lysogenic state. Due to these factors, we decided to study differences seen in elicited response, as well as observe phage success, in a suite of related Roseobacters strains.

High phage-host specificity has been previously described, and well-illustrated with *Salmonella* phages (reviewed in Joerger 2003). It has been suggested that narrow host ranges are the result of immunity stemming from lysogeny, as seen in *Lactobacillus casei* Shirota phage PL-1 and the subgenus *Streptobacterium* (Stetter 1977). Others report observation of a wider host range, as seen by infection of both *Vibrio minicus* and *V. cholera* by CTXϕ (Boyd et al 2000), and by the broad host range phage, ϕ-OT8, that facilities high-efficiency transduction in *Serratia* strain ATCC 39006 (*Serratia* 39006) and *Pantoea agglomerans* 9Rz4 (Evans et al 2010). Other systems describe the capability of phages to infect several hosts, which may facilitate HGT amongst susceptible hosts, thus widening the dispersal of virulence genes (Casas et al 2006). There is further evidence to

suggest that a singular phage can infect several different hosts, thus proliferating major genetic transfer (Casas et al 2006). Different lineages of phage have been seen to have different host ranges. For instance, Podoviridae are known to have relatively narrow host ranges. Furthermore, different phages can exhibit varying ranges of specificity on strains of the same species (Holmfeldt et al 2014). Not much is known regarding why some phages have broad host ranges while others have narrow ones.

To our knowledge, this study provides the only evidence identifying the degree of temperate phage specificity of roseobacter-roseophage model systems. This study seeks to assess the degree of host specificity of temperate phage, ϕ-A, and prophage, ϕ-D. We used a suite of eighteen roseobacters which represent a spectrum of phylogenetic relatedness to the native host, *Sulfitobacter* sp. strain CB-D. This collection contained strains of the same genus to those distantly related and presence/absence of the *attB* putative integration site. Spot plate assays were conducted to identify host killing by infecting phage. Subsequent infection experiments of strains that contain the *attB* site only were done and screened through colony PCR to assess possibility of integration.

MATERIALS AND METHODS

Bacterial propagation.

Bacteria were routinely grown on standard marine media (SMM) in 10 ml cultures at 25ºC at 200 rpm. Overnight cultures were sub-cultured, and samples of cultures were taken at $OD_{540nm} \approx 0.17$. See Table 1 for a list of all strains and their sources. Organisms were grown in biological triplicates.

Induction experiments.

Mitomycin C was added at a concentration of 0.5µg/ml to induce prophage when cultures reached $OD_{540nm} \approx 0.6$. *Sulfitobacter* sp. strains CB-D and CB-A were induced to obtain fresh ϕ-D and ϕ-A lysate, respectively. Phages from these *Sulfitobacter* sp. strains were harvested the subsequent day by pelleting of host biomass via centrifugation for 30 minutes at 4,000 rpm. Supernatants were decanted and 0.2 µm filter sterilized. Viral lysate was left at room temperature in the light for 24-48 hours to allow for Mitomycin C degradation. Plaque assays, using *Sulfitobacter* sp. strains CB-D and CB-A as hosts were conducted to determine PFU/ml. Phages from *Sulfitobacter* sp. strain CB-D was concentrated by ultracentrifugation for 3 hours at 29,900 rpm.

Spot plating assays for phage infection detection.

Roseobacter strains were inoculated in duplicate and incubated overnight in 10 ml of SMM at 200 rpm at 25ºC. Roseobacter strains were sub-cultured in SMM, and at $OD_{540nm} \approx 0.17$, 200 µl of bacterial culture was added to 3 ml top agar aliquots and plated. Top agar was prepared ahead of time using 0.57-0.6 g (0.55-0.60%) noble agar. Once this top layer dried, 10ul of ϕ-D and ϕ-A lysate were spot plated for all strains. This was done in technical duplicate. Serial dilutions were done for viral lysate of ϕ-A and ϕ-D. Serial dilutions ranging from undiluted to 10^{-5} were plated for ϕ-A. Dilutions ranging from undiluted to 10^{-3} were plated for ϕ-D. The schematic included an SMM only and an uninduced control. Plates were incubated at room temperature, and zones of clearing were observed 24-48 hours after plating.

Screening for integration in Sulfitobacter sp. strains with attB site.

Roseobacter strains containing an *attB* site were inoculated in duplicate and incubated overnight in 10 ml of SMM at 200 rpm at 25ºC. These strains were sub-cultured in SMM, and at $OD_{540nm} \approx 0.17$, ϕ-A was added to *Sulfitobacter* sp. strain EE-36 (AALV00000000), 03SOLIMAR (AXZR00000000) and 01FIGIMAR (JEMU00000000) at a multiplicity of infection (MOI) of 0.6 and 0.06. Samples were collected at 4 hours and 8 hours post infection (h.p.i.). Optical density (OD) readings were taken over 24 hours, every hour for the first 9 hours, then every hour from 21-24 hours. 1 ml of bacterial culture was taken for serial dilutions (plating 10^{-5}, 10^{-6}, 10^{-7} dilutions), to obtain viable counts data. All sampling was conducted in biological triplicate. Blanks were used as negative controls. Optical density readings and viable counts were conducted for the biological triplicates at OD_{540nm}. Twenty colonies were randomly selected from both time points and patch plates were made. Colonies grown on patch plates were used for colony PCR screening and subsequent gel imaging.

Colony PCR and gel electrophoresis.

Colonies from infection experiments were suspended in 50 µl of 10 mM Tris buffer (pH 8.0), vortexed, and heated at 95ºC for 10 minutes. Samples were then spun on a benchtop centrifuge for 5 minutes to pellet cell debris. The supernatant was used as template for PCR amplification using phage specific primers (Table 3.1). (All tables and figures are located in the appendix). Thermocycling conditions for AC (specific for ϕ-A) and PP1 (specific for ϕ-D) primer sets were as follows: 95ºC for 2 min, 40 cycles of 95ºC for 20 sec, 57ºC for 20 sec, 72ºC for 20 sec, followed by 72ºC for 5 min.

Analysis of integration site conservation.

Gene organization around putative integration site, *attB*, in *Sulfitobacter* sp. strain EE-36 (AALV00000000), 03SOLIMAR (AXZR00000000) and 01FIGIMAR (JEMU00000000) was determined using BLASTn as previously described (Ankrah 2015).

Phylogenetic tree.

FASTA files of 16S rRNA gene sequences and whole genome sequences were obtained through NCBI (National Center for Biotechnology Information). For organisms with multiple 16S rRNA sequences, alignments were conducted in CLC Genomics Workbench version 8.5.4 (Qiagen). RNAammer 1.2 Server was used to predict 16S rRNA sequences within genomes sequences which lacked 16S rRNA annotations. MEGA (Molecular Evolutionary Genetics Analysis) was used to conduct sequence alignments using MUSCLE (MUltiple Sequence Comparison by Log Expectation) and trimming. Aligned sequences were exported and the phylogeny software ATGC:PhyML was used to create a phylogenic tree using the substitution model HKY85 and bootstrapping. The phylogenic tree was constructed and managed through using the iTOL (interative Tree Of Life) online tool (http://itol.embl.de).

Identification of restriction modification (RM) systems.

RefSeq GCF accession numbers were obtained through NCBI. These numbers were used to conduct BLAST searches for RM systems.

RESULTS

Differences in viral yields of ϕ-D and ϕ-A.

Induction experiments were conducted to obtain viral lysate from *Sulfitobacter* sp. strains CB-A and CB-D. We found that there were differences in viral yield between strains as we obtained 2.14 x 10^9 PFU/ml of ϕ-A and 7.28 x 10^6 PFU/ml of ϕ-D. To increase ϕ-D phage yields we ultracentrifuged ϕ-D lysate to concentrate ϕ-D particles which yielded 1.41 x 10^7 PFU/ml. Here, concentrations of ϕ-D were still considerably lower than that of ϕ-A, preventing comparable MOIs. Therefore, integration experiments described herein were conducted using ϕ-A only.

Roseobacter relatedness, identification of attB site and presence of restriction modification systems.

Sulfitobacter sp. strain EE-36 (AALV00000000), NAS-14.1 (AALZ00000000), *Sulfitobacter* sp. strain 03SOLIMAR (AXZR00000000) and *Sulfitobacter* sp. strain 01FIGIMAR (JEMU00000000) all contain putative integration site (*attB*), and share 99.93, 100, 99.93 and 98.31% sequence identity respectively to *Sulfitobacter* sp. strain CB-D (Ankrah et al 2014b) (Fig 3.1). These strains were isolated from diverse locations (Fig 3.2) and none appear to be lysogenized by a prophage. We also tested fourteen additional roseobacters that lack the *attB* site and evidence for prophages. Restriction modification (RM) systems were identified in CB-D, CB-A, EE-36, NAS 14.1, 3SOLIMAR, 1FIGIMAR, Y4I, E37 and 217 (Table 3.2). Phylogenetic analyses identified the relatedness of these strains, seeking to show the range of our screening individuals (Fig 3.3).

Spot plating indicates high infection specificity of roseophages.

Our data indicate that only *Sulfitobacter* sp. strain CB-D and CB-A are infected by ϕ-A and ϕ-D respectively, as marked by plaques on SMM agar plates. No plaques were observed with *Sulfitobacter* strains EE-36, 3SOLIMAR, 1FIGIMAR, NAS-14.1. This may indicate that even with the presence of a putative integration site, it is possible that there is

no receptor recognition for the virus in these strains. This suggests that the roseophages of our system have a very narrow host range.

Colony PCR screenings reveal high host specificity.

Previous preliminary investigations demonstrated that integration of ϕ-A was possible in all the listed *Sulfitobacter* sp. strains that contain putative integration site *attB* (Ankrah 2015). Subsequent integration experiments were conducted with roseobacter strains that contained the *attB* site only. Due to low PFU/ml yields of ϕ-D, ϕ-A was used for these series of experiments only. Colony PCR screening and gel imaging determined that none of the strains were ϕ-A positive for the conditions tested (data not shown). This result may also be an indication of the level of specificity of this roseophage.

DISCUSSION

Host-phage systems are complex. The presence of putative integration site, *attB* can influence site specific recombination and the formation of this phage-host relationship (Ankrah 2015, reviewed in Howard-Varona et al 2017). Aspects such as host range remains not well characterized in roseobacter-roseophage model systems. The presence of this *attB* site in several roseobacter strains marks the appropriateness of this kind of study.

Individuals of the Roseobacter clade are ecologically important in global biogeochemical cycles (Ankrah et al 2014c, Buchan et al 2005, Buchan et al 2014), and are often lysogenized by phages (Ankrah et al 2014a). As previously identified, lysogens of our roseobacter-roseophage model system, *Sulfitobacter* sp. strains CB-D and CB-A are lysogenized by phages ϕ-D and ϕ-A respectively. Spot plate assay results identified obvious infection only of *Sulfitobacter* sp. strain CB-D by ϕ-A, and *Sulfitobacter* sp. strain CB-A by ϕ-D. These phages share 79% sequence identity and exhibit hetero-susceptibility. Partial plaque formation were observed in *Sagittula stellata* E37**,** *Rhodobacteraceae* strain SE62**,** *Silicibacter lacuscaerulensis* ITI-1157 in response to both phages. We also report possible zones of clearing for *Rhodobacteraceae* strain pspc.2 and *Phaeobacter* sp. strain Y3F in response to just ϕ-D. For these strains zones of clearing were not obvious, therefore definitive conclusion about infection cannot be made, but may suggest incidence of lysis from without. These findings indicate high specificity of roseophages in our system, which may assist in the maintenance of microbial diversity in ecosystems and support the concepts of the Kill the Winner (KtW) hypothesis (reviewed in Johnke et al 2014, Thingstad and Lignell 1997).

Sulfitobacter strains EE-36, 3SOLIMAR, 1FIGIMAR, NAS-14.1 showed no plaques in response to either phage. This indicates that the presence of putative attachment site, *attB*, is not the only factor dictating host infection. Bacteria possess protective mechanisms from phage infection and still survive through adsorption resistance, temperate phage infection and restriction mechanisms, favoring use of mechanisms regulating parasitic negative effects (reviewed in Hyman and Abedon 2010). The potential use of restriction mechanisms helps prevent irreversible high-jacking of host metabolism

by phages. This post-adsorption mechanism describes the survival of the host and subsequent death of the phage (reviewed in Hyman and Abedon 2010). Restriction modification (RM) systems of hosts can negatively impact a wide range of phages and are described as anti-phage mechanisms (reviewed in Hyman and Abedon 2010). Restriction modification systems (RM) can provide profiles that will help dictate the possibility of infectivity. CB-D, CB-A, EE-36, NAS 14.1, 3SOLIMAR, 1FIGIMAR Y4I, E37 and 217 also contain numerous RM systems (Table 3.2).

In using spot assay tests for infection, we are limited to observations of only bacterial killing, but not phage infection specifically. Perhaps more stringent broth-based assays or efficiency of center of infection (ECOI) is required for determination of productive host range, as is suggested (reviewed in Hyman and Abedon 2010). It is additionally important to note that spot plating assays help in the identification of phage killing as determined by plaques. We are therefore unable to determine whether phages are integrating into the genomes of the non-lysogenized roseobacters.

A possible explanation for our observations is that no receptor recognition exists for roseophages ϕ-D and ϕ-A in these other strains. Adsorption inhibition mechanisms block chance encounters of phage and host (reviewed in Hyman and Abedon 2010). Bacteria can decorate their cell surfaces with extracellular polymers (which may be facilitated by plasmids) though it is not always successful and is more prominent in incidence of biofilm formation (reviewed in Hyman and Abedon 2010) compared to free-living physiologies (Sule and Belas 2013). Bacteria found in biofilms may not exhibit a physiological state that favors active phage infection (reviewed in Hyman and Abedon 2010).

It is not uncommon to find phages with narrow host range (Hambly and Suttle 2005, Joerger 2003, Stetter 1977, Wang and Chen 2008), though using terminology such as ‘narrow’ and ‘broad’ has been suggested to add difficulty and complexity of defining host range (Ross et al 2016). An underlying problem may be that hosts kept as part of lab collections may unknowingly be biased against phage adsorption. This therefore allows for the observation of hosts exhibiting resistance mechanisms, which provide for host propagation in the presence of phage (reviewed in Hyman and Abedon 2010). Additionally,

we cannot make conclusions for susceptibility to infection under other conditions. It is likely that components of laboratory standard marine media, such as yeast extract and tryptone provide environments that are nutrient rich, which create high host abundance, and perpetuate a high phage-host specificity state. It is suggested that the chance of lysogeny is greater under more oligotrophic conditions (Jiang and Paul 1994). In considering aspects of the phage-host arms race, it is possible that resistance to specific phages has evolved, where the number of phages is reflective of bacterial species diversity as a within-community mechanism (Vage et al 2016).

We demonstrate that there is only one true host that is infected by either roseophage. We also demonstrate that integration is not observed for the growth conditions that tested, and we cannot distinguish viral susceptibility under other conditions. These data indicate the high specificity of roseophages in our system.

ACKNOWLEDGEMENTS

We would like to thank the undergraduate students who contributed to the development of this research chapter: Alex Grossman and Avery Bullock. This research was supported by NSF grant (OCE-106352) to A.B.

REFERENCES

Ankrah NYD, Budinoff CR, Wilson WH, Wilhelm SW, Buchan A (2014a). Genome Sequences of Two Temperate Phages, ΦCB2047-A and ΦCB2047-C, Infecting Sulfitobacter sp. Strain 2047. *Genome Announcements* **2**.

Ankrah NYD, Lane T, Budinoff CR, Hadden MK, Buchan A (2014b). Draft Genome Sequence of Sulfitobacter sp. CB2047, a Member of the Roseobacter Clade of Marine Bacteria, Isolated from an Emiliania huxleyi Bloom. *Genome Announcements* **2**.

Ankrah NYD, May AL, Middleton JL, Jones DR, Hadden MK, Gooding JR *et al* (2014c). Phage infection of an environmentally relevant marine bacterium alters host metabolism and lysate composition. *Isme Journal* **8:** 1089-1100.

Ankrah NYD (2015). Elucidating the Impact of Roseophage on Roseobacter Metabolism and Marine Nutrient Cycles.

Bergh O, Borsheim KY, Bratbak G, Heldal M (1989). High Abundance of Viruses Found in Aquatic Environments. *Nature* **340:** 467-468.

Billerbeck S, Wemheuer B, Voget S, Poehlein A, Giebel HA, Brinkhoff T *et al* (2016). Biogeography and environmental genomics of the Roseobacter-affiliated pelagic CHAB-I-5 lineage. *Nature Microbiology* **1**.

Boyd EF, Moyer KE, Shi L, Waldor MK (2000). Infectious CTXPhi and the vibrio pathogenicity island prophage in Vibrio mimicus: evidence for recent horizontal transfer between V. mimicus and V. cholerae. *Infection and immunity* **68:** 1507-1513.

Breitbart M (2012). Marine Viruses: Truth or Dare. In: Carlson CA, Giovannoni SJ (eds). *Annual Review of Marine Science, Vol 4*. pp 425-448.

Brinkhoff T, Giebel HA, Simon M (2008). Diversity, ecology, and genomics of the Roseobacter clade: a short overview. *Archives of Microbiology* **189:** 531-539.

Buchan A, Gonzalez JM, Moran MA (2005). Overview of the marine Roseobacter lineage. *Applied and Environmental Microbiology* **71:** 5665-5677.

Buchan A, LeCleir GR, Gulvik CA, Gonzalez JM (2014). Master recyclers: features and functions of bacteria associated with phytoplankton blooms. *Nature Reviews Microbiology* **12:** 686-698.

Canchaya C, Fournous G, Chibani-Chennoufi S, Dillmann ML, Brussow H (2003). Phage as agents of lateral gene transfer. *Current Opinion in Microbiology* **6:** 417-424.

Casas V, Miyake J, Balsley H, Roark J, Telles S, Leeds S *et al* (2006). Widespread occurrence of phage-encoded exotoxin genes in terrestrial and aquatic environments in Southern California. *Fems Microbiology Letters* **261:** 141-149.

Evans TJ, Crow MA, Williamson NR, Orme W, Thomson NR, Komitopoulou E *et al* (2010). Characterization of a broad-host-range flagellum-dependent phage that mediates high-efficiency generalized transiduction in, and between, Serratia and Pantoea. *Microbiology-Sgm* **156:** 240-247.

Feiner R, Argov T, Rabinovich L, Sigal N, Borovok I, Herskovits AA (2015). A new perspective on lysogeny: prophages as active regulatory switches of bacteria. *Nature Reviews Microbiology* **13:** 641-650.

Fuhrman JA, Lee SH, Masuchi Y, Davis AA, Wilcox RM (1994). Characterization of Marine Prokaryotic Communities via DNA and RNA. *Microbial Ecology* **28:** 133-145.

Gonzalez JM, Covert JS, Whitman WB, Henriksen JR, Mayer F, Scharf B *et al* (2003). Silicibacter pomeroyi sp nov and Roseovarius nubinhibens sp nov., dimethylsulfoniopropionate-demethylating bacteria from marine environments. *International Journal of Systematic and Evolutionary Microbiology* **53:** 1261-1269.

Hambly E, Suttle CA (2005). The viriosphere, diversity, and genetic exchange within phage communities. *Current Opinion in Microbiology* **8:** 444-450.

Hargreaves KR, Kropinski AM, Clokie MRJ (2014). Bacteriophage behavioral ecology. *Bacteriophage* **4:** e29866.

Hendrix RW (2002). Bacteriophages: Evolution of the majority. *Theoretical Population Biology* **61:** 471-480.

Holmfeldt K, Howard-Varona C, Solonenko N, Sullivan MB (2014). Contrasting genomic patterns and infection strategies of two co-existing Bacteroidetes podovirus genera. *Environmental Microbiology* **16:** 2501-2513.

Howard-Varona C, Hargreaves KR, Abedon ST, Sullivan MB (2017). Lysogeny in nature: mechanisms, impact and ecology of temperate phages. *Isme Journal* **11:** 1511-1520.

Hyman P, Abedon ST (2010). Bacteriophage Host Range and Bacterial Resistance. In: Laskin AI, Sariaslani S, Gadd GM (eds). *Advances in Applied Microbiology, Vol 70*. pp 217-248.

Jiang SC, Paul JH (1994). Seasonal and Diel Abundance of Viruses and Occurrence of Lysogeny/Bacteriocinogeny in the Marine Environment. *Marine Ecology Progress Series* **104:** 163-172.

Joerger RD (2003). Alternatives to antibiotics: Bacteriocins, antimicrobial peptides and bacteriophages. *Poultry Science* **82:** 640-647.

Johnke J, Cohen Y, de Leeuw M, Kushmaro A, Jurkevitch E, Chatzinotas A (2014). Multiple micro-predators controlling bacterial communities in the environment. *Current Opinion in Biotechnology* **27:** 185-190.

Mas-Lladó M, Piña-Villalonga JM, Brunet-Galmés I, Nogales B, Bosch R (2014). Draft Genome Sequences of Two Isolates of the Roseobacter Group, Sulfitobacter sp. Strains 3SOLIMAR09 and 1FIGIMAR09, from Harbors of Mallorca Island (Mediterranean Sea). *Genome Announcements* **2:** e00350-00314.

Paul JH (2008). Prophages in marine bacteria: dangerous molecular time bombs or the key to survival in the seas? *Isme Journal* **2:** 579-589.

Ross A, Ward S, Hyman P (2016). More Is Better: Selecting for Broad Host Range Bacteriophages. *Frontiers in Microbiology* **7**.

Slightom RN, Buchan A (2009). Surface Colonization by Marine Roseobacters: Integrating Genotype and Phenotype. *Applied and Environmental Microbiology* **75:** 6027-6037.

Stetter KO (1977). Evidence for frequent lysogeny in lactobacilli: temperate bacteriophages within the subgenus Streptobacterium. *Journal of virology* **24:** 685-689.

Sturino JM, Klaenhammer TR (2006). Engineered bacteriophage-defence systems in bioprocessing. *Nature Reviews Microbiology* **4:** 395-404.

Sule P, Belas R (2013). A Novel Inducer of Roseobacter Motility Is Also a Disruptor of Algal Symbiosis. *Journal of Bacteriology* **195:** 637-646.

Susskind MM, Botstein D, Wright A (1974a.). Superinfection exclusion by P22 prophage in lysogens of Salmonella typhimurium III. Failure of superinfecting phage DNA to enter sieA+ lysogens. *Virology* **62:** 350-366.

Thingstad TF, Lignell R (1997). Theoretical models for the control of bacterial growth rate, abundance, diversity and carbon demand. *Aquatic Microbial Ecology* **13:** 19-27.

Thomas R, Berdjeb L, Sime-Ngando T, Jacquet S (2011). Viral abundance, production, decay rates and life strategies (lysogeny versus lysis) in Lake Bourget (France). *Environmental Microbiology* **13:** 616-630.

Touchon M, Bernheim A, Rocha EPC (2016). Genetic and life-history traits associated with the distribution of prophages in bacteria. *Isme Journal* **10:** 2744-2754.

Vage S, Pree B, Thingstad TF (2016). Linking internal and external bacterial community control gives mechanistic framework for pelagic virus-to-bacteria ratios. *Environmental Microbiology* **18:** 3932-3948.

Wang K, Chen F (2008). Prevalence of highly host-specific cyanophages in the estuarine environment. *Environmental Microbiology* **10:** 300-312.

Zhan YC, Chen F (2019). Bacteriophages that infect marine roseobacters: genomics and ecology. *Environmental Microbiology* **21:** 1885-1895.

APPENDIX

Table legend.

Table 3.1. Oligonucleotides used in this study.

Table 3.2. General features and host infectivity range of roseobacters in this study.

Table 3.3. List of annotated restriction modification (RM) systems in genomes of roseobacters investigated as part of this study.

Table 3.1. Oligonucleotides used in this study.

Primer name	Primer sequence (5'->3')	Gene target	Purpose/experiment
2047PP1_for	TATTCATAGCGAGGCGCAGT	endolysin	ϕ-D identification
2047PP1_rev	ATACCTGCCCAACGTCACAG	endolysin	ϕ-D identification
2047A-C_for	CCCATGTGTATGTCGCCTCT	endolysin	ϕ-A identification
2047A-C_rev	CAGCGTTGAAAAAGGCTCTG	endolysin	ϕ-A identification

Table 3.2. General features and host infectivity range of roseobacters investigated as part of this study. +++ denotes clear zones of clearing and + denotes possible zones of clearing during spot plate assays.

Roseobacter species strains[a]	Host infectivity		Isolation location	genome size (bp) [main chromosome]	G+C %	Accession number	Information source
	ϕ-A	ϕ-D					
Sulfitobacter sp. strain EE-36	-	-	Coastal Georgia, USA	3,547,243	60	AALV00000000	Brinkhoff et al. 2008.
Sulfitobacter sp. strain NAS 14.1	-	-	North Atlantic Ocean	4,002,069	60	AALZ00000000	Brinkhoff et al. 2008, Slightom and Buchan. 2009.
Sulfitobacter sp. strain FIGIMAR	-	-	Cala Figuera harbor, Mallorca Island, Spain	3,861,701	58	JEMU00000000	Mas-Lladó et al. 2014.
Sulfitobacter sp. strain SOLIMAR	-	-	Sóller harbor, Mallorca Island, Spain	3,453,172	60	AXZR00000000	Mas-Lladó et al. 2014.
Sulfitobacter sp. strain CB-D (CB: 2047)	+++	-	Raunefjorden, Norway	3,767,790	60	JPOY00000000	Ankrah et al. 2014. Draft genome sequence of *Sulfitobacter* sp. CB2047.
Sulfitobacter sp. strain CB-A (CB: YM3A)	-	+++	Raunefjorden, Norway		60	PYUG00000000	Basso et al. 2019. unpublished.
Citreicella SE45	-	-	Southeastern US salt marshes off Skidaway Island, from *Spartina alterniflora* (smooth cordgrass) detritus, GA, USA	5,523,231	67	AF388308	Sightom and Buchan. 2009.
Phaeobacter sp. strain Y4I	-	-	Coastal seawater near St. Mary's, Georgia, USA	4,344,244	64	ABXF00000000	Sightom and Buchan. 2009.
Roseovarius nubinhibens ISM	-	-	Caribbean Sea	3,668,667	63	AF098495	Furhman et al. 1994, González et al. 2003.
Sagittula stellata E37	+	+	Coastal Georgia, USA	5,262,893	65	AAYA00000000	Sightom and Buchan. 2009.
Rhodobacteraceae strain pspc.2	-	+	Dean Creek site, from ascomata found on late-decay blades, Georgia, USA			AY149624	Slightom and Buchan. 2009, Buchan et al. 2003.
Rhodobacteraceae strain SE62	+	+	Coast of Sapelo Island, from decaying *Spartina*, Georgia, USA	4,581,948	57	AY038920	Buchan et al. 2001.
Roseovarius sp. 217	-	-	Surface seawater from a methyl halide oxidizing enrichment culture, collected near Plymouth, England	4,762,632	60	AAMV00000000	Sightom and Buchan. 2009.
Phaeobacter sp. strain Y3F	-	+	Collected from Skidaway River, Georgia, USA			AF253467	Sightom and Buchan. 2009, Buchan et al. 2004.
Ruegaria pomeroyi DSS.3	-	-	Coastal Georgia, USA	4,109,442	64	CP000031.2; CP000032.1	Moran, Buchan et al. 2004, Slightom and Buchan. 2009.
Silicibacter lacuscaerulensis ITI-1157	+	+	Icelandic geothermal lake	3,523,710	63	U77644	Sightom and Buchan. 2009.
Ruegaria sp. TM1040	-	-	The phycosphere of the dinoflagellate *Pfiesteria piscicida* cell	3,201,640	60	NC_008044	Miller and Belas 2004, Slightom and Buchan. 2009.
Sulfitobacter pontiacus Chlg10	-	-				NR_026418	Sorokin, D. Y. 1995, Slightom and Buchan. 2009.
Jannaschia strain CCS1	-	-	Pacific coastal waters	4,317,977	62	NC_007802	Moran et al. 2007.
Phaeobacter daeponensis KCTC 12794	-	-	Tidal flat sediment of the Yellow Sea, Korea		65	DQ981486	Yoon et al. 2007.

[a]The following strains can be found in NCBI under the following nomenclature: Bacterium NAS 14.1; Marine bacterium SE45; Marine bacterium Y4I; *Roseobacter sp. ISM;* Uncultured bacterium clone E37; Marine bacterium SIMO IS-S76-282 pspc.2; Marine bacterium SE62; Rhodobacteraceae bacterium 217; Alphaproteobacterium Y3F; *Silicibacter pomeroyi strain DSS.3; Ruegaria lacuscaerulensis strain ITI 1157, Phaeobacter daeponensis strain TF-218*.

Table 3.3. List of annotated restriction modification (RM) systems in genomes of roseobacters investigated as part of this study.

Roseobacter species strains	Genome size (bp) [main chromosome]	G+C %	Accession number	RefSeq assembly Accession no.	Accession	Domain(s) Found	Protein length	Product	TopBLAST; evalue; bitscore
Sulfitobacter sp. strain EE-36	3,547,243	60	AALV000 00000	GCF_0001 52605.1	NZ_CH959311|1 4108..15229	DNA methylase	373	DNA (cytosine-5-)-methyltransfera se	N/A
					NZ_CH959310|c omplement(6614 41..662541)	N6 N4 Mtase	366	site-specific DNA-methyltransfera se	N/A
					NZ_CH959310|c omplement(1631 795..1632562)	N/A	255	HNH endonuclease	R1.BbrUI;6.3 4e-38;131.0
					NZ_CH959310|2 043421..2044824	HsdM N;N6 Mtase	467	type I restriction endonuclease	N/A
					NZ_CH959310|2 044817..2046445	Methylase S;Methylas e S	542	type I restriction endonuclease subunit S	N/A
					NZ_CH959310|2 337827..2338981	DNA methylase	384	DNA (cytosine-5-)-methyltransfera se	N/A
					NZ_CH959310|2 489174..2490016	N6 Mtase	280	peptide chain release factor N(5) glutamine methyltransfera se	N/A

Table # 3.3 continued

Roseobacter species strains	Genome size (bp) [main chromosome]	G+C %	Accession number	RefSeq assembly Accession no.	Accession	Domain(s) Found	Protein length	Product	TopBLAST; evalue; bitscore
Sulfitobacter sp. strain NAS 14.1	4,002,069	60	AALZ000 00000	GCF_0001 52645.1	NZ_CH959317|c omplement(1140 9..14549)	N6 Mtase	1046	DNA methyltransfera se	BbuB31II;1.1 09999999999 9996e-139;444.0
					NZ_CH959316|5 6508..60047	N6 Mtase	1179	SAM-dependent methyltransfera se	AhyYL17I;2. 29999999999 99993e-130;431.0
					NZ_CH959312|7 2055..72897	N6 Mtase	280	peptide chain release factor N(5) glutaminemethy ltransferase	N/A
					NZ_CH959312|c omplement(6451 34..646042)	NaeI	302	hypothetical protein	N/A
					NZ_CH959312|c omplement(6461 09..647068)	DNA methylase	319	DNA cytosine methyltransfera se	N/A
					NZ_CH959312|c omplement(1248 047..1249147)	N6 N4 Mtase	366	site-specific DNA methyltransfera se	N/A
					NZ_CH959312|1 959695..1960879	Mrr cat	394	putative prophage LambdaCh01, restriction endonuclease	N/A

Table #3.3 continued

Roseobacter species strains	Genome size (bp) [main chromosome]	G+C %	Accession number	RefSeq assembly Accession no.	Accession	Domain(s) Found	Protein length	Product	TopBLAST; evalue; bitscore
					NZ_CH959312|complement(2237554..2238321)	N/A	255	HNH endonuclease	R1.BbrUI;5.4e-38;131.0
					NZ_CH959312|2966881..2968035	DNA methylase	384	DNA (cytosine-5-)-methyltransferase	N/A
Sulfitobacter sp. strain FIGIMAR	3,861,701	58.43	JEMU000000000	GCF_000647535.1	NZ_JEMU01000005|127085..128185	N6 N4 Mtase	366	site-specific DNA methyltransferase	N/A
					NZ_JEMU01000011|complement(146377..147660)	RE LlaJI	427	LlaJI family restriction endonuclease	N/A
					NZ_JEMU01000011|complement(147650..149458)	N/A	602	hypothetical protein	R2.BsuMI;1.91999999999999998e-45;160.0
					NZ_JEMU01000011|complement(149981..151246)	DNA methylase; DNA methylase	421	restriction endonuclease subunit M	N/A

Table #3.3 continued

Roseobacter species strains	Genome size (bp) [main chromosome]	G+C %	Accession number	RefSeq assembly Accession no.	Accession	Domain(s) Found	Protein length	Product	TopBLAST; evalue; bitscore
Sulfitobacter sp. strain SOLIMAR	3,453,172	60.35	AXZR00000000	GCF_000647675.1	NZ_AXZR01000002|13880..15226	N6 N4 Mtase	448	hypothetical protein	N/A
					NZ_AXZR01000003|complement(472475..473860)	DNA methylase;DNA methylase	461	DNA (cytosine-5-)-methyltransferase	N/A
					NZ_AXZR01000004|complement(138065..139165)	N6 N4 Mtase	366	site-specific DNA-methyltransferase	N/A
					NZ_AXZR01000006|complement(16061..16903)	N6 Mtase	280	peptide chain release factor N(5)-glutaminemethyltransferase	N/A
					NZ_AXZR01000006|complement(167161..168315)	DNA methylase	384	DNA (cytosine-5-)-methyltransferase	N/A
					NZ_AXZR01000011|complement(<33639..34748)	DNA methylase	370	DNA (cytosine-5-)-methyltransferase	N/A

Table #3.3 continued

Roseobacter species strains	Genome size (bp) [main chromosome]		G+C %	Accession number	RefSeq assembly Accession no.	Accession	Domain(s) Found	Protein length	Product	TopBLAST; evalue; bitscore
Sulfitobacter sp. strain CB-D (CB: 2047)	3,767,790	60	JPOY00000000		GCF_000735125.1	NZ_JPOY01000010|319302..320402	N6 N4 Mtase	366	site-specific DNA-methyltransferase	N/A
						NZ_JPOY01000011|469409..471700	Mrr cat	763	hypothetical protein	N/A
						NZ_JPOY01000011|complement(659892..660659)	N/A	255	HNH endonuclease	R1.BbrUI; 1.85e-38;132.0
						NZ_JPOY01000011|complement(693061..694791)	Methylase S;Methylase S	576	hypothetical protein	N/A
						NZ_JPOY01000011|complement(694788..696236)	HsdMN;N6 Mtase	482	SAM-dependent DNA methyltransferase	M.CfrAI;5.4e-08;43.9
						NZ_JPOY01000011|complement(696240..698702)	ResIII;EcoEI R C;HSDR N	820	restriction_endonuclease	N/A
						NZ_JPOY01000011|complement(1249791..1250921)	DNA methylase	376	DNA (cytosine-5-)-methyltransferase	N/A
						NZ_JPOY01000011|complement(1251000..1252049)	NotI	349	hypothetical_protein	N/A

Table #3.3 continued

Roseobacter species strains	Genome size (bp) [main chromosome]	G+C %	Accession number	RefSeq assembly Accession no.	Accession	Domain(s) Found	Protein length	Product	TopBLAST; evalue; bitscore
					NZ_JPOY01000011|1310061..1311215	DNA methylase	384	DNA (cytosine-5-)-methyltransferase	N/A
					NZ_JPOY01000011|1471193..1472035	N6 Mtase	280	peptide chain release factor N(5)-glutaminemethyltransferase	N/A
Sulfitobacter sp. strain CB-A (CB: YM3A)		60.3	PYUG00000000	GCF_003028485.1	NZ_PYUG01000006|319302..320402	N6 N4 Mtase	366	site-specific DNA-methyltransferase	N/A
					NZ_PYUG01000007|469409..471700	Mrr cat	763	hypothetical protein	N/A
					NZ_PYUG01000007|complement(659892..660659)	N/A	255	HNH endonuclease	R1.BbrUI;1.67e-38;132.0
					NZ_PYUG01000007|complement(693061..694791)	Methylase S;Methylase S	576	hypothetical protein	N/A
					NZ_PYUG01000007|complement(694788..696236)	HsdMN;N6 Mtase	482	SAM-dependent DNA methyltransferase	M.CfrAI;4.860000000000005e-08;43.9

Table #3.3 continued

Roseobacter species strains	Genome size (bp) [main chromosome]	G+C %	Accession number	RefSeq assembly Accession no.	Accession	Domain(s) Found	Protein length	Product	TopBLAST; evalue; bitscore
					NZ_PYUG01000007|complement(696240..698702)	ResIII;EcoEI RC;HSDRN	820	restriction endonuclease	N/A
					NZ_PYUG01000007|complement(1249791..1250921)	DNA methylase	376	DNA (cytosine-5-)-methyltransferase	N/A
					NZ_PYUG01000007|complement(1251000..1252049)	NotI	349	hypothetical protein	N/A
					NZ_PYUG01000007|1310061..1311215	DNA methylase	384	DNA (cytosine-5-)-methyltransferase	N/A
					NZ_PYUG01000007|1471193..1472035	N6 Mtase	280	peptide chain release factor N(5)-glutaminemethyltransferase	N/A
Citreicella SE45	5,523,231	67	AF388308	N/A	Genome is not sequenced				
Phaeobacter sp. strain Y4I	4,344,244	64	ABXF00000000	GCF_000156135.1	NZ_DS995281|82712..84025	DNA methylase	437	DNA (cytosine-5-)-methyltransferase	N/A
					NZ_DS995281|269348..269722	Mrr cat	124	hypothetical protein	N/A
					NZ_DS995281|569150..570676	N6 N4 Mtase	508	site-specific DNA-methyltransferase	N/A

Table #3.3 continued

Roseobacter species strains	Genome size (bp) [main chromosome]	G+C %	Accession number	RefSeq assembly Accession no.	Accession	Domain(s) Found	Protein length	Product	TopBLAST; evalue; bitscore
				NZ_DS995281	570673..573357	ResIII	894	hypothetical protein	N/A
				NZ_DS995281	complement(907218..908144)	Mrr N;Mrr cat	308	restriction endonuclease	N/A
				NZ_DS995281	complement(954578..>955012)	NaeI	144	hypothetical protein	N/A
				NZ_DS995281	complement(<955186..955460)	NaeI	91	hypothetical protein	N/A
				NZ_DS995281	complement(955563..956522)	DNA methylase	319	DNA cytosine methyltransferase	N/A
				NZ_DS995281	1286180..1287037	N6 Mtase	285	peptide chain release factor N(5)-glutaminemethyltransferase	N/A
				NZ_DS995281	complement(1324411..1325904)	DNA methylase; DNA methylase	497	DNA cytosine methyltransferase	N/A
				NZ_DS995281	complement(<1377899..1379773)	ResIII;HSDR N	625	deoxyribonuclease	N/A

Table #3.3 continued

Roseobacter species strains	Genome size (bp) [main chromosome]	G+C %	Accession number	RefSeq assembly Accession no.	Accession	Domain(s) Found	Protein length	Product	TopBLAST; evalue; bitscore
					NZ_DS995281|complement(1380602..1381207)	N/A	201	hypothetical protein	S.EcoR15I;1.27e-14;64.7
					NZ_DS995281|2522408..2524858	ResIII;EcoEIR C;HSDR N	816	DEAD	N/A
					NZ_DS995281|2525398..2526843	HsdM N;N6 Mtase	481	SAM-dependent DNA methyltransferase	M.CfrAI;1.0800000000000002e-09;48.9
					NZ_DS995281|2527919..2529649	Methylase S;Methylase S	576	type I site-specific deoxyribonuclease chain S	N/A
					NZ_DS995281|3729282..3730385	N6 N4 Mtase	367	site-specific DNA-methyltransferase	N/A
Roseovarius nubinhibens ISM	3,668,667	63	AF098495	N/A	Genome is not sequenced				

Table #3.3 continued

Roseobacter species strains	Genome size (bp) [main chromosome]	G+C %	Accession number	RefSeq assembly Accession no.	Accession	Domain(s) Found	Protein length	Product	TopBLAST; evalue; bitscore
Sagittula stellata E37	5,262,893	65	AAYA00000000	GCF_000169415.1	NZ_AAYA01000020|49982..53377	N/A	1131	class I SAM-dependent DNA methyltransferase	SstE37I;0.0; 2338.0
					NZ_AAYA01000014|complement(97254..101087)	N6 Mtase;TaqI C N6 N4	1277	restriction endonuclease subunit M site-specific DNA-methyltransferase	N/A
					NZ_AAYA01000001|170219..171316	Mtase	365		N/A
Rhodobacteraceae strain pspc.2			AY149624	N/A	Genome is not sequenced				
Rhodobacteraceae strain SE62	4,581,948	57	AY038920	N/A	Genome is not sequenced				

Table #3.3 continued

Roseobacter species strains	Genome size (bp) [main chromosome]	G+C %	Accession number	RefSeq assembly Accession no.	Accession	Domain(s) Found	Protein length	Product	TopBLAST; evalue; bitscore
Roseovarius sp. 217	4,762,632	60	AAMV00000000	GCF_000152845.1	NZ_CH902587|complement(17010..17918)	Mrr cat	302	hypothetical protein	N/A
					NZ_CH902586|complement(42653..45415)	N/A	920	class I SAM-dependent DNA methyltransferase	Cba4G11III;0.0;1387.0
					NZ_CH902584|complement(878447..880114)	DNA methylase	555	DNA cytosine methyltransferase	N/A
					NZ_CH902584|complement(1175035..1176150)	N6 N4 Mtase	371	site-specific DNA-methyltransferase	N/A
					NZ_CH902584|complement(1859991..1863359)	ResIII Helicase C;ResIII;Mrr cat	1122	hypothetical protein	N/A
					NZ_CH902584|3270737..3272410	DNA methylase;DNA methylase	557	DNA helicase	N/A
					NZ_CH902584|3273398..3274558	NA	386	multidrug DMT transporter	N/A

Table #3.3 continued

Roseobacter species strains	Genome size (bp) [main chromosome]	G+C %	Accession number	RefSeq assembly Accession no.	Accession	Domain(s) Found	Protein length	Protein Product	TopBLAST; evalue; bitscore
				NZ_CH902584|complement(3274555..3275313)		RE Eco29kI	252	Eco29kI family restriction endonuclease	N/A
				NZ_CH902584|3284230..3285603		N6 N4 Mtase	457	DNA methylase	N/A
				NZ_CH902584|3304206..3307463		N/A	1085	SAM-dependent methyltransferase	Bgl2196IV;0.0; 904.0
				NZ_CH902584|3318549..3319829		N6 N4 Mtase	426	DNA methylase	N/A
Phaeobacter sp. strain Y3F			AF253467	N/A	Genome is not sequenced				
Ruegaria pomeroyi DSS.3	4,109,442	64.2	CP000031.2; CP000032.1	N/A	Genome is not sequenced				
Silicibacter lacuscaerulensis ITI-1157	3,523,710	63	U77644	N/A	Genome is not sequenced				
Ruegaria sp. TM1040	3,201,640	60	NC_008044	N/A	Genome is not sequenced				

Table #3.3 continued

Roseobacter species strains	Genome size (bp) [main chromosome]	G+C %	Accession number	RefSeq assembly Accession no.	Accession	Domain(s) Found	Protein length	Product	TopBLAST; evalue; bitscore
Sulfitobacter pontiacus Chlg1ϕ			NR_026418	N/A	Genome is not sequenced				
Jannaschia strain CCS1	4,317,977	62.2	NC_007802	N/A	Genome is not sequenced				
Phaeobacter daeponensis KCTC 12794		64.9	DQ981486	N/A	Genome is not sequenced				

Figure legend.

Fig 3.1. Sequence alignment of *Sulfitobacter* sp. strains that contain putative attachment site (*attB*). Genomes were organized from greatest to least sequence similarity to *Sulfitobacter* sp. strain CB-D.

Fig 3.2. Geographical isolation location of Sulfitobacter strains that contain putative attachment site (*attB*). These strains show diversity in isolation location.

Fig 3.3. Phylogenic tree showing relatedness of roseobacter strains analyzed in this study. Full length 16S rRNA sequences were obtained from NCBI. *E. coli* K-12 was used as the outgroup. Strains shown in orange contain the *attB* site of prophage integration.

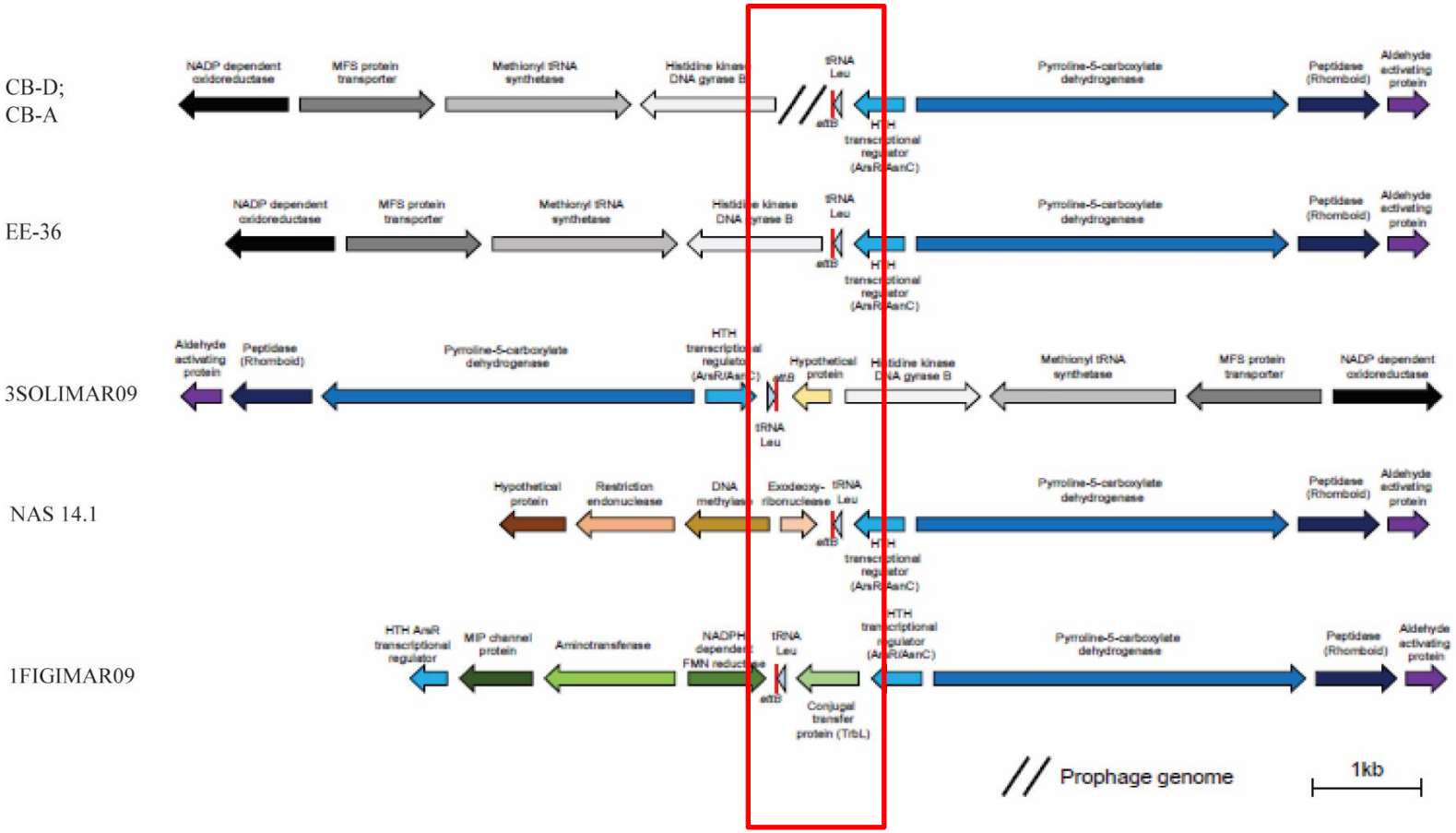

Fig 3.1. Sequence alignment of *Sulfitobacter* sp. strains that contain putative attachment site (*attB*). Genomes were organized from greatest to least sequence similarity to *Sulfitobacter* sp. strain CB-D.

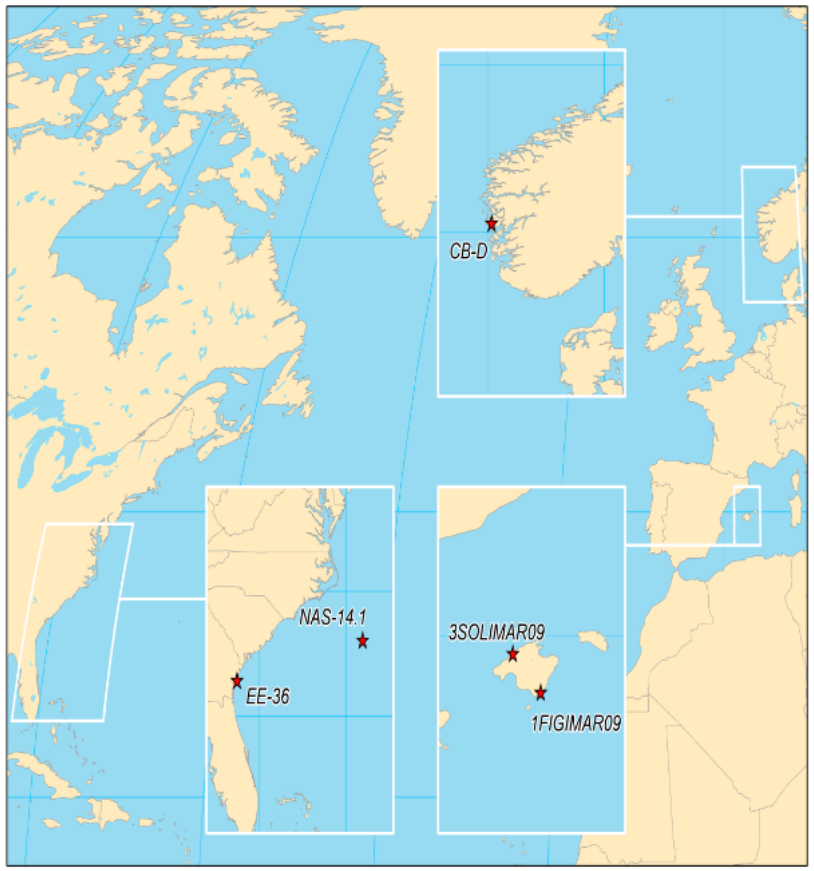

Fig 3.2. Geographical isolation location of Sulfitobacter strains that contain putative attachment site (*attB*). These strains show diversity in isolation location.

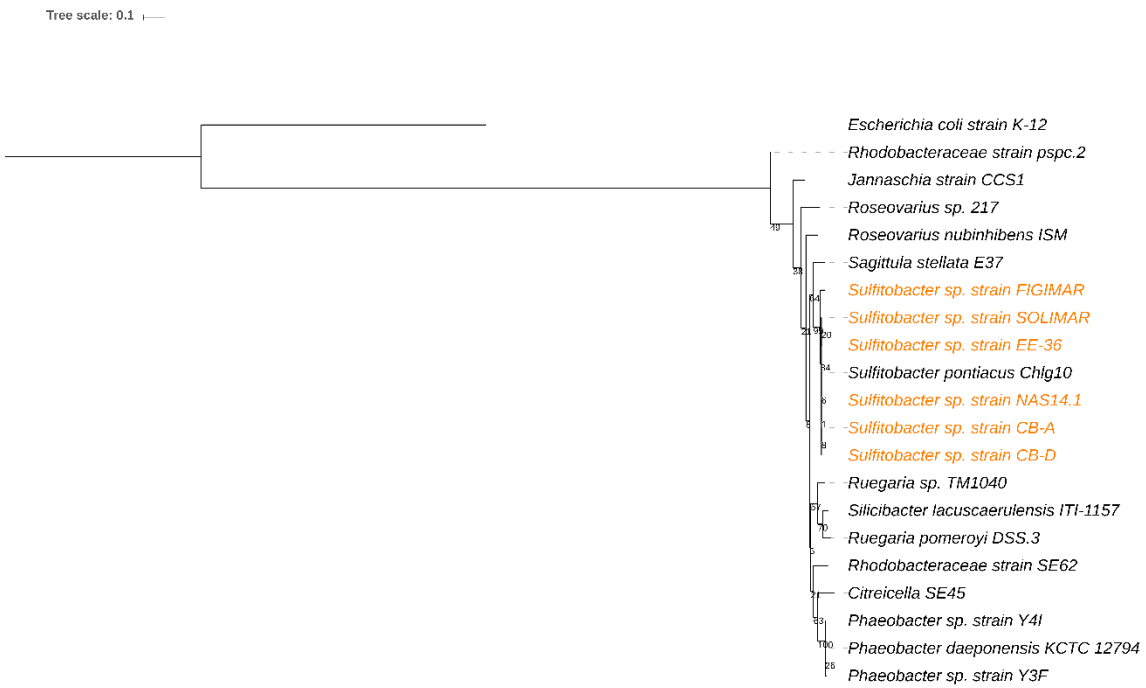

Fig 3.3. Phylogenic tree showing relatedness of roseobacter strains analyzed in this study. Full length 16S rRNA sequences were obtained from NCBI. *E. coli* K-12 was used as the outgroup. Strains shown in orange contain the *attB* site of prophage integration.

CHAPTER 4

SELECT METABOLITES AND LIPIDS SIGNIFICANTLY CONTRIBUTE TO HOST TCA CYCLING AND PHOSPHOLIPID BIOSYNTHESIS PATHWAYS IN A ONE-HOST-TWO-PHAGE MODEL SYSTEM WITH GENETICALLY SIMILAR PROPHAGES

A version of this chapter will be submitted for publication by Jonelle T.R. Basso, Haley Fielland, Katarina Jones, Kaylee Jacobs, Shawn R. Campagna and Alison Buchan.

JTRB and HF conducted sampling of strains for omics analyses. JTRB conducted bacterial culturing, SPI assays, viable counts experiments, and drafted the manuscript. HF conducted metabolomics and lipidomics processing. KAJ generated restructured heatmaps and PLSDA plots used in the presentation of metabolites and lipids. HF, KAJ and JTRB conducted statistical analyses on datasets. KRJ and JTRB conducted further modulation of growth dynamics, viable counts and SPI in custom-made XL test tubes (data reported in Appendix). AB aided with crafting the manuscript. AB also aided with the design and data interpretation of the study. AB and Alex Grossman reviewed this manuscript.

ABSTRACT

We have previously found evidence for the modification of specific physiologies of the lysogens *Sulfitobacter* sp. strains CB-D and CB-A. Additionally, we see evidence for spontaneous prophage induction (SPI) in these strains, which is linked to physiological differences. As a result, here I aimed to identify alterations in intracellular components. This study focused on growth dynamics, spontaneous prophage induction, metabolome and lipidome of both virocells (infected cells). Using untargeted metabolomics and lipidomics technologies a suite of 78 metabolites and 6 lipid groups were detected over a 27-hour experiment. Our results show that distinct metabolites (glutamate, aspartate, leucine/isoleucine and malate) and lipid species (phosphatidylglycerol and phosphatidylcholine) are the significant drivers of differences seen in carbon and lipid metabolic pools between virocells, rather than by a singular pathway. The aforementioned amino acids are either part of, or directly feed into the TCA cycle. The lipids are part of lipid biosynthesis through the CDP-DAG pathway. These data aim to improve the understanding of the role of temperate viruses in influencing internal cellular metabolism.

INTRODUCTION

Bacteriophages are ubiquitous in marine systems, where they are estimated to infect a third of bacteria at any given time (Bergh et al 1989). Viral lysis can lead to the release of gigatons of carbon in the oceans (Suttle 2007). Viruses are typically differentiated as either obligately lytic or temperate, though other forms have been suggested (Feiner et al 2015, Sturino and Klaenhammer 2006). Studies examining viral influence on host metabolism have almost exclusively focused on obligately lytic infections. Furthermore, knowledge of host cellular global changes is principally derived from lytic phage studies conducted in *E. coli* (Miller et al 2003, Poranen et al 2006). Reports have demonstrated that *E. coli* K-12 infection JE2571 with lytic phage PRD1 leads to changes in host gene expression, while lytic infection in *Sulfitobacter* strains has resulted in phage redirection of nutrients and shifts in host metabolism (Ankrah et al 2014b, Poranen et al 2006). The influence of temperate phage on host metabolism, however, is to a much lesser extent known or studied in model marine systems despite a dominance of lysogeny in marine systems. Temperate phages (also known as prophages when integrated into host genome) have been described as "time bombs". The precise drivers for the switch between the lysogeny and lytic cycle remain largely unknown (Paul 2008).

Prophages can influence their hosts in many ways (Wang et al 2010, Yu et al 2015). For example, the presence of phage genes can mediate host phenotypic changes. These phenotypic changes are referred to as lysogenic conversion (Bondy-Denomy and Davidson 2014). Bacterial host cells that exist in this altered state can be described as virocells, whereby infected cells behave differently from their uninfected counterparts (Forterre 2013). Through influence of host metabolism, it is suggested that such virocells may exhibit conferred competitive advantages (Harrison and Brockhurst 2017, Lai et al 2018, Paul 2008). Phages may possess Auxiliary Metabolic Genes (AMGs) that can result in significant manipulation in host carbon metabolism, nucleotide biosynthesis and/or lipid metabolism (reviewed in Breitbart et al 2018, Hurwitz et al 2013, Thompson et al 2011, reviewed in Warwick-Dugdale et al 2019).

Sulfitobacter strains and *Pseudomonas aeruginosa* studies have illustrated that viral infection causes increases of select host metabolites through phage-driven manipulation to host metabolism (Ankrah et al 2014b, De Smet et al 2016). In *P. aeruginosa*, phage-specific changes are also evident in the modification of host physiology (De Smet et al 2016). While viral infection

of the alga *Emiliania huxleyi* with *E. huxleyi* virus (EhV) have resulted in viral manipulation of the host lipidome (Fulton et al 2014, Malitsky et al 2016).

Spontaneous prophage induction (SPI), is described as the incidence whereby induction of a subset of a population occurs in the absence of a known factor or stimulus. This phenomenon is linked to differences in intracellular compounds, such as cAMP in *E. coli* (Czyz et al 2001, Nanda et al 2015, Wang et al 2010). Phenotypic differences are linked to SPI, though little is known of this phenomenon in other organisms, including roseobacters. Previously observed incidence of SPI in roseobacters provides the rationale for the investigation of intracellular composition of these lysogenized bacteria. These investigations complement observations of physiological changes. There is increasing recognition of phage-host interactions in a variety of environments (Reyes-Robles et al 2018), particularly in this virocell state, yet little is known about the effects of prophages on the metabolome and lipidome of their hosts. As a result, we wanted to investigate specific pathways using these technologies.

Marine bacteria belonging to the Roseobacter clade are ubiquitous, ecologically important, and have important implications in global biogeochemical cycles (Ankrah et al 2014b, Buchan et al 2005, Buchan et al 2014). Roseobacters are often lysogenized by prophage (Ankrah et al 2014a, Zhan and Chen 2019), and previously identified, virocells *Sulfitobacter* sp. strains CB-A and CB-D are lysogenized by ϕ-A and ϕ-D, respectively. These roseophages share 79% sequence identity and help bring about phenotypic differences to their host (Chapter 2 of this dissertation). To our knowledge, we are the first to explore the influence of two very similar temperate phages on a singular host, simultaneously investigating host growth dynamics, incidence of SPI and metabolism. We predict that temperate phage influence will be apparent in general pathways that contribute to producing biochemical building blocks. We anticipate this be reflected in differences in the relative contributions of intracellular metabolites and lipids between the two strains.

MATERIALS AND METHODS

Different growth conditions sampling methodology.

Sulfitobacter sp. strains CB-A and CB-D were inoculated and incubated overnight in Standard Marine Media (SMM) in 10 ml cultures at 25ºC at 200 rpm. Overnight cultures were sub-cultured, and samples of cultures at T0 hours were taken at $OD_{540nm} \approx 0.17$. Growth was monitored every two hours for 24 hours. Samples were taken at T0 hours, T4 hours, T8 hours and T21 hours Both bacterial species strains were grown in biological triplicate in 10 ml test tubes, 200 ml unbaffled flasks and 200 ml baffled flasks to test the effects of growth dynamics, viable counts and SPI on growth conditions. Subsequent experiments were conducted in 200 ml baffled flasks only.

200 ml baffled flasks sampling methodology.

Samples were taken at T0 hours, T2 hours, T4 hours, T6 hours, T8 hours, T14 hours, T21 hours and T27 hours. 5 ml of bacterial culture was filtered at each time point for metabolomics processing and analysis. 5 ml of bacterial culture was placed in 15ml conical tubes, centrifuged at 4,000 rpm for 30 minutes @ 4ºC, then taken for lipidomics processing and analysis. 1 ml of bacterial culture was additionally taken for serial dilutions (plating 10^{-5}, 10^{-6}, 10^{-7} dilutions), to obtain viable counts data and CFU/ml calculations. All sampling was conducted in biological triplicate. Blanks were used as negative controls, and T0 hours data was used for data normalization. Optical density readings and viable counts were conducted for the biological triplicates at OD_{540nm}.

Spot plating assays for SPI detection.

1 ml of bacterial culture was taken for spontaneous prophage induction (SPI) detection. *Sulfitobacter* sp. strains CB-A and CB-D were inoculated in duplicate and incubated overnight in 10 ml of SMM at 200 rpm at 25ºC. *Sulfitobacter* sp. strains were sub-cultured in SMM, and at an optical density of 0.10 (OD_{540nm}), 500ul of bacterial culture was added to 3 ml top agar aliquots and plated. Top agar was prepared ahead of time using 0.57-0.6 g (0.55-0.60%) noble agar. Once this top layer dried, 10 µl of ϕ-D and ϕ-A lysate were spot plated for all strains. This was done in technical triplicate. Serial dilutions were done for viral lysate of ϕ-A and ϕ-D. Serial dilutions ranging from undiluted to 10^{-5} were plated for ϕ-A. Dilutions ranging from undiluted to 10^{-3} were

plated for ϕ-D. The schematic included an SMM only and an uninduced control. Plates were incubated at room temperature, and zones of clearing were observed 24-48 hours after plating.

Metabolomics.

1.3 ml of extraction solvent (4:4:2 acetonitrile:methanol:water with 0.1% formic acid) was added to each petri dish, with the filter cell side down. Samples were kept at -20^{o}C for 20 minutes. Samples were thawed at 4^{o}C for 30-60 minutes. Filters were flipped over, and the back of the filters rinsed with solvent in the petri dish. These samples were then transferred into tubes, which were centrifuged for 5 minutes at 4,000 rpm. Supernatant was transferred into new tubes, and cells from the first set of tubes were resuspended in 200ul of solvent, were kept at -20^{o}C for 20 minutes, then transferred to the second set of tubes. These samples were dried under a steady flow of nitrogen. Solid residue was resuspended in 300ul of MilliQ water and transferred to autosampler vials. Samples were analyzed through liquid chromatography-mass spectrometry (LC-MS).

Lipidomics.

Methodology for lipidomics analysis is greatly derived from Xue, 2010. 1000 µl of sample were centrifuged @ 9,000 rpm for 5 minutes. The supernatant was decanted, and the pellet resuspended in 1 ml of 15:15:5:1:0.18 95% EtOH, water, diethyl ether, pyridine, and 4.2 N ammonium hydroxide. 100ul of glass beads were added and the mixture vortexed. Samples were kept in a water bath at 60^{o}C for 20 minutes, then centrifuged at 10,000 rpm for 10 minutes. Supernatant was removed, then added to dram vials. Resuspension and water bath steps previously described were repeated, added to same dram vials, then dried under a steady stream of nitrogen. Samples were then resuspended in 300 µl of water saturated butanol and 150 µl of water. These were then centrifuged at 10,000 rpm for 2 minutes, and the top butanol phase was added to dram vials. The aqueous phase was re-extracted with 300ul of water saturated butanol, vortexed, then centrifuged at 10,000 rpm for 2 minutes. The top butanol phase was added to the dram vials. Samples were then dried under a steady stream of nitrogen, resuspended in 300 µl of a 9:1 ratio of MeOH:$CHCl_3$. Samples were analyzed through liquid chromatography-mass spectrometry (LC-MS).

Statistical analysis.

Analysis of Similarities (ANOSIM) was conducted in Primer 7 using a two-way cross with organism and time being factors. Tests were conducted for differences between unordered organism groups and across all time groups using 999 permutations. Significance level of sample statistic was 0.1%. Similarity percentage (SIMPER) two-way analyses and non-metric Multi-Dimensional Scaling (nMDS). were conducted in Primer 7 to determine species contribution. Euclidean distance was chosen for resemblance parameters and the cut-off for low contributions was 70%. Square distance and square distance standard deviation (SD) are reported. Partial least squares discriminant analysis (PLSDA) was conducted in R statistical program to determine the relationship between two matrices to explain differences between organism groups and time. Data were square root transformed in Primer 7.

RESULTS

Growth dynamics, viable counts and SPI.

Previous investigations conducted in 10 ml cultures show significant differences in growth dynamics of *Sulfitobacter* sp. strains CB-A and CB-D (Fig 4.1). (All tables and figures are located in the appendix). Here, 200 ml baffled flasks were used to reduce overt differences in cell growth due to high incidence of spontaneous prophage induction (SPI) in CB-A (Chapter 2 of this dissertation). Colony PCR confirmed that *Sulfitobacter* sp. strains CB-A and CB-D were ϕ-A and ϕ-D, positive respectively (data not shown). There was no observed significant difference in growth dynamics (OD_{540nm}) between strains grown in 200 ml baffled flasks cultures (Fig 4.1), and these data corresponded with viable counts (Table 4.1). This describes a caveat of scalability that is seldom reported in the literature. To address modulation of growth dynamics, viable counts and SPI in different vessels, we compared these parameters for cultures grown in 10 ml tubes, 200 ml baffled flasks and 200 ml unbaffled flasks (Fig 4.1). We report that from least to most aerated conditions (10 ml tube, 200 ml unbaffled flask and baffled flask, respectively), growth dynamics modulate from most distinctly different to most similar. Viable counts averages correspond with growth dynamics data (4.35×10^9 ($\pm 6.89 \times 10^8$) and 2.56×10^9 ($\pm 3.06 \times 10^8$); 4.15×10^9 ($\pm 3.94 \times 10^8$) and 5.74×10^9 ($\pm 4.65 \times 10^8$); 5.36×10^9 ($\pm 5.11 \times 10^8$) and 4.37×10^9 ($\pm 4.94 \times 10^8$), CFU/ml) for CB-A and CB-D, in 10 ml tube, 200 ml unbaffled flask and baffled flask respectively (Fig 4.1). For the same aeration gradient, we observed incidence of SPI in CB-A cultures from most to least average incidence (Fig 4.1). No plaques were observed for CB-D strains regardless of culture conditions. No significant deviation in pH from the buffered media was observed (± 0.5) and therefore pH was not a significant contributing factor to any other observed differences (data not shown).

Metabolomics data identify relative elevation in select amino acids/amino acid derivatives and differentiation by time over 27 hours.

Seventy-eight metabolites were detected and were grouped in heat maps according to general metabolic pathways (Fig 4.2). In the early phase of the cycle (0-8 hours), the following metabolites were significantly elevated in CB-A relative to CB-D: uridine, N-acetylglucosamine, glucose-6-phosphate, glucose 1-phosphate, hydroxyphenylacetate and salicylate. For the same early phase, the following metabolites were significantly elevated in CB-D relative to CB-A: we

observed significant increases in UDP, ornithine, UDP-glucose, dTDP, dTMP, IMP, hydroxybenzoate, and 3,4, dihydroxyphenylacetate (DOPAC). In late phase (14-27 hours), the following metabolites were significantly elevated in CB-A relative to CB-D: asparagine, glutamine, hydroxyphenylpyruvate, hydroxyproline, lysine, N-acetyl-beta-alanine, ornithine, dCMP, dTDP, dTMP, uridine, alpha-ketoglutarate, acetylphosphate, aminoimidazole ribotide (AIR) and citraconate. For the same late phase, the following metabolites were significantly elevated in CB-D relative to CB-A: citrate/isocitrate, trehalose/sucrose/cellobiose, FMN, purine and kynurenic acid. There was no identified pathway-specific alteration to the metabolome of CB-A or CB-D and no significant difference in metabolic pools between the strains. We observed differentiation according to time and normalized the data according to optical density. Partial Least Squares Discriminant Analysis (PLSDA) plots were created for CB-D versus CB-A (Fig 4.4A) and individually (Fig 4.4B and 4.4C). PLSDA plots identified that there was general clustering of samples according to organism (Fig 4.4A). Time point T0 and T14 were greatly differentiated, relative to all other time points which clustered together (Fig 4.4B and 4.4C). ANOSIM analysis for metabolomics experiments showed no significant difference by organism (average R sample statistic 0.218). Significance level of sample statistic was 2.9%. ANOSIM analysis for these data, however, identified significant difference by time (average R sample statistic 0.828). Significance level of sample statistic was 0.1%.

Lipidomics data reveal significant differences in select lipid species and differentiation by time.

We conducted lipidomics analysis and detected six lipid species, namely phosphatidic acid (PA), phosphatidylserine (PS), phosphatidylethanolamine (PE), phosphatidylcholine (PC), phosphatidylglycerol (PG), and phosphatidylinositol (PI) (Fig 4.3). In the early phase of the cycle (0-8 hours), the following lipids were significantly elevated in CB-A relative to CB-D: PA (34:1, 34:2, 36:1, 36:2), PE (30:6), PG (36:0) and PS (40:8). For the same early phase, the following lipids were significantly elevated in CB-D relative to CB-A: PE (30:6, 32:2, 34:2, 36:3, 36:2), PG (34:2, 34:3, 36:2, 36:3), PI (42:0), and PS (26:0, 36:1). In late phase (14-27 hours), the following lipids were significantly elevated in CB-A relative to CB-D: PA (34:2), PC (30:1, 32:1, 32:2, 34:1, 34:2, 36:0, 36:2, 36:3, 36:4, 38:2, 38:5, 42:10), PE (32:2, 32:6), PG (34:4) and PS (34:0, 40:8, 42:9, 44:9). For the same late phase, the following lipids were significantly elevated in CB-D

relative to CB-A: PC (42:6), PI (38:10), and PS (38:5). PLSDA plots showed similar patterns of differentiation as metabolites (Fig 4.5A, 4.5B and 4.5C). ANOSIM analysis for lipids experiments showed no significant difference by organism (average R sample statistic 0.398). ANOSIM analysis for these data, however, identified significant difference by time (average R sample statistic 0.53). Significance level of sample statistic was 0.1%.

Statistical analysis.

SIMPER analysis corresponding to metabolomics data across all time points identified that aspartate, malate, glutamate and leucine/isoleucine collectively accounted for 74.41% contribution observed differences in CB-D scene through the growth cycle (7.85% (± 0.35), 9.6% (± 0.31), 12.54% (± 0.35), 44.42% (± 0.3) respectively). SIMPER analysis across all time points identified that this identical group of metabolites were responsible for 76.75% contribution to differences in CB-A across time points (7.71% (± 0.33), 14.31% (± 0.29), 16.47% (± 0.3), 38.26% (± 0.4) respectively). This group was also found to be significantly different between organisms and over time. There is significant difference between glutamate, glutamine, and aspartate in CB-D and CB-A at 14 hours. There is significant difference between glutamate and aspartate in CB-D and CB-A at 27 hours (Fig 4.6). Due to the direct relationship between glutamate and glutamine, glutamate:glutamine ratios were determined. Glutamate normalized peak values were two orders of magnitude greater than those of glutamine (Fig 4.6A), with significant difference between these ratios at 21 hours (Fig 4.6B). This group of metabolites are either part of the TCA cycle, or directly feed into the cycle (Fig 4.8).

SIMPER analysis corresponding to lipidomics data across all time points identified that PG (36:2) and PC (36:2) accounted for 76.97% of the observed differences in CB-D (31.81% (± 0.42), 45.16% (± 0.25) respectively). SIMPER analysis across all time points identified that this identical pair of lipids were collectively responsible for 72.34% of the differences in CB-A (24.78% (± 0.58), 47.56% (± 0.36) respectively). This pair continued to be significant lipids distinguishing both organisms over time. There is significant difference between PC in CB-D and CB-A at 27 hours only (Fig 4.9). These two lipids feed into the CDP-DAG pathway of lipid biosynthesis (Fig 4.10).

DISCUSSION

Though lysogeny is prevalent in marine systems (Paul 2008), there are relatively few models present that demonstrate the extent of how lysogeny shapes host carbon and lipid metabolism. To address this, we use a two-phage-one-host model system to highlight the factors influencing roseobacters-roseophage interactions. Ankrah et al. were the first to use metabolomics to identify changes in metabolic pools during a lytic viral infection between *Sulfitobacter* sp. CB-D and lytic phage ϕ-B, and identified glutamate and glutamine as key drivers (Ankrah et al 2014b). Here, we used metabolomics and lipidomics to report on the metabolome and lipidome of virocells *Sulfitobacter* sp. strains CB-D and CB-A, where a singular host is lysogenized by different temperate phages that share 79% sequence identity. We wished to determine how the presence of each temperate phage influences host internal pools and physiology. We have previously reported that ϕ-A and ϕ-D bring about physiological differences in their host, specifically growth dynamics and biofilm formation (Chapter 2 of this dissertation), which may be linked to differences in SPI and intracellular metabolic pools. In an attempt to diminish potentially conflicting effects of high cell lysis, we first identified growth conditions that minimized SPI in CB-A.

Previous research identified that cell lysis leads to the release of intracellular components that can be readily taken up by non-lysogenized cells of a community (Ankrah et al 2014b, Zhao et al 2019). In order to reduce the complexity of metabolomics and lipidomics data interpretation, we aimed to identify a method by which to decrease incidence of SPI in *Sulfitobacter* sp. strain CB-A. By modulating volume of bacterial culture and vessel type, we identified a pattern of greatest disparity in growth dynamics in least aerated conditions, and least disparity in most aerated conditions. Viable counts data correspond with these findings. Incidence of SPI follows the trend seen with growth dynamics along the same gradient. We demonstrate that experiments conducted in 10 ml tubes, 200 ml baffled flasks, and 200 ml unbaffled flasks help identify changes in growth dynamics, viable counts and SPI along an aeration gradient. This may suggest that less aerated conditions present more stressful conditions that prompt the release of more phage. We additionally tested pH of cultures grown in these vessels and identified no significant deviation in pH from these buffered media (pH 7.5 ± 0.5). We therefore suggest that differences in growth dynamics may be due to variation in aeration or the presence of reactive oxygen species (ROS). We were successful in achieving minimization of SPI in CB-A by growing cultures in 200 ml

baffled flasks. Modulations in scalability of model systems, however, highlights a level of complexity to these systems whereby caution must be considered when attempting to make definitive claims to global scale occurrences in compared to laboratory settlings.

Of the 78 metabolites that were detected and grouped by general class/pathway, no individual class of metabolites was identified that showed a consistent trend in relative abundance over the growth cycle. However, discrete metabolites within the metabolic pool were significantly elevated in one organism relative to the other at specific time points. We, therefore, conclude that there is no massive metabolic difference between the two virocells. We additionally suggest that the individual profile identities for specific amino acids are more important contributing factors of observed differences. Glutamate, aspartate, malate and isoleucine/leucine were significant drivers of virocell carbon metabolism over time. The presence of glutamate as a driver is supported by previously conducted research (Ankrah et al 2014b). Glutamate and glutamine collectively account for 99% of inorganic nitrogen shuttled into biomolecules (Yu et al 2015). Furthermore, glutamate and glutamine are greatly abundant in metabolic pools of *E. coli* (Bennett et al 2009). Significant differences in the normalized peak area for both glutamate and aspartate in the late phase of the growth cycle between virocells may suggest possible redirection of these metabolites by prophage requirements. These four metabolites either form part of the TCA cycle, or directly feed into the cycle. Nitrogen regulation in bacteria are notoriously complex, in terms of regulation at transcription and post-transcriptional levels. In order to fully evaluate nitrogen regulation in these cells, global cellular analyses of the transcriptome and proteome need to be conducted, which are both beyond the scope of the study.

Similar to the metabolomics data, we detected no discrete lipid group that showed a significant trend over time. We do identify that across all time points PG (36:2) and PC (36:2) significantly contributed to observed differences. Here, we can also conclude that there is no massive lipid difference between the two virocells and suggest that individual lipid species profiles are more significant factors. Detection of PC is an indication of cell wall degradation (Ankrah et al 2014b, Jørgensen et al 2003, Pedersen et al 2001), as would be expected as ϕ-A reverts to a lytic cycle. Others have identified a redirection of intracellular carbon during viral infection for fatty acid metabolism (Hurwitz et al 2013). These data may suggest a relationship between stress and lipid metabolism. PG and PC are both important in phospholipid biosynthesis, directly feeding into the CDP-DAG pathway.

This unique influence of temperate phages on their host is addressed by the relatively new concept of a virocell, as proposed by Patrick Forterre (Forterre 2013). A virocell is different from an uninfected cell, in terms of behavior, and others suggest there be competitive advantage conferred to existing as such (Bondy-Denomy and Davidson 2014, Chen et al 2005). Future works can seek to generate a prophage-less variant and conduct similar research in parallel with the virocells that make up our model system, in order to truly test the influence of prophage on the metabolism of this singular host. Interestingly, others have shown that by generating a phage-free variant of *Vibrio natriegens*, this new strain has greater competitive advantage over lysogenized counterparts (Pfeifer et al 2019). Altogether, these findings identify the importance of lysogeny studies and the need for associated model systems. The decreased complexity of model systems such as ours, allows for the investigation of carbon and lipid metabolism alterations during growth cycles, to allow for a systems-level approach for the elucidation of complex intracellular mechanisms.

ACKNOWLEDGEMENTS

This research was supported by NSF grant (OCE-106352) to A.B. and S.R.C.

REFERENCES

Ankrah NYD, Budinoff CR, Wilson WH, Wilhelm SW, Buchan A (2014a). Genome Sequences of Two Temperate Phages, ΦCB2047-A and ΦCB2047-C, Infecting Sulfitobacter sp. Strain 2047. *Genome Announcements* **2**.

Ankrah NYD, May AL, Middleton JL, Jones DR, Hadden MK, Gooding JR *et al* (2014b). Phage infection of an environmentally relevant marine bacterium alters host metabolism and lysate composition. *Isme Journal* **8:** 1089-1100.

Bennett BD, Kimball EH, Gao M, Osterhout R, Van Dien SJ, Rabinowitz JD (2009). Absolute metabolite concentrations and implied enzyme active site occupancy in Escherichia coli. *Nature Chemical Biology* **5:** 593-599.

Bergh O, Borsheim KY, Bratbak G, Heldal M (1989). High Abundance of Viruses Found in Aquatic Environments. *Nature* **340:** 467-468.

Bondy-Denomy J, Davidson AR (2014). When a Virus is not a Parasite: The Beneficial Effects of Prophages on Bacterial Fitness. *Journal of Microbiology* **52:** 235-242.

Breitbart M, Bonnain C, Malki K, Sawaya NA (2018). Phage puppet masters of the marine microbial realm. *Nature Microbiology* **3:** 754-766.

Buchan A, Gonzalez JM, Moran MA (2005). Overview of the marine Roseobacter lineage. *Applied and Environmental Microbiology* **71:** 5665-5677.

Buchan A, LeCleir GR, Gulvik CA, Gonzalez JM (2014). Master recyclers: features and functions of bacteria associated with phytoplankton blooms. *Nature Reviews Microbiology* **12:** 686-698.

Chen Y, Golding I, Sawai S, Guo L, Cox EC (2005). Population fitness and the regulation of Escherichia coli genes by bacterial viruses. *Plos Biology* **3:** 1276-1282.

Czyz A, Los M, Wrobel B, Wegrzyn G (2001). Inhibition of spontaneous induction of lambdoid prophages in Escherichia coli cultures: simple procedures with possible biotechnological applications. *BMC Biotechnology* **1:** 1-1.

De Smet J, Zimmermann M, Kogadeeva M, Ceyssens PJ, Vermaelen W, Blasdel B *et al* (2016). High coverage metabolomics analysis reveals phage-specific alterations to Pseudomonas aeruginosa physiology during infection. *Isme Journal* **10:** 1823-1835.

Feiner R, Argov T, Rabinovich L, Sigal N, Borovok I, Herskovits AA (2015). A new perspective on lysogeny: prophages as active regulatory switches of bacteria. *Nature Reviews Microbiology* **13:** 641-650.

Forterre P (2013). The virocell concept and environmental microbiology. *Isme Journal* **7:** 233-236.

Fulton JM, Fredricks HF, Bidle KD, Vardi A, Kendrick BJ, DiTullio GR *et al* (2014). Novel molecular determinants of viral susceptibility and resistance in the lipidome of Emiliania huxleyi. *Environmental Microbiology* **16:** 1137-1149.

Harrison E, Brockhurst MA (2017). Ecological and Evolutionary Benefits of Temperate Phage: What Does or Doesn't Kill You Makes You Stronger. *BioEssays* **39:** 1700112.

Hurwitz BL, Hallam SJ, Sullivan MB (2013). Metabolic reprogramming by viruses in the sunlit and dark ocean. *Genome biology* **14:** R123-R123.

Jørgensen NOG, Stepanaukas R, Pedersen A-GU, Hansen M, Nybroe O (2003). Occurrence and degradation of peptidoglycan in aquatic environments. *FEMS Microbiology Ecology* **46:** 269-280.

Lai JYH, Zhang H, Chiang MHY, Lun CHI, Zhang R, Lau SCK (2018). The putative functions of lysogeny in mediating the survivorship of Escherichia coli in seawater and marine sediment. *Fems Microbiology Ecology* **94**.

Malitsky S, Ziv C, Rosenwasser S, Zheng S, Schatz D, Porat Z *et al* (2016). Viral infection of the marine alga Emiliania huxleyi triggers lipidome remodeling and induces the production of highly saturated triacylglycerol. *The New phytologist* **210:** 88-96.

Miller ES, Kutter E, Mosig G, Arisaka F, Kunisawa T, Rüger W (2003). Bacteriophage T4 Genome. *Microbiology and Molecular Biology Reviews* **67:** 86.

Nanda AM, Thormann K, Frunzke J (2015). Impact of Spontaneous Prophage Induction on the Fitness of Bacterial Populations and Host-Microbe Interactions. *Journal of Bacteriology* **197:** 410-419.

Paul JH (2008). Prophages in marine bacteria: dangerous molecular time bombs or the key to survival in the seas? *Isme Journal* **2:** 579-589.

Pedersen A-GU, Thomsen TR, Lomstein BA, Jørgensen NOG (2001). Bacterial influence on amino acid enantiomerization in a coastal marine sediment. *Limnology and Oceanography* **46:** 1358-1369.

Pfeifer E, Michniewski S, Gatgens C, Munch E, Muller F, Polen T *et al* (2019). Generation of a Prophage-Free Variant of the Fast-Growing Bacterium Vibrio natriegens. *Applied and Environmental Microbiology* **85**.

Poranen MM, Ravantti JJ, Grahn AM, Gupta R, Auvinen P, Bamford DH (2006). Global Changes in Cellular Gene Expression during Bacteriophage PRD1 Infection. *Journal of Virology* **80:** 8081.

Reyes-Robles T, Dillard RS, Cairns LS, Silva-Valenzuela CA, Housman M, Ali A *et al* (2018). Vibrio cholerae Outer Membrane Vesicles Inhibit Bacteriophage Infection. *Journal of Bacteriology* **200:** e00792-00717.

Sturino JM, Klaenhammer TR (2006). Engineered bacteriophage-defence systems in bioprocessing. *Nature Reviews Microbiology* **4:** 395-404.

Suttle CA (2007). Marine viruses - major players in the global ecosystem. *Nature Reviews Microbiology* **5:** 801-812.

Thompson LR, Zeng Q, Kelly L, Huang KH, Singer AU, Stubbe J *et al* (2011). Phage auxiliary metabolic genes and the redirection of cyanobacterial host carbon metabolism. *Proceedings of the National Academy of Sciences* **108:** E757.

Wang X, Kim Y, Ma Q, Hong SH, Pokusaeva K, Sturino JM *et al* (2010). Cryptic prophages help bacteria cope with adverse environments. *Nature Communications* **1:** 147.

Warwick-Dugdale J, Buchholz HH, Allen MJ, Temperton B (2019). Host-hijacking and planktonic piracy: how phages command the microbial high seas. *Virology Journal* **16:** 15.

Yu Z-C, Chen X-L, Shen Q-T, Zhao D-L, Tang B-L, Su H-N *et al* (2015). Filamentous phages prevalent in Pseudoalteromonas spp. confer properties advantageous to host survival in Arctic sea ice. *The ISME journal* **9:** 871-881.

Zhan YC, Chen F (2019). Bacteriophages that infect marine roseobacters: genomics and ecology. *Environmental Microbiology* **21:** 1885-1895.

Zhao Z, Gonsior M, Schmitt-Kopplin P, Zhan Y, Zhang R, Jiao N *et al* (2019). Microbial transformation of virus-induced dissolved organic matter from picocyanobacteria: coupling of bacterial diversity and DOM chemodiversity. *The ISME Journal* **13:** 2551-2565.

APPENDIX

Table legend.

Table 4.1. Optical density and viable counts data for different growth conditions experiments for *Sulfitobacter* sp. strains CB-D and CB-A. 10 ml cultures, 200 ml unbaffled flasks and 200 ml baffled flasks were used to grow *Sulfitobacter* sp. strain CB-D and CB-A over 21 hours. Three replicates were done per time point.

Table 4.1. Optical density and viable counts data for different growth conditions experiments for *Sulfitobacter* sp. strains CB-D and CB-A.

10 ml

	CB-A				CB-D			
	optical density		viable counts		optical density		viable counts	
Time	Av	Stdev	Av	Stdev	Av	Stdev	Av	Stdev
-1	0.13	0.01			0.11	0.08		
0	0.17	0.02	2.77E+08	3.11E+07	0.18	0.01	2.44E+08	4.68E+07
2	0.31	0.03			0.33	0.01		
4	0.51	0.02	6.51E+08	1.38E+08	0.56	0.01	9.24E+08	1.47E+08
6	0.67	0.02			0.77	0.02		
8	0.82	0.03	1.84E+09	3.92E+08	0.95	0.01	1.96E+09	3.56E+08
10	0.93	0.03			1.13	0.00		
12	0.98	0.02			1.24	0.00		
18	1.05	0.03			1.48	0.02		
21	1.05	0.01	4.35E+09	6.89E+08	1.49	0.01	2.56E+09	3.06E+08

200 ml unbaffled

	CB-A				CB-D			
	optical density		viable counts		optical density		viable counts	
Time	Av	Stdev	Av	Stdev	Av	Stdev	Av	Stdev
-1	0.08	0.00			0.07	0.00		
0	0.16	0.00	3.33E+08	2.33E+07	0.17	0.00	3.91E+08	5.33E+07
2	0.30	0.01			0.36	0.00		
4	0.50	0.01	1.12E+09	1.93E+08	0.57	0.01	1.37E+09	2.37E+08
6	0.67	0.02			0.75	0.01		
8	0.82	0.02	3.17E+09	6.81E+08	0.88	0.01	3.32E+09	3.05E+08
10	0.93	0.02			0.98	0.01		
12	1.01	0.02			1.05	0.00		
18	1.13	0.01			1.20	0.00		
21	1.14	0.00	4.15E+09	3.94E+08	1.20	0.00	5.74E+09	4.65E+08

Table # 4.1 continued

200 ml baffled								
	CB-A				CB-D			
	optical density		viable counts		optical density		viable counts	
Time	Av	Stdev	Av	Stdev	Av	Stdev	Av	Stdev
-1	0.07	0.01			0.07	0.01		
0	0.14	0.03	2.93E+08	6.67E+07	0.15	0.02	4.59E+08	7.38E+07
2	0.28	0.04			0.30	0.02		
4	0.49	0.03	1.37E+09	1.80E+08	0.50	0.02	1.25E+09	1.82E+08
6	0.69	0.01			0.64	0.04		
8	0.81	0.01	3.67E+09	3.68E+08	0.75	0.06	2.80E+09	2.35E+08
10	0.89	0.02			0.87	0.05		
12	0.97	0.03			0.96	0.03		
18	1.12	0.03			1.13	0.03		
21	1.13	0.01	5.36E+09	5.11E+08	1.14	0.03	4.37E+09	4.94E+08

Figure legend.

Fig 4.1. Modulation of growth dynamics, viable counts and spontaneous prophage induction (SPI), between different vessels, over time. (A) 10 ml cultures, (B) 200 ml unbaffled flasks and (C) 200 ml baffled flasks were used to grow *Sulfitobacter* sp. strain CB-D and CB-A over 21 hours. Three replicates were done per time point.

Fig 4.2. Metabolomics heatmap analysis. Metabolomics heat map for standard marine media (SMM) showing fold change between *Sulfitobacter* sp. strain CB-D and CB-A over time. All data are normalized according to optical density. Three replicates were done per time point.

Fig 4.3. Lipidomics heatmap analysis. Lipidomics heat map for standard marine media (SMM) showing fold change between *Sulfitobacter* sp. strain CB-D and CB-A over time. All data are normalized according to optical density. Three replicates were done per time point.

Fig 4.4. Significant difference only by time. (A) PLSDA *Sulfitobacter* sp. strain CB-D and CB-A metabolites comparison for standard marine media (SMM). PLSDA by time points for metabolites for (B) *Sulfitobacter* sp. strain CB-D and (C) CB-A. All data are normalized according to optical density. Three replicates were done per time point. Numbers correspond to samples taken per organism replicate per time point. Significance level of sample statistic for ANOSIM histograms was 2.9% (organism) and 0.1% (time) for 999 permutations. Sample statistic between organisms (Average R): 0.218. Sample statistic between time points (Average R): 0.828.

Fig 4.5. Significant difference only by time. (A) PLSDA *Sulfitobacter* sp. strain CB-D and CB-A lipids comparison for standard marine media (SMM). PLSDA by time points for lipids for (B) *Sulfitobacter* sp. strain CB-D and (C) CB-A. All data are normalized according to optical density. Three replicates were done per time point. Numbers correspond to samples taken per organism replicate per time point. Significance level of sample statistic for ANOSIM histograms was 0.1% for 999 permutations. Sample statistic between organisms (Average R): 0.389. Sample statistic between time points (Average R): 0.53.

Fig 4.6. Malate, aspartate, Leucine/Isoleucine and glutamate are the highest contributors to differences in both *Sulfitobacter* sp. strain CB-D and CB-A, determined by Similarity Percent (SIMPER) statistical test. There is significant difference between glutamate, glutamine, and aspartate in CB-D and CB-A at 14 hours. There is significant difference between Glutamate and aspartate in CB-D and CB-A at 27 hours. Significant differences (Student's T-tests) are denoted by asterisks (* = $p<0.05$; ** = $p<0.01$). Averages of biological triplicates are reported for all treatments. Error bars denote standard deviation and are obscured by the data markers in some instances.

Fig 4.7. Relationship between glutamate and glutamine normalized peak area values and glutamate:glutamine ratios. (A) Glutamate normalized peak values are two orders of magnitude greater than those of glutamine. (B) There is significant difference between glutamate:glutamine ratios at 21 hours. Significant differences (Student's T-tests) are denoted by asterisks (* = $p<0.05$). Averages of biological triplicates are reported for all treatments. Error bars denote standard deviation and are obscured by the data markers in some instances.

Fig 4.8. Significant metabolite contributors to differences feed into the TCA cycle. Malate, aspartate, Leucine/Isoleucine and glutamate are the highest contributors to differences in both *Sulfitobacter* sp. strain CB-D and CB-A, determined by Similarity Percent (SIMPER) statistical test. There is significant difference between glutamate, glutamine, and aspartate in CB-D and CB-A at 14 hours. There is significant difference between glutamate and aspartate in CB-D and CB-A at 27 hours. Significant differences (Student's T-tests) are denoted by asterisks (* = $p<0.05$; ** = $p<0.01$). Averages of biological triplicates are reported for all treatments. Error bars denote standard deviation and are obscured by the data markers in some instances.

Fig 4.9. (A) Phosphotidylglycerol (PG) and (B) phosphotidylcholine (PC) are the highest contributors to differences in both *Sulfitobacter* sp. strain CB-D and CB-A, determined by Similarity Percent (SIMPER) statistical test. There is significant difference between PC in CB-D and CB-A at 27 hours only. Significant differences (Student's T-tests) are denoted by

asterisks (* = p<0.05). Averages of biological triplicates are reported for all treatments. Error bars denote standard deviation and are obscured by the data markers in some instances.

Fig 4.10. Significant phospholipid contributors to differences feed into the CDP-DAG pathway. Phosphotidylglycerol (PS) and phosphotidylcholine (PC) are the highest contributors to differences in both *Sulfitobacter* sp. strain CB-D and CB-A, determined by Similarity Percent (SIMPER) statistical test. There is significant difference between PC in CB-D and CB-A at 27 hours only. Significant differences (Student's T-tests) are denoted by asterisks (* = p<0.05). Averages of biological triplicates are reported for all treatments. Error bars denote standard deviation and are obscured by the data markers in some instances.

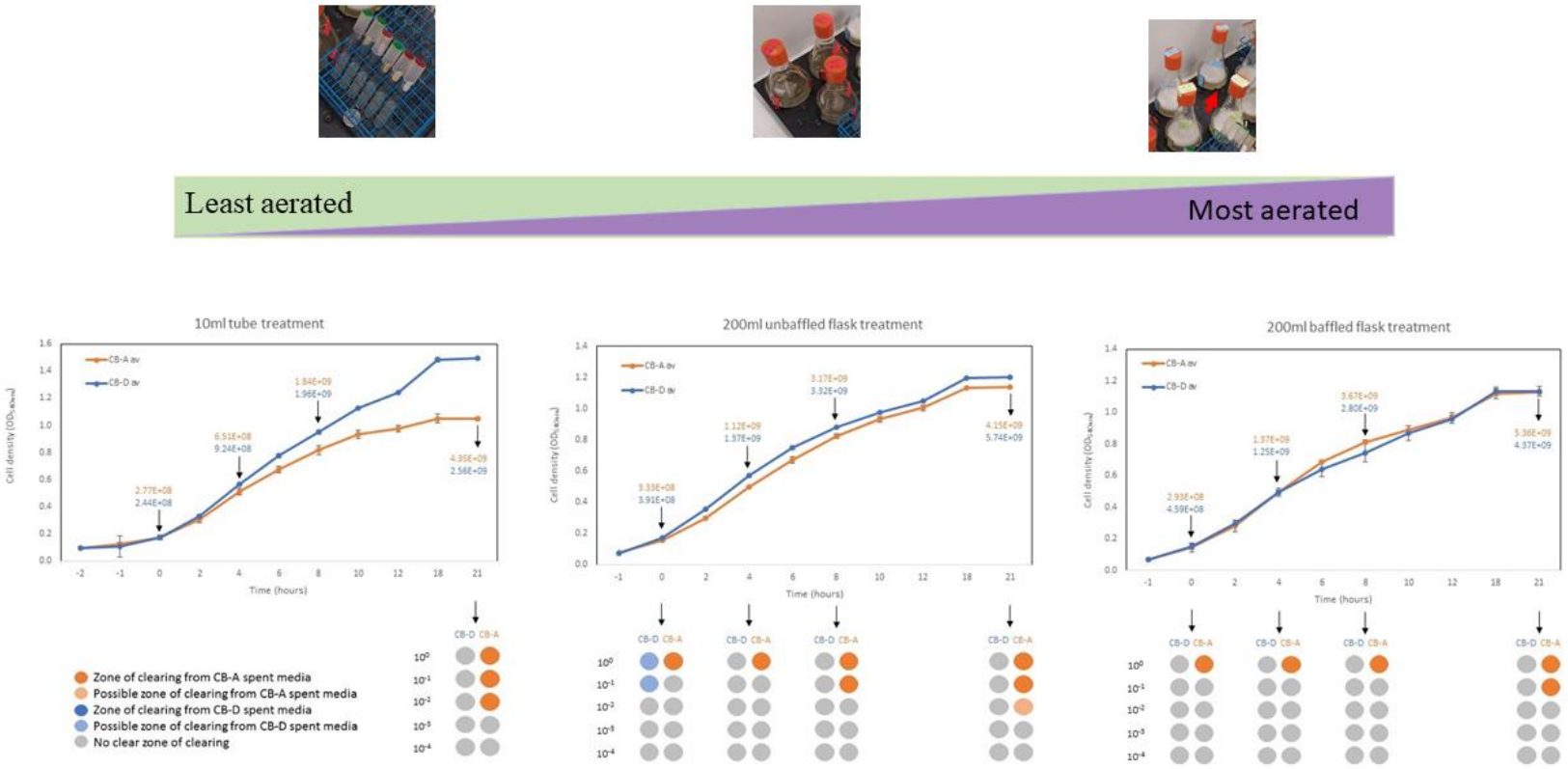

Fig 4.1. Modulation of growth dynamics, viable counts and spontaneous prophage induction (SPI), between different vessels, over time. (A) 10 ml cultures, (B) 200 ml unbaffled flasks and (C) 200 ml baffled flasks were used to grow *Sulfitobacter* sp. strain CB-D and CB-A over 21 hours. Three replicates were done per time point.

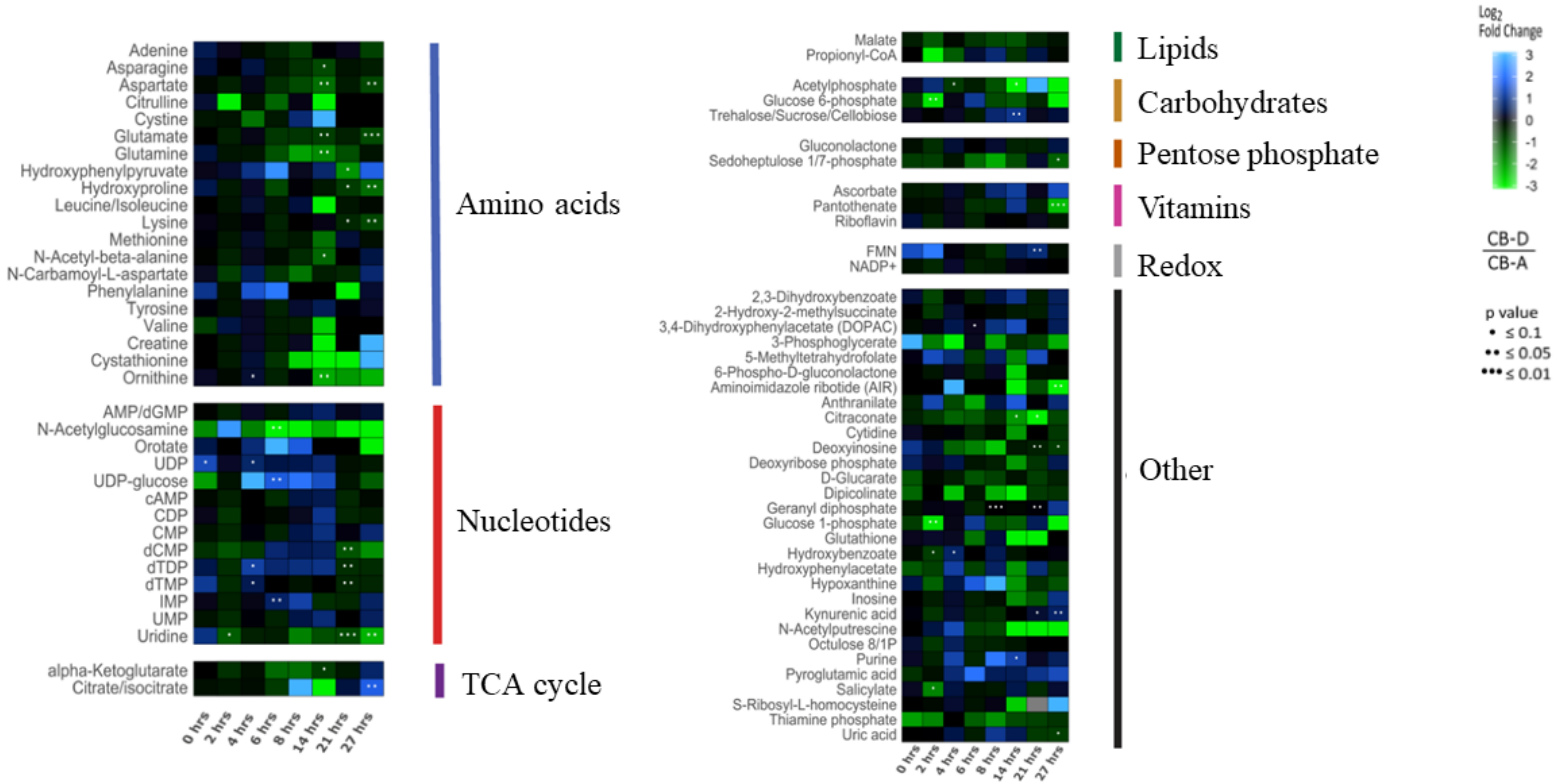

Fig 4.2. Metabolomics and lipidomics heatmap analysis. (A) Metabolomics heat maps for standard marine media (SMM) showing fold change between *Sulfitobacter* sp. strain CB-D and CB-A over time.

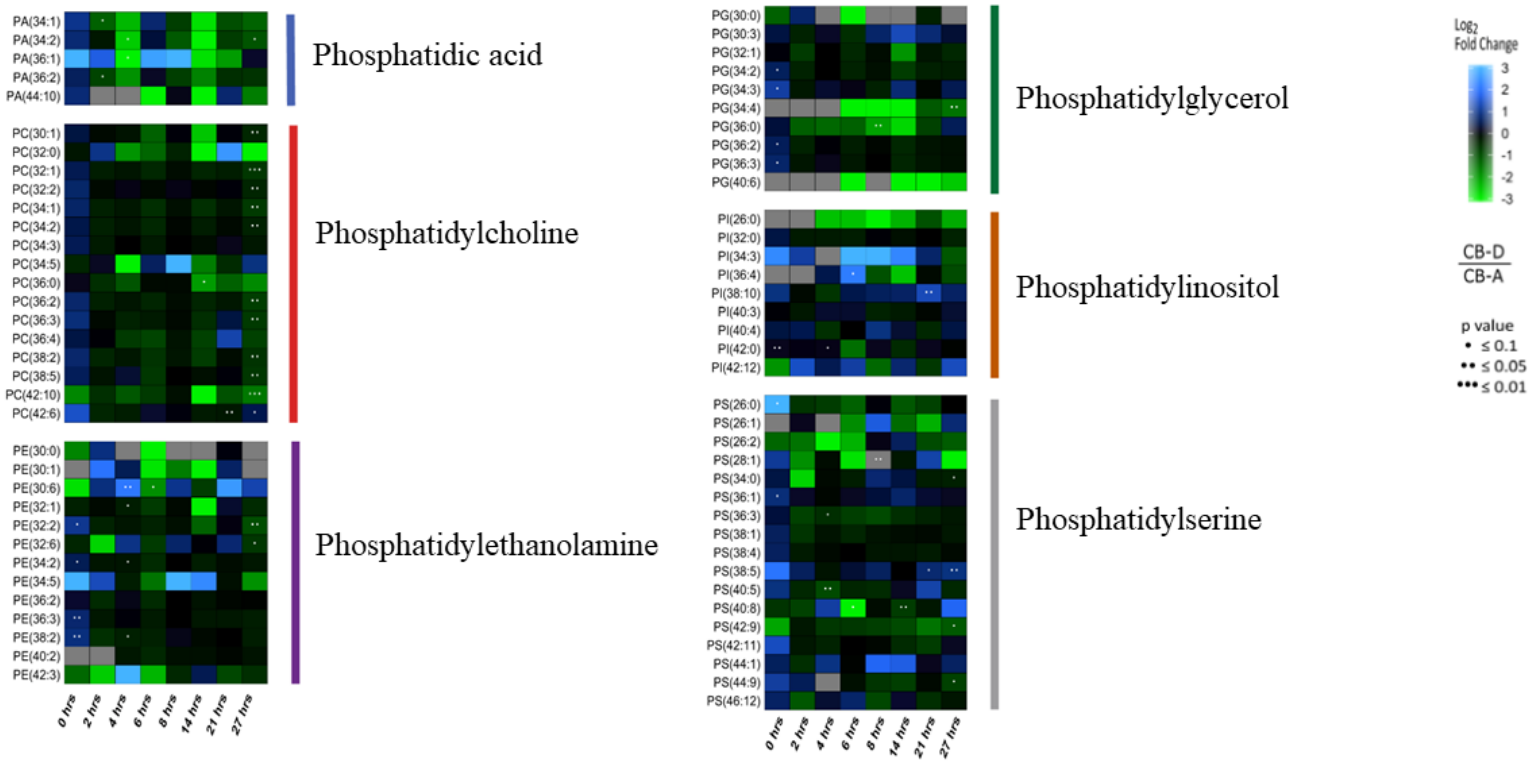

Fig 4.3. Metabolomics and lipidomics heatmap analysis. Lipidomics heat maps for standard marine media (SMM) showing fold change between *Sulfitobacter* sp. strain CB-D and CB-A over time.

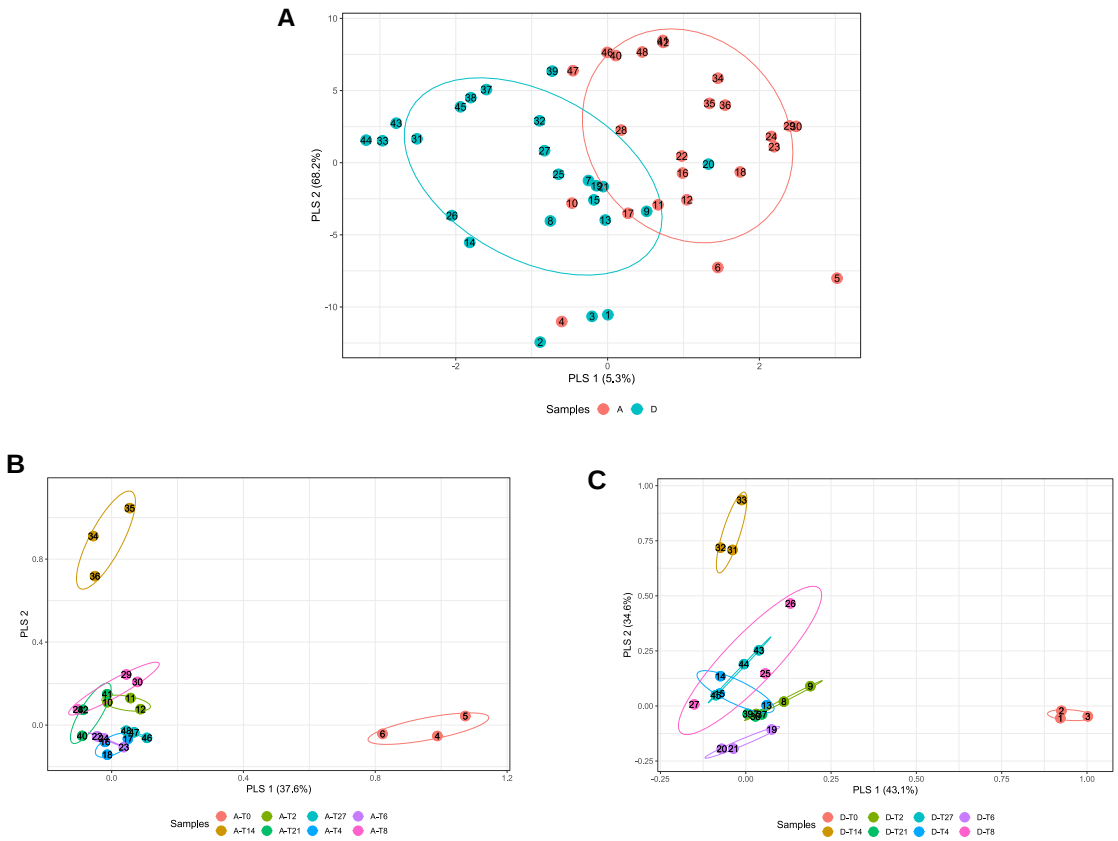

Fig 4.4. Significant difference only by time. (A) PLSDA *Sulfitobacter* sp. strain CB-D and CB-A metabolites comparison for standard marine media (SMM). PLSDA by time points for metabolites for (B) *Sulfitobacter* sp. strain CB-D and (C) CB-A. All data are normalized according to optical density. Three replicates were done per time point. Numbers correspond to samples taken per organism replicate per time point.

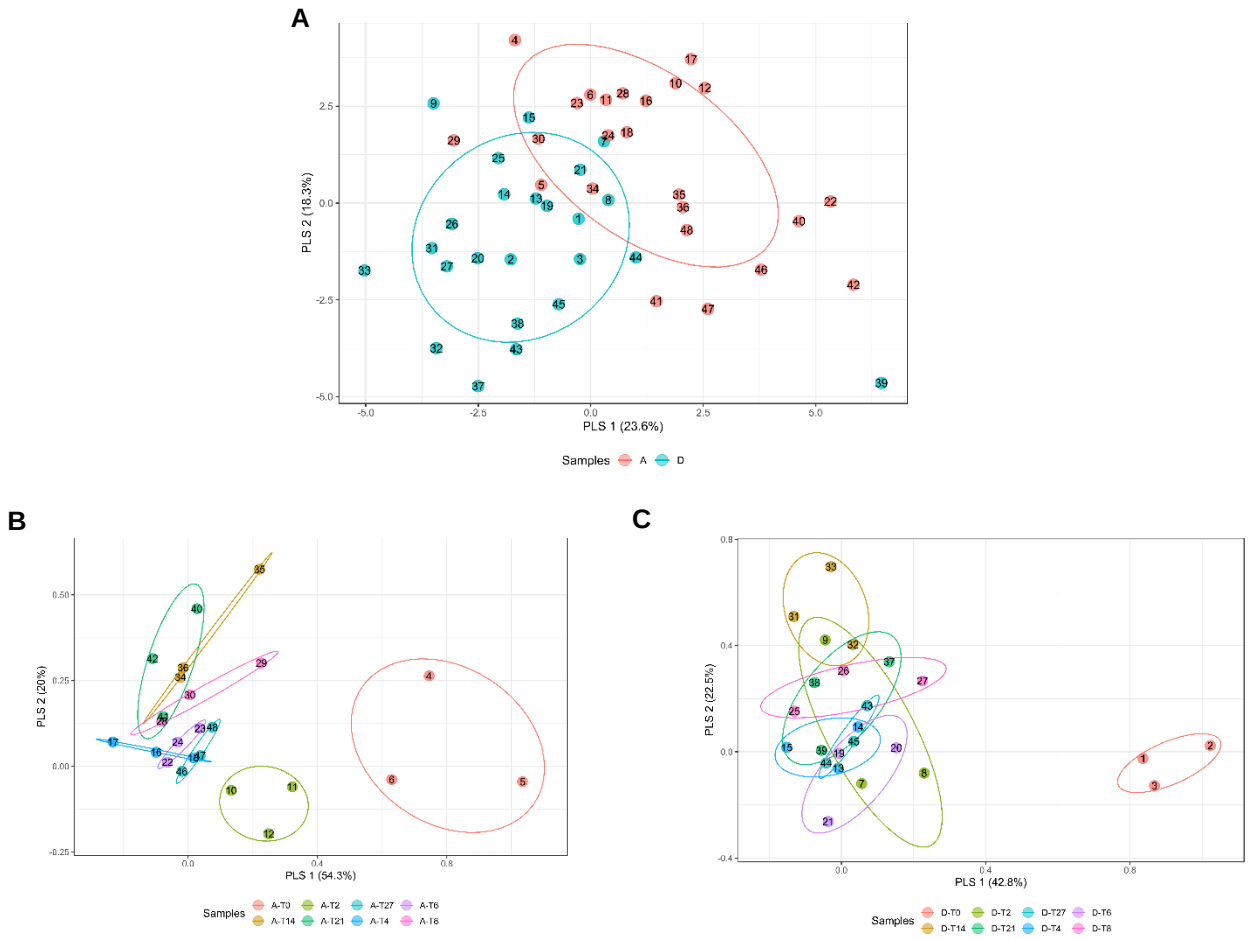

Fig 4.5. Significant difference only by time. (A) PLSDA *Sulfitobacter* sp. strain CB-D and CB-A lipids comparison for standard marine media (SMM). PLSDA by time points for lipids for (B) *Sulfitobacter* sp. strain CB-D and (C) CB-A. All data are normalized according to optical density. Three replicates were done per time point. Numbers correspond to samples taken per organism replicate per time point.

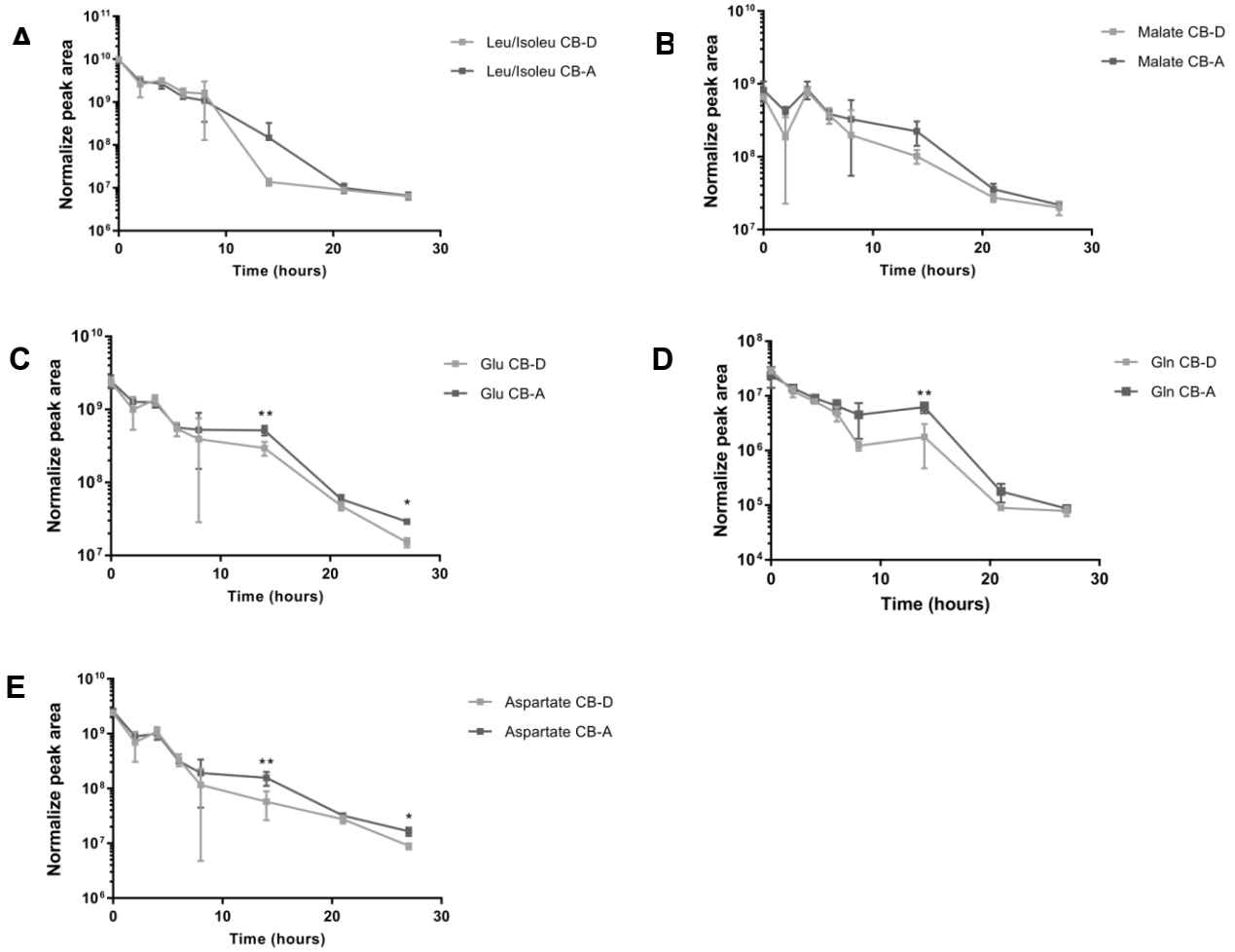

Fig 4.6. Malate, aspartate, Leucine/Isoleucine and glutamate are the highest contributors to differences in both *Sulfitobacter* sp. strain CB-D and CB-A, determined by Similarity Percent (SIMPER) statistical test.

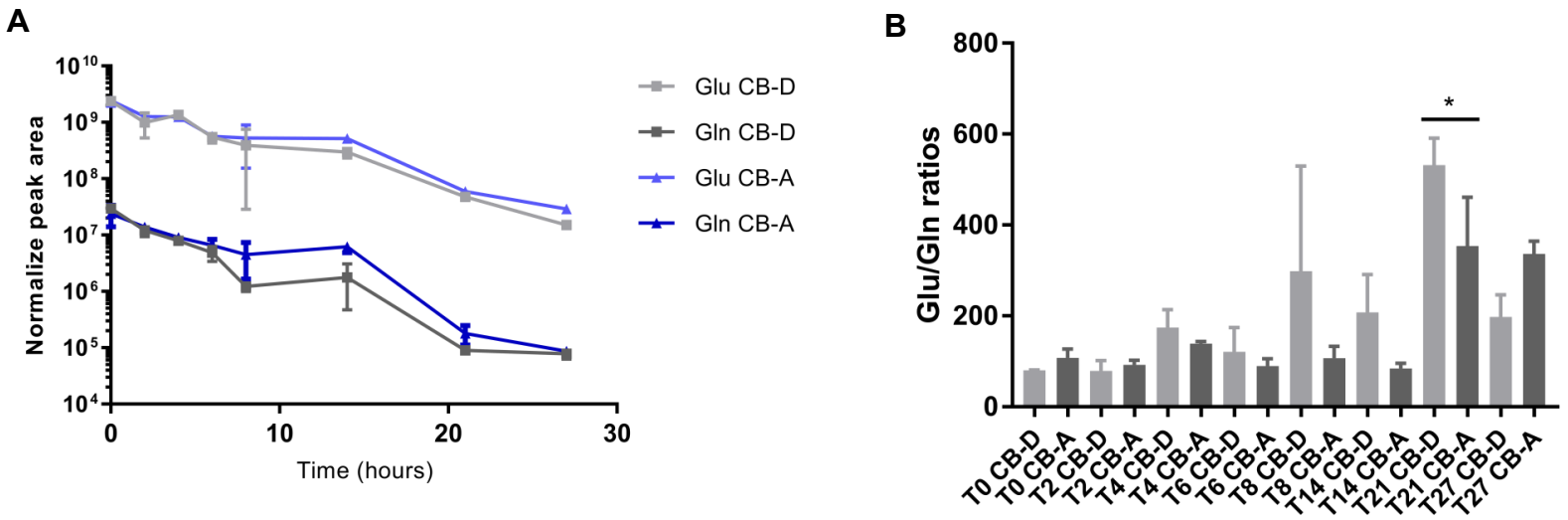

Fig 4.7. Relationship between glutamate and glutamine normalized peak area values and glutamate:glutamine ratios. (A) Glutamate normalized peak values are two orders of magnitude greater than those of glutamine. (B) There is significant difference between glutamate:glutamine ratios at 21 hours.

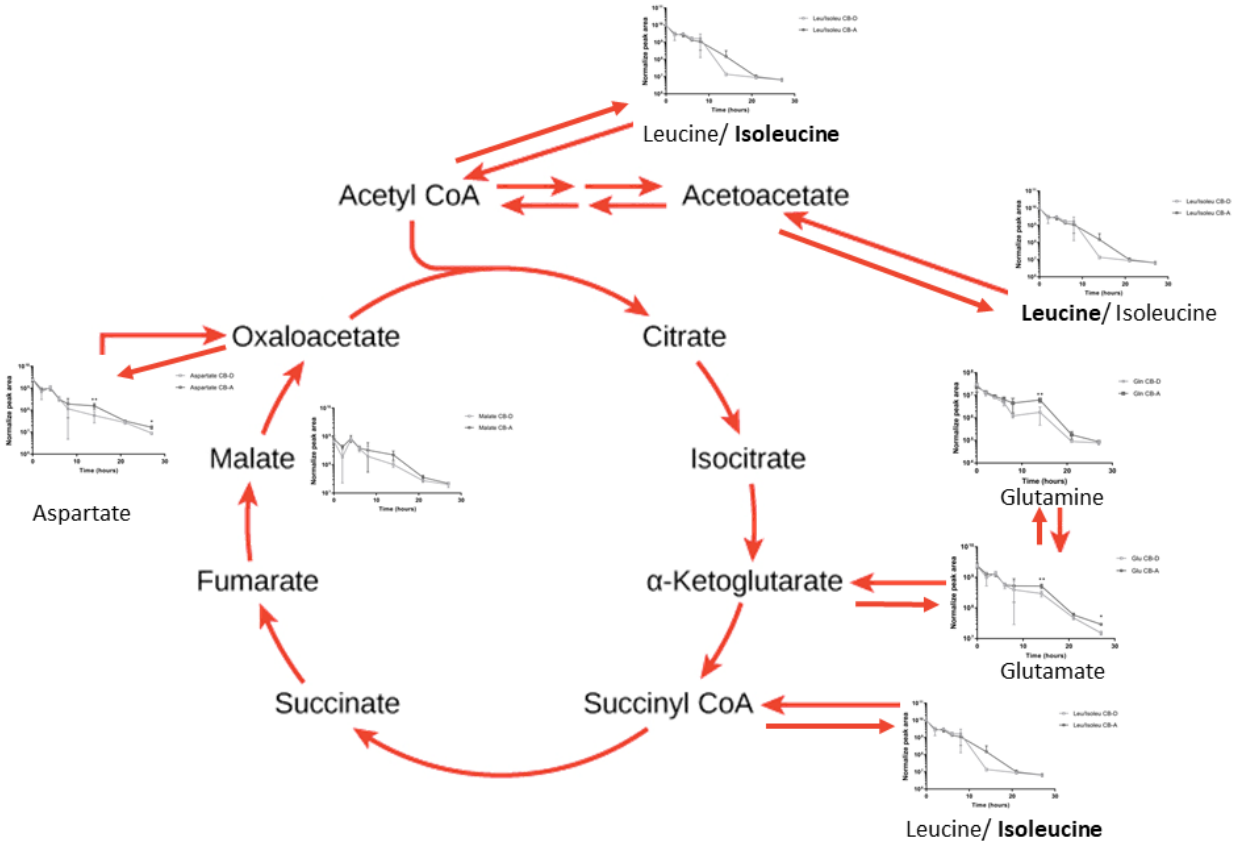

Fig 4.8. Significant metabolite contributors to differences feed into the TCA cycle. Malate, aspartate, Leucine/Isoleucine and glutamate are the highest contributors to differences in both *Sulfitobacter* sp. strain CB-D and CB-A, determined by Similarity Percent (SIMPER) statistical test.

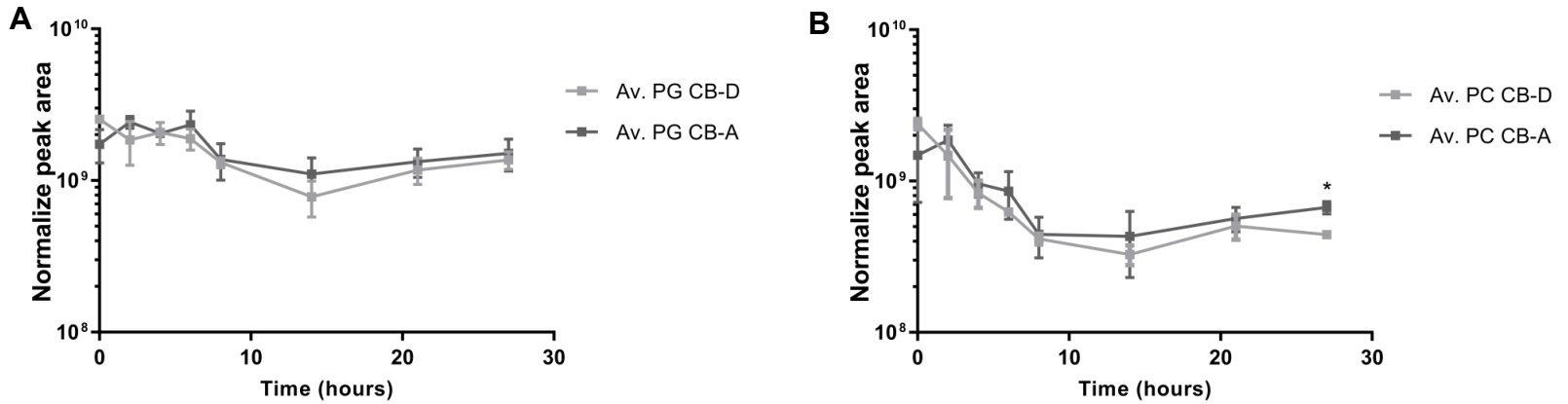

Fig 4.9. (A) Phosphatidylglycerol (PG) and (B) phosphatidylcholine (PC) are the highest contributors to differences in both *Sulfitobacter* sp. strain CB-D and CB-A, determined by Similarity Percent (SIMPER) statistical test. There is significant difference between PC in CB-D and CB-A at 27 hours only.

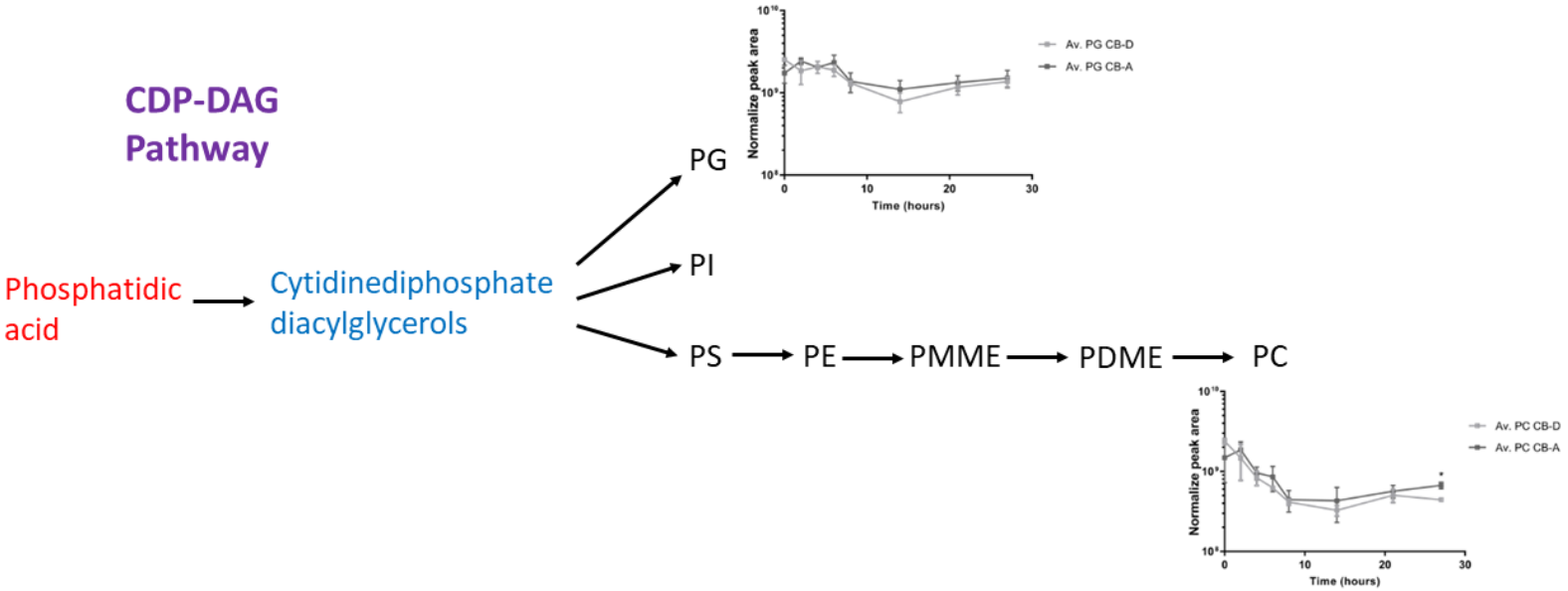

Fig 4.10. Significant phospholipid contributors to differences feed into the CDP-DAG pathway. Phosphotidylglycerol (PS) and phosphotidylcholine (PC) are the highest contributors to differences in both *Sulfitobacter* sp. strain CB-D and CB-A, determined by Similarity Percent (SIMPER) statistical test.

CHAPTER 5

A SUBSTRATE OF CHOICE: GENETICALLY SIMILAR PROPHAGES OF A ONE-HOST-TWO-PHAGE MODEL SYSTEM EXHIBIT DIFFERENCES IN HOST METABOLITE AND LIPID PROFILES DURING GROWTH ON GLUTAMATE AND ACETATE

A version of this chapter will be submitted for publication by Jonelle T.R. Basso, Katarina A. Jones, Kaylee R. Jacobs, Courtney J. Christopher, Shawn R. Campagna and Alison Buchan.

JTRB, KAJ, KRJ and CJC conducted sampling of strains for omics analyses. JTRB conducted bacterial culturing, viable counts experiments, and drafted the manuscript. KRJ conducted SPI assays. KAJ and CJC conducted metabolomics and lipidomics processing. KAJ generated restructured heatmaps and PLSDA plots used in the presentation of metabolites and lipids. KAJ and JTRB conducted statistical analyses on datasets. KRJ and JTRB conducted further modulation of growth dynamics, viable counts and SPI in custom-made XL test tubes on glutamate and acetate grown cultures (data reported in appendix 1). AB aided with crafting the manuscript and data interpretation of the study. AB and SRC aided with the design of the study. AB and KAJ reviewed this manuscript.

ABSTRACT

We have previously found evidence for the modification of specific physiologies of our model virocells, *Sulfitobacter* sp. strains CB-D and CB-A. We have additionally identified incidence of spontaneous prophage induction (SPI), which is linked to physiological differences. I therefore aimed to determine alterations in intracellular composition. This study focused on growth dynamics, SPI, metabolome, and lipidome of both lysogenized cells during growth on glutamate and acetate. Using untargeted metabolomics and lipidomics, a suite of 127 metabolites and 33 lipid groups were detected over a 24-hour experiment in glutamate. Additionally, a suite of 77 metabolites and 24 lipid groups were detected for the same time course in acetate. We determine that distinct metabolites (glutamate, pyroglutamic acid, malate, and aspartate in glutamate grown cells; glutamate, citraconate and succinate/methylmalonate in acetate grown cells) are the most dominant metabolites detected in carbon metabolic pools between virocells, as opposed to a singular pathway. Furthermore, we determine that distinct lipid species (phosphatidylglycerol and phosphatidylserine in glutamate grown cells; phosphatidylserine in acetate grown cells) are the most dominant lipids detected. Most of the aforementioned metabolites either form part of, or directly feed into the TCA cycle, and the lipids are directly part of lipid biosynthesis through the CDP-DAG pathway. These data aim to elucidate the role of temperate phages in influencing intracellular bacterial host metabolism.

INTRODUCTION

Marine bacteria are an integral part of the marine web, that form close associations with phytoplankton and phages (Sule and Belas 2013, Zhan and Chen 2019). Phage lysis influences the release of organic matter from phytoplankton and bacteria through the viral shunt thus mediating feedback of dissolved and particulate organic matter into the marine system and contributing to global nutrient cycling (Wilhelm and Suttle 1999). For example, viral lysis or grazing of the alga *Emiliania huxleyi* results in dimethylsulfonioprionate (DMSP) that can be utilized as both carbon releases and sulfur sources for heterotrophic marine bacteria (Alcolombri et al 2015). Phages are ubiquitous, and with estimates of millions of viral particles per milliliter of seawater, thus highlighting the importance of aquatic phage investigation (Bergh et al 1989, Fuhrman 1999).

Phages are capable of mediating horizontal gene transfer, eliciting phenotypic changes, altering host metabolism and providing resistance to infection by closely related phages (Bondy-Denomy et al 2016, Canchaya et al 2003, Hurwitz et al 2013, Wang et al 2010). Phages may carry auxiliary metabolic genes (AMGs), that appear to be derived from bacteria, and thus phages can influence nutrient cycling, bring about changes to host fitness, and alter host metabolic activity through redirection of pathway-specific mechanisms (Breitbart et al 2018, Lindell et al 2004, Thompson et al 2011). Phages may also enhance particulate to dissolved organism matter transitions, thereby aiding in the diversity of dissolved organic matter (Weinbauer 2004). Spontaneous prophage induction (SPI), can be defined as the phenomenon whereby phage induction of a subset of a given bacterial population occurs in the absence of a known stimulus or inducer. SPI is linked to physiological differences, though much of current knowledge is derived from studies conducted with *E. coli* (Czyz et al 2001). Metabolomic analyses help complement observations of physiological changes.

Previous studies have therefore used targeted and untargeted metabolomics approaches on uninfected *Synechococcus elongatus*, *Pseudoalteromonas lipidolytica* TC8, and other marine bacteria, or lytically infected *Sulfitobacter* strains to identify changes to the metabolome (Ankrah et al 2014, Favre et al 2017, Favre et al 2018, Fiore et al 2015). Though lysogeny is prevalent, a limited number of metabolomics studies focus on marine bacteria, and less so on temperate phages (Paul 2008). Due to the influence of temperate phages on their hosts, the term virocell has been used to describe this unique system that operates with its own phage-manipulated metabolic state

(Forterre 2013, Rosenwasser et al 2016). Currently, little is known about the effect of lysogeny on host carbon and lipid metabolism.

Roseobacters are an environmentally relevant clade of marine bacteria that are ubiquitous and are lysogenized by phage (Billerbeck et al 2016, Slightom and Buchan 2009, Zhan and Chen 2019). As a result, roseobacters and their temperate phages make idea model system components for such a study. Others have use strains of roseobacters, such as *Phaeobacter gallaeciensis* strain DSM 17395 grown on glucose to elucidate aspects of host metabolism (Zech et al 2009). There are however, few representative marine systems that study temperate phage-mediated metabolism on cells grown on different defined carbon sources.

Here, we use a two-phage-one-host model system of an ecologically relevant marine bacteria, to quantify relative abundances of metabolites and lipids in virocells *Sulfitobacter* sp. strains CB-D and CB-A, grown on glutamate and acetate over a 24-hour experiment. Since we previously observed no significant difference in the metabolome of these strains grown in standard marine media, we sought to identify differences by use of alternate carbon sources. The phages that comprise this model system share 79% sequence identity. We used an untargeted approach of metabolomics and lipidomics technologies using mass spectrometry. We aimed to identify differences in carbon and lipid metabolic pools between the virocells. We also aimed to determine incidence of SPI, differences in biomass and cell size, and conduct cell counts for cultures grown in these media. We hypothesize that different carbon substrates will differentially influence host metabolism. We suggest that glutamate is the substrate of choice, because the greater abundance of organic nitrogen that can be readily utilized by the cells, and as a result would lead to greater biomass and cell counts. The TCA cycle is the mainly used catabolic pathway for a variety of bacteria, (Han et al 2008), though some grown on acetate or iron replete conditions may alternatively use the glyoxylate shunt (Ahn et al 2016, Han et al 2008, Koedooder et al 2018). As a result, we anticipate that there will be a difference in the group of dominant metabolites and lipids detected between these carbon sources.

MATERIALS AND METHODS

Bacterial propagation- different substrates experiments.

Sulfitobacter sp. strains CB-A and CB-D were inoculated in Roseobacter Minimal Media (RMM), supplemented with either (4 mM L-glutamic acid [glutamate], 10 mM sodium acetate [acetate], 2 mM p-hydroxycinnamic acid [coumarate], 2 mM 4-hydroxy-3-methoxybenzoic acid [vanillate], glycerol, phytoplankton exudate from *Emiliana huxleyi*, 4-hydroxybenzoic acid [POB], Dimethyl sulfoxide [DSMO] or 4 mM dimethylsulfoniopropionate [DMSP]) as sole carbon source. Cultures were incubated at 25ºC at 200 rpm. Overnight cultures were sub-cultured, and samples of cultures at T0h were taken at $OD_{540nm} \approx 0.17$. Growth was monitored every two hours for 24 hours. Both bacterial species strains were grown in five biological replicates of 200 ml per flask.

Sampling methodology.

Samples were taken at time points T0 hours, T10 hours, T18 hours, and T24 hours, in order to achieve good coverage along the whole growth cycle. 5 ml of bacterial culture was filtered at each time point and taken for metabolomics processing and analysis. 5 ml of bacterial culture was also placed in 15 ml conical tubes, centrifuged at 4,000 rpm for 5 minutes @ 4ºC, then taken for lipidomics processing and analysis. Blanks were used as negative controls, and T0 hours data was used as references points for data normalization. All data were normalized by cell count. 1 ml of bacterial culture was taken for serial dilutions (plating 10^{-5}, 10^{-6}, 10^{-7} dilutions), to obtain viable counts data and CFU/ml calculations. Serial dilutions were plated in technical triplicate. Optical density readings and viable counts were conducted for the five biological replicates at OD_{540nm}. 12 ml of bacterial culture was filtered at each time point, flash frozen in liquid nitrogen, and archived at -80ºC for future transcriptomics analysis. 2 ml of culture was taken for flow cytometry. All sampling was conducted for five biological replicates for all time points.

Metabolomics.

1.3 ml of extraction solvent (4:4:2 acetonitrile:methanol:water with 0.1% formic acid) was added to each petri dish, with the filter cell side down. Samples were kept at -20ºC for 20 minutes. Filters were flipped over, and the back of the filters rinsed with solvent in the petri dish. The

solvent was then transferred into 2 ml conical tubes. 400 µl of extraction solvent was added to filters. Filters were rinsed and compressed. Solvent was transferred into the same 2 ml tubes. These samples were then centrifuged for 5 minutes at 4,000 rpm. Supernatant was transferred into new tubes, and cells from the first set of tubes were resuspended in 200 µl of solvent, were kept at -20^{o}C for 20 minutes, then transferred to the second set of tubes. These samples were dried under a steady flow of nitrogen. Solid residue was resuspended in 300 µl of MilliQ water and transferred to autosampler vials. Samples were analyzed through liquid chromatography-mass spectrometry (LC-MS). These data were normalized according to cell count.

Lipidomics.

Methodology for lipidomics analysis is greatly derived from Xue, 2010. 1000ul of sample were centrifuged @ 9,000 rpm for 5 minutes. The supernatant was decanted, and the pellet resuspended in 1 ml of 15:15:5:1:0.18 95% EtOH, water, diethyl ether, pyridine, and 4.2 N ammonium hydroxide. 100ul of glass beads were added and the mixture vortexed. Samples were kept in a water bath at 60^{o}C for 20 minutes, then centrifuged at 10,000 rpm for 10 minutes. Supernatant was removed, then added to dram vials. Resuspension and water bath steps previously described were repeated, added to same dram vials, then dried under a steady stream of nitrogen. Samples were then resuspended in 300 µl of water saturated butanol and 150ul of water. These were then centrifuged at 10,000 rpm for 2 minutes, and the top butanol phase was added to dram vials. The aqueous phase was re-extracted with 300 µl of water saturated butanol, vortexed, then centrifuged at 10,000 rpm for 2 minutes. The top butanol phase was added to the dram vials. Samples were then dried under a steady stream of nitrogen, resuspended in 300 µl of a 9:1 ratio of MeOH:$CHCl_3$. Samples were analyzed through liquid chromatography-mass spectrometry (LC-MS). These data were normalized according to cell count.

Spot plating assays for SPI detection.

1 ml of bacterial culture was taken for SPI detection. *Sulfitobacter* sp. strains CB-A and CB-D were inoculated in duplicate and incubated overnight in 10 ml of RMM supplemented with 4 mM glutamate or 10 mM acetate, at 200 rpm at 25^{o}C. *Sulfitobacter* sp. strains were sub-cultured in RMM, and at an optical density of 0.10 (OD_{540nm}), 500 µl of bacterial culture was added to 3 ml top agar aliquots and plated. Top agar was prepared ahead of time using 0.57-0.6 g (0.55-0.60%)

noble agar. Once this top layer dried, 10 µl of ϕ-D and ϕ-A lysate were spot plated for all strains. This was done in technical triplicate. Serial dilutions were done for viral lysate of ϕ-A and ϕ-D. Serial dilutions ranging from undiluted to 10^{-5} were plated for ϕ-A. Dilutions ranging from undiluted to 10^{-3} were plated for ϕ-D. The schematic included an RMM only and an uninduced control. Plates were incubated at room temperature, and zones of clearing were observed 24-48 hours after plating.

Statistical analysis.

All data are normalized according to cell count. Five replicates were done per time point. Heat maps show fold change of CB-D/CB-A and significant differences are denoted by asterisks (* = $p<0.05$; ** = $p<0.01$; *** = $p<0.001$). Analysis of Similarities (ANOSIM) was conducted in Primer 7 (Quest Research Limited, Auckland, NZ) using a two-way cross with organism and time being factors. Tests were conducted for differences between unordered organism groups and across all time groups using 999 permutations. Significance level of sample statistic was 0.1%. Similarity percentage (SIMPER) two-way analyses and non-metric Multi-Dimensional Scaling (nMDS). were conducted in Primer 7 to determine species contribution. Euclidean distance was chosen for resemblance parameters and the cut-off for low contributions was 70%. Square distance and square distance standard deviation (SD) are reported. Partial least squares discriminant analysis (PLSDA) was conducted in R statistical program to determine the relationship between two matrices to explain differences between organism groups and time. Data were square root transformed in Primer 7.

RESULTS

Sulfitobacter sp. strains CB-D and CB-A exhibit limited ability to grow on diverse set of substrates.

We used a variety of substrates that differed in terms of chemical complexity and points of entry into central catabolic pathways (Fig 5.1) (All tables and figures are located in the appendix). We first tested growth dynamics in 10 ml cultures in all substrate types. We observed that *Sulfitobacter* sp. strains CB-D and CB-A did not grow on coumarate (Fig 5.1A), *E. huxleyi* exudate (Fig 5.1B), DMSO (Fig 5.1D), or POB (Fig 5.1E). We also observed that these *Sulfitobacter* strains were unable to grow on vanillate, glycerol, or DMSP (data not shown). We did however observe growth on acetate (Fig 5.1C) and glutamate (Fig 5.1F). As a result, these two substrates were used for subsequent experiments.

Differences in growth dynamics, viable counts and cell size.

For metabolomics and lipidomics experiments, *Sulfitobacter* sp. strains CB-D and CB-A growth dynamics were monitored and sampled for 36 hours. Growth on glutamate was more favorable than on acetate. Both strains reached higher ODs on glutamate (Fig 5.2A) compared to acetate (Fig 5.2B). At 36 hours the OD_{540nm} reached 0.436 (± 0.005) and 0.416 (± 0.038), respectively, for CB-D and CB-A in RMM supplemented with 4 mM glutamate. In comparison, at the same time point, OD_{540nm} reached 0.354 (± 0.085) and 0.257 (± 0.053), respectively, for CB-D and CB-A in RMM supplemented with 10 mM acetate. For both substrates, CB-D reached higher optical densities than CB-A. Viable counts data corroborated OD_{540nm} measurements data. Average CB-D colony counts for all time points (Fig 5.2). Cell size was determined through use of flow cytometry. We observed that CB-D is significantly larger than CB-A grown on 4 mM glutamate (Fig 5.2A). In contrast, no significant difference was observed between strains grown on acetate (Fig 5.2B).

Spontaneous prophage induction is observed during growth on both substrates.

CB-A strains undergo SPI when growing on both substrates. We had previously determined that the concentration of ϕ-D that is spontaneously induced from CB-D is significantly less than ϕ-A counterparts derived from CB-A (Chapter 2 of this dissertation). As a result, we were unable

to detect SPI in response to the presence of ϕ-D in lysate for any treatment, at any time point (Table 5.1 and 5.2). Alternatively, we see that the presence of ϕ-A in lysate is detected by observation of plaques for all time points. Generally, more plaques were observed, indicating the presence of ϕ-A in lysate, for a greater range of dilutions, over time (Table 5.1 and 5.2).

Differences in glutamate metabolomics and lipidomics.

A total of 127 metabolites were detected in glutamate grown cultures (Fig 5.3). In the early phase of the cycle in glutamate grown cells (0-10 hours), 101 metabolites were significantly elevated in CB-A relative to CB-D, while one metabolite was significantly elevated in CB-D relative to CB-A. In late phase (18-24 hours), 41 metabolites were significantly elevated in CB-A relative to CB-D, while one metabolite was significantly elevated in CB-D relative to CB-A (Fig 5.3). Comparisons to T0 hours were also done for both CB-D and CB-A (Fig 5.4). There was no singular identified pathway-specific alteration to the metabolome of CB-A or CB-D. Partial Least Squares Discriminant Analysis (PLSDA) plots were created for CB-D versus CB-A (Fig 5.5A) and individually (Fig 5.5B and 5.5C). PLSDA plots identified that there was general clustering of samples according to organism (Fig 5.5A). In *Sulfitobacter* sp. strain CB-A, time point T0 and T10 were greatly differentiated, as opposed to time point T18 and T24 which clustered together (Fig 5.5B). This pattern of clustering according to time point was also observed in *Sulfitobacter* sp. strain CB-D (Fig 5.5C). ANOSIM analysis for glutamate metabolomics experiments showed significant difference by organism and time (average R sample statistic 0.389 and 0.53 respectively). Significance level of sample statistic was 0.1%. Glutamate, malate and aspartate were the most abundant metabolites as determined by normalized peak area (Fig 5.6). The highest composite average normalized peak area was of a value of ≈ 80. Overall, there was a greater relative abundance of metabolites detected for CB-A than CB-D, though the differences diminished with time (greatest differences at T0 hours, while least differences at T24 hours).

We detected 33 lipid species in these cultures (Fig 5.7), specifically phosphatidylethanolamine (PE) (34:1, 34:2, 35:1, 35:2, 36:2, 37:2, 37:3), PG (26:1, 32:0, 32:1, 34:2, 35:1, 35:2, 36:2, 36:3, 37:2, 38:2), and phosphatidylserine (PS) (26:0, 28:1, 28:2, 30:2, 33:0, 33:1, 35:0, 35:1, 35:2, 36:0, 36:1, 36:3, 37:1, 37:2, 37:3). In the early phase of the cycle in glutamate grown cells (0-10 hours), 12 lipids were significantly elevated in CB-A relative to CB-D, while 14 lipids were significantly elevated in CB-D relative to CB-A. In late phase (18-24

hours), 2 lipids were significantly elevated in CB-A relative to CB-D, while 35 lipids were significantly elevated in CB-D relative to CB-A (Fig 5.7). Comparisons to T0 hours were also done for both CB-D and CB-A (Fig 5.8). As with the metabolomics data, PLSDA plots identified general clustering of samples according to organism (Fig 5.9A). Additionally, T0 and T10 samples were also greatly differentiated, as opposed to clustering seen in T18 and T24 for both *Sulfitobacter* sp. strain CB-A (Fig 5.9B) and CB-D (Fig 5.9C). ANOSIM analysis for glutamate lipidomics also showed significant difference by organism and time (average R sample statistic 0.447 and 0.609 respectively). The average normalized peak area identified that phosphatidylcholine (PC) 34:2, phosphatidylserine (PS) 37:1, PS 35:0 and phosphatidylglycerol (PG) 36:2 were greatly detected (Fig 5.10). The highest composite average normalized peak area was of a value of ≈ 6.0. Overall, there was a greater relative abundance of lipids detected in CB-D compared to CB-A, except at T10.

Glutamate statistical analyses.

SIMPER analysis across all time points identified that aspartate, malate and glutamate collectively accounted for 77.91% contribution to differences observed in CB-D across time points (10.32% (± 0.49), 21.34% (± 0.49), 46.25% (± 0.36) respectively). SIMPER analysis across all time points identified that pyroglutamic acid, malate and glutamate collectively accounted for 88.51% contribution to differences observed in CB-A across time points (2.98% (± 0.23), 3.6% (± 0.42), 81.93% (± 0.25) respectively). Glutamate continued to be the single most contributor to observed differences between organisms and over time. SIMPER analysis across all time points identified that PC (42:11), PG (36:2) and PS (37:1) collectively accounted for 75.68% contribution of the differences in CB-D (19.38% (± 0.45), 26.15% (± 0.43), 30.19% (± 0.42) respectively). SIMPER analysis across all time points identified that PC (42:11), PC (34:1) and PS (37:1) collectively accounted for 36.38% contribution of the differences in CB-A (8.47% (± 0.5), 12.66% ± (0.25), 15.25% (± 0.41) respectively). PS (37:1) and PG (36:2) continued to be dominant lipids contributing to differences between organisms and over time. There is significant difference between glutamate, pyroglutamic acid, malate, aspartate, and glutamine in CB-D and CB-A at T0 and T10 hours (Fig 5.11). Due to the direct relationship between glutamate and glutamine, glutamate:glutamine ratios were determined and are significantly different at T10 hours (Fig 5.10F). These metabolites are either part of the TCA cycle, or feed into the cycle (Fig 5.12). There

is significant difference between both PG and PS in CB-D and CB-A at T0 and T18 hours only (Fig 5.13). These two lipids feed into the CDP-DAG pathway, contributing to lipid biosynthesis (Fig 5.14).

Differences in acetate metabolomics and lipidomics.

We detected 77 metabolites from acetate grown cultures (Fig 5.15). In the early phase of the cycle in acetate grown cells (0-10 hours), 30 metabolites were significantly elevated in CB-A relative to CB-D, while 14 metabolites were significantly elevated in CB-D relative to CB-A. In late phase (18-24 hours), 13 metabolites were significantly elevated in CB-A relative to CB-D, while 19 metabolites were significantly elevated in CB-D relative to CB-A (Fig 5.15). Comparisons to T0 hours were also done for both CB-D and CB-A (Fig 5.16). PLSDA plots were created for CB-D versus CB-A (Fig 5.17A) and individually (Fig 5.17B and 5.17C). As with glutamate there was a general clustering of samples according to organism (Fig 5.17A). Time points T0 and T10 were greatly differentiated, relative to time point T18 and T24 (Fig 5.17B and 17C). ANOSIM analysis for acetate metabolomics experiments showed significant difference by organism and time (average R sample statistic 0.549 and 0.67 respectively). Significance level of sample statistic was 0.1%. Glutamate, malate and succinate/methylmalonate were dominant metabolites as determined by normalized peak area (Fig 5.18). The highest composite average normalized peak area was of a value of ≈ 12. Overall, there was a greater relative abundance of metabolites detected for CB-A than CB-D at every time point.

We detected 24 lipids from these cultures (Fig 5.19), specifically phosphatic acid (PA) (34:1, 34:2, 36:2), phosphatidylethanolamine (PE) (34:1, 34:2, 35:1, 36:2, 37:2, 44:10),PG (32:1, 33:1, 34:1, 34:2, 35:1, 35:2, 36:2, 37:2), PS (31:1), and phosphatidylcholine (PC) (34:1, 34:2, 36:1, 36:2, 36:3, 36:4). In the early phase of the cycle in acetate grown cells (0-10 hours), no lipids were significantly elevated in CB-A relative to CB-D, while 3 lipids were significantly elevated in CB-D relative to CB-A. In late phase (18-24 hours), no lipids were significantly elevated in CB-A relative to CB-D, while 18 lipids were significantly elevated in CB-D relative to CB-A (Fig 5.19A). Comparisons to T0 hours were also done for both CB-D and CB-A (Fig 5.19B). As with the metabolomics data, non-metric Multi-Dimensional (nMDS) analysis identified general clustering of samples according to organism (Fig 5.20A). ANOSIM analysis for glutamate lipidomics also showed significant difference by organism and time (average R sample statistic 0.687 and 0.236

respectively) (Fig 5.20B). The average normalized peak area identified that PG 36:2, PG 34:2, and PG 34:1 were greatly detected (Fig 5.21). The highest composite average normalized peak area was of a value of ≈ 5.0. Overall, there was a greater relative abundance of lipids detected in CB-D compared to CB-A at all time points.

Acetate statistical analyses.

SIMPER analysis across all time points identified that malate, citraconate and glutamate collectively accounted for 42.52% contribution of the differences in CB-D (9.35% (± 0.46), 12.87% (± 0.38), 20.3% (± 0.5) respectively). SIMPER analysis across all time points identified that malate, adenine and succinate/ methylmalonate collectively accounted for 40.34% contribution of the differences in CB-A (10.16% (± 0.45), 14.76% (± 0.21), 15.42% (± 0.33) respectively). Succinate/ methylmalonate continued to be a dominant metabolite contributing to differences between organisms and over time. SIMPER analysis across all time points identified that PG (34:2), PG (34:1) and PG (36:2) were responsible for 86.31% contribution observed in CB-D (5.23% (± 0.45), 24.6% (± 0.44), 56.48% (± 0.45) respectively). SIMPER analysis across all time points identified that PC (36:2), PG (34:1) and PG (36:2) were responsible for 63.67% contribution in CB-A (11.42% (± 0.31), 13.73% ± (0.34), 38.52% (± 0.37) respectively). PG (34:1) and PG (36:2) continued to be dominant lipids metabolite contributing to differences between organisms and over time. There is significant difference between citraconate and succinate/methylmalonate, in CB-D and CB-A at T0 and T10 hours (Fig 5.22B and 5.22C). Due to the direct relationship between glutamate and glutamine, glutamate:glutamine ratios were determined, and are significantly different at T0 hours (Fig 5.22H). Most of these metabolites feed into the TCA cycle (Fig 5.23). There is significant difference between PG in CB-D and CB-A at T24 hours only (Fig 5.22I). This lipid group feeds into the CDP-DAG pathway, contributing to lipid biosynthesis (Fig 5.24).

DISCUSSION

Previous research has identified that a significant proportion of well characterized marine bacteria contain prophage signatures (Paul 2008, Touchon et al 2016). To acknowledge this uniqueness, lysogenized hosts have been deemed metabolically unique and are termed virocells (Forterre 2013). This "metabolic rewiring' may be due to the influence by phage auxiliary metabolic genes (AMGs), active lysogeny and other forms of genetic misregulation (Breitbart et al 2018, reviewed in Rosenwasser et al 2016, reviewed in Warwick-Dugdale et al 2019). It has also been acknowledged that nutrient availability can influence lysogeny (Jiang and Paul 1994). Here we report differences in host carbon and lipid metabolic pools when virocells *Sulfitobacter* sp. strains CB-A and CB-D are grown on glutamate and acetate as sole carbon sources.

Initial screening for growth in a variety of substrates that vary in terms of points entry into central catabolic pathways showed that these strains have least preference for growth on minimal media supplemented with aromatic compounds or organic sulfur compounds, which may demonstrate that they may not be able to metabolize these compounds in quantities or within a time that is detected by the conditions tested. Select *Roseobacter* strains, however, have demonstrated the ability to grow on media containing aromatic compounds such as vanillate, coumarate and p-hydroxybenzoate (POB) through studies focused on the protocatechuate component of the beta-ketoadipate pathway (Buchan et al 2000).

Between both substrates tested, we observe a much longer lag phase in organisms grown in acetate rather than glutamate and viable counts data corresponded with growth dynamics and highlight that a smaller number of cells are present in acetate rather than glutamate. Additionally, we observe a significant difference in cell size in glutamate rather than acetate, suggesting these nutrients are not being utilized. A preferred carbon source can result in the best yields or growth rates, as is illustrated previously and is reflected in our observations (Monod 1949). Spontaneous prophage induction has been previously observed in our model system in standard marine media (SMM) (Chapter 2 of this dissertation) and has been reported in other systems as it relates to host fitness and may also be linked to substrate preference (Liu et al 2019, Nanda et al 2015).

In glutamate, we detected 127 metabolites and 33 lipids, compared to acetate where we report 77 metabolites and 24 lipids. This observation may be due to few and smaller cells in acetate-grown cultures. For both substrates, there is significant differentiation according to

organism and time, demonstrating that samples of a specific time-point and strain are more similar to each other, rather than other samples. Select metabolites were dominant and consistent within the quantified intracellular compounds accounting for observed differences (aspartate, malate, glutamate, pyroglutamic acid, in cells grown in glutamate; malate, citraconate, glutamate, adenine, and succinate/ methylmalonate in cells grown in acetate). Though malate and glutamate are dominant and consistent metabolites within the quantified intracellular compounds, glutamate was the most dominant metabolite contributing to observed differences in glutamate-grown cells. Though previous studies have shown that both glutamate and glutamine are major contributors to differences during a lytic cycle, here, glutamine never contributed to more than 1% of the observed differences in either treatment (Ankrah et al 2014). Asparagine, tryptophan and histidine require both glutamate and glutamine as nitrogen donors for their production, while glutamate is the donor for the other amino acids (reviewed in Richardson et al 2015). Asparagine, tryptophan and histidine are not greatly detected and may explain the low contribution of glutamine. Glutamate can be used to replenish TCA cycle intermediates and synthesize other non-essential amino acids (Moloughney et al 2016). Though uninfected cells, others using *Phaeobacter gallaeciensis* strain DSM 17395 as a model organism have also observed modification of a select number of metabolites (Zech et al 2009). Where SPI is apparent, released DOM can be available to other microbes found in proximity, which is important in microbe-microbe interactions. Others using *Synechococcus elongatus* demonstrate that the organism is a constant source of amino acids and nucleotides that, if released, can influence the metabolism of nearby members of the microbial community (Fiore et al 2015). Furthermore, others explain that several metabolites may serve as a protective measure in instances of adaptive response to environmental or competitive alternations (Dang and Lovell 2016).

Key lipids were detected (phosphatidylcholine (PC), phosphatidylglycerol (PG), and phosphatidylserine (PS) in glutamate grown cells; PG and PC in acetate grown cells). For metabolism of fatty acids and acetate the glyoxylate cycle is a necessary alternative to the TCA cycle for cells that needing to produce glucose and may play a role in response to oxidative stress and infection (Ahn et al 2016, Clark and Cronan 2005). This redirection of cellular metabolism through the glyoxylate shunt (GS) may act as a form of metabolic acclimation of marine bacteria if grown in an iron limited environment (Koedooder et al 2018). Others have observed possible detection of phospholipids such as PG (Favre et al 2018). Phospholipids are thought to play a role

in bacterial membrane lipid plasticity in response to a variety of environmental conditions and may be linked to physiology (Favre et al 2018).

These data provide valuable complementary insights into the physiological changes in growth dynamics, cell size, and biofilm formation that we have previously observed (Chapter 2 of this dissertation).

ACKNOWLEDGEMENTS

This research was supported by NSF grant (OCE-106352) to A.B. and S.R.C. Expertise for flow cytometry was received by Benjamin Carter Calfee.

REFERENCES

Ahn S, Jung J, Jang IA, Madsen EL, Park W (2016). Role of Glyoxylate Shunt in Oxidative Stress Response. *Journal of Biological Chemistry* **291:** 11928-11938.

Alcolombri U, Ben-Dor S, Feldmesser E, Levin Y, Tawfik DS, Vardi A (2015). Identification of the algal dimethyl sulfide–releasing enzyme: A missing link in the marine sulfur cycle. *Science* **348:** 1466.

Ankrah NYD, May AL, Middleton JL, Jones DR, Hadden MK, Gooding JR *et al* (2014). Phage infection of an environmentally relevant marine bacterium alters host metabolism and lysate composition. *Isme Journal* **8:** 1089-1100.

Bergh O, Borsheim KY, Bratbak G, Heldal M (1989). High Abundance of Viruses Found in Aquatic Environments. *Nature* **340:** 467-468.

Billerbeck S, Wemheuer B, Voget S, Poehlein A, Giebel HA, Brinkhoff T *et al* (2016). Biogeography and environmental genomics of the Roseobacter-affiliated pelagic CHAB-I-5 lineage. *Nature Microbiology* **1**.

Bondy-Denomy J, Qian J, Westra ER, Buckling A, Guttman DS, Davidson AR *et al* (2016). Prophages mediate defense against phage infection through diverse mechanisms. *The ISME Journal* **10:** 2854-2866.

Breitbart M, Bonnain C, Malki K, Sawaya NA (2018). Phage puppet masters of the marine microbial realm. *Nature Microbiology* **3:** 754-766.

Buchan A, Collier LS, Neidle EL, Moran MA (2000). Key Aromatic-Ring-Cleaving Enzyme, Protocatechuate 3,4-Dioxygenase, in the Ecologically Important MarineRoseobacter Lineage. *Applied and Environmental Microbiology* **66:** 4662.

Canchaya C, Fournous G, Chibani-Chennoufi S, Dillmann ML, Brussow H (2003). Phage as agents of lateral gene transfer. *Current Opinion in Microbiology* **6:** 417-424.

Clark DP, Cronan JE (2005). Two-Carbon Compounds and Fatty Acids as Carbon Sources. *EcoSal Plus* **1**.

Czyz A, Los M, Wrobel B, Wegrzyn G (2001). Inhibition of spontaneous induction of lambdoid prophages in Escherichia coli cultures: simple procedures with possible biotechnological applications. *BMC Biotechnology* **1:** 1-1.

Dang H, Lovell CR (2016). Microbial Surface Colonization and Biofilm Development in Marine Environments. *Microbiology and Molecular Biology Reviews* **80:** 91.

Favre L, Ortalo-Magné A, Greff S, Pérez T, Thomas OP, Martin J-C *et al* (2017). Discrimination of Four Marine Biofilm-Forming Bacteria by LC–MS Metabolomics and Influence of Culture Parameters. *Journal of Proteome Research* **16:** 1962-1975.

Favre L, Ortalo-Magne A, Pichereaux C, Gargaros A, Burlet-Schiltz O, Cotelle V *et al* (2018). Metabolome and proteome changes between biofilm and planktonic phenotypes of the marine bacterium Pseudoalteromonas lipolytica TC8. *Biofouling* **34:** 132-148.

Fiore CL, Longnecker K, Kido Soule MC, Kujawinski EB (2015). Release of ecologically relevant metabolites by the cyanobacterium Synechococcus elongatus CCMP 1631. *Environmental Microbiology* **17:** 3949-3963.

Forterre P (2013). The virocell concept and environmental microbiology. *Isme Journal* **7:** 233-236.

Fuhrman JA (1999). Marine viruses and their biogeochemical and ecological effects. *Nature* **399:** 541-548.

Han SO, Inui M, Yukawa H (2008). Effect of carbon source availability and growth phase on expression of Corynebacterium glutamicum genes involved in the tricarboxylic acid cycle and glyoxylate bypass **154:** 3073-3083.

Hurwitz BL, Hallam SJ, Sullivan MB (2013). Metabolic reprogramming by viruses in the sunlit and dark ocean. *Genome biology* **14:** R123-R123.

Jiang SC, Paul JH (1994). Seasonal and Diel Abundance of Viruses and Occurrence of Lysogeny/Bacteriocinogeny in the Marine Environment. *Marine Ecology Progress Series* **104:** 163-172.

Koedooder C, Guéneuguès A, Van Geersdaële R, Vergé V, Bouget F-Y, Labreuche Y *et al* (2018). The Role of the Glyoxylate Shunt in the Acclimation to Iron Limitation in Marine Heterotrophic Bacteria **5**.

Lindell D, Sullivan MB, Johnson ZI, Tolonen AC, Rohwer F, Chisholm SW (2004). Transfer of photosynthesis genes to and from Prochlorococcus viruses. *Proceedings of the National Academy of Sciences of the United States of America* **101:** 11013.

Liu XX, Tang KH, Zhang DL, Li YM, Liu Z, Yao JY *et al* (2019). Symbiosis of a P2-family phage and deep-sea Shewanella putrefaciens. *Environmental Microbiology*.

Moloughney JG, Kim PK, Vega-Cotto NM, Wu C-C, Zhang S, Adlam M *et al* (2016). mTORC2 Responds to Glutamine Catabolite Levels to Modulate the Hexosamine Biosynthesis Enzyme GFAT1. *Molecular Cell* **63:** 811-826.

Monod J (1949). The Growth of Bacterial Cultures. *Annual Review of Microbiology* **3:** 371-394.

Nanda AM, Thormann K, Frunzke J (2015). Impact of Spontaneous Prophage Induction on the Fitness of Bacterial Populations and Host-Microbe Interactions. *Journal of Bacteriology* **197:** 410-419.

Paul JH (2008). Prophages in marine bacteria: dangerous molecular time bombs or the key to survival in the seas? *Isme Journal* **2:** 579-589.

Richardson AR, Somerville GA, Sonenshein AL (2015). Regulating the Intersection of Metabolism and Pathogenesis in Gram-positive Bacteria. *Microbiol Spectr* **3:** 10.1128/microbiolspec.MBP-0004-2014.

Rosenwasser S, Ziv C, Van Creveld SG, Vardi A (2016). Virocell Metabolism: Metabolic Innovations During Host-Virus Interactions in the Ocean. *Trends in Microbiology* **24:** 821-832.

Slightom RN, Buchan A (2009). Surface Colonization by Marine Roseobacters: Integrating Genotype and Phenotype. *Applied and Environmental Microbiology* **75:** 6027-6037.

Sule P, Belas R (2013). A Novel Inducer of Roseobacter Motility Is Also a Disruptor of Algal Symbiosis. *Journal of Bacteriology* **195:** 637-646.

Thompson LR, Zeng Q, Kelly L, Huang KH, Singer AU, Stubbe J *et al* (2011). Phage auxiliary metabolic genes and the redirection of cyanobacterial host carbon metabolism. *Proceedings of the National Academy of Sciences* **108:** E757.

Touchon M, Bernheim A, Rocha EPC (2016). Genetic and life-history traits associated with the distribution of prophages in bacteria. *Isme Journal* **10:** 2744-2754.

Wang XX, Kim Y, Ma Q, Hong SH, Pokusaeva K, Sturino JM *et al* (2010). Cryptic prophages help bacteria cope with adverse environments. *Nature Communications* **1**.

Warwick-Dugdale J, Buchholz HH, Allen MJ, Temperton B (2019). Host-hijacking and planktonic piracy: how phages command the microbial high seas. *Virology Journal* **16:** 15.

Weinbauer MG (2004). Ecology of prokaryotic viruses. *Fems Microbiology Reviews* **28:** 127-181.

Wilhelm SW, Suttle CA (1999). Viruses and Nutrient Cycles in the Sea - Viruses play critical roles in the structure and function of aquatic food webs. *Bioscience* **49:** 781-788.

Zech H, Thole S, Schreiber K, Kalhöfer D, Voget S, Brinkhoff T *et al* (2009). Growth phase-dependent global protein and metabolite profiles of Phaeobacter gallaeciensis strain DSM 17395, a member of the marine Roseobacter-clade. *PROTEOMICS* **9:** 3677-3697.

Zhan YC, Chen F (2019). Bacteriophages that infect marine roseobacters: genomics and ecology. *Environmental Microbiology* **21:** 1885-1895.

APPENDIX

Table legend.

Table 5.1. Incidence of SPI in glutamate grown cells. Spot plating assays used serial dilutions ranging from 10^0 to 10^{-3}. The presence of ϕ-D in lysate was below the limit of detection. Data for five biological replicates are reported for all treatments and all time points. Plating was done in technical triplicates of the five biological replicates. Detection of SPI is denoted by asterisks (* = detection at 10^0 dilution; ** = detection at 10^{-1} dilution; * = detection at 10^{-2} dilution; n.d. = not detected).**

Table 5.2. Incidence of SPI in acetate grown cells. Spot plating assays used serial dilutions ranging from 10^0 to 10^{-3}. The presence of ϕ-D in lysate was below the limit of detection. Data for five biological replicates are reported for all treatments and all time points. Plating was done in technical triplicates of the five biological replicates. Detection of SPI is denoted by asterisks (* = detection at 10^0 dilution; ** = detection at 10^{-1} dilution; * = detection at 10^{-2} dilution; **** = detection at 10^{-3} dilution; n.d. = not detected).**

Table 5.1. Incidence of SPI in glutamate grown cells. Spot plating assays used serial dilutions ranging from 10^0 to 10^{-3}. The presence of ϕ-D in lysate was below the limit of detection. Data for five biological replicates are reported for all treatments and all time points. Plating was done in technical triplicates of the five biological replicates. Detection of SPI is denoted by asterisks (* = detection at 10^0 dilution; ** = detection at 10^{-1} dilution; * = detection at 10^{-2} dilution; n.d. = not detected).**

4mM glutamate							
Time	**Treatment**	**Biological Replicate**	**SPI detected**	**Time**	**Treatment**	**Biological Replicate**	**SPI detected**
T0	CB-A	A	**	**T18**	CB-A	A	***
	(addition of 0.2um	B	**		(addition of 0.2um	B	**
	filter sterilized CB-A	C	**		filter sterilized CB-A	C	**
	spent media to host	D	**		spent media to host	D	***
	CB-D)	E	**		CB-D)	E	***
	CB-D	A	n.d.		CB-D	A	n.d.
	(addition of 0.2um	B	n.d.		(addition of 0.2um	B	n.d.
	filter sterilized CB-D	C	n.d.		filter sterilized CB-D	C	n.d.
	spent media to host	D	n.d.		spent media to host	D	n.d.
	CB-A)	E	n.d.		CB-A)	E	n.d.
T10	CB-A	A	**	**T24**	CB-A	A	***
	(addition of 0.2um	B	**		(addition of 0.2um	B	***
	filter sterilized CB-A	C	**		filter sterilized CB-A	C	n.d.
	spent media to host	D	**		spent media to host	D	n.d.
	CB-D)	E	**		CB-D)	E	***
	CB-D	A	n.d.		CB-D	A	n.d.
	(addition of 0.2um	B	n.d.		(addition of 0.2um	B	n.d.
	filter sterilized CB-D	C	n.d.		filter sterilized CB-D	C	n.d.
	spent media to host	D	n.d.		spent media to host	D	n.d.
	CB-A)	E	n.d.		CB-A)	E	n.d.

Table 5.2. Incidence of SPI in acetate grown cells. Spot plating assays used serial dilutions ranging from 10^0 to 10^{-3}. The presence of ϕ-D in lysate was below the limit of detection. Data for five biological replicates are reported for all treatments and all time points. Plating was done in technical triplicates of the five biological replicates. Detection of SPI is denoted by asterisks (* = detection at 10^0 dilution; ** = detection at 10^{-1} dilution; * = detection at 10^{-2} dilution; **** = detection at 10^{-3} dilution; n.d. = not detected).**

10mM acetate							
Time	**Treatment**	**Biological Replicate**	**SPI detected**	**Time**	**Treatment**	**Biological Replicate**	**SPI detected**
T0	CB-A	A	*	**T18**	CB-A	A	**
	(addition of 0.2um	B	*		(addition of 0.2um	B	*
	filter sterilized CB-A	C	*		filter sterilized CB-A	C	*
	spent media to host	D	n.d.		spent media to host	D	*
	CB-D)	E	***		CB-D)	E	****
	CB-D	A	n.d.		CB-D	A	n.d.
	(addition of 0.2um	B	n.d.		(addition of 0.2um	B	n.d.
	filter sterilized CB-D	C	n.d.		filter sterilized CB-D	C	n.d.
	spent media to host	D	n.d.		spent media to host	D	n.d.
	CB-A)	E	n.d.		CB-A)	E	n.d.
T10	CB-A	A	**	**T24**	CB-A	A	*
	(addition of 0.2um	B	**		(addition of 0.2um	B	n.d.
	filter sterilized CB-A	C	*		filter sterilized CB-A	C	*
	spent media to host	D	***		spent media to host	D	****
	CB-D)	E	*		CB-D)	E	*
	CB-D	A	n.d.		CB-D	A	n.d.
	(addition of 0.2um	B	n.d.		(addition of 0.2um	B	n.d.
	filter sterilized CB-D	C	n.d.		filter sterilized CB-D	C	n.d.
	spent media to host	D	n.d.		spent media to host	D	n.d.
	CB-A)	E	n.d.		CB-A)	E	n.d.

Figure legend.

Fig 5.1. Growth dynamics of *Sulfitobacter* sp. strains CB-D and CB-A, on a variety of growth substrates, which differ in terms of chemical complexity and points of entry into central catabolic pathways. Three replicates were done per time point.

Fig 5.2. Growth dynamics, cell size, and viable counts data for *Sulfitobacter* sp. strain CB-D and CB-A in glutamate and acetate. Cell size was measured by forward scatter through flow cytometry. Averages and standard deviations were calculated for CFU/ml. Significant difference in cell size (Student's T-tests) is denoted by asterisks (* = $p<0.05$). Averages of five biological replicates are reported for all treatments. Plating was done in technical replicates of the five biological replicates.

Fig 5.3. Metabolomics heatmap analysis. Heat maps for glutamate grown cells showing fold change between *Sulfitobacter* sp. strain CB-D and CB-A over time. All data are normalized according to cell counts. Five replicates were done per time point.

Fig 5.4. Metabolomics heatmap analysis. Heat maps for glutamate grown cells showing T0 hour comparisons with T10, T18 and T24 hours for both organisms. All data are normalized according to cell counts. Five replicates were done per time point.

Fig 5.5. Significant difference by organism and time. (A) PLSDA *Sulfitobacter* sp. strain CB-D and CB-A metabolites comparison for glutamate grown cells. PLSDA by time points for metabolites for (B) *Sulfitobacter* sp. strain CB-A and (C) CB-D. All data are normalized according to cell counts. Five replicates were done per time point. Numbers correspond to samples taken per organism replicate per time point. Significance level of sample statistic for ANOSIM histograms was 0.1% for 999 permutations. Sample statistic between organisms (Average R): 0.389. Sample statistic between time points (Average R): 0.53.

Fig 5.6. Comparison of select metabolites in glutamate grown cells. Glutamate, malate and aspartate are dominant metabolites in both *Sulfitobacter* sp. strains CB-D and CB. All data are normalized according to cell counts. Five replicates were done per time point.

Fig 5.7. Lipidomics heatmap analysis. Heat maps for glutamate grown cells showing (A) fold change between *Sulfitobacter* sp. strain CB-D and CB-A over time. All data are normalized according to cell counts. Five replicates were done per time point.

Fig 5.8. Lipidomics heatmap analysis. Heat maps for glutamate grown cells showing T0 hour comparisons with T10, T18 and T24 hours for both organisms. All data are normalized according to cell counts. Five replicates were done per time point.

Fig 5.9. Significant difference by organism and time. (A) PLSDA *Sulfitobacter* sp. strain CB-D and CB-A lipids comparison for glutamate grown cells. PLSDA by time points for lipids for (B) *Sulfitobacter* sp. strain CB-A and (C) CB-D. All data are normalized according to cell counts. Five replicates were done per time point. Numbers correspond to samples taken per organism replicate per time point. Significance level of sample statistic for ANOSIM histograms was 0.1% for 999 permutations. Sample statistic between organisms (Average R): 0.447. Sample statistic between time points (Average R): 0.609.

Fig 5.10. Comparison of select lipids in glutamate grown cells. Phosphatidylserine (PS), phosphatidylcholine (PC) and phosphatidylglycerol (PG) are dominant lipids in both *Sulfitobacter* sp. strains CB-D and CB-A. All data are normalized according to cell counts. Five replicates were done per time point.

Fig 5.11. Glutamate, pyroglutamic acid, malate and aspartate are the highest contributors to differences in both *Sulfitobacter* sp. strain CB-D and CB-A, determined by Similarity Percent (SIMPER) statistical test. There is significant difference between all aforementioned metabolites, and glutamine, in CB-D and CB-A at T0 and T10 hours. There is significant difference between glutamate:glutamine ratios at T10 hours. Significant differences (Student's T-tests) are denoted by asterisks (* = $p<0.05$; ** = $p<0.01$; *** = $p<0.001$).

Averages of five biological replicates are reported for all treatments. Error bars denote standard deviation and are obscured by the data markers in some instances.

Fig 5.12. Significant metabolite contributors to differences feed into the TCA cycle. Glutamate, pyroglutamic acid, malate and aspartate are the highest contributors to differences in both *Sulfitobacter* sp. strain CB-D and CB-A, determined by Similarity Percent (SIMPER) statistical test. There is significant difference between all aforementioned metabolites, and glutamine, in CB-D and CB-A at T0 and T10 hours. There is significant difference between glutamate:glutamine ratios at T10 hours. Significant differences (Student's T-tests) are denoted by asterisks (* = p<0.05; ** = p<0.01; *** = p<0.001). Averages of five biological replicates are reported for all treatments. Error bars denote standard deviation and are obscured by the data markers in some instances.

Fig 5.13. (A) Phosphotidylglycerol (PG) and (B) phosphotidylserine (PS) are the highest contributors to differences in both *Sulfitobacter* sp. strain CB-D and CB-A, determined by Similarity Percent (SIMPER) statistical test. There is significant difference between both PG and PS in CB-D and CB-A at T0 and T18 hours only. Significant differences (Student's T-tests) are denoted by asterisks (= p<0.01; *** = p<0.001). Averages of five biological replicates are reported for all treatments. Error bars denote standard deviation and are obscured by the data markers in some instances.**

Fig 5.14. Significant phospholipid contributors to differences feed into the CDP-DAG pathway. Phosphotidylglycerol (PS) and phosphotidylserine (PS) are the highest contributors to differences in both *Sulfitobacter* sp. strain CB-D and CB-A, determined by Similarity Percent (SIMPER) statistical test. Significant differences (Student's T-tests) are denoted by asterisks (= p<0.01; *** = p<0.001). Averages of five biological replicates are reported for all treatments. Error bars denote standard deviation and are obscured by the data markers in some instances.**

Fig 5.15. Metabolomics heatmap analysis. Heat maps for acetate grown cells showing fold change between *Sulfitobacter* sp. strain CB-D and CB-A over time. All data are normalized according to cell counts. Five replicates were done per time point.

Fig 5.16. Metabolomics heatmap analysis. Heat maps for acetate grown cells showing T0 hour comparisons with T10, T18 and T24 hours for both organisms. All data are normalized according to cell counts. Five replicates were done per time point.

Fig 5.17. Significant difference by organism and time. (A) PLSDA *Sulfitobacter* sp. strain CB-D and CB-A metabolites comparison for acetate grown cells. PLSDA by time points for metabolites for (B) *Sulfitobacter* sp. strain CB-A and (C) CB-D. All data are normalized according to cell counts. Five replicates were done per time point. Numbers correspond to samples taken per organism replicate per time point. Significance level of sample statistic for ANOSIM histograms was 0.1% for 999 permutations. Sample statistic between organisms (Average R): 0.549. Sample statistic between time points (Average R): 0.67.

Fig 5.18. Comparison of select metabolites in acetate grown cells. Glutamate, malate and succinate/methylmalonate are dominant metabolites in both *Sulfitobacter* sp. strains CB-D and CB. All data are normalized according to cell counts. Five replicates were done per time point.

Fig 5.19. Lipidomics heatmap analysis. Heat maps for acetate grown cells showing (A) fold change between *Sulfitobacter* sp. strain CB-D and CB-A over time, and (B) T0 hour comparisons with T10, T18 and T24 hours for both organisms. All data are normalized according to cell counts. Five replicates were done per time point.

Fig 5.20. Significant difference by organism and time. (A) non-metric Multi-Dimensional (nMDS) analysis for acetate grown cells. All *Sulfitobacter* sp. strain CB-D samples are denoted by blue triangles. All *Sulfitobacter* sp. strain CB-A samples are denoted by inverted red triangles. Numbers correspond to samples taken per organism replicate per time point. (B) Analysis of Similarity (ANOSIM) analysis shows significant difference by organism and

time. All data are normalized according to cell counts. Five replicates were done per time point. Significance level of sample statistic for ANOSIM histograms was 0.1% for 999 permutations. Sample statistic between organisms (Average R): 0.687. Sample statistic between time points (Average R): 0.236.

Fig 5.21. Comparison of select lipids in acetate grown cells. Phosphatidylglycerol (PG) is the dominant lipid group in both *Sulfitobacter* sp. strains CB-D and CB-A. All data are normalized according to cell counts. Five replicates were done per time point.

Fig 5.22. Glutamate, citraconate, succinate/methylmalonate, pyroglutamic acid, malate and adenine are the highest contributors to differences in both *Sulfitobacter* sp. strain CB-D and CB-A, determined by Similarity Percent (SIMPER) statistical test. There is significant difference between citraconate and succinate/methylmalonate, in CB-D and CB-A at T0 and T10 hours. There is significant difference between glutamate:glutamine ratios at T0 hours. Phosphotidylglycerol (PG) is the highest lipid contributor to differences in both *Sulfitobacter* sp. strain CB-D and CB-A, determined by Similarity Percent (SIMPER) statistical test. There is significant difference between PG in CB-D and CB-A at T24 hours only. Significant differences (Student's T-tests) are denoted by asterisks (* = $p<0.05$). Averages of five biological replicates are reported for all treatments. Error bars denote standard deviation and are obscured by the data markers in some instances.

Fig 5.23. Significant metabolite contributors to differences feed into the TCA cycle. Glutamate, citraconate, succinate/methylmalonate, pyroglutamic acid, malate and adenine are the highest contributors to differences in both *Sulfitobacter* sp. strain CB-D and CB-A, determined by Similarity Percent (SIMPER) statistical test. There is significant difference between citraconate and succinate/methylmalonate, in CB-D and CB-A at T0 and T10 hours. There is significant difference between glutamate:glutamine ratios at T0 hours. Significant differences (Student's T-tests) are denoted by asterisks (* = $p<0.05$). Averages of five biological replicates are reported for all treatments. Error bars denote standard deviation and are obscured by the data markers in some instances.

Fig 5.24. Significant phospholipid contributor to differences feeds into the CDP-DAG pathway. Phosphotidylglycerol (PG) is the highest lipid contributor to differences in both *Sulfitobacter* sp. strain CB-D and CB-A, determined by Similarity Percent (SIMPER) statistical test. There is significant difference between PG in CB-D and CB-A at T24 hours only. Significant differences (Student's T-tests) are denoted by asterisks (* = $p<0.05$). Averages of five biological replicates are reported for all treatments. Error bars denote standard deviation and are obscured by the data markers in some instances.

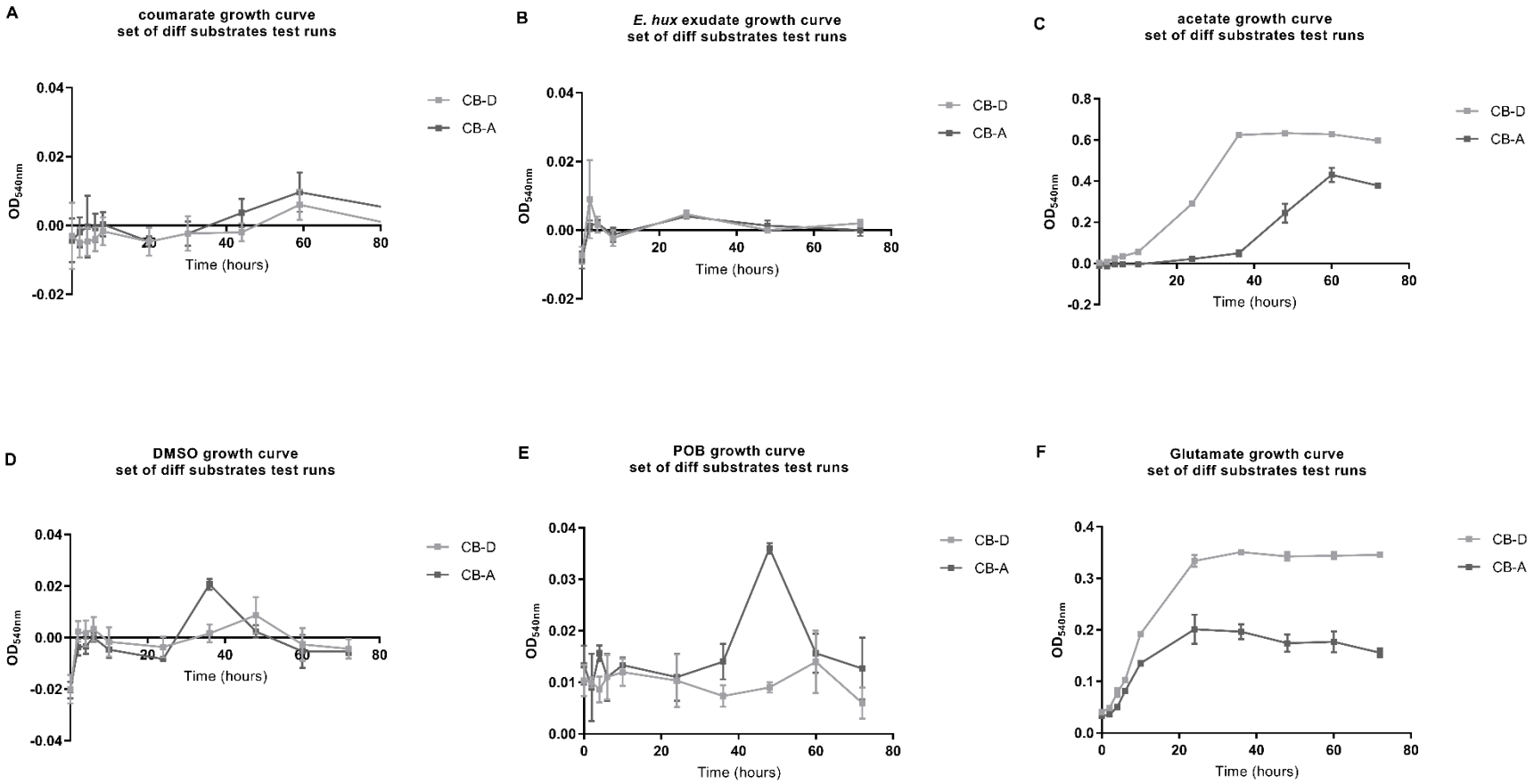

Fig 5.1. Growth dynamics of *Sulfitobacter* sp. strains CB-D and CB-A, on a variety of growth substrates, which differ in terms of chemical complexity and points of entry into central catabolic pathways. Three replicates were done per time point.

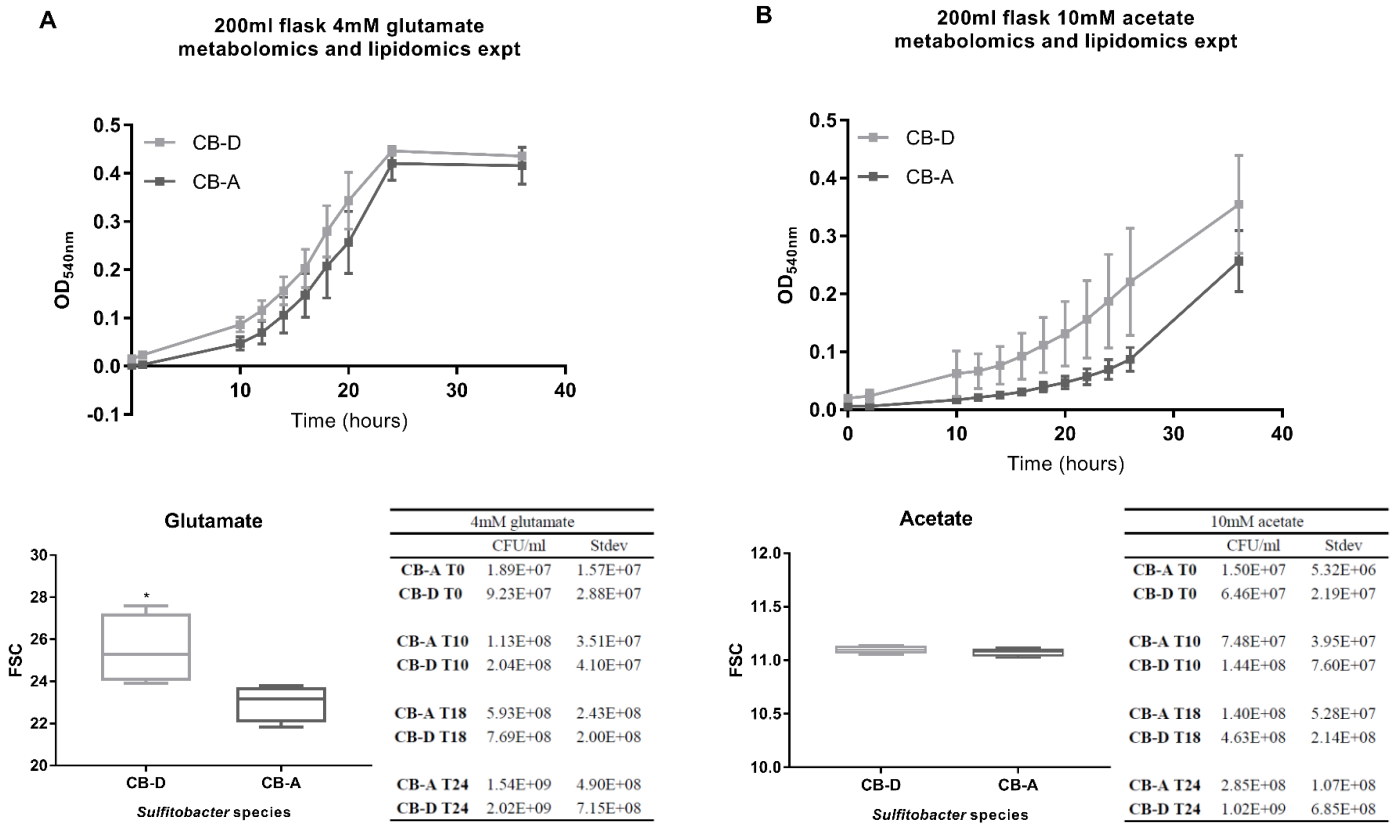

	4mM glutamate	
	CFU/ml	Stdev
CB-A T0	1.89E+07	1.57E+07
CB-D T0	9.23E+07	2.88E+07
CB-A T10	1.13E+08	3.51E+07
CB-D T10	2.04E+08	4.10E+07
CB-A T18	5.93E+08	2.43E+08
CB-D T18	7.69E+08	2.00E+08
CB-A T24	1.54E+09	4.90E+08
CB-D T24	2.02E+09	7.15E+08

	10mM acetate	
	CFU/ml	Stdev
CB-A T0	1.50E+07	5.32E+06
CB-D T0	6.46E+07	2.19E+07
CB-A T10	7.48E+07	3.95E+07
CB-D T10	1.44E+08	7.60E+07
CB-A T18	1.40E+08	5.28E+07
CB-D T18	4.63E+08	2.14E+08
CB-A T24	2.85E+08	1.07E+08
CB-D T24	1.02E+09	6.85E+08

Fig 5.2. Growth dynamics, cell size, and viable counts data for *Sulfitobacter* sp. strain CB-D and CB-A in glutamate and acetate. Cell size was measured by forward scatter through flow cytometry. Averages and standard deviations were calculated for CFU/ml. Significant difference in cell size (Student's T-tests) is denoted by asterisks (* = p<0.05). Averages of five biological replicates are reported for all treatments. Plating was done in technical replicates of the five biological replicates.

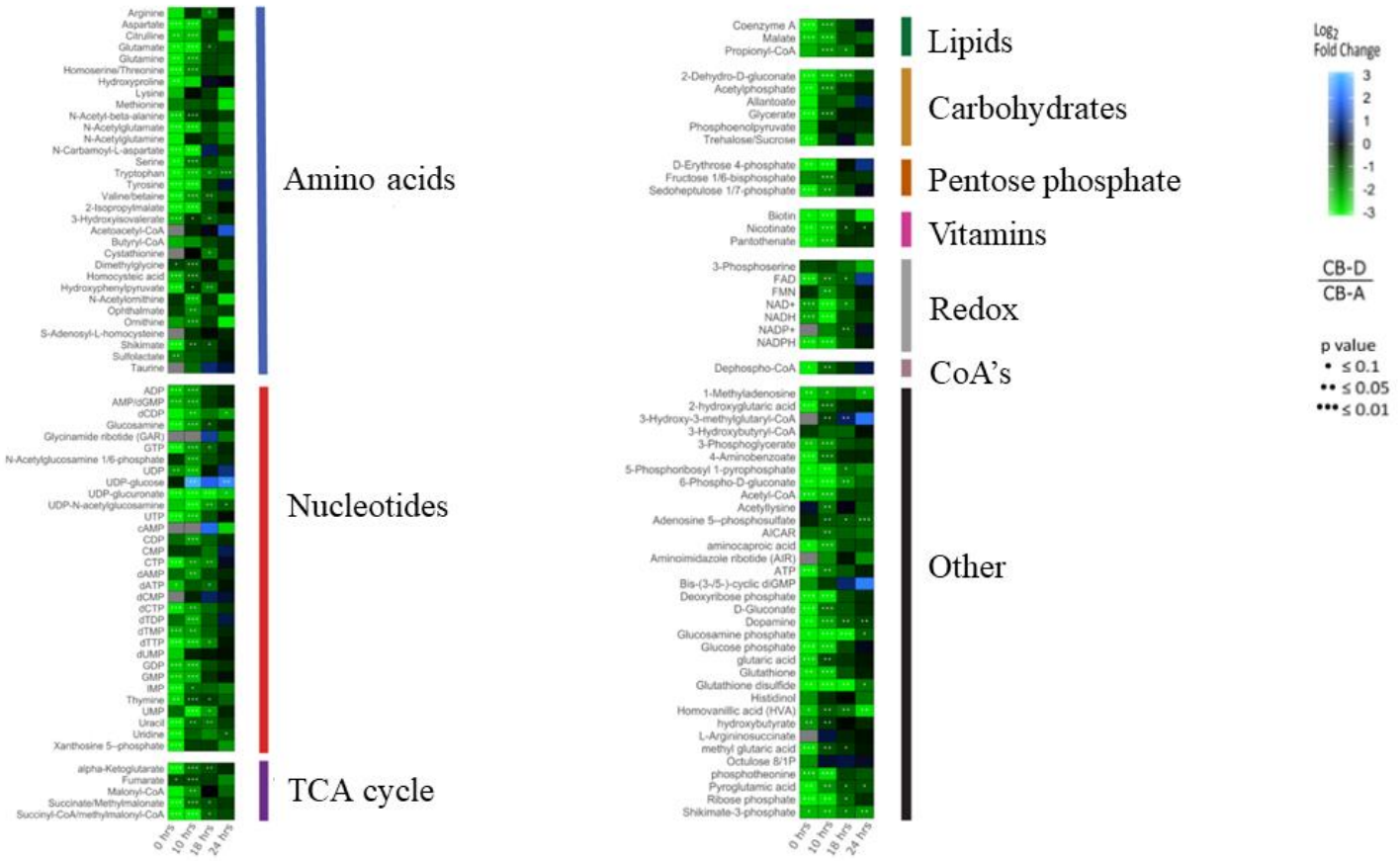

Fig 5.3. Metabolomics heatmap analysis. Heat maps for glutamate grown cells showing fold change between *Sulfitobacter* sp. strain CB-D and CB-A over time. Five replicates were done per time point.

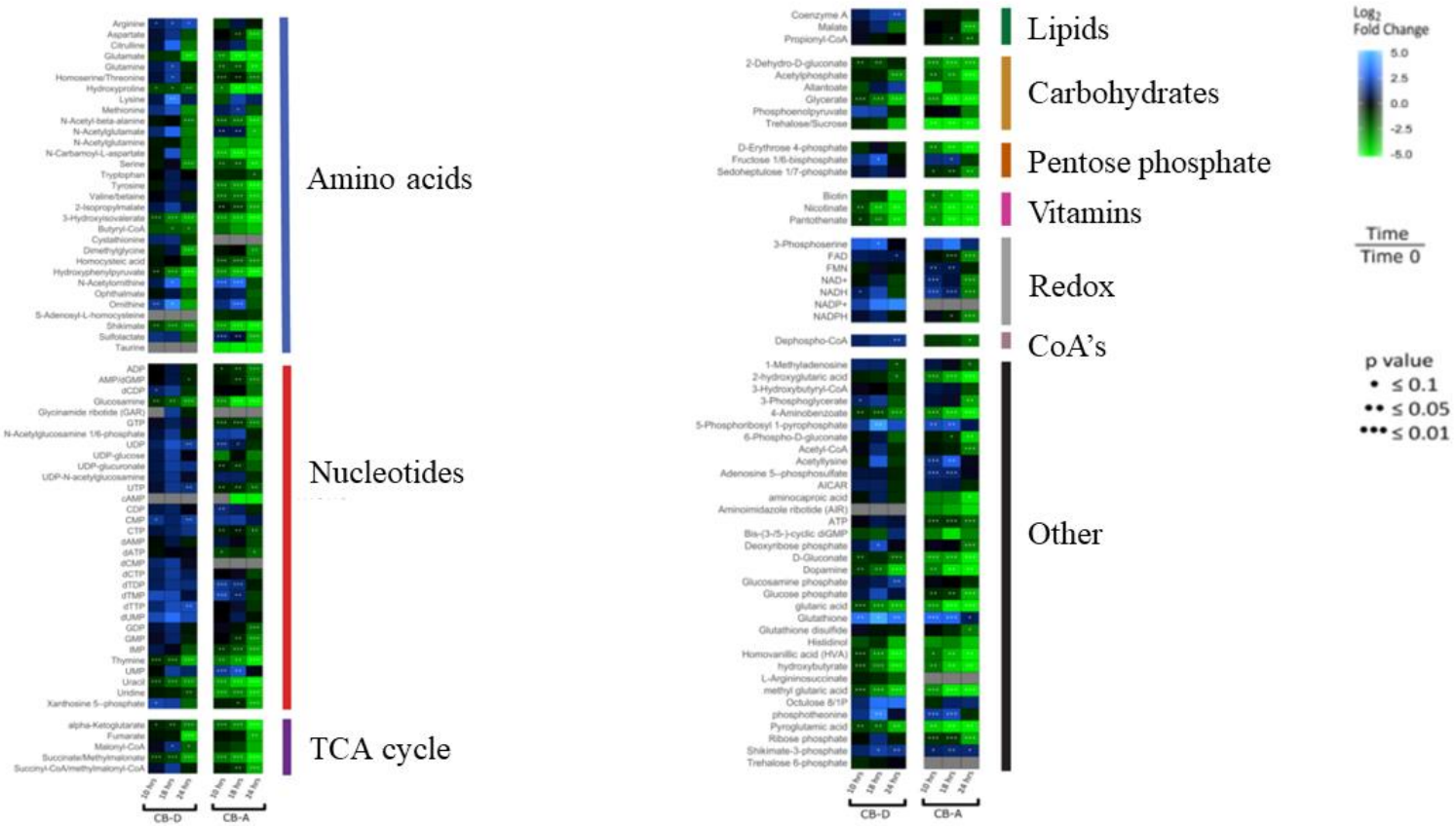

Fig 5.4. Metabolomics heatmap analysis. Heat maps for glutamate grown cells showing T0 hour comparisons with T10, T18 and T24 hours for both organisms. All data are normalized according to cell counts. Five replicates were done per time point.

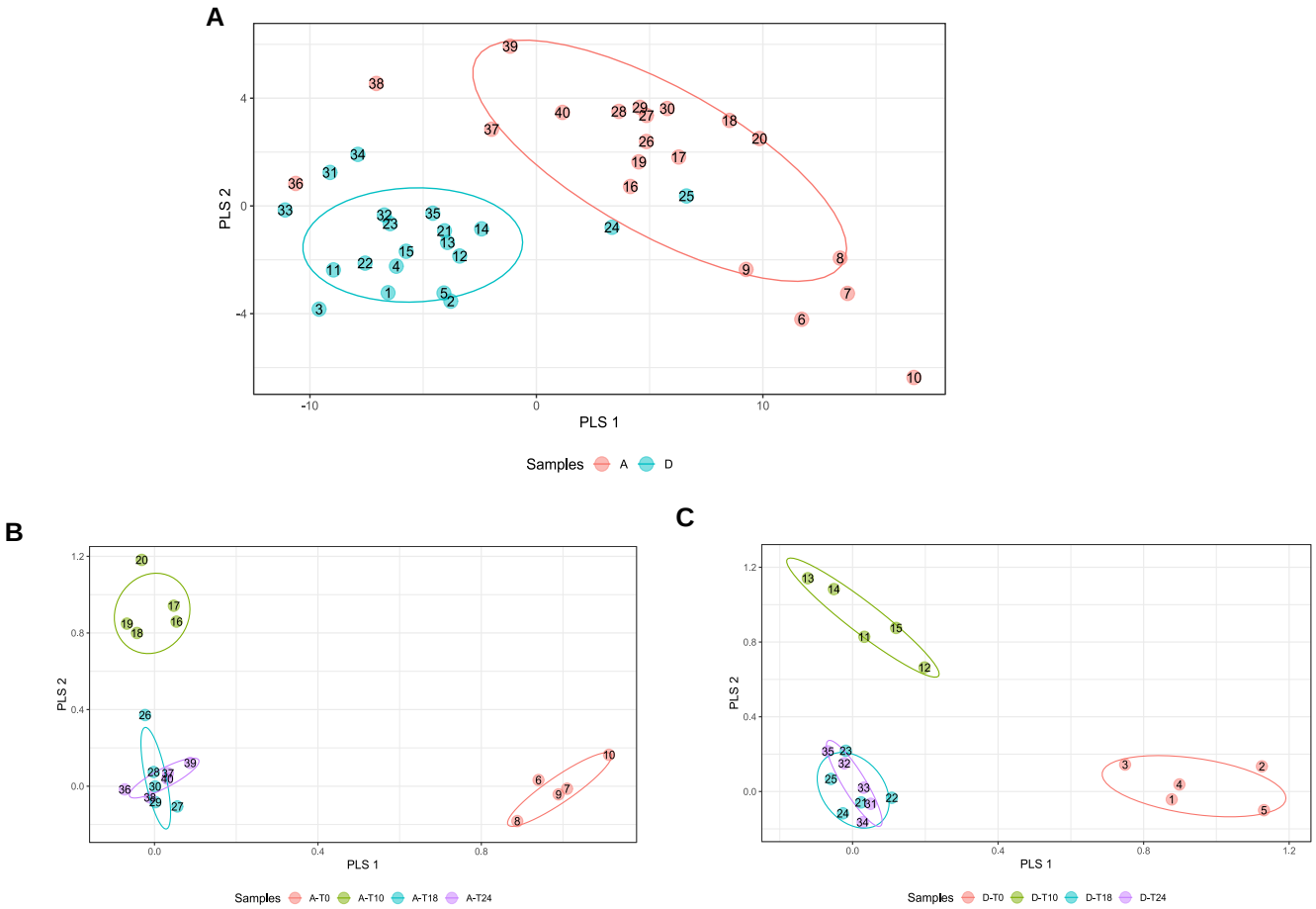

Fig 5.5. Significant difference by organism and time. (A) PLSDA *Sulfitobacter* sp. strain CB-D and CB-A metabolites comparison for glutamate grown cells. PLSDA by time points for metabolites for (B) *Sulfitobacter* sp. strain CB-D and (C) CB-A. All data are normalized according to cell counts. Five replicates were done per time point. Numbers correspond to samples taken per organism replicate per time point.

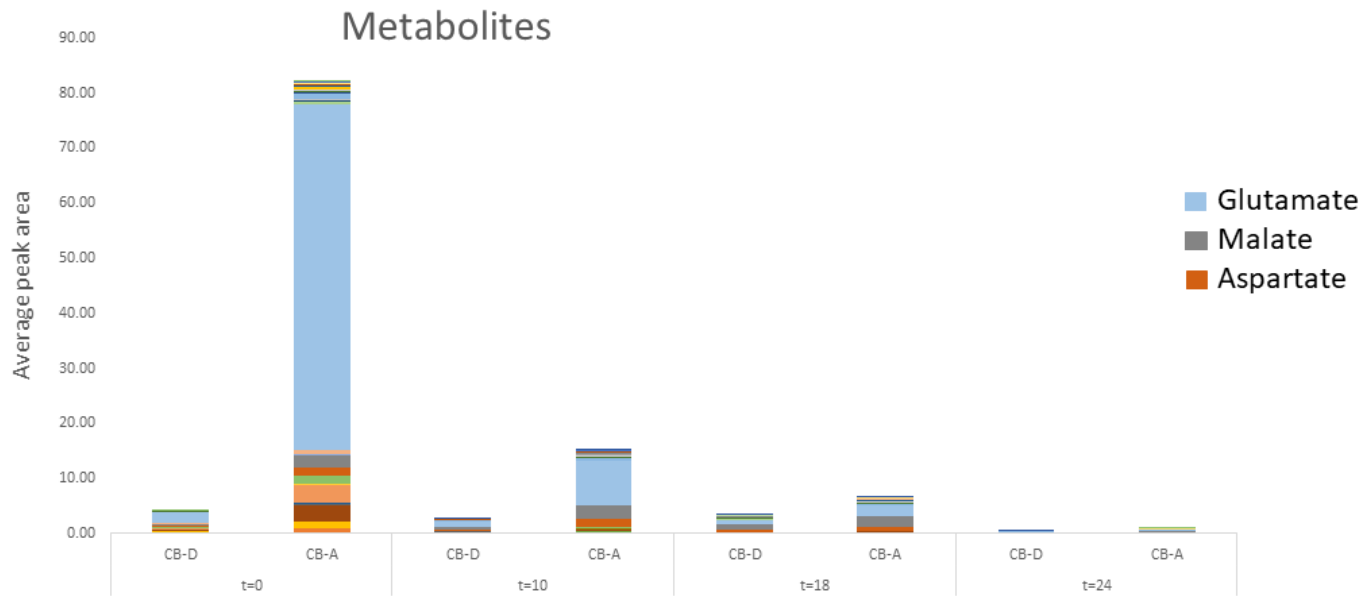

Fig 5.6. Comparison of select metabolites in glutamate grown cells. Glutamate, malate and aspartate are dominant metabolites in both *Sulfitobacter* sp. strains CB-D and CB. All data are normalized according to cell counts. Five replicates were done per time point.

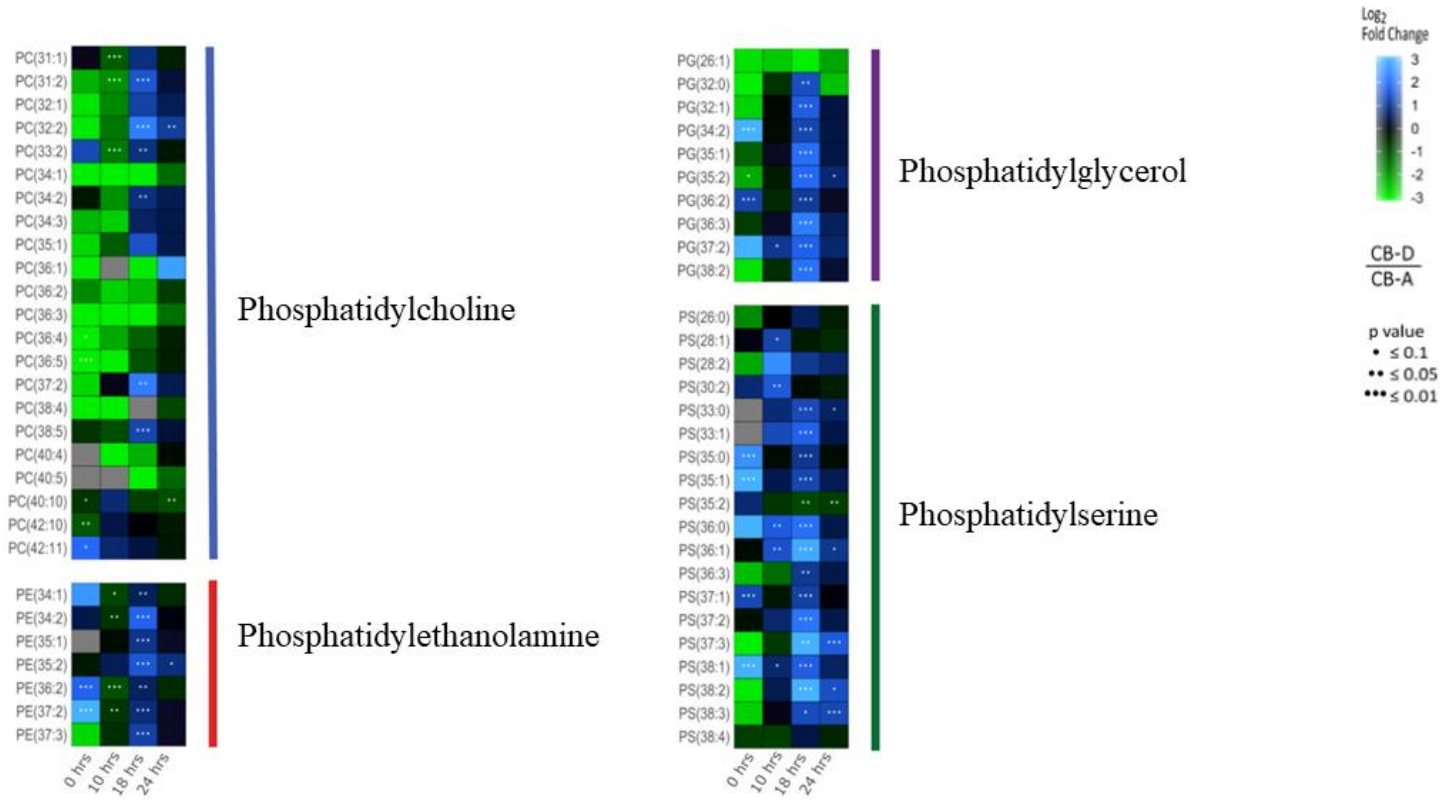

Fig 5.7. Lipidomics heatmap analysis. Heat maps for glutamate grown cells showing fold change between *Sulfitobacter* sp. strain CB-D and CB-A over time. All data are normalized according to cell counts. Five replicates were done per time point.

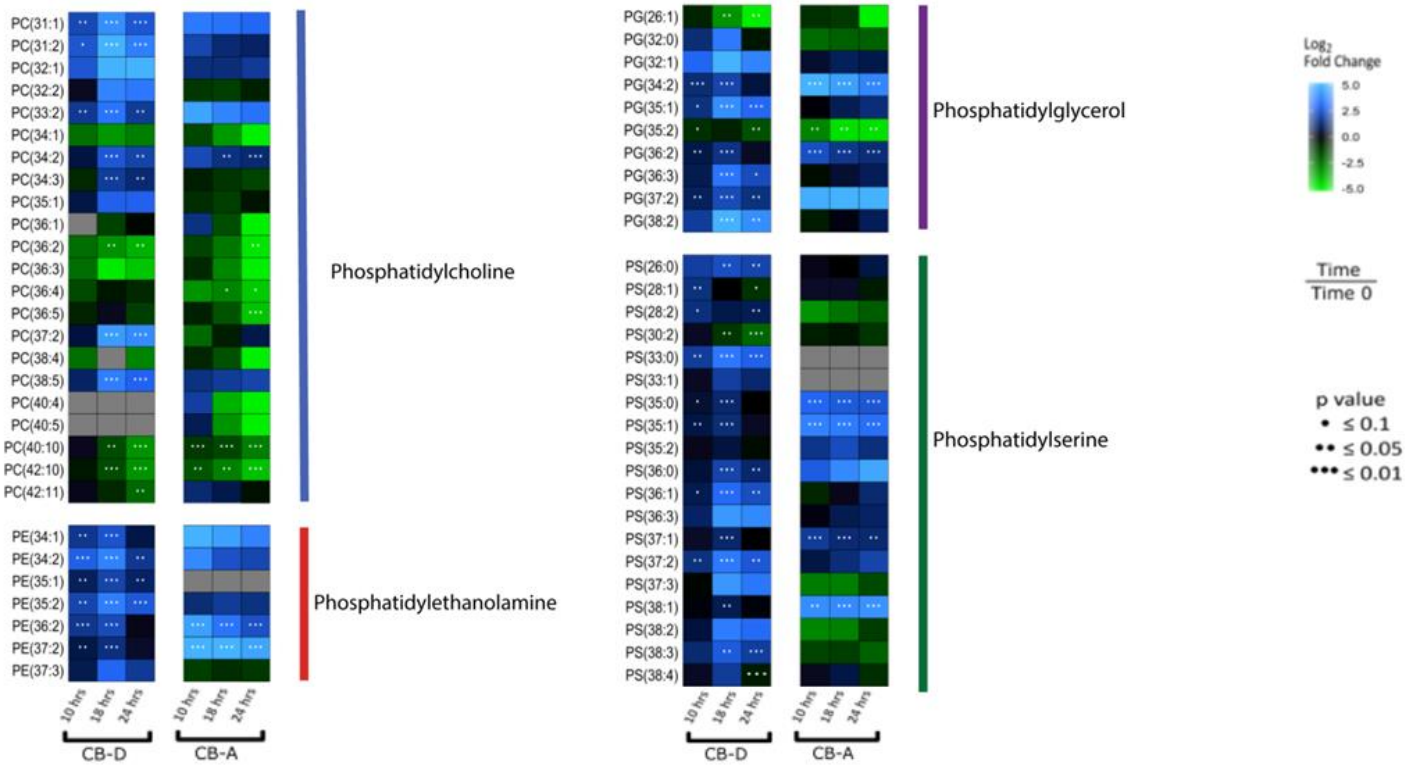

Fig 5.8. Lipidomics heatmap analysis. Heat maps for glutamate grown cells showing T0 hour comparisons with T10, T18 and T24 hours for both organisms. All data are normalized according to cell counts. Five replicates were done per time point.

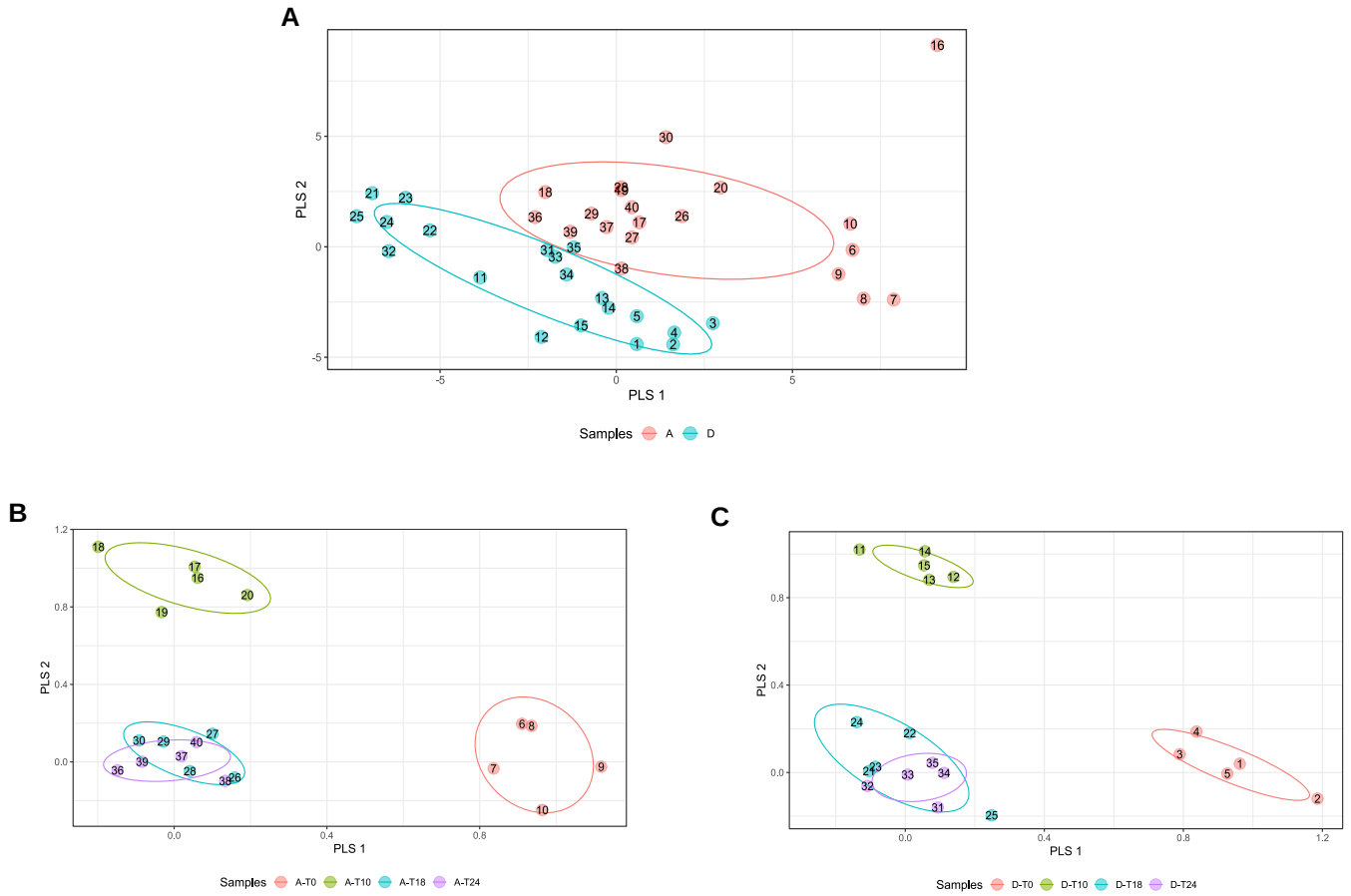

Fig 5.9. Significant difference by organism and time. (A) PLSDA *Sulfitobacter* sp. strain CB-D and CB-A lipids comparison for glutamate grown cells. PLSDA by time points for lipids for (B) *Sulfitobacter* sp. strain CB-D and (C) CB-A. All data are normalized according to cell counts. Five replicates were done per time point. Numbers correspond to samples taken per organism replicate per time point.

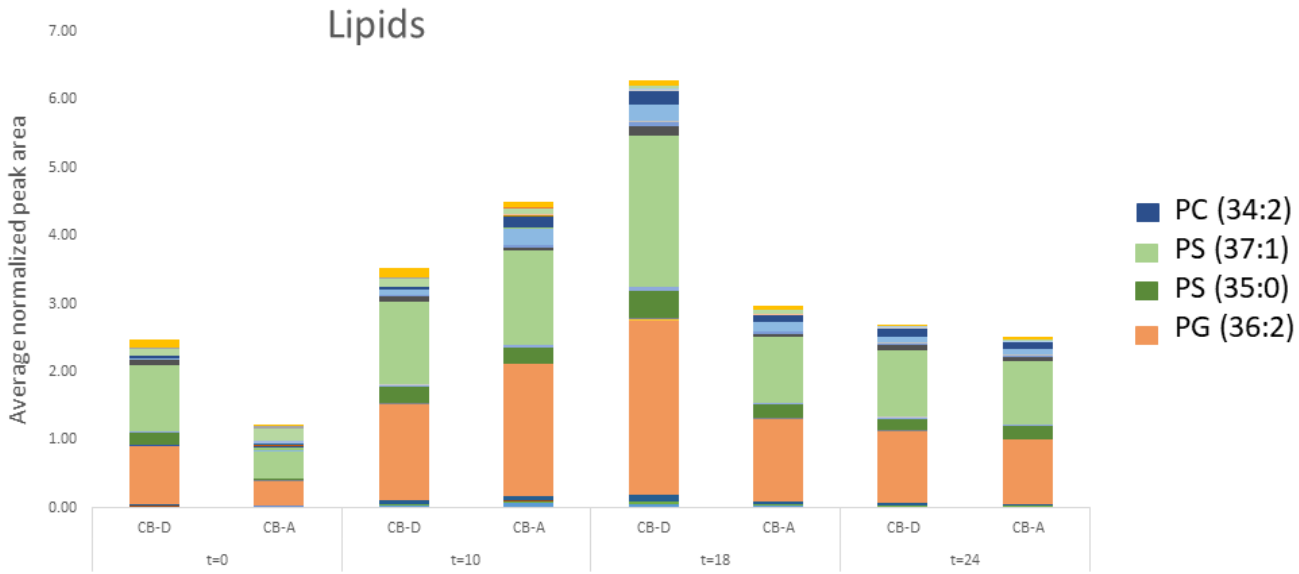

Fig 5.10. Comparison of select lipids in glutamate grown cells. Phosphatidylserine (PS), phosphatidylcholine (PC) and phosphatidylglycerol (PG) are dominant lipids in both *Sulfitobacter* sp. strains CB-D and CB-A. All data are normalized according to cell counts. Five replicates were done per time point.

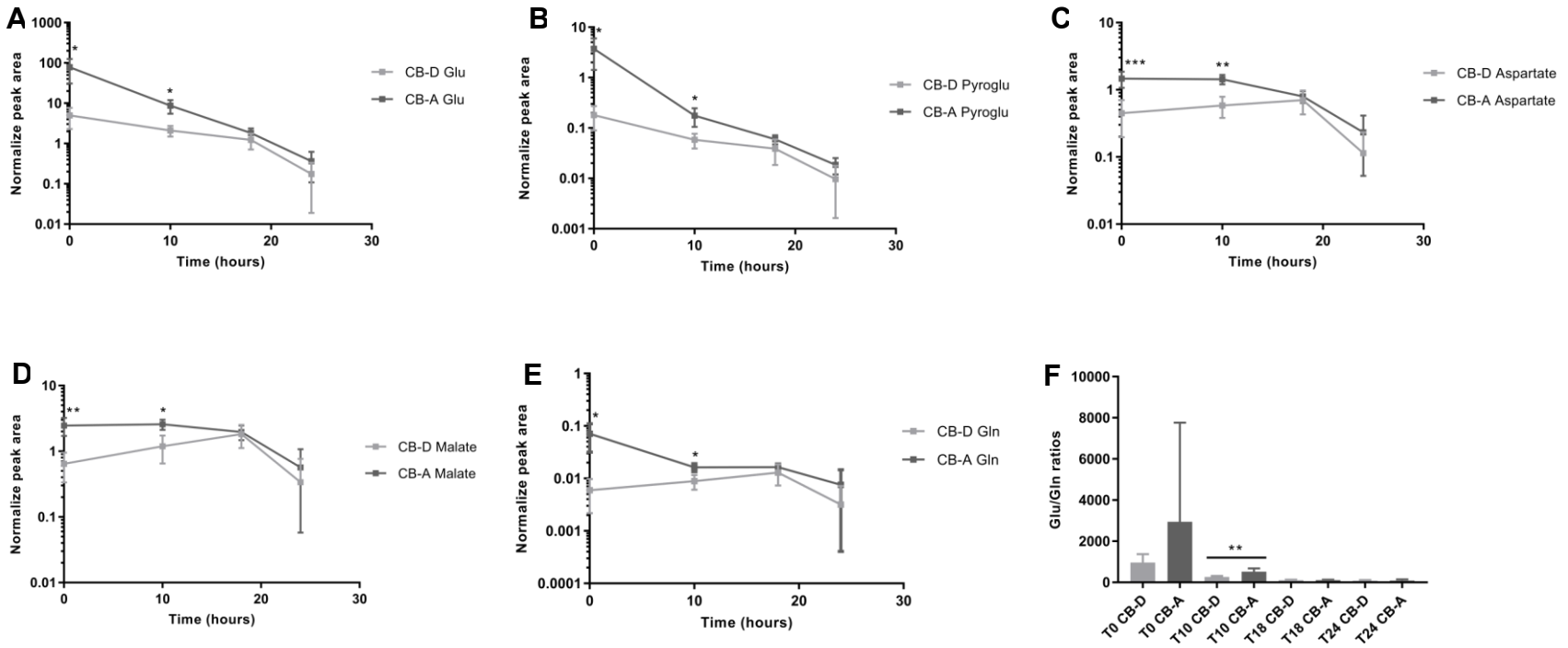

Fig 5.11. Glutamate, pyroglutamic acid, malate and aspartate are the highest contributors to differences in both *Sulfitobacter* sp. strain CB-D and CB-A, determined by Similarity Percent (SIMPER) statistical test. There is significant difference between all aforementioned metabolites, and glutamine, in CB-D and CB-A at T0 and T10 hours. There is significant difference between glutamate:glutamine ratios at T10 hours.

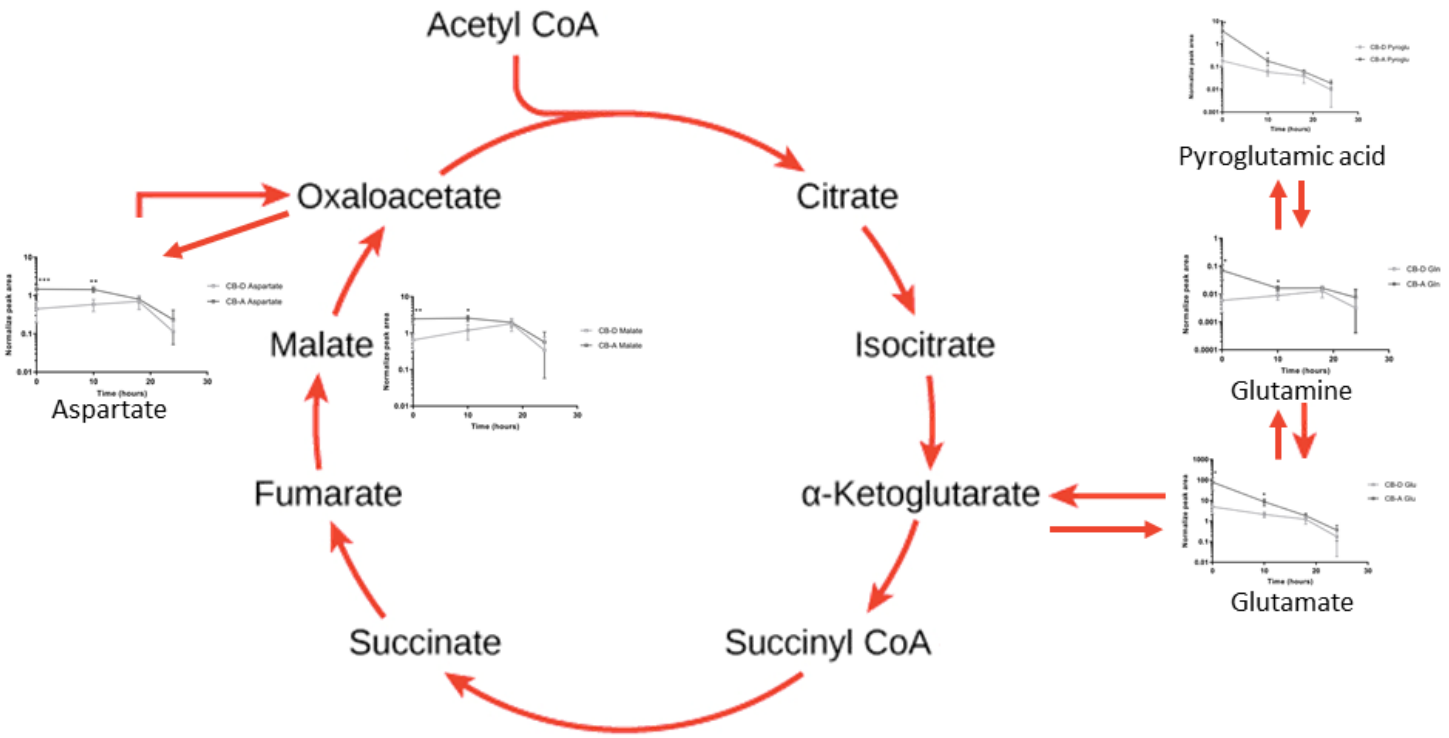

Fig 5.12. Significant metabolite contributors to differences feed into the TCA cycle. Glutamate, pyroglutamic acid, malate and aspartate are the highest contributors to differences in both *Sulfitobacter* sp. strain CB-D and CB-A, determined by Similarity Percent (SIMPER) statistical test. There is significant difference between all aforementioned metabolites, and glutamine, in CB-D and CB-A at T0 and T10 hours.

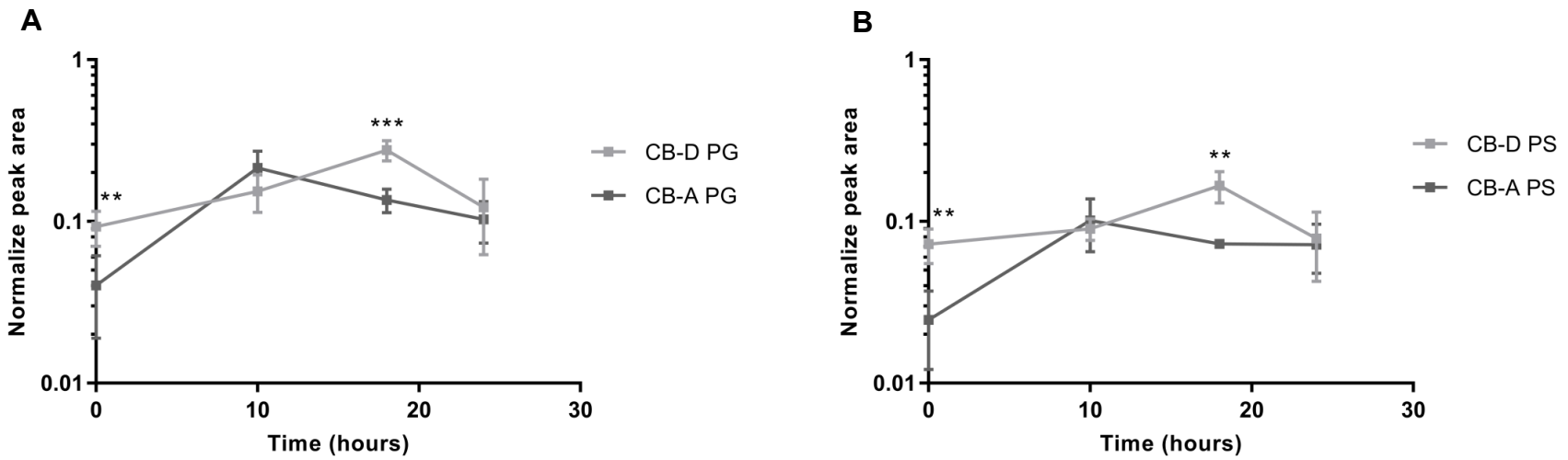

Fig 5.13. (A) Phosphatidylglycerol (PG) and (B) phosphatidylserine (PS) are the highest contributors to differences in both *Sulfitobacter* sp. strain CB-D and CB-A, determined by Similarity Percent (SIMPER) statistical test. There is significant difference between both PG and PS in CB-D and CB-A at T0 and T18 hours only.

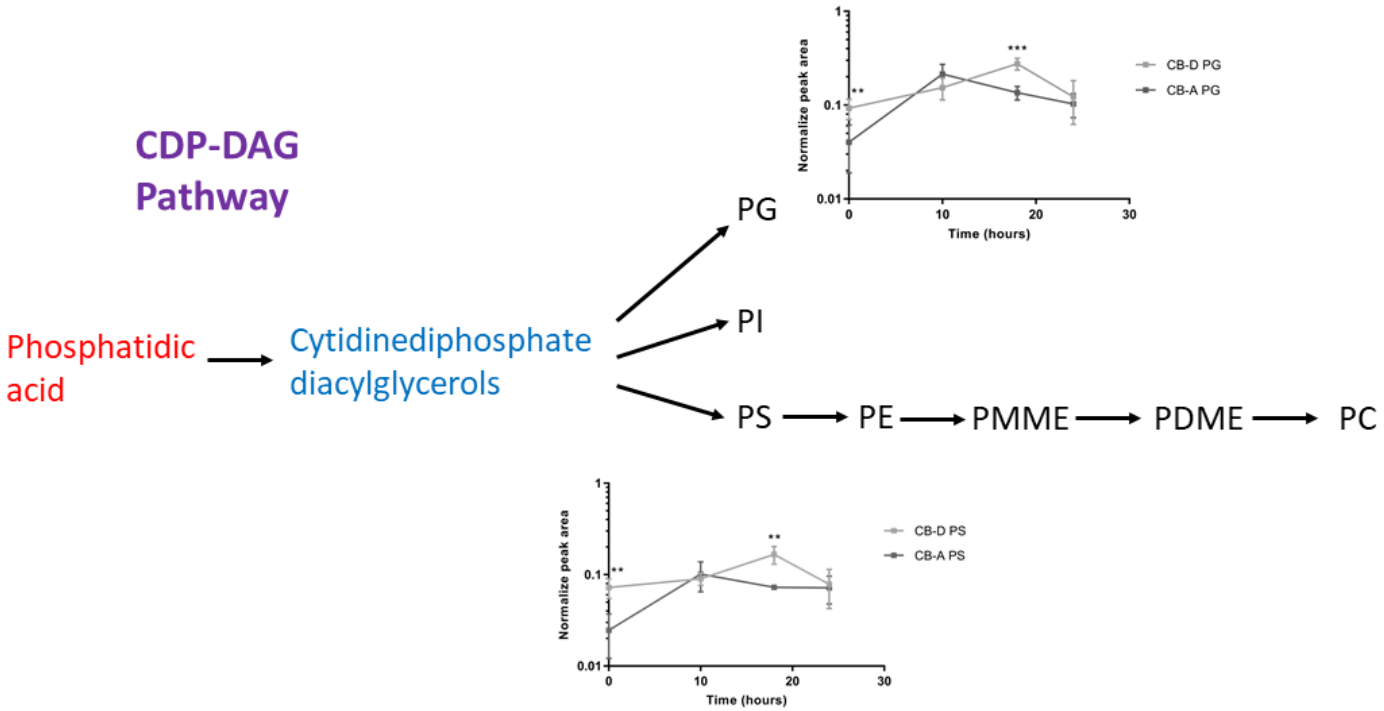

Fig 5.14. Significant phospholipid contributors to differences feed into the CDP-DAG pathway. Phosphatidylglycerol (PS) and phosphatidylserine (PS) are the highest contributors to differences in both *Sulfitobacter* sp. strain CB-D and CB-A, determined by Similarity Percent (SIMPER) statistical test.

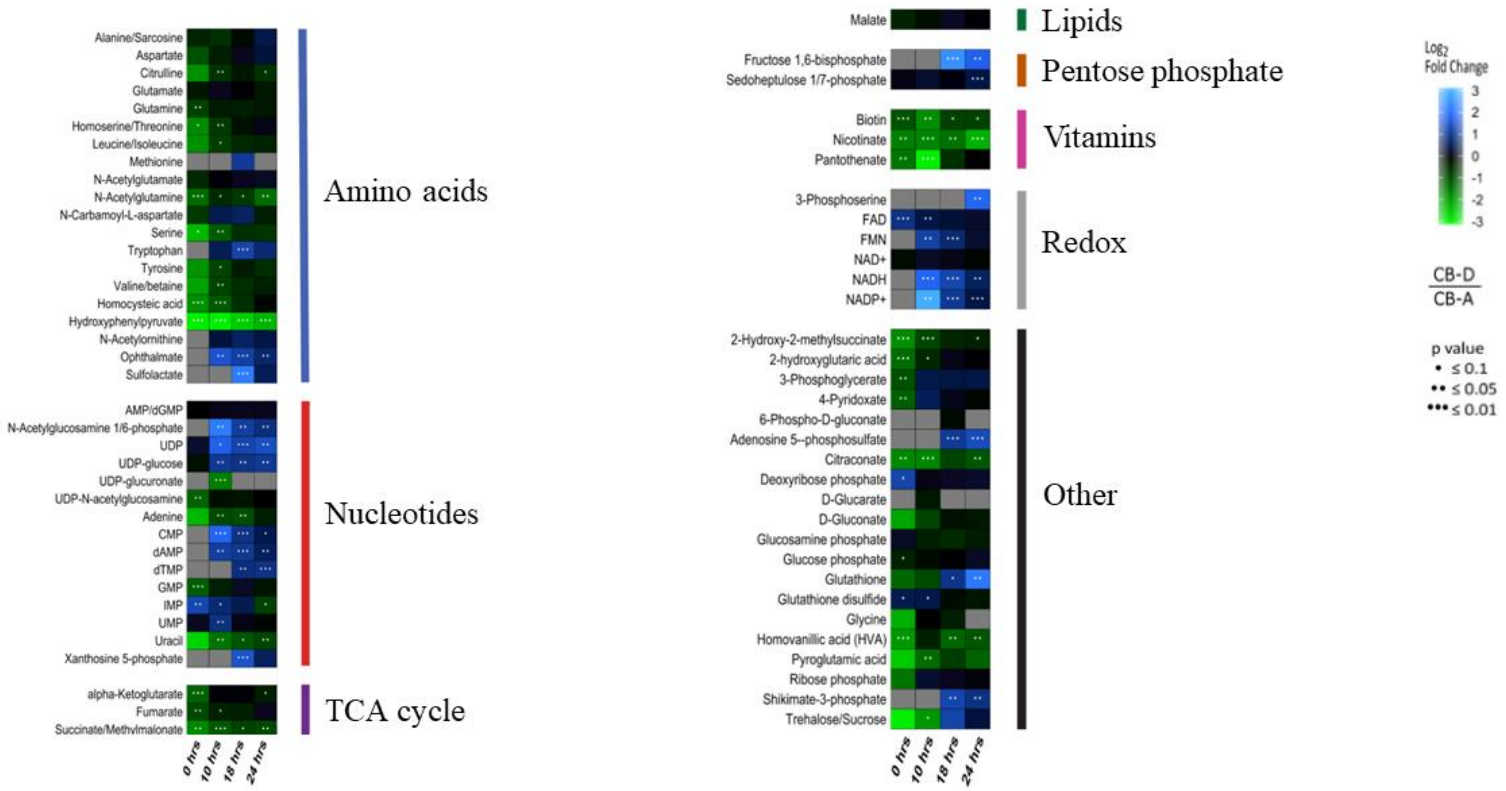

Fig 5.15. Metabolomics heatmap analysis. Heat maps for acetate grown cells showing fold change between *Sulfitobacter* sp. strain CB-D and CB-A over time All data are normalized according to cell counts. Five replicates were done per time point.

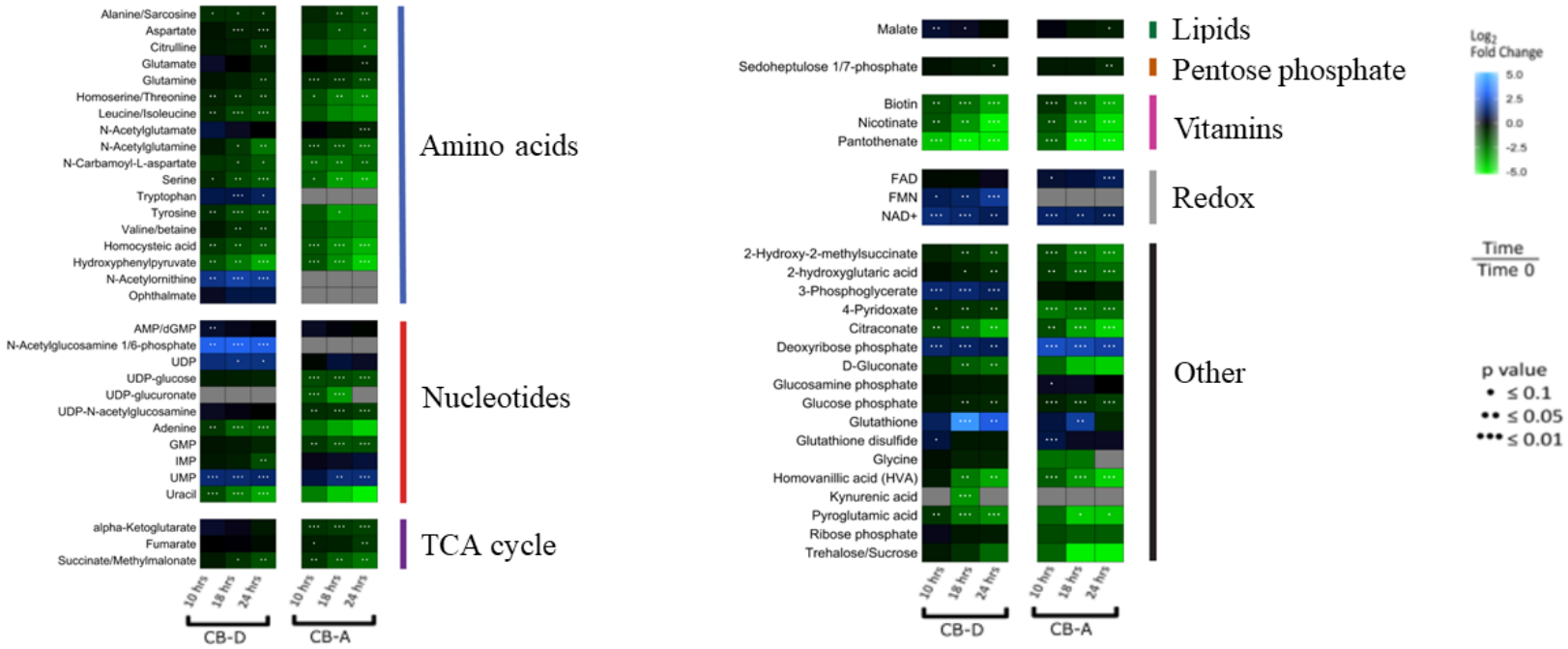

Fig 5.16. Metabolomics heatmap analysis. Heat maps for acetate grown cells showing T0 hour comparisons with T10, T18 and T24 hours for both organisms. All data are normalized according to cell counts. Five replicates were done per time point.

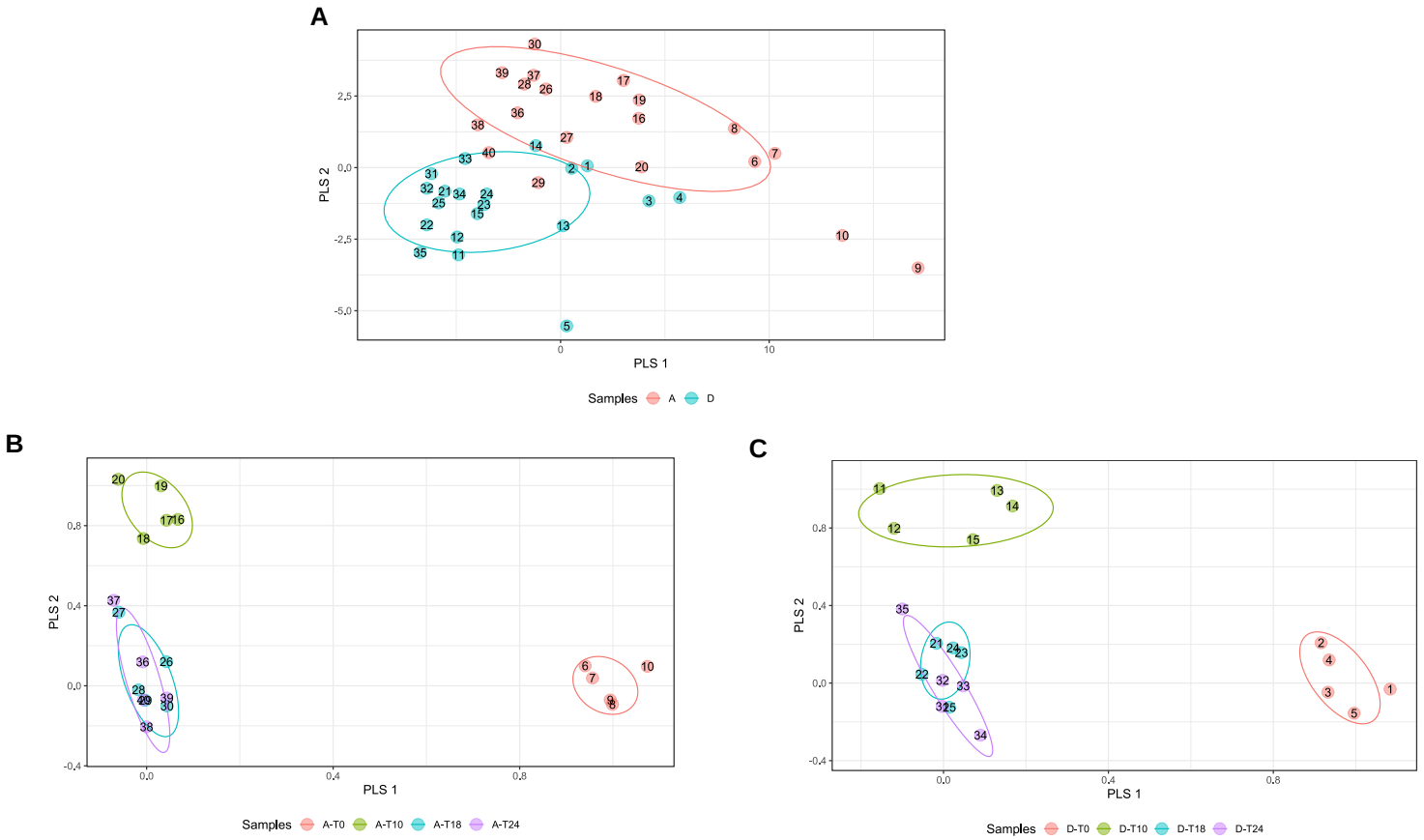

Fig 5.17. Significant difference by organism and time. (A) PLSDA *Sulfitobacter* sp. strain CB-D and CB-A metabolites comparison for acetate grown cells. PLSDA by time points for metabolites for (B) *Sulfitobacter* sp. strain CB-D and (C) CB-A. All data are normalized according to cell counts. Five replicates were done per time point. Numbers correspond to samples taken per organism replicate per time point.

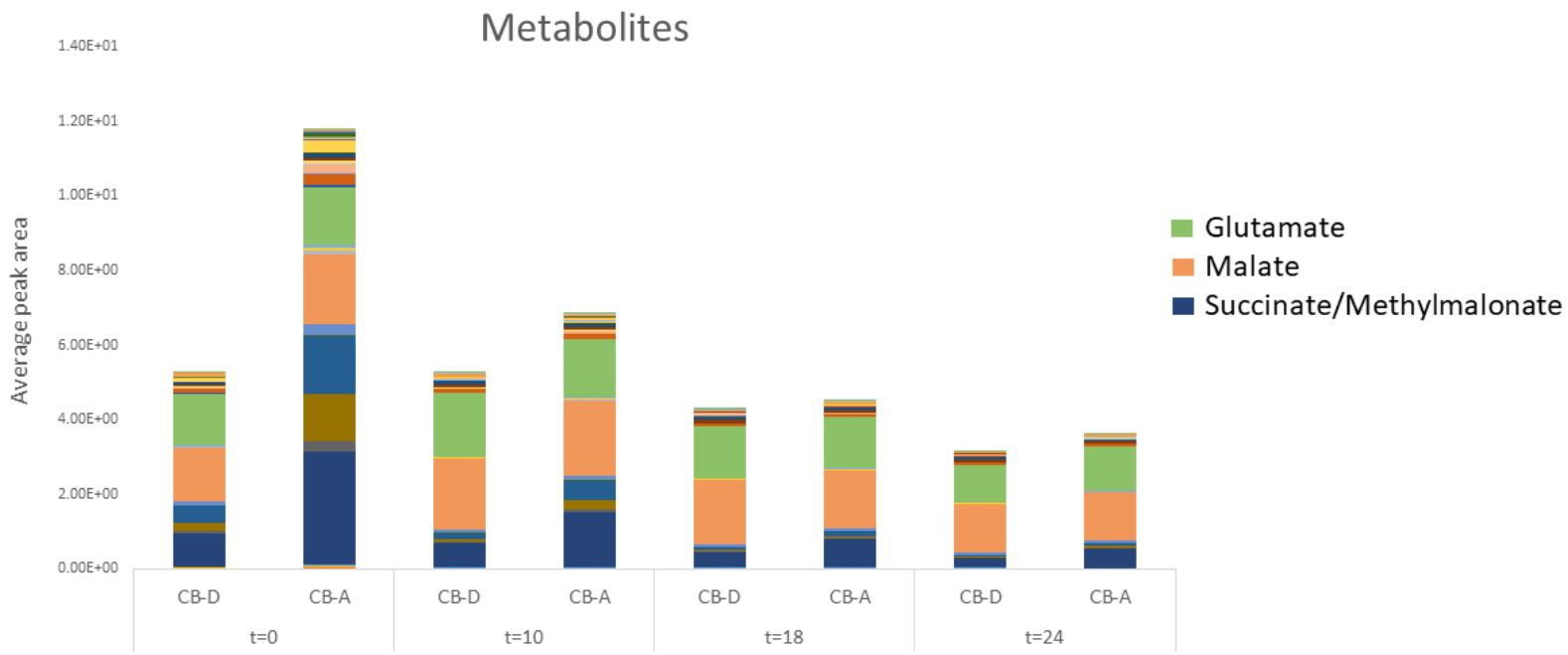

Fig 5.18. Comparison of select metabolites in acetate grown cells. Glutamate, malate and succinate/methylmalonate are dominant metabolites in both *Sulfitobacter* sp. strains CB-D and CB. All data are normalized according to cell counts. Five replicates were done per time point.

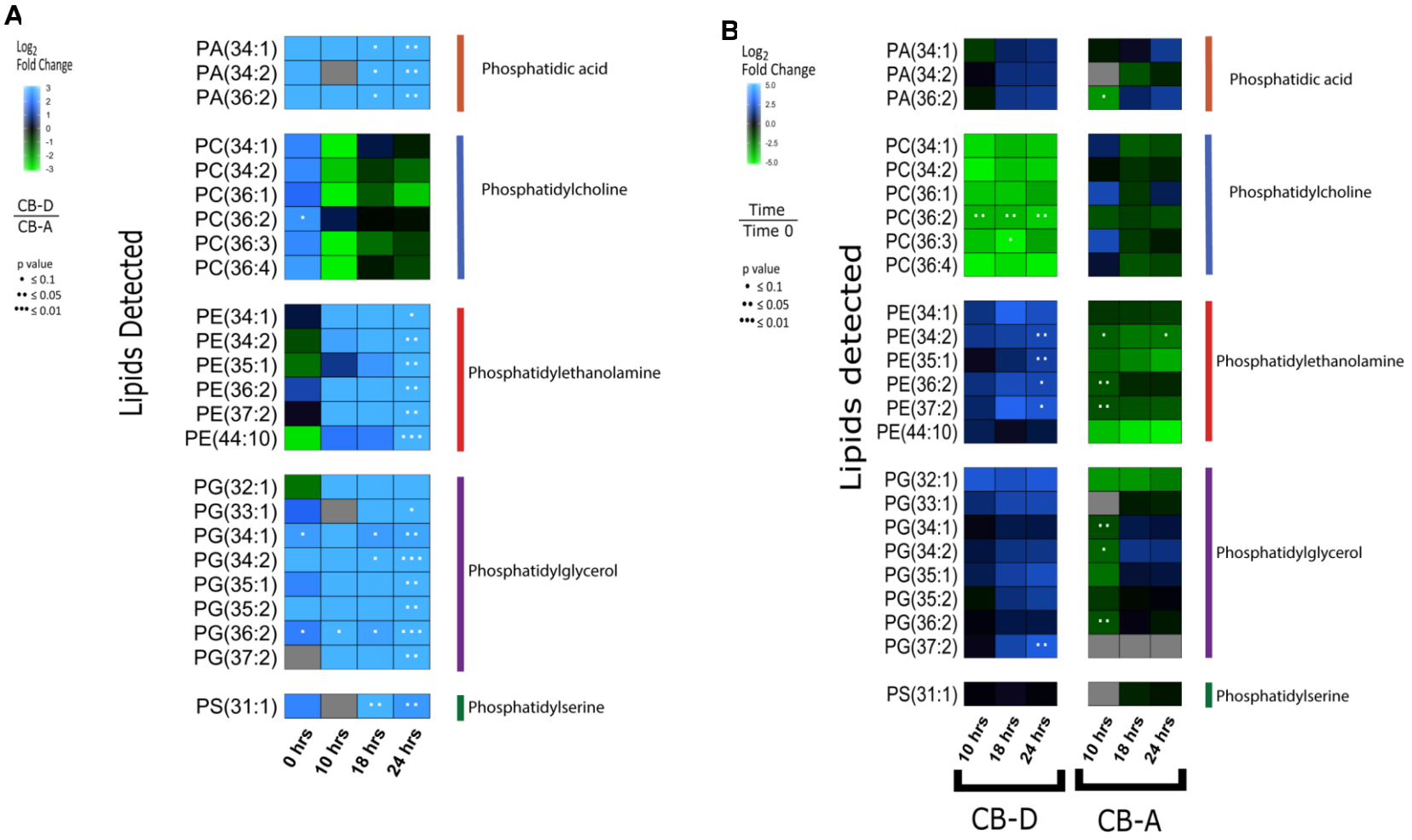

Fig 5.19. Lipidomics heatmap analysis. Heat maps for acetate grown cells showing (A) fold change between *Sulfitobacter* sp. strain CB-D and CB-A over time, and (B) T0 hour comparisons with T10, T18 and T24 hours for both organisms. All data are normalized according to cell counts. Five replicates were done per time point.

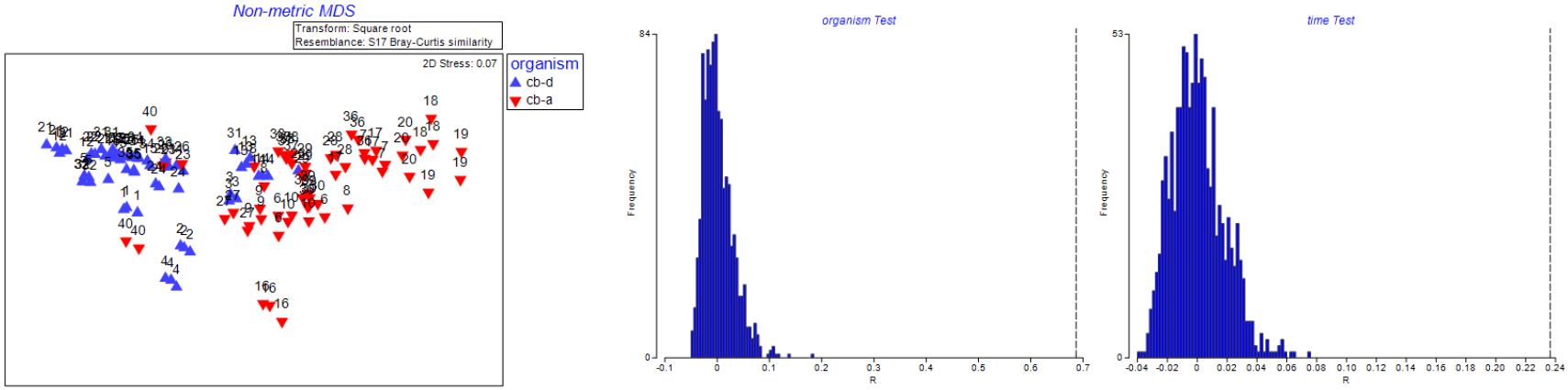

Fig 5.20. Significant difference by organism and time. (A) non-metric Multi-Dimensional (nMDS) analysis for acetate grown cells. All *Sulfitobacter* sp. strain CB-D samples are denoted by blue triangles. All *Sulfitobacter* sp. strain CB-A samples are denoted by inverted red triangles. Numbers correspond to samples taken per organism replicate per time point. (B) Analysis of Similarity (ANOSIM) analysis shows significant difference by organism and time. All data are normalized according to cell counts. Five replicates were done per time point.

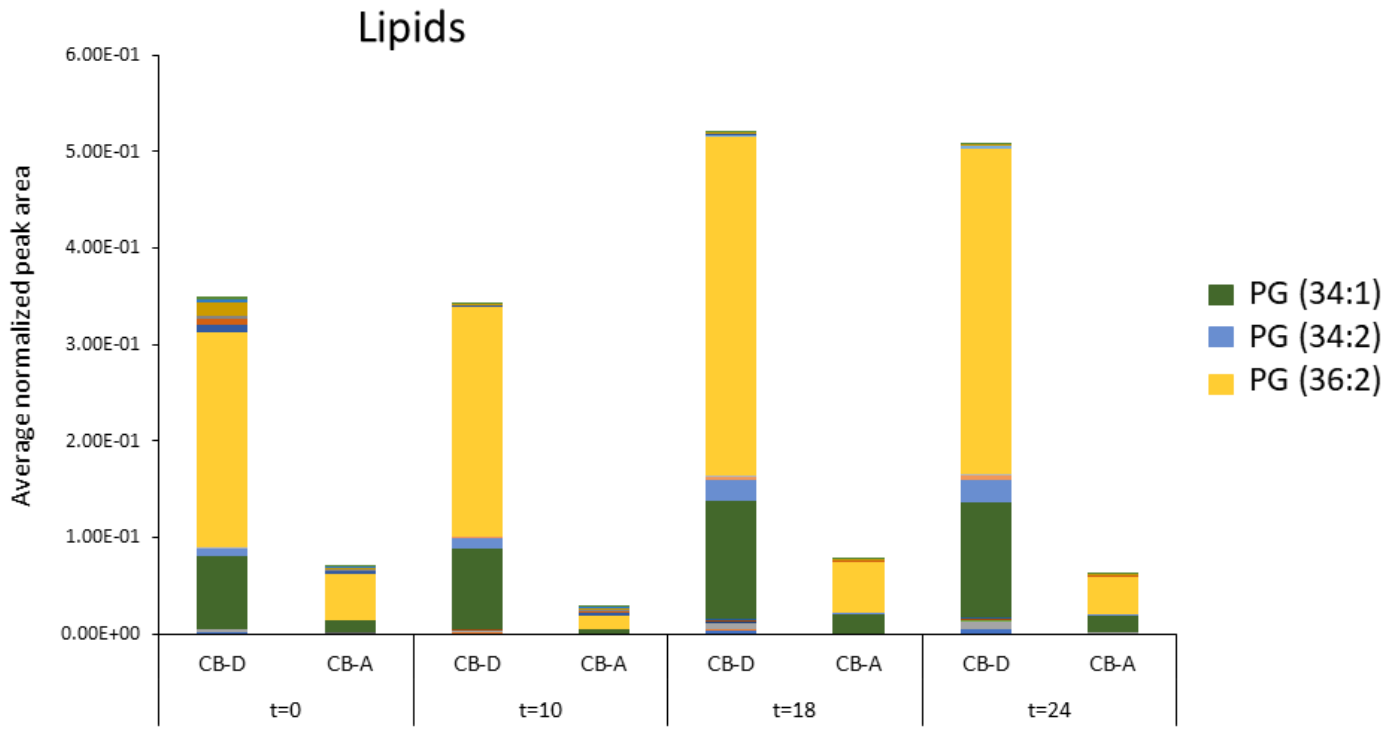

Fig 5.21. Comparison of select lipids in acetate grown cells. Phosphatidylglycerol (PG) is the dominant lipid group in both *Sulfitobacter* sp. strains CB-D and CB-A. All data are normalized according to cell counts. Five replicates were done per time point.

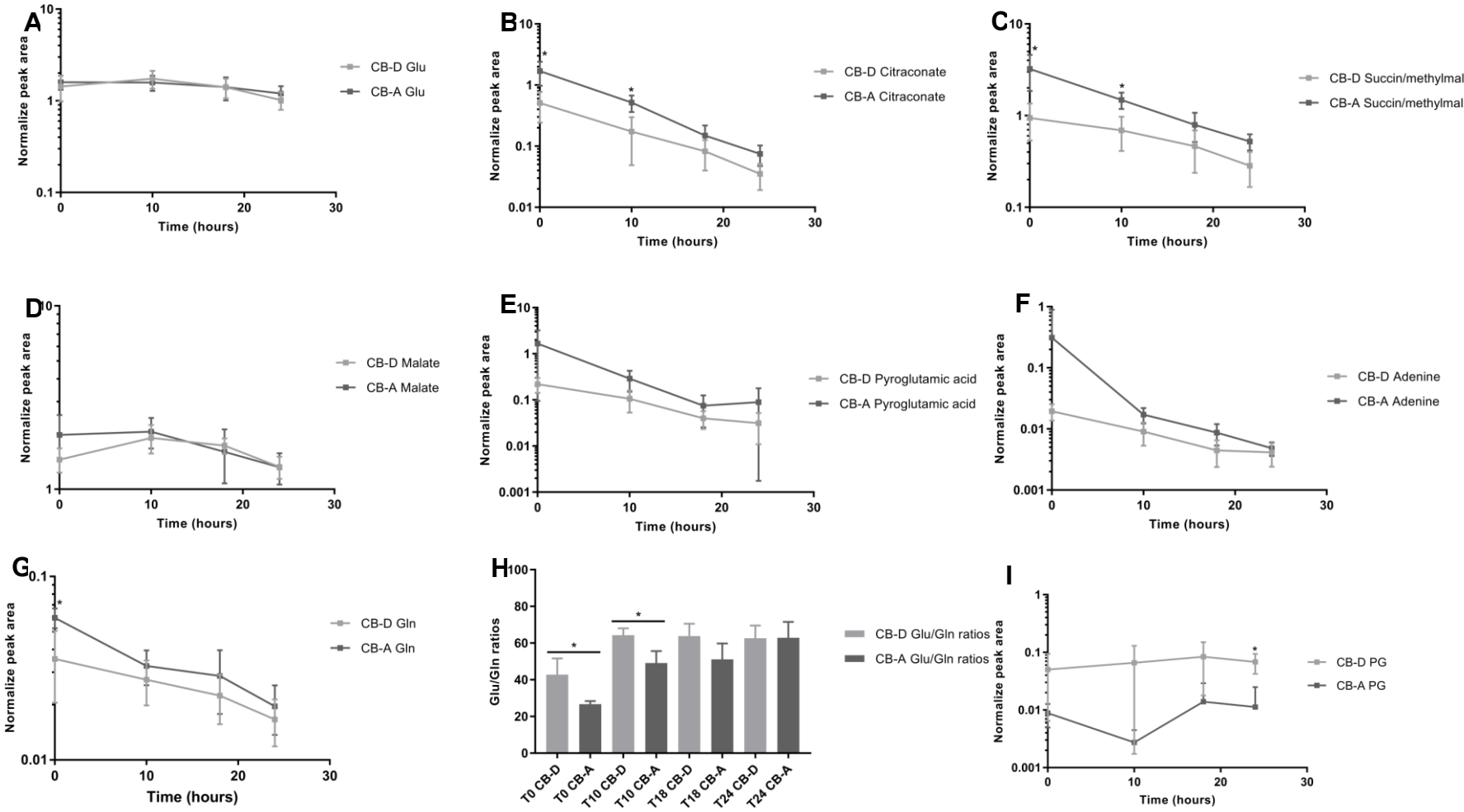

Fig 5.22. Glutamate, citraconate, succinate/methylmalonate, pyroglutamic acid, malate and adenine are the highest contributors to differences in both *Sulfitobacter* sp. strain CB-D and CB-A. There is significant difference between glutamate:glutamine ratios at T0 hours. Phosphatidylglycerol (PG) is the highest lipid contributor to differences in both strains.

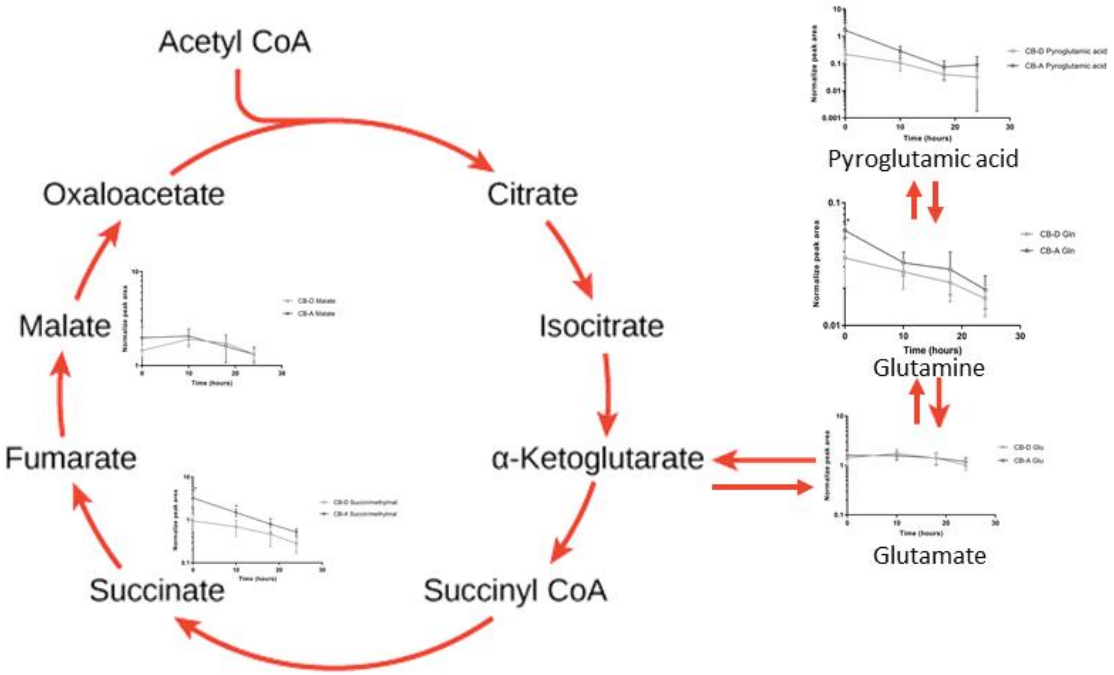

Fig 5.23. Significant metabolite contributors to differences feed into the TCA cycle. Glutamate, citraconate, succinate/methylmalonate, pyroglutamic acid, malate and adenine are the highest contributors to differences in both *Sulfitobacter* sp. strain CB-D and CB-A. There is significant difference between glutamate:glutamine ratios at T0 hours. Phosphatidylglycerol (PG) is the highest lipid contributor to differences in both strains.

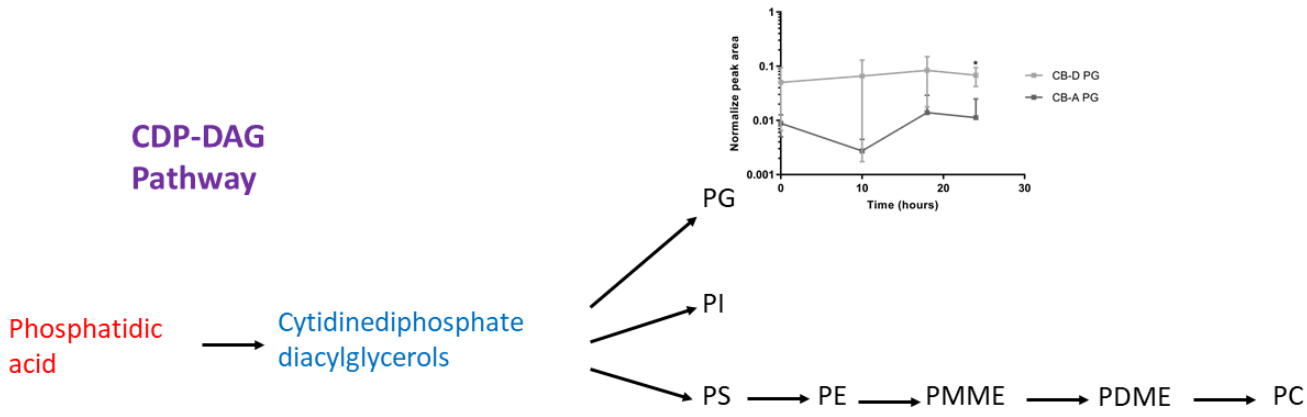

Fig 5.24. Significant phospholipid contributor to differences feeds into the CDP-DAG pathway. Phosphatidylglycerol (PG) is the highest lipid contributor to differences in both *Sulfitobacter* sp. strain CB-D and CB-A, determined by Similarity Percent (SIMPER) statistical test. There is significant difference between PG in CB-D and CB-A at T24 hours only.

CHAPTER 6

CONCLUSIONS

Where ‘I’ is used, this denotes where I primarily led the investigation into the project data generation. Where ‘we’ is used, this denotes where collaborators were involved in the generation of data.

With global estimates of upwards of 10^{30}, viruses are the most abundant biological entities on the planet that significantly impact shuttling of carbon and other nutrients in marine systems (Bergh et al 1989, Fuhrman 1999, Hambly and Suttle 2005, Hendrix 2002, Suttle 2007, Wilhelm and Suttle 1999). Temperate phages specifically may form long-term mutualistic symbioses with their hosts, which can allow for conferred host competitive advantage, modulation of biofilm formation, immunity from superinfection, and enhanced virulence (Bondy-Denomy and Davidson 2014, Brussow et al 2004, Canchaya et al 2003, Feiner et al 2015, Harrison and Brockhurst 2017, Nanda et al 2015, Paul 2008). The ways in which prophages effect increased fitness, of both phage and host, in these complex relationships are currently less understood. Observed prophage induction may be the result of the presence of chemical compounds or UV radition, but knowledge of the mechanisms that cause spontaneous induction of these “time bombs” in nature is much less understood (Feiner et al 2015, Fortier and Sekulovic 2013, Paul 2008). The fate of prophages is so intertwined with their hosts that it propels the need for a better understanding of the lysogenized state as a unique living entity, i.e. virocell (Forterre 2013). *Sulfitobacter* sp. strain CB-D (lysogenized by ϕ-D) and temperate phage ϕ-A were directly derived from mesocosm studies conducted in Raunefjorden, Norway, while CB-A was generated through superinfection experiments conducted with ϕ-A and CB-D in the laboratory. Herein, we developed and characterized a new one-host-two-phage roseobacter model system in order to elucidate roseophage host range and effects of prophage on bacterial physiologies and metabolism. Roseobacters are ideal model organisms due to their abudance, ecological relevance, contribution to global biogeochemistry, presence of cultured isolates, and intimate relationships formed with phages (Billerbeck et al 2016, Buchan et al 2014, Zhan and Chen 2019, Zhao et al 2010). Roseobacter host *Sulfitobacter* sp. strain CB-D and temperate phage, ϕ-A, were originally isolated from an *Emiliani huxleyi* bloom mesocosm experiment (Ankrah et al 2014a, Ankrah et al 2014b). CB-D is lysogenized by ϕ-D, and strain CB-A was derived from superinfection experiments conducted in the lab. ϕ-D and ϕ-A share 79% sequence identity and provide an opportunity to study host-phage interactions in terms of lysogeny.

Through genome analyses, we determine that temperate ϕ-A and prophage ϕ-D share high sequence similarity, both carrying a suite of genes for phage structure, replication/host regulations, host integration/excision, lysis/structure, and share the same DNA Bre-C-like integrase anticipated to facilitate integration into the host genome (Ankrah et al 2014a, Ankrah et al 2014b). Sequence variation between the phages is localized to two 4-6 kb regions, which primarily encode genes of unknown function, but also includes putative tail fibers protein genes, anticipated to be important for binding to host cell surface receptors, and transcriptional regulators that may repress lytic genes during lysogeny. In Chapter 2, we elucidate that infection of *Sulfitobacter* sp. strains with temperate phage ϕ-A results in prophage induction, production of both phage types and cell lysis. We show that each of the two lysogens demonstrates homoimmunity yet are hetero-susceptible to lytic infection by the other phage type. I show that these phages influence host physiology, specifically growth dynamics, biofilm formation, and spontaneous prophage induction (SPI). We further competed our strains and discovered that these strains grow to lower abundance together, but alternatively form significantly more robust biofilms. We observe differences in phage titers between our roseophages, but phage burst size of either phage remains unknown. To further characterize this model system, I propose that one-step growth curves be used in order to determine phage burst size. Methods for this proposed experiment can be found in Appendix I.

In Chapter 3, I provide novel findings for the host range of these temperate *Podoviridae* in a one-host-two-phage model system. Though different phage lineages have been observed to show variation as it relates to host range, podoviridae tend to have relatively narrow host ranges. Not much is known about this discrepancy and host range remains not well characterized in roseobacter-roseophage model systems. The presence of a putative attachment site, *attB*, in Roseobacter strains makes these organisms appropriate for this research. By using a wide selection of roseobacters that vary in relatedness to the *Sulfitobacter* host that are part of the model system, as well as presence or absence of the *attB* site, I determined a narrow host range of both phages through spot plate assays. I was unable to determine phage integration into the genomes of the non-lysogenized roseobacters, for the conditions tested, since our methods limit our observations to phage killing. I was also unable to determine phage integration of *Sulfitobacters* that contain *attB* site through colony PCR screening. I suggest that the presence of restriction modification (RM) systems may play a role in host evasion of phage infection (reviewed in Hyman and Abedon 2010). Future work may employ selection versus screening techniques that will overcome these

limitations. I initially designed use of a biomolecular method which proposes the insertion of a Kanamycin resistance (KanR) marker into the genome of the respective prophage (Appendix 2). This seeks to capture incidence of integration that may be occurring at low frequencies. I identified intergenic regions in the phage genome (>100 bp in length), that are located far from genes required for phage integration. One such region was identified (173 bp in length) and is homologous for both phages (Fig 2). This method may be a more efficient and effective for phage integration identification. Using a selection method such as this may allow for probing of additional biological questions about roseobacter-roseophage interactions. Additionally, I propose use of lectins to determine factors concerning phage binding recognition. It remains unknown what cell surface receptors facilitate phage adsorption in our strains. Lectins have been previously used in studies to identify the blocking ability (inhibition) of these compounds of host cells to phage infection (Ishibashi et al 1982, Valyasevi et al 1990, Wendlinger et al 1996). *Sulfitobacter* cells would be grown in standard marine media (SMM) and pretreated with an additional 20ul in 2 ml for lectins with a concentration of 2 mg/ml, and 40 μl in 2 ml for lectins with a concentration of 1 mg/ml. Cells would be pretreated at room temperature for 5 minutes. Cells would be kept at 4^0C for 1 hour, then centrifuged at 5,000 rpm, and resuspended in SMM. Roseophages would be added and the mixture and incubated for 15 minutes. Prevention of phage adsorption by lectins would be tested via plaque assay, using a plating range of 10^0 to 10^{-7}.

Due to the increased acknowledgement of phage-host interactions, particularly as a virocell entity, I led an effort to explore the influence of lysogeny on carbon and lipid metabolism of our virocells that is described in Chapter 4. Currently little is known about how prophages influence host metabolism, whereby most systems focus on lytic phages. These studies were further driven by previously identified phenotypic differences, that are linked to SPI, though little is known about SPI in roseobacters. To first control complexity of data interpretation by SPI, I addressed the modulation of SPI, growth dynamics and viable counts by growing our strains in different vessels and volumes. I determined that these factors change along an aeration gradient, and successfully minimize SPI by growing cultures in 200 ml baffled flasks. I also determined that change to pH is not a significantly contributing factor. We used metabolomics and lipidomics technologies to determine that distinct metabolites and lipids, as opposed to holistic pathways or classes, are responsible for observed differences in the metabolome and lipidome. These select compounds form part of, or directly feed into the TCA cycle or lipid biosynthesis pathways. Future directions

may aim to measure reactive oxygen species (ROS) in different vessel types and volumes to determine why I observe variation according to aeration.

In my final research chapter, I led an effort to explore the ways in which differences in carbon substrates influence virocells, thus affecting host physiologies, SPI and metabolism. Previous research has shown that season changes may influence lysogeny and that preferred carbon sources have a directly positive impact on bacterial growth rates and host yields (Jiang and Paul 1994, Monod 1949). Some systems have identified that different substrates influence host physiology, specifically biomass for example, however, few representative marine phage-host systems currently exist that study how carbon source changes mediate lysogeny and host metabolism (Wendisch et al 2000). Here, we provide new data that suggest that glutamate is preferred over acetate as a substrate. We illustrate that different substrates dictate differentiation in growth dynamics, viable counts and cell size. We also observe incidence of SPI of ϕ-A only in cultures grown in these substrates. We see that there is differentiation of samples according to organism and by time. As seen in SMM, select metabolites and lipids more so contribute to observed differences, rather than entire pathways. Future works can aim to conduct transcriptome data analysis, which will identify gene expression over time and help reveal metabolic shifts. As part of this study, samples were collected and archived for such research to be pursued. Substrates can also be complex mixtures to be more indicative of carbon pools in natural environments. Here, I was unable to truly determine the effects of prophage compared to un-lysogenized cells, and I propose that the generation of a phage-less variant will help in such experiments.

ACKNOWLEDGEMENTS

I would like to thank the undergraduate and graduate students who contributed to the development of future works that are written in this Chapter: Avery Bullock, Courtney Christopher, Katarina Jones, Kaylee Jacobs and Dr. Joseph Jackson. Avery contributed to the development of proposed selection methods of *Sulfitobacter* sp. strains conducted as part of Chapter 3. Lectins were provided by Dr. Joseph Jackson and Dr. Gladys Alexandre for initial study conducted as part of Chapter 3. Katarina, Kaylee and Courtney helped conduct sampling for transcriptomics archiving conducted as part of Chapter 4. AB and Dr. Sanjeev Dahal reviewed this chapter. This research was supported by NSF grant (OCE-106352) to A.B. and S.R.C.

REFERENCES

Ankrah NYD, Budinoff CR, Wilson WH, Wilhelm SW, Buchan A (2014a). Genome Sequences of Two Temperate Phages, ΦCB2047-A and ΦCB2047-C, Infecting Sulfitobacter sp. Strain 2047. *Genome Announcements* **2**.

Ankrah NYD, Lane T, Budinoff CR, Hadden MK, Buchan A (2014b). Draft Genome Sequence of Sulfitobacter sp. CB2047, a Member of the Roseobacter Clade of Marine Bacteria, Isolated from an Emiliania huxleyi Bloom. *Genome Announcements* **2**.

Bergh O, Borsheim KY, Bratbak G, Heldal M (1989). High Abundance of Viruses Found in Aquatic Environments. *Nature* **340:** 467-468.

Billerbeck S, Wemheuer B, Voget S, Poehlein A, Giebel HA, Brinkhoff T *et al* (2016). Biogeography and environmental genomics of the Roseobacter-affiliated pelagic CHAB-I-5 lineage. *Nature Microbiology* **1**.

Bondy-Denomy J, Davidson AR (2014). When a Virus is not a Parasite: The Beneficial Effects of Prophages on Bacterial Fitness. *Journal of Microbiology* **52:** 235-242.

Brussow H, Canchaya C, Hardt WD (2004). Phages and the evolution of bacterial pathogens: From genomic rearrangements to lysogenic conversion. *Microbiology and Molecular Biology Reviews* **68:** 560-+.

Buchan A, LeCleir GR, Gulvik CA, Gonzalez JM (2014). Master recyclers: features and functions of bacteria associated with phytoplankton blooms. *Nature Reviews Microbiology* **12:** 686-698.

Canchaya C, Fournous G, Chibani-Chennoufi S, Dillmann ML, Brussow H (2003). Phage as agents of lateral gene transfer. *Current Opinion in Microbiology* **6:** 417-424.

Feiner R, Argov T, Rabinovich L, Sigal N, Borovok I, Herskovits AA (2015). A new perspective on lysogeny: prophages as active regulatory switches of bacteria. *Nature Reviews Microbiology* **13:** 641-650.

Forterre P (2013). The virocell concept and environmental microbiology. *Isme Journal* **7:** 233-236.

Fortier LC, Sekulovic O (2013). Importance of prophages to evolution and virulence of bacterial pathogens. *Virulence* **4:** 354-365.

Fuhrman JA (1999). Marine viruses and their biogeochemical and ecological effects. *Nature* **399:** 541-548.

Hambly E, Suttle CA (2005). The viriosphere, diversity, and genetic exchange within phage communities. *Current Opinion in Microbiology* **8:** 444-450.

Harrison E, Brockhurst MA (2017). Ecological and Evolutionary Benefits of Temperate Phage: What Does or Doesn't Kill You Makes You Stronger. *BioEssays* **39:** 1700112.

Hendrix RW (2002). Bacteriophages: Evolution of the majority. *Theoretical Population Biology* **61:** 471-480.

Hyman P, Abedon ST (2010). Bacteriophage Host Range and Bacterial Resistance. In: Laskin AI, Sariaslani S, Gadd GM (eds). *Advances in Applied Microbiology, Vol 70*. pp 217-248.

Ishibashi K, Takesue S, Watanabe K, Oishi K (1982). Use of Lectins to Characterize the Receptor Sites for Bacteriophage PL-1 of Lactobacillus casei. *Journal of General Microbiology* **128:** 2251-2259.

Jiang SC, Paul JH (1994). Seasonal and Diel Abundance of Viruses and Occurrence of Lysogeny/Bacteriocinogeny in the Marine Environment. *Marine Ecology Progress Series* **104:** 163-172.

Monod J (1949). The Growth of Bacterial Cultures. *Annual Review of Microbiology* **3:** 371-394.

Nanda AM, Thormann K, Frunzke J (2015). Impact of Spontaneous Prophage Induction on the Fitness of Bacterial Populations and Host-Microbe Interactions. *Journal of Bacteriology* **197:** 410-419.

Paul JH (2008). Prophages in marine bacteria: dangerous molecular time bombs or the key to survival in the seas? *Isme Journal* **2:** 579-589.

Suttle CA (2007). Marine viruses - major players in the global ecosystem. *Nature Reviews Microbiology* **5:** 801-812.

Valyasevi R, Sandine WE, Geller BL (1990). The Bacteriophage-KH Receptor of Lactococcus lactis subsp. cremoris KH is the Rhamnose of the Extracellular Wall Polysaccharide. *Applied and Environmental Microbiology* **56:** 1882-1889.

Wendisch VF, de Graaf AA, Sahm H, Eikmanns BJ (2000). Quantitative Determination of Metabolic Fluxes during Coutilization of Two Carbon Sources: Comparative Analyses withCorynebacterium glutamicum during Growth on Acetate and/or Glucose. *Journal of Bacteriology* **182:** 3088.

Wendlinger G, Loessner MJ, Scherer S (1996). Bacteriophage receptors on Listeria monocytogenes cells are the N-acetylglucosamine and rhamnose substituents of teichoic acids or the peptidoglycan itself. *Microbiology-Uk* **142:** 985-992.

Wilhelm SW, Suttle CA (1999). Viruses and Nutrient Cycles in the Sea - Viruses play critical roles in the structure and function of aquatic food webs. *Bioscience* **49:** 781-788.

Zhan YC, Chen F (2019). Bacteriophages that infect marine roseobacters: genomics and ecology. *Environmental Microbiology* **21:** 1885-1895.

Zhao YL, Wang K, Ackermann HW, Halden RU, Jiao NZ, Chen F (2010). Searching for a "Hidden" Prophage in a Marine Bacterium. *Applied and Environmental Microbiology* **76:** 589-595.

APPENDIX

Figure legend.

Fig 6.1. Proposed optimization method.

Fig 6.2. Proposed location of a KanR marker into the genome of phages ϕ-D and ϕ-A.

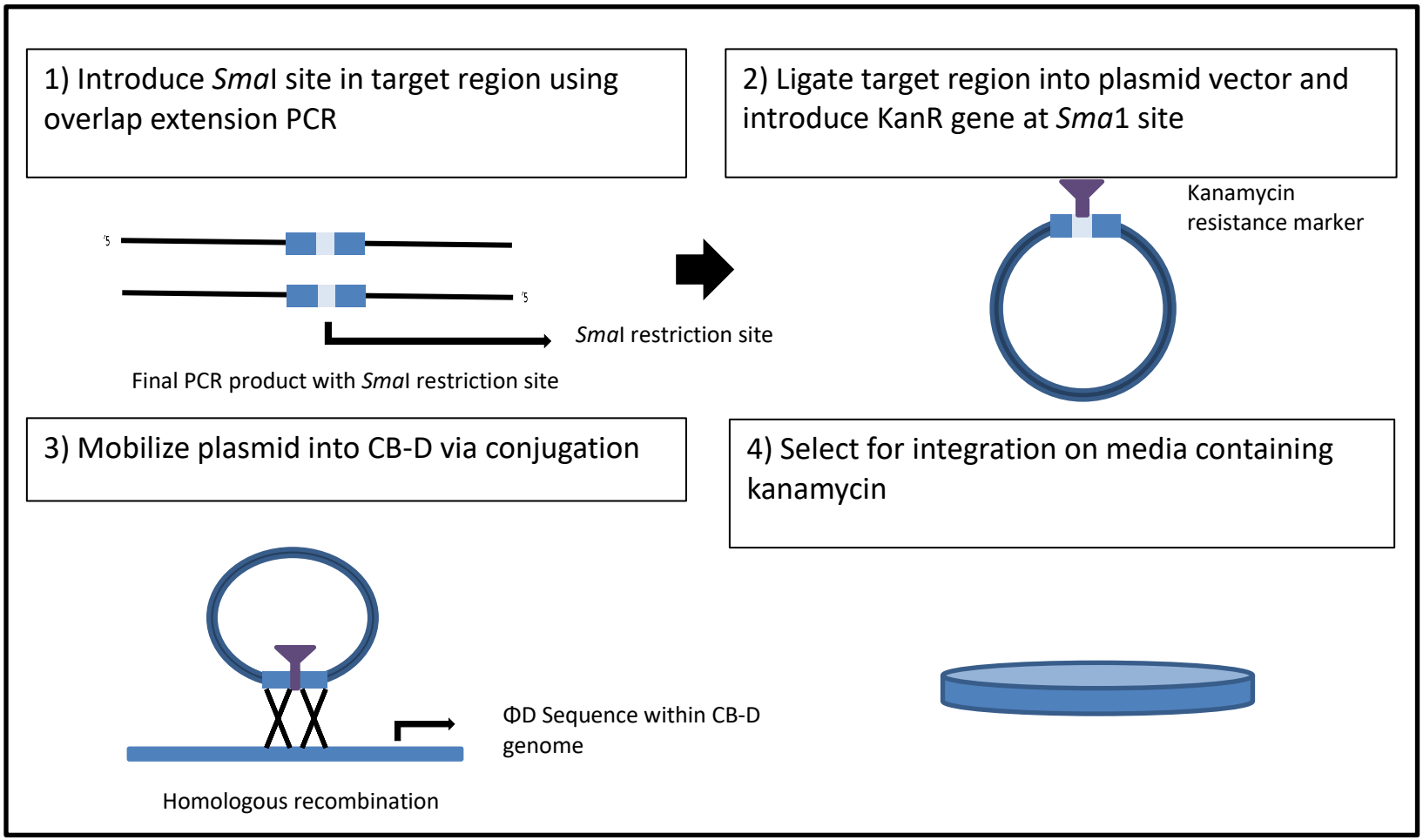

Fig 6.1. Proposed optimization method.

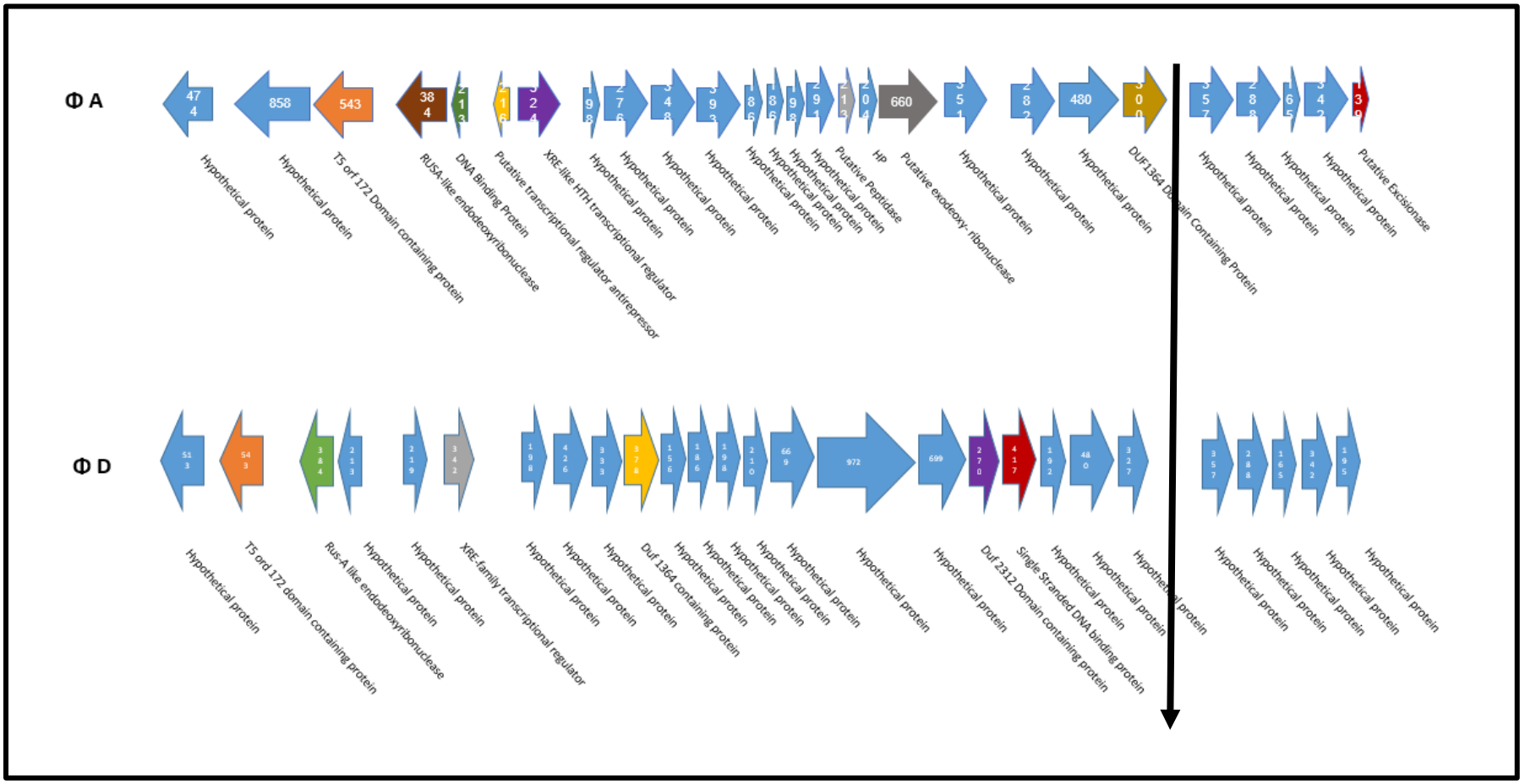

Fig 6.2. Proposed location of a KanR marker into the genome of phages ϕ-D and ϕ-A.

One-step growth curves for *Sulfitobacter sp.* phages_mod1

Jonelle Basso
An adaptation from the protocol developed by Bonnie Poulos

Pre-steps:

i. First determine when the host exhibits exponential growth. Also, calculate the phage lysate titer to be used for the experiment.
ii. Store all media at 25^{o}C prior to experiment to keep the temperature constant.
iii. All incubation will be done at 25^{o}C at 200 rpm

Host growth:

1. Inoculate a new culture, i.e. pick a colony into a new flask containing 10 ml of ½ cbud media (at 25^{o}C, 200 rpm).
2. Immediately after the transfer, take a 'time 0' growth reading (T0), at OD 540nm
3. Continue taking readings periodically.
   -Graph the results as you go. It is best to infect the host in mid-exponential (log linear) phage, when OD is ≈ 0.2.
   -You can start with longer intervals (1-2 hours) until you start to see growth, then shorter intervals (15-30 minutes) until the growth starts to level off. If it's taking a while, you can go back to reading at longer intervals.
4. Do a plaque assay to determine the PFU/ml of the lysate you plan to use.
5. Calculate the volume needed for 10^7 phages.
   -If 10^7 phages are contained in less than 1 ul, you will need to dilute the lysate prior to performing the growth curve experiment.
6. Determine the concentration of your culture at the time you start the infection.
   -Use the correlation of readings from the spec and cell counts (CFU, DAPI, or FCM counts) to estimate this.
7. Calculate the volume of host culture needed for 10^8 cells.

One-step protocol:

8. Add 10^7 of phages to the tube. Allow the phages to adsorb to the host cells for 20 minutes. At host OD 0.17 (@540nm), infect using an MOI of 0.5 (10 ml of host culture).
9. Centrifuge for 5 min at 4,000 rpm.
10. Carefully pour off supernatant.
11. Resuspend pellet in 10 ml of fresh media (don't dilute here).
12. Set up two flasks. Dilute the infection 1:1000 in ½ cbud media in a 250 ml flask.
    -If you have 50 ml of ½ cbud in the flask, add 50 ul of host for a 1:1000 dilution.
13. Take a sample immediately after dilution- this is T0.
    -At T0 do centrifuged and not centrifuged samples.
14. Steps for centrifuged sample:
    -Pipet 100 ul from the flask into 900 ul of ½ cbud in a 15 ml tube (you are diluting your sample 10x: 10^{-1}).

Note that if you're using a different MOI, you will need to calculate the expected number of phage at T0 to guide you in what dilution to plate. This will depend on the total volume of the initial infection (i.e. the volume of cells plus phages). So the concentration at T0 should be total phage added/volume of infection, divided by 1000 (for the 1:1000 dilution). Convert this to phages per ml.
-Vortex briefly.
-Very carefully remove the tube (do not disturb the pellet!) and plate 100 ul.

15. Continue sampling in this way for 4 hours
-Monitor OD every hour and take samples for plaque assay, for **free** phage only, at T0, T1 (after 1 hr), T2 (2hrs), T3 (2.5hrs), T4 (3hrs), T5 (3.5hrs), T6 (4hrs)
-Centrifuge 0.5 ml for 5 minutes at 4000 rpm, assaying phage in supernatant.
-At later time points, more dilutions will need to be plated. On the first trial, be generous with what you plate (i.e. plate, 10^{-2}, 10^{-3}, 10^{-4}, 10^{-5}), and use the results as a guide for what you should plate in repeat experiments.
-Store the filtered samples at 4^{o}C.
16. The next day, count the plaques on all plates that have a countable number of them.
17. Decide which dilution gives the best count at each time point for the next time you do this same phage-host pair
-depending on the size of the plaques, a 'good' count will be somewhere between 10 and a few hundred.
18. The next day, count any new plaques that have appeared and add these to your original count.
19. Count again on the third day.
20. Calculate PFU/ml at each time point for both the centrifuged (free phage only) and not centrifuged (total phage) samples.
21. Graph the results.
22. Calculate burst size.
23. Take the **free** phage average of the time points on the plateau before the burst (A).
24. Take the **free** phage average of the time points on the plateau after the burst (B).
25. Subtract A from B; This is the **total** burst or new phages released (C).
26. Divide C by the number of infected phage (**total** phages at T0 minus **free** at T0); This is the burst size.

APPENDIX

Modulation of growth dynamics, viable counts and spontaneous prophage induction in custom made extra-large test tubes

We have previously found evidence for the modification of specific physiologies of *Sulfitobacter* sp. strains CB-D and CB-A by modulating vessel type and volume of bacterial cultures. We see incidence of spontaneous prophage induction (SPI) in these strains, which is linked to physiological differences. By scaling up standard 10 ml cultures by 20-fold and growing cultures in baffled or unbaffled flasks, we have previously identified a pattern of greatest disparity in growth dynamics in least aerated conditions, and least disparity in most aerated conditions. As a result, we aimed to further characterize this modulation through scaling up the vessel type, while keeping the volume to surface ratio constant. To address this, custom made extra-large tubes were made and used to characterize growth dynamics, viable counts and spontaneous prophage induction of both strains. Our results show that physiologies are more alike those seen in 10 ml cultures, though not as distinct. These data aim to improve the understanding of the implications of scalability on *Sulfitobacter* lysogens.

To our knowledge, we are the first to investigate modulation of growth dynamics, viable counts and incidence of SPI in custom-made XL test tubes. As previously conducted, we increased the culture volume by 20-fold compared to 10 ml test tube cultures. By using these custom-made tubes, we maintained a constant surface area to volume ratio. Here, we use a two-phage-one-host model system of an ecologically relevant marine bacteria, in order to determine incidence of SPI, differences in biomass and cell size, and conduct cell counts for cultures grown in standard marine media, glutamate or acetate.

This study seeks to characterize modulation of physiology and SPI by vessel type and culture volume. We hypothesize that the volume to surface area ratio of these tubes will replicate growth dynamics, corroborated by viable counts data, as seen in 10 ml test tubes. We hypothesize that different carbon substrates will differentially influence host physiology and incidence of SPI. We suggest that standard marine media is the preferred substrate, followed by glutamate then acetate. As a result, we anticipate that biomass and cell counts will range from greatest to smallest for these media respectively.

MATERIALS AND METHODS

Production of XL tubes and custom-made tube racks.

XL test tubes were custom-made by the glass blower affiliated with Department of Chemistry at The University. Test tube racks were made at the woodshop affiliated with the College of Engineering at The University.

Bacterial propagation.

Sulfitobacter sp. strains CB-A and CB-D were inoculated in, Standard Marine Media (SMM), or Roseobacter Minimal Media (RMM) supplemented with either (4 mM L-glutamic acid [glutamate] or 10 mM sodium acetate [acetate]) as a sole carbon source. Cultures were incubated at 25^{o}C at 200 rpm. Overnight cultures were sub-cultured, and samples of cultures at 0 hours were taken at $OD_{540nm} \approx 0.17$ or ≈ 0.10 respectively. Growth was monitored every two hours for 24 hours. Both bacterial strains were grown in biological triplicate of 200 ml per XL tube.

Sampling methodology and spot plating assays for SPI detection have been previously described in chapters 4 and 5.

RESULTS

Growth dynamics, viable counts and SPI.

Extra-large (XL) tubes were made (UT chemistry department) to replicate scaled up growth vessel conditions present in 10 ml test tubes. 200 ml cultures were grown in SMM and their growth dynamics compared to other growth treatments (Fig 1). There was no significant difference in growth dynamics of 200 ml cultures grown in baffled or unbaffled flasks. Growth dynamics in XL tubes were not as pronounced as in 10 ml test tubes but were more differentiated than in 200 ml unbaffled flasks and 200 ml baffled flasks. In subsequent experiments with XL tubes, 10 ml tubes were grown in tandem for comparison control purposes only.

In order to test growth dynamics in a minimal media, 10 ml test tube cultures and XL tube cultures were grown on glutamate as sole carbon source. Cultures grown in glutamate had longer lag phase and more distinct differentiation between organisms in both treatments 10 ml and XL tubes (Fig 2). Viable counts data corroborated with growth dynamics data (Table 1). We see incidence of SPI in XL tube cultures grown in SMM and glutamate (data not shown.

We suggest that differences in growth dynamics may be due to variation in aeration or the presence of reactive oxygen species (ROS). We illustrate that SPI was minimized greatest in 200 ml baffled flasks. Modulations in scalability of model systems however highlights a level of complexity to these systems whereby caution must be taken when attempting to make definitive claims to global scale occurrences in compared to laboratory settlings.

ACKNOWLEDGEMENTS

We would like to thank Kaylee Rae Jacobs for her great to the development of this research chapter: Kaylee contributed to testing of growth dynamics of roseobacters in SMM, glutamate and acetate. She also conducted SPI tests in each substrate. JTRB wrote the manuscript for this study and conducted sampling for growth dynamics determination and viable counts data acquisition. JTRB made custom-made XL test tube racks at the Perkins Hall woodshop through the assistance of Mr. Michael Allen, College of Engineering. This research was supported by NSF grant (OCE-106352) to A.B.

Table legend.

Table A1. Viable counts data conducted for *Sulfitobacter* sp. strain CB-D and CB-A over 27 hours.

Table A1. Viable counts data conducted for *Sulfitobacter* sp. strain CB-D and CB-A over 27 hours.

10 ml tubes in SMM								
	CB-A				CB-D			
	optical density		viable counts		optical density		viable counts	
Time	Av	Stdev	Av	Stdev	Av	Stdev	Av	Stdev
0	0.07	0.01			0.07	0.01		
2	0.15	0.01			0.16	0.01		
4	0.30	0.01			0.29	0.02		
6	0.49	0.01			0.52	0.04		
8	0.62	0.02			0.69	0.06		
10	0.82	0.03			0.90	0.07		
12	0.91	0.03			1.03	0.07		
14	0.96	0.05			1.12	0.05		
16	1.03	0.07			1.21	0.05		
18	1.04	0.09			1.30	0.06		
20	1.08	0.11			1.37	0.06		
22	1.08	0.12			1.44	0.06		
24	1.02	0.15			1.45	0.04		

20 ml XL tubes in SMM								
	CB-A				CB-D			
	optical density		viable counts		optical density		viable counts	
Time	Av	Stdev	Av	Stdev	Av	Stdev	Av	Stdev
0	0.06	0.00	1.61E+07	3.18E+06	0.07	0.01	2.66E+06	
2	0.11	0.00			0.11	0.01		
4	0.22	0.01			0.22	0.02		
6	0.40	0.02			0.37	0.05		
8	0.56	0.02			0.54	0.04		
10	0.72	0.02	7.68E+07	7.18E+07	0.69	0.04	4.41E+06	
12	0.86	0.02			0.81	0.04		
14	0.93	0.01			0.92	0.03		
16	1.01	0.01			1.00	0.04		
18	0.97	0.01	7.28E+07	1.20E+07	1.05	0.04	1.38E+07	
20	1.05	0.00			1.10	0.04		
22	1.06	0.01			1.14	0.03		
24	0.99	0.01	8.64E+07	1.68E+07	1.16	0.00	8.20E+06	

Table # A1 continued

10 ml tubes in 4 mM glutamate								
	CB-A				CB-D			
	optical density		viable counts		optical density		viable counts	
Time	Av	Stdev	Av	Stdev	Av	Stdev	Av	Stdev
0	0.02	0.00			0.03	0.00		
2	0.02	0.00			0.03	0.00		
10	0.10	0.01			0.14	0.00		
12	0.11	0.02			0.17	0.01		
14	0.11	0.01			0.21	0.01		
16	0.14	0.02			0.29	0.02		
18	0.20	0.04			0.38	0.02		
20	0.27	0.04			0.51	0.03		
22	0.32	0.04			0.56	0.02		
24	0.38	0.03			0.55	0.01		
26	0.43	0.03			0.54	0.01		

20 ml XL tubes in 4 mM glutamate								
	CB-A				CB-D			
	optical density		viable counts		optical density		viable counts	
Time	Av	Stdev	Av	Stdev	Av	Stdev	Av	Stdev
0	0.01	0.00	7.20E+06	1.31E+06	0.03	0.01	9.40E+06	2.56E+06
2	0.02	0.00			0.03	0.01		
10	0.05	0.01	1.07E+07	2.87E+06	0.07	0.01	1.86E+07	4.93E+06
12	0.06	0.01			0.08	0.01		
14	0.08	0.01			0.11	0.01		
16	0.10	0.01			0.15	0.02		
18	0.13	0.01	3.47E+07	5.27E+06	0.20	0.04	4.21E+07	1.33E+07
20	0.16	0.01			0.25	0.05		
22	0.20	0.01			0.32	0.07		
24	0.23	0.01			0.39	0.08		
26	0.29	0.01	5.61E+07	3.75E+07	0.43	0.03	6.35E+07	4.73E+07

Figure legend.

Fig A1. Growth dynamics comparison of *Sulfitobacter* sp. strain CB-D (light grey) and CB-A (dark grey) in 10 ml tubes (A), 200 ml baffled flask cultures (B), 200 ml baffled flask cultures (C) and XL tubes (D). Organisms were grown in standard marine media (SMM).

Fig A2. Growth dynamics of *Sulfitobacter* sp. strain CB-D (light grey) and CB-A (dark grey) in XL tubes and 10 ml test tubes grown in standard marine media (SMM) (panels A and B), and 4 mM glutamate (panels C and D).

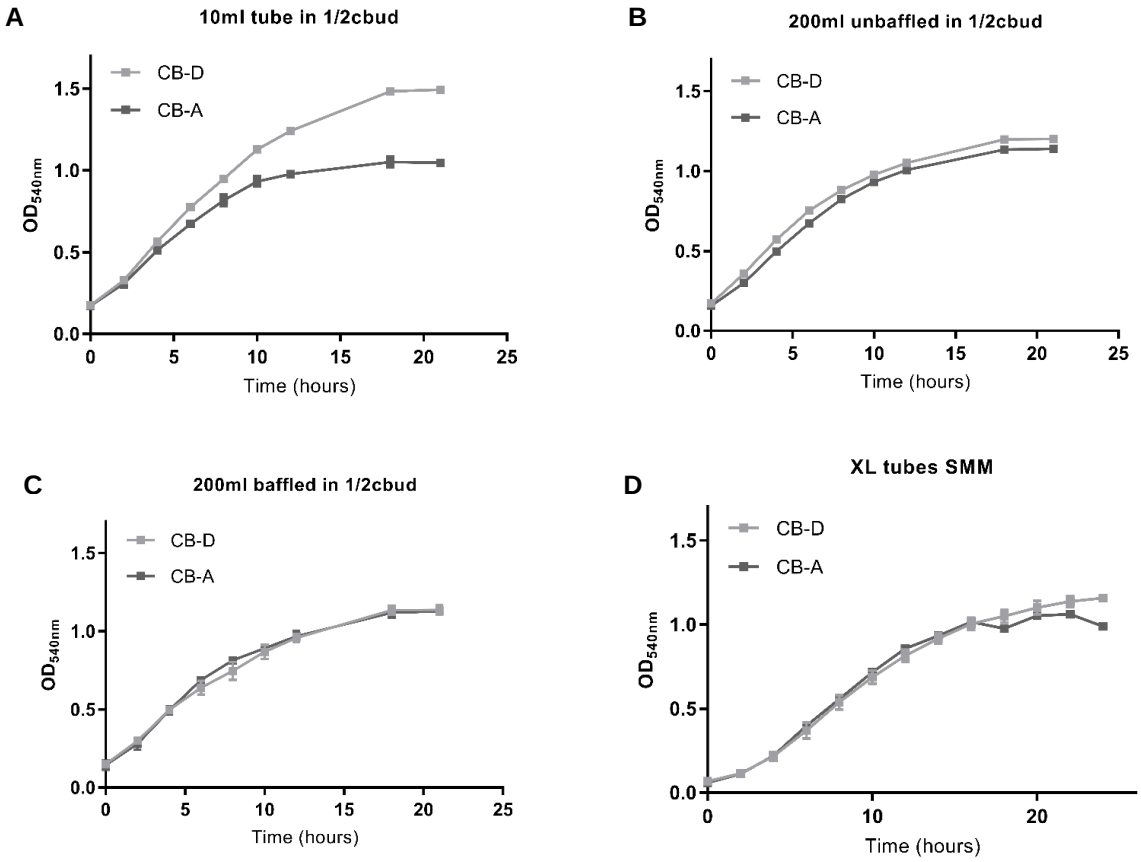

Fig A1. Growth dynamics comparison of *Sulfitobacter* sp. strain CB-D (light grey) and CB-A (dark grey) in 10 ml tubes (A), 200 ml baffled flask cultures (B), 200 ml baffled flask cultures (C) and XL tubes (D). Organisms were grown in standard marine media (SMM).

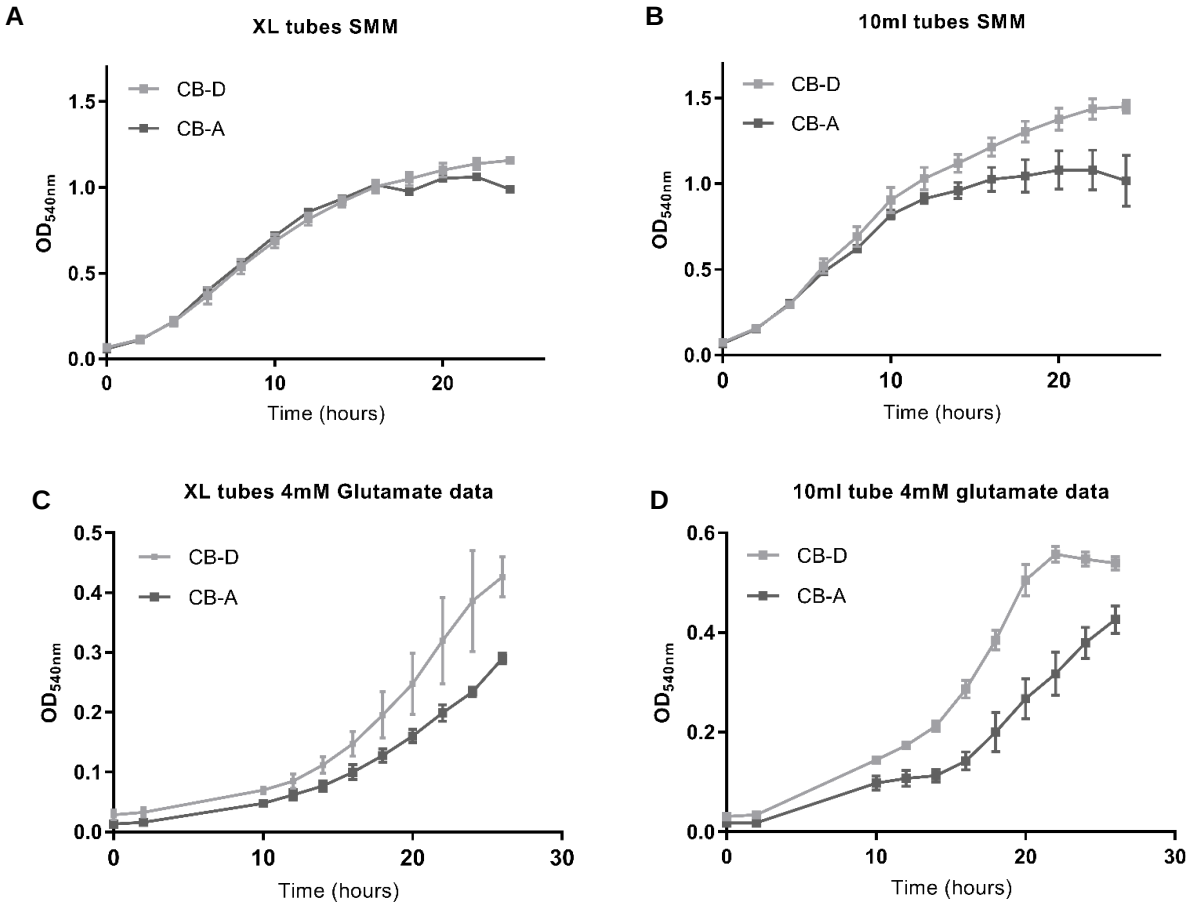

Fig A2. Growth dynamics of *Sulfitobacter* sp. strain CB-D (light grey) and CB-A (dark grey) in XL tubes and 10 ml test tubes grown in standard marine media (SMM) (panels A and B), and 4 mM glutamate (panels C and D).

VITA

Jonelle Tamara Rose Basso was born in the beautiful twin island republic of Trinidad and Tobago. She graduated from St. Joseph's Convent Secondary School in 2003 and pursued a double major in Environmental biology at the University of the West Indies, Mona, Jamaica. Upon graduating U.W.I. in 2003, she worked for two years in the Health, Safety and Environmental department at the Petroleum Company of Trinidad and Tobago (Petrotrin). Although going aboard helicopters for offshore audits and traversing the island of Trinidad for onshore oilfield audits was quite fun, Jonelle wanted to pursue a master's degree. From 2008-2011, Jonelle was enrolled in the Environmental Science and Policy MSc. program at the University of South Florida, St. Petersburg, Fl. While completing an environmental chemistry-based research thesis, she served as a microbiology teacher's assistant. It was through this teaching opportunity, Jonelle became employed as a researcher by USF College of Marine Science, Distinguished University Professor, Dr. John Paul. For three years, post Gulf of Mexico Maconda Oil spill, Jonelle was part of thirteen research cruises that went to sea approximately six times a year, six to ten days at a time. She collected water samples to help monitor the health of the Gulf. During her time in the Paul lab, Dr. Paul hosted the Aquatic Virus Workshop (AVW) 7, which served as a great turning point in her career. She fell in love with aquatic virus research, and the people who were a part of that realm. Through that experience, she was encouraged to pursue a PhD. She enrolled in the PhD program in Microbiology at the University of Tennessee Knoxville, where she received her terminal degree in December 2019.